# SAPIENZA
## UNIVERSITÀ DI ROMA

DOTTORATO DI RICERCA IN BIOCHIMICA

CICLO XXXI (A.A. 2015-2018)

# Study of new potential therapeutic approaches for the Rett syndrome in murine models

Dottorando:

**Daniele Vigli**

Docente guida:                    Coordinatore:

**Dr. Bianca De Filippis**          **Prof. Stefano Gianni**

Tutor interno:

**Prof. Maria d'Erme**

Dicembre 2018

*Again…To my Family*

**Index**

*Chapter 1*

# 1. Introduction

## 1.1 Rett syndrome

### 1.1.1 Story and Clinical aspects: symptomatology, neurobiology, biochemical alterations and variants

Rett syndrome (RTT) [OMIM 312750] is a rare neurodevelopmental disorder, that almost exclusively affects females with a incidence of 1 in every 10,000 births, characterized by severe behavioural and physiological symptoms (Rett, 1966; Hagberg et al., 2002; Ricceri et al., 2012). RTT was reported for the first time by Dr. Andreas Rett, paediatric neurologist: he studied the clinical cases of two female children showing an unusual compulsive behaviour and physical and cognitive deficits, symptomatology very similar to patients with Autism. He started to investigate deeply on this strange symptoms finding 22 cases of this new disorder in Europe, publishing results in 1966 (Rett, 1966) without impacting the scientific community until 1983, when Dr. Hagberg described 35 clinical cases displaying the Rett's described symptomatology (Hagberg et al., 1983; Hagberg, 1985).

One essential feature of RTT is the apparently normal perinatal development until about 6-18 months of age, when RTT patients start a regression period, losing their acquired cognitive, social, and motor skills and develop a wide variety of symptoms (Hagberg, 2002) (Fig. 1). Indeed, most of the severe symptoms in RTT are not quite detectable in the first stage of the disorder. After the first "normal development" phase, at 6 months of age starts the "developmental stagnation" phase, characterized by microcephaly, growth arrest and hypotonia. Already after the first year of life, child enters in a phase called "rapid regression", phase where child loses the hands skills, the speech,

3

the social interaction, developing all autistic features, including severe mental retardation. Moreover, the child displays hands stereotypies, breathing impairments and seizures. Despite everything there are more and more evidences supporting the absence of this regression phase, suggesting that already from the first days of life, some morphological and biochemical alterations are just detectable in RTT patients (Cosentino et al., in preparation). After this phase of rapid regression, about three years of age the clinical picture goes to a "stationary stage" characterized by scoliosis defect and the anxiety behaviour onset accompanied by a late motor deterioration leading to motor rigidity and Parkinsonian features that will accompanied child for all life, causing complications often deadly (Chahrour and Zoghbi, 2007).

Classic RTT is caused in about 90–95% of cases mutations in the X-linked MECP2 gene, which encodes the methyl CpG-binding protein 2 (MECP2), a multifunctional protein that binds to methylated DNA and mainly acts as a key transcriptional regulator (Guy et al., 2011). This protein was identified in 1992 by Dr. Adrian Bird and colleagues (Meehan et al., 1992). Only 7 years later, mutations in MECP2 were associated to be the most important cause of RTT (Amir et al., 1999). Most of the mutations arise *de novo* in the paternal germline and many times involve a C to T transition at CpG dinucleotides (Trappe et al., 2001). A wide range of mutations occurs on MECP2 gene; eight missense and nonsense mutations in about 70% of cases, small C-terminal deletion in about 10% of cases and complex rearrangements in about 6% of cases (Christodoulou and Weaving, 2003).
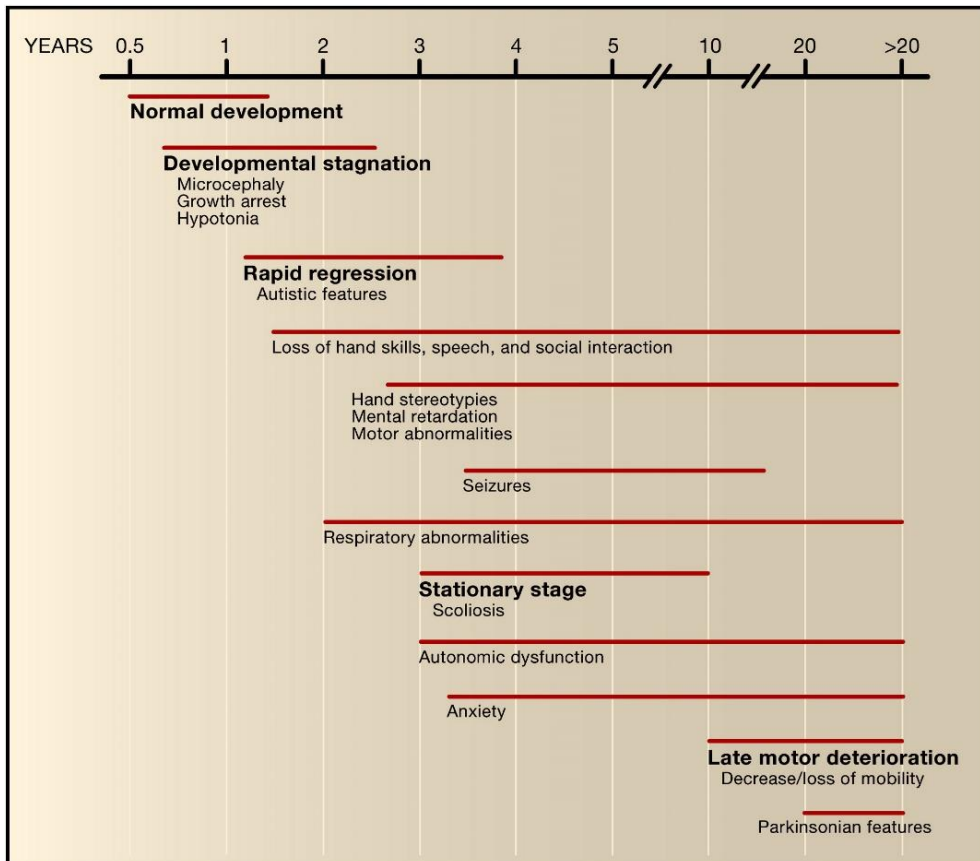
Fig.1: **Developmental phases in the Rett syndrome**: at each phase corresponds a wide range of symptoms (Chahrour and Zoghbi, 2007)

After the first initial description and characterization of RTT, to better define its neuro-biology and pathology features at the end of 80's many neuroimaging and neuropathological studies have been carried out on RTT patients. The head growth deceleration and cognitive decline suggested alterations in neocortex, whereas gait disturbances involved extrapyramidal and cerebellar dysfunction. Actually, there is a generalized brain atrophy (12-34% reduction in brain weight and volume in RTT patients (Armstrong, 2005)) involving cerebrum and cerebellum (Nomura et al., 1985; Reiss et al., 1993; Armstrong, 2005). Contrary to what was expected, no evidence of neuronal

5

loss was detected (Armstrong et al., 1995), suggesting the absence of a neurodegeneration over time. However, from RTT post-mortem brain studies several changes in neurons synaptic growth and architecture regarding the number of dendrites as well as the presence of regions without dendritic spines were observed (Belichenko et al., 1994). Post-mortem studies characterizing different brain regions cell types, have tried to correlate cells alterations and symptoms occurrence (Leontovich et al., 1999). In addition, several neurochemical alterations in RTT patients were also reported, mainly related to cholinergic and dopaminergic systems (Brucke et al., 1987; Wenk et al., 1993). Nevertheless, all these results suggest a fundamental role for MeCP2 in neuronal maturation and maintenance. Considering that the reported alterations are linked with a lacking general brain growth and functionality, several studies focused on the levels of neurotrophic factors in cerebrospinal fluid and serum, using them as markers of pathogenesis too. Indeed, low concentrations of cerebrospinal fluid nerve growth factor (NGF) that acts on cholinergic neurons of the basal forebrain and high level of glutamate were reported in patients with RTT. In particular, the forebrain is more severely affected in RTT than the other cortical areas. These data suggested that alterations in RTT dendritic development could be the consequence of cholinergic deficiency and of NGF/glutamate imbalance (Calamandrei et al., 2001; Riikonen, 2003). In addition, RTT brain post mortem studies showed a reduced quantity of dopamine, serotonin and noradrenaline and higher levels of markers associated to bioaminergic metabolism (Lekman et al., 1989). These results were confirmed in studies on brain of RTT mouse models, in which the same alterations were detected (Viemari et al., 2005; Panayotis et al., 2011).

To complicate the clinical picture, the presence of different mutations leads to different phenotype-genotype correlations with severe symptoms and alterations. *MeCP2* mutations involving the nuclear localization signal (NLS) or early truncated mutations cause a severe phenotype, whereas C-terminal deletion lead to milder phenotype with prolonged life-span (Smeets et al., 2005; De Filippis et al., 2010). In all reported cases of classic RTT, the syndrome was caused by the partial or complete loss of MeCP2 functions, including DNA binding and protein-protein interactions. From the first RTT description, several atypical forms have been described. These variants range from milder phenotype with a later age of onset to more severe clinical symptomatology. This high variability in the phenotype shown by females RTT patients is due to the phenomenon of casual inactivation of the X-chromosome, which is altered in some patients (Renieri et al., 2003; Weaving et al., 2005). Moreover, somatic mosaicism in females with *MECP2* alterations is another source of variability (Bourdon et al., 2001). The wide clinic heterogeneity reporting in RTT patients allowed the description of four major RTT variants:

1) The "forme fruste" ("Worndown form"): it is characterized by a later age of symptoms onset, with the hypothetical regression phase starting between 1 to the 3 years of age, and less severe stereotyped hands movements.

2) The congenital form: it is the most severe variant, lacking the "apparently normal development" period with the first seizure episode at 6 months of age. Most of the symptoms appear already from the first day of life. The gene involved in this form is FOXG1, codifying for the transcriptional repressor "winged-elix", important for telencephalons development (Ariani et al., 2008).

7

3) The Zappella variant (Preserved speech variant): the essential feature of this form is the ability of the patients to speak some few words, even if often out of context. In addition, the head size can be considered normal and the stereotypic hands movement are absent. However, patients display a severe kyphosis and are often overweight (Zappella et al., 2001).

4) CDKL5 deficiency disorder (CDD) or Hanefeld variant (early infantile epileptic encephalopathy type 2): comparing it with classical RTT, in this variants the main diagnostic symptom is the early-onset seizures, occurring by the 6 month of life, accompanied with several RTT-like features (Hanefeld, 1985b, a). In this variant, no alteration in *MECP2* gene are present; mutation of gene codifying for Cyclin-Dependent Kinase-Like 5 (CDKL5), previously known as serine/threonine kinase 9 (STK9) (Montini et al., 1998) leads to the Hanefeld variant, that will change its name in CDKL5 deficiency disorder.

## CDKL5 deficiency disorder (CDD)

CDD is a severe X-linked neurodevelopmental disease characterized by severe mental retardation, generalized developmental delay (symptoms in common with RTT) and the typical early-onset intractable seizures. It is caused by mutation of *CDKL5* gene, leading to CDKL5 protein with altered functionality. This protein is highly expressed in the brain in physiological condition. CDD affects mostly females and, after the first descriptions reporting most of the symptomatology of RTT, was initially termed Hanefeld variant of RTT. The first described mutations were reported in 2003 by Dr. Vera Kalscheuer which identified *CDKL5* gene disruption by a breakpoint on

the X-chromosome, in two different girls displaying infantile spasms and severe developmental delay (Kalscheuer et al., 2003). The interest for CDKL5 is growing because there are many patients affected by RTT symptomatology, but they were negative to MeCP2 testing (Weaving et al., 2004). Subsequent studies allowed the identification of intragenic CDKL5 alterations in girls showing early onset seizures (Weaving et al., 2004).

Many works have tried to understand the relationship between MeCP2 and CDKL5. Mutations in both genes are involved in the genesis of neurodevelopmental and behavioural impairments, whereas the characteristics of the linked-epilepsy are different (Guerrini and Parrini, 2012). Despite that, MeCP2 and CDKL5 are widely co-expressed in the brain and both activated during neuronal maturation (Rusconi et al., 2008). Moreover, it has been demonstrated that CDKL5 can bind and phosphorylate MeCP2 *in vitro*, and that MeCP2 exerts a precise regulation of CDKL5 gene expression (Mari et al., 2005; Bertani et al., 2006). Finally, both proteins can bind DNA methyltransferase I, suggesting a participation to common pathway (Kameshita et al., 2008).

As mentioned, the clinical features in CDD are the early-onset seizures, severe mental retardation and gross motor impairment. In 2010, the diagnostic criteria for atypical RTT were published (Neul et al., 2010) and included five specific diagnostic items: seizures onset before 5 months of age, infantile spasms, refractory myoclonic epilepsy, seizures onset before regression and decreased of typical RTT features. Considering the diverse profiles displayed by RTT and CDKL5, in 2013 it has been proposed to consider the two disorders separately (Fehr et al., 2013).

Despite extensive effort understanding RTT and, recently CDD, how mutations in *MECP2* and *CDKL5* lead to the symptomatology of RTT/CDD is still unknown. Moreover, no effective therapy is currently available for these devastating disorders.

## 1.1.2 MECP2 (gene location and protein structure and function, regulation and mutations in classic RTT)

The methyl-CpG binding protein 2 (*MECP2*; OMIM 300005) gene is located at q28 on the human X chromosome. It is long about 76kb and it is localized on X chromosome antisense strand and has been demonstrated to go through X inactivation in human and mice (D'Esposito et al., 1996). The gene is flanked by Interleukin-1 Receptor Associated Kinase gene (*IRAK1*) and by the Red Opsin gene (*RCP*) (Fig. 2). It was localized for the first time in mouse in 1994, in a region equivalent to region 28 of the human X-chromosome long arm (Quaderi et al., 1994). *MECP2* encodes for the homonym protein (MeCP2), which belongs to a large family of DNA-binding proteins that bind 5-methylcytosine residue in CpG dinucleotides. In 1999, MeCP2 has been identified as clear etiological factor in more than 95% of RTT cases (Amir et al., 1999).

Primary transcript (pre-mRNA) encloses four exon regions (exon 1-2-3-4) and three intronic regions, leading to two main splicing variants; the first encloses the exons 1-3-4 codifying for MeCP2e1 isoform (486 amino acids) (in human MeCP2B), the second one encloses exons 1-2-3-4, but it uses the translation starting codon AUG on exon 2 to encodes the MeCP2e2 isoform (498 amino acids) (in human MeCP2A) (Kriaucionis and Bird, 2004; Mnatzakanian et al., 2004). Region 3'UTR differs in length in the two main transcripts containing multiple polyadenylation sites leading to functional or

not functional transcripts (Kriaucionis and Bird, 2004) (Fig 2) MeCP2B seems to be more prevalent in brain, thymus and lungs (Kriaucionis and Bird, 2004), whereas MeCP2A is highly expressed in fibroblast and lymphoblast (Mnatzakanian et al., 2004). Expression level of *MeCP2* changes during the development, raising higher levels during embryonal development, short post-natal decrease following by an increase during the growth (Shahbazian et al., 2002; Pelka et al., 2005). The functional significance of these temporal fluctuations is still unknown.
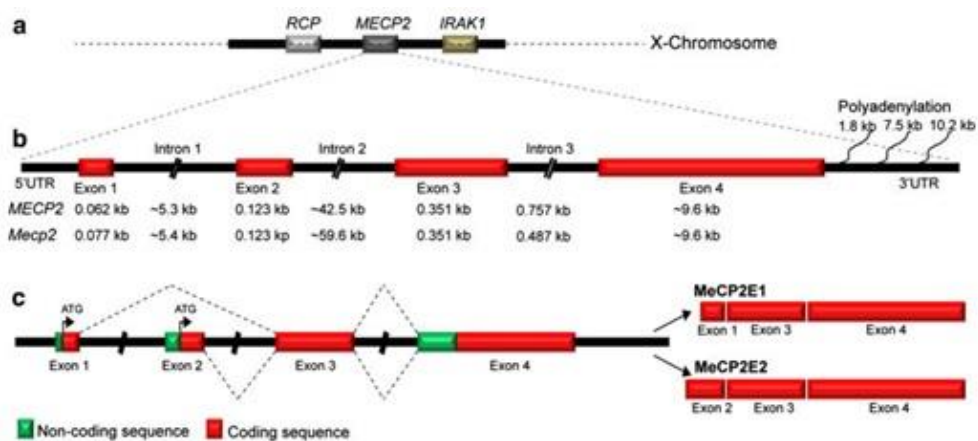


Fig.2: **Methyl-CpG binding protein 2 gene (*MECP2*)**
**(a)** *MECP2* gene is located at q28 on the human X chromosome and is flanked by Interleukin-1 Receptor Associated Kinase gene (*IRAK1*) and by the Red Opsin gene (*RCP*); **(b)** primary transcript of MeCP2 and **(c)** the two splicing variants (Liyanage and Rastegar, 2014)

MeCP2 is a very plenty nuclear protein that weights about 53kDa belonging to Methyl Binding Protein family (Lewis et al., 1992) (Fig.3). MeCP2 was defined as member of protein family of Intrinsically disordered proteins (IDP) as MeCP2 is lacking secondary and tertiary structures (Fig. 4) and like other IDP can interact with a wide variety of complexes and nucleic

11

acids (Adams et al., 2007). The methyl CpG binding domain (MBD), forming by a short α/β tertiary structure, is highly conserved in all proteins of this family and in MeCP2 starts from position 92 to 176. This domain is fundamental for the DNA binding: it recognizes and binds methyl groups on 5' position of CpG cytosines leading to chromatin compacting and transcription repression. Besides MBD, MeCP2 contains a transcriptional repression domain (TRD), which extends from position 215 to 326, and several DNA binding domains in not methylated positions, such as three domains able to bind the DNA in the zones full of AT sequences (A-T hook domains) and two sites of chromatin binding (Fig.4) (Nan et al., 1996; Ghosh et al., 2010; Baker et al., 2013). TRD domain interacts with repressor complexes NCoR/SMRT and Sin3a/HDAC. Inside the TRD there is the Nuclear localization site (NLS), which allows the transport in the nucleus, and one of the AT-hooks.
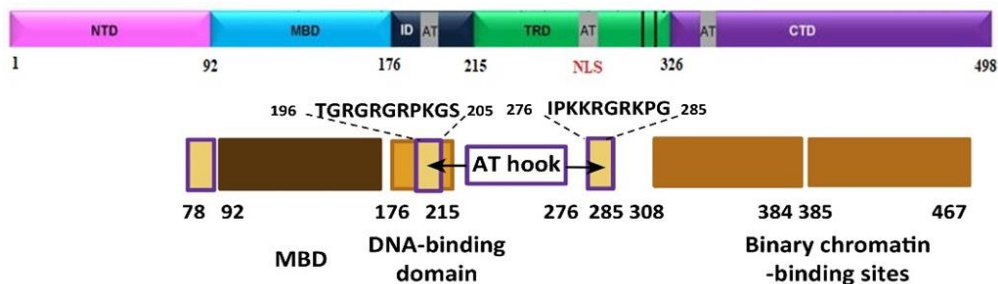


Fig 3: **MeCP2 domains;** MeCP2 is characterized by an aminoacidic sequence (498 amino acids) which are divided in domains. Protein starts with N-terminal domain (NTD; pink) followed by methyl CpG binding domain (MBD; blue), transcriptional repression domain (TRD; green) and C-terminal domain (CTD, purple); DNA binding domains include the AT-Hooks (purple outline) and MDB (in brown and blue). Chromatin interaction domains include the DNA-binding domain (orange) and the Binary chromatin-binding sites (light brown). Modified by (Ausio et al., 2014) and (Rastegar et al., 2009).

MeCP2 binds the NCoR/SMRT complex by TRD terminal residues (285-319), forming the NCoR/SMRT interaction domains (NID). When mutations occurs in this site, the MeCP2 repressor role fails (Lyst et al., 2013). Regarding the Sin3a/HDAC complex, no clear information is available about its interaction with MeCP2. It is known that this complex contributes to MeCP2 repression activity interacting directly with Sin3a-MeCP2 (TRD/CTD) or indirectly through NCoR/SMRT complex and the histone-deacetylases (HDACs) and the histone Methyl transferases (HMTs) (Nan et al., 1998; Samaco and Neul, 2011; Lyst and Bird, 2015).
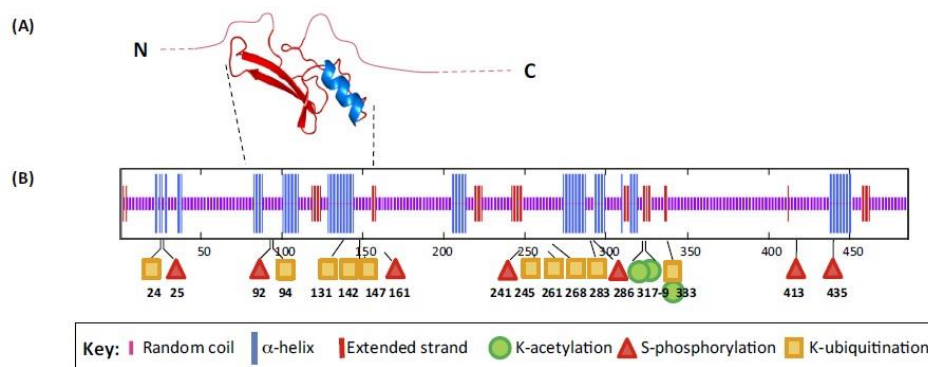


Fig.4: **Secondary and tertiary structure of MeCP2 and Post Translational Mutations (PTM)**

**(A)** Tertiary structure of MDB, obtained by crystallographic studies; **(B)** MeCP2 secondary structures with the possible secondary structures that can be assumed by the protein and the PTMs with the involved aminoacidic residues (modified by Ausio et al., 2014)

MeCP2 was thought to act mainly as transcriptional repression factor, which binds the dinucleotides CpG, leading to further chromatin compacting (Lewis et al., 1992). Subsequent studies have clearly showed that MeCP2 can both activate and repress transcription and can also globally regulate chromatin

remodelling (Horike et al., 2005) (Chahrour et al., 2008) (Fig. 5). MDB domain is able to interact and bind the 5'Methyl Cytosines (5mC) and the 5'-hydroxy Methyl Cytosines (5hmC) (Szulwach et al., 2011). When MeCP2 binds target genes CpG methylated, its TRD domain recruits the corepressor Sin3a, the HDAC 1 and 2 associated with it, and the NCoR/SMRT complex (Heinzel et al., 1997; Nan et al., 1998). The MeCP2 transcriptional repressor activity leads to the chromatin compacting, promoting the nucleosome clustering, both by deacetylation HDAC-mediated and direct interaction between CTD and the chromatin (Nikitina et al., 2007). Moreover, it has been demonstrated a direct interaction between MeCP2 and the nuclear receptor co-repressor (NCoR), which composes the NCoR/SMRT complex. NCoR is a transcriptional repressor which recruits the HDACs and other repressors to down-regulate target genes. It has been demonstrated that MeCP2 stably interacts with NCoR and that TRD mutations could compromise the bind between MeCP2 and the complexes disrupting their repression function on promotors genes MeCP2-regulated (Kokura et al., 2001; Lyst et al., 2013).

Of note, besides the transcriptional repression activity, MeCP2 can acts as transcriptional activator, directly or indirectly. This role needs to be explored deeper: it has been showed an interaction between MeCP2 and the transcriptional repressor CREB1 at the promoter of an activated target but not a repressed target, suggesting a possible transcriptional activator function, but the reason of this interaction remains unclear (Chahrour et al., 2008)(Fig.5).

MeCP2 may also act as splicing regulator. The RNA-binding protein "Y-box-binding protein 1" (YB1), one of the main components of ribonucleoproteins controlling the pre-mRNA in mRNA processing, has been identified as MeCP2 partner. Indeed, when MeCP2 is absent, the splicing of

14

some transcripts results altered leading to transcripts aberrant forms (Young et al., 2005).
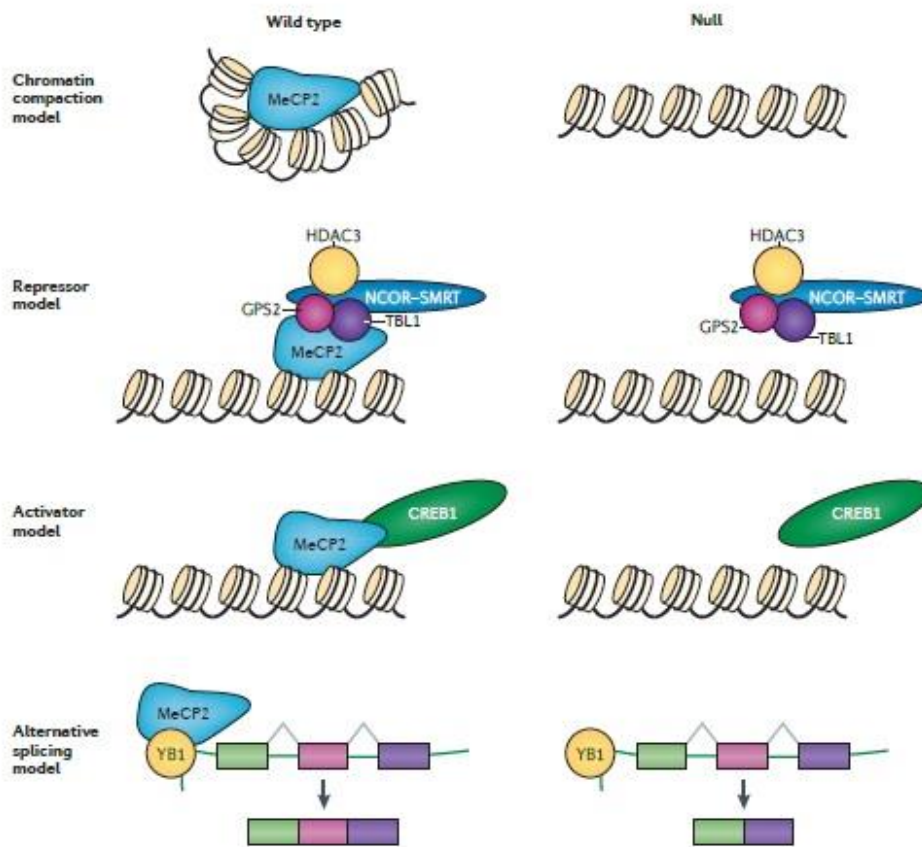


Fig.5: **Different MeCP2 functions (modified by Lyst and Bird, 2015)**

## MeCP2 mutations and RTT mouse model

Several efforts have been made to understand the role of MeCP2 in the brain and in the developing brain. Indeed, many studies on post mortem brain of RTT patients have demonstrated the MeCP2 involvement in the central nervous system (CNS) development and neuronal maturation (Armstrong, 2005) and in dendritic morphology (Armstrong, 2002; Chapleau et al., 2009), signs which contribute to the neuropathology of RTT.

Two research groups demonstrated that one of the MeCP2 targets are the methylated CpG sites near the promoter III region of Bdnf in rats and near the promoter IV region of Bdnf in mice (Chen et al., 2003; Martinowich et al., 2003) suggesting that the *Bdnf* gene is under MeCP2 transcriptional control. BDNF is a member of the neurotophin family of growth factors having critical roles in neuronal survival and differentiation in early development and in modulation of synaptic plasticity in adult brain.

As mentioned above, MeCP2 mutations have been documented in more than 95% of RTT cases and in the recent years more than 2000 pathogenic mutations have been reported in females with RTT (Amir et al., 1999; Weaving et al., 2005; Lyst and Bird, 2015) among which:

- 8 mutations, among missense and nonsense, finding in 70% of RTT patients:
- Total or partial deletion of the CTD, in about 10% of RTT cases;
- Complex gene rearrangements finding in 6% of the patients.

Using genotype-phenotype correlation studies, it has been showed that mutations involving the NLS and nonsense mutations (creators of premature

STOP codon) lead to more severe phenotype compared to the phenotype derived from mutation on CTD (Calfa et al., 2011).
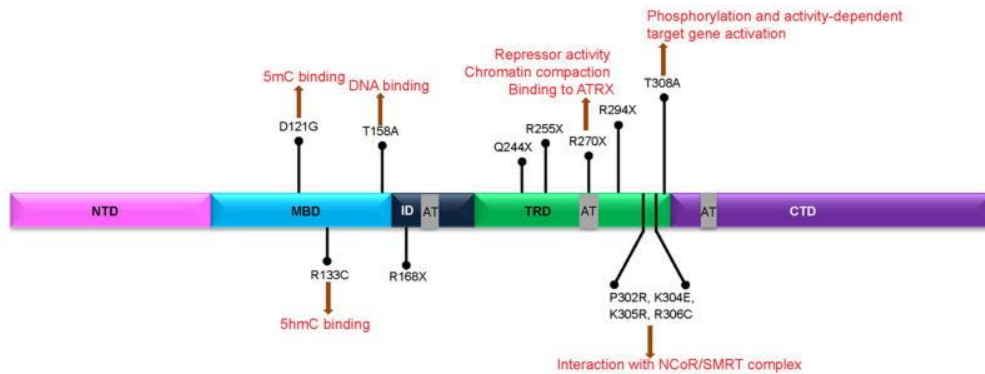


Fig. 6: **Main mutations occurring in the MeCP2 (Liyanage and Rastegar, 2014)**

Mutations on MDB and the TRD determine a very severe phenotype , because they affect the DNA binding and the correct recruitment of repressor factors (Ebert et al., 2013; Lyst et al., 2013) (Fig. 6-7). In particular, three important missense mutations on residues R106, R133 and T158 are found on MBD, compromising MeCP2 primary function and destabilizing the methylated DNA binding (Kucukkal et al., 2015). The fourth missense mutation is on R306 residue, in the TRD, which destabilizes DNA binding thus not allowing NCoR/SMRT binding. (Lyst and Bird, 2015). C-terminal deletions lead to less severe phenotype because they eliminate only the phosphorylation site S421, important for protein regulation and turnover, maintaining the principal functions (Thambirajah et al., 2009). The patients display all RTT symptomatology but with a less severe phenotype (Bebbington et al., 2010). In addition, Arg270X mutation on TRD resulting in a truncated protein is associated with increased mortality (Cuddapah et al., 2014).

a Co-repressor recruitment or bridge model    b Chromatin compaction model

Wild type

R306C

R270X

R106
R133
R158
MBD mutant

○ NID or basic patch  ⬯ MBD  AT-hook  ✿ Mutation
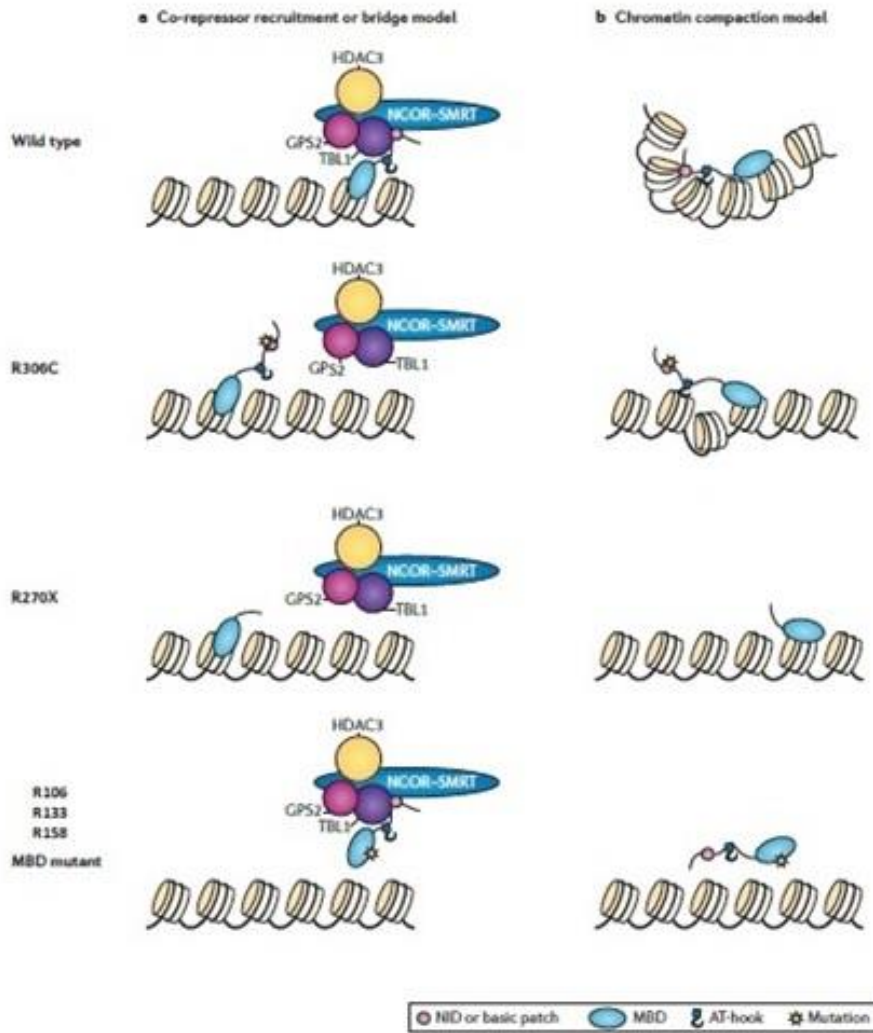
Fig.7: **Different MeCP2 mutations lead to different complexes or DNA binding impairments (modified by Lyst and Bird, 2015)**

The discovery of a monogenic origin for classical RTT (Amir et al., 1999), initially led to the creation of mice models carrying mutations in the *Mecp2* gene. The first RTT mouse was the MeCP2-*null* and was described in 2001 (Chen et al., 2001; Guy et al., 2001). In the case of Guy et al., their mouse model lacks exons 3 and 4 (hemizygous males; -/Y), leading to MeCP2 block

18

expression in whole organism (MeCP2Bird). Chen et al. generated a full knockout (KO) by the targeting deletion of exon 3 (MeCP2Jae), a conditional KO in which embryonic MeCP2 expression was blocked only in the brain (CNS KO) and a conditional KO in which MeCP2 expression was blocked only in the postmitotic neurons in the forebrain (Forebrain KO). All models displayed the same pathological traits similar to RTT patients. Heterozygous Female MeCP2-*null* mice (MeCP2 +/-) show the same alterations but with a later stage of onset. Subsequently, considering that MeCP2 mutations can occur in the C-terminal too, a model bears a truncating mutation on the gene exon 4, leading to the expression of a protein truncated at amino acid 308, was created (MeCP2-308) (Shahbazian et al., 2002). This model appears associated with a milder phenotype and prolonged life-span in comparison with KO mice.

## 1.1.3 CDKL5 (gene location and protein structure and function, mutations in patients)

The cyclin-dependent kinase-like 5 gene (CDKL5), is located on the X-chromosome in the Xp22 region and was identified in 1998 and initially called Serine threonine Kinase 9 (STK9)(Montini et al., 1998) Mutations on *CDKL5* have been associated with a form of epileptic encephalopathy classified as early infantile epileptic encephalopathy 2. The human *CDKL5* gene is long about 240kb, composed of 24 exons: exons 1, 1a and 1b are untranslated, whereas the coding sequence are contained within exons 2-21. Moreover, *CDKL5* is characterized by different isoforms and splicing variants (Kalscheuer et al., 2003; Williamson et al., 2012). The 107 kDa isoform (CDKL5$_{107}$) is the predominant isoform in human and in mouse brain, suggesting it to be of primary pathogenic importance for CDD (Williamson et al., 2012). CDKL5 protein contains a serine/threonine kinase domain in its N-terminal and belongs to a large superfamily of homologous proteins which conserve the kinase domain of 250-300 amino acids. Mutations in this gene were found in epileptic patients and in 2003 Dr. Vera Kalscheuer suggested *STK9* as the etiological key of X-linked infantile spasm (Kalscheuer et al., 2003), a pathology characterized by early onset seizures and mental retardation (symptoms of the CDD) and caused in the most of cases by mutation in the aristaless-related homebox gene (*ARX*), located on the Xp21.3-p22.1 (same *CDKL5* region).

The CDKL5 belongs to the CMGC family of serine-threonine kinases (cyclin-dependent kinases (**C**DKs), mitogen-activated protein kinases (**M**APK), glycogen synthase kinases (**G**SK) and **C**DK-like kinases) characterized by a N-terminal catalytic domain (amino acid 13-297). This catalytic domain contains the ATP-binding region (amino acid 14-47), the

20

serine-threonine kinase active site (amino acid 127-144) and a Thr-Xaa-Tyr motif (TEY) (amino acid 169-171), site of a possible auto phosphorylation (Bertani et al., 2006). Unlike other protein of its family, CDKL5 has an unusual long C-terminal tail of more than 600 amino acids containing signals for nuclear import (NLS) and export (NES), which could be involved in the cellular localization of protein and either the catalytic activity (Bertani et al., 2006; Rusconi et al., 2008) (Fig.8).
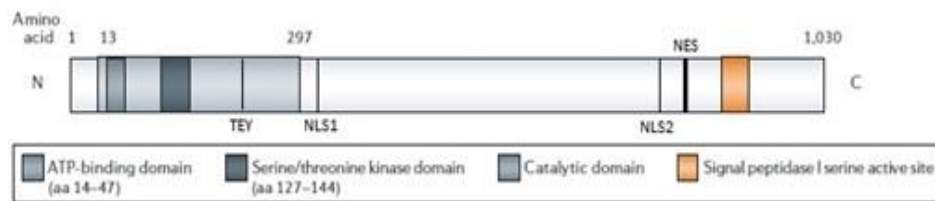


Fig.8: **Schematic representation of CDKL5 (Bienvenu and Chelly, 2006)**

CDKL5 function seems to be critical in the CNS by regulating different molecular pathways, involving the synaptic function, structure and plasticity. Unfortunately, the lack of mouse model for *Cdkl5* functions does not allowed to clarify the fair situations. Despite all, many studies tried to explain the real role of CDKL5, adding year by year several pieces. The CDKL5 protein shuttles between cytoplasm and nucleus, where exerts different functions (Fig.9).

Using RNA interference (RNAi) to downregulate CDKL5 in cultured cortical rat neurons, Cdkl5 has been demonstrated to be critically involved in the regulation of neuronal morphogenesis through mechanisms involving Rac1 (Chen et al., 2010) (Fig.9), a protein belonging to the Rho GTPase family, a group of low-molecular-weight guanine nucleotide binding proteins with a well-established role as regulators of actin cytoskeleton dynamics (Etienne-

21

Manneville and Hall, 2002) leading to formation and maturation of neuronal spines (Tolias et al., 2011). The loss of Cdkl5 influences mice neuronal morphogenesis by deregulating BDNF-Rac1 signalling pathway (Chen et al., 2010), suggesting that Cdkl5 has a role in the maintaining of the neuronal function during life. Recently, different authors have reported that Cdkl5 phosphorylates amphiphyn 1 (AMPH1), brain specific protein involved in neuronal transmission (Sekiguchi et al., 2013) exclusively at Ser[293]. This phosphorylation does not occur if a mutation is present in the CDKL5 catalytic domain. Interestingly , mice lacking AMPH1 display severe cognitive deficits and seizures, suggesting its involvement in the CDD pathogenesis (Sekiguchi et al., 2013).

*Possible link between Cdkl5 and MeCP2*

Link between MeCP2 and Cdkl5 has been described *in vitro* (Mari et al., 2005; Bertani et al., 2006), suggesting a possible link between RTT and CDD. However, considering that Cckl5-mediated MeCP2 phosphorylation is weak (Kameshita et al., 2008), is not plausible that MeCP2 and Cdkl5 linked-activities are due to only this phosphorylation. Indeed, it is well known that DNA methyltransferase 1 (DNMT1) and netrin-G1 ligand (NGL-1) are phosphorylated by Cdkl5 (Kameshita et al., 2008) (Fig.9): DNMT1 has the function to maintain the DNA CpG methylations after the replication and it is well known its interaction with MeCP2 suggesting Cdkl5 critical role in controlling gene expression (Kameshita et al., 2008); NGL-1 is involved in synapse formation and maturation, indirectly suggesting Cdkl5 involvement in spine and synapses development (Ricciardi et al., 2012).

22
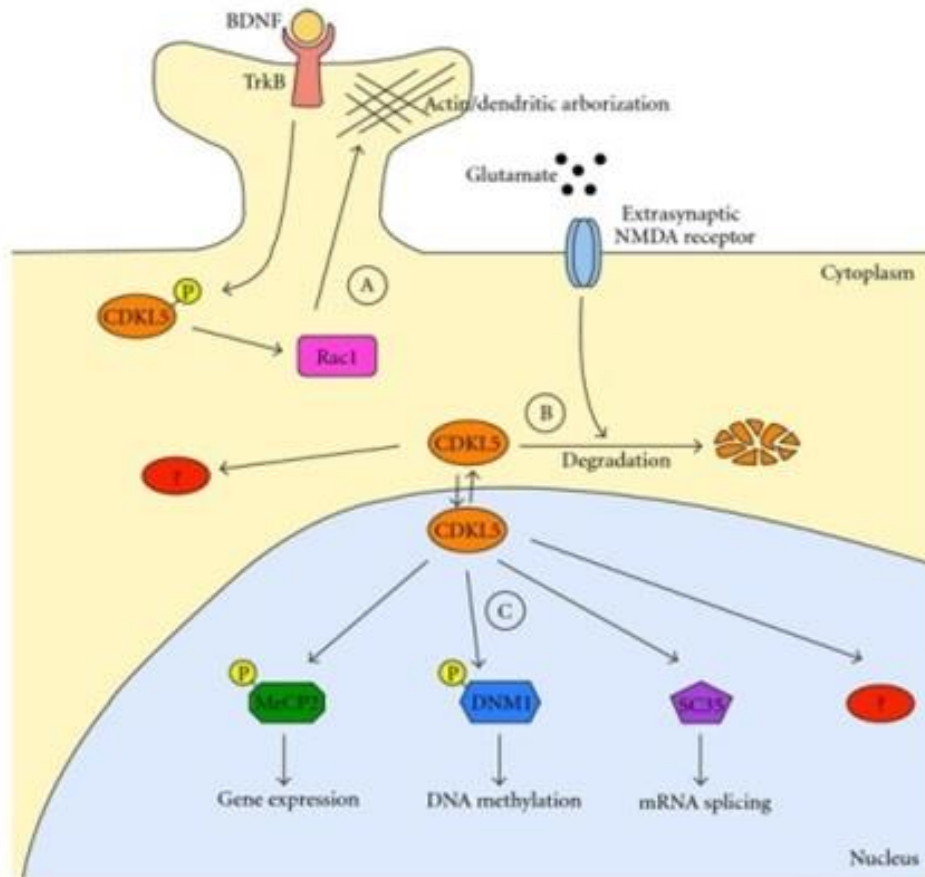
Fig. 9: **CDKL5 functions in cytoplasmatic and nuclear environment**

(A) in the cytoplasm CDKL5 regulates actin cytoskeleton and dendritic arborisation, using the interaction with Rac1; (B) degradation is the pathway to regulate levels of CDKL5 in the cytoplasmic compartment; (C) in the nucleus, CDKL5 regulates epigenetic events by interacting with MeCP2 and DNMT1 (Kilstrup-Nielsen et al., 2012)

## Pathogenic CDKL5 mutations and CDD mouse models

As in RTT, in CDD is present a relationship between CDKL5 mutations and phenotype showed. All reported cases of CDD are sporadic. From the first

23

CDKL5 identified mutation (Kalscheuer et al., 2003), a wide range of pathogenic mutations have been described, reaching over a hundred of CCD patients types (Fig.10).
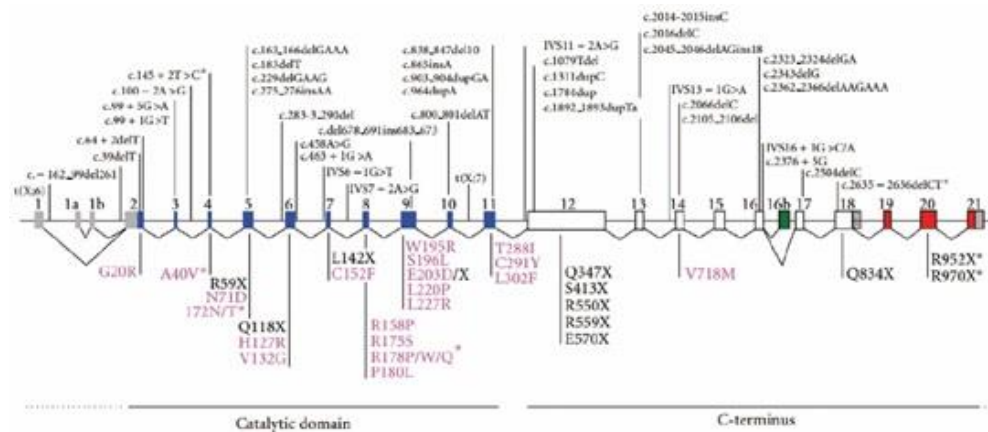


Fig.10: **Pathogenic CDKL5 mutations**

Mutations can involve the catalytic domain (the blue exons) or the C-terminal region (the white exons). The green and the red parts show different versions of the protein (isoforms). Mutations reported on the upper part of the figure represent deletions or frameshift mutations, whereas in fuchsia and black respectively are reported below the gene and represent the missense and nonsense mutations (Kilstrup-Nielsen et al., 2012).

These mutations include missense and nonsense mutations, deletions, frameshifts and aberrant splicing. Missense mutations re localized in the N-terminal domain, compromising the kinase activity of CDKL5. These kinds of mutations are associated with a more severe phenotype. On the contrary, patients bearing missense mutations on the ATP binding site display less severe symptomatology. Conversely, truncating mutations can occur anywhere on the gene. Many pathogenic alterations involve the C-terminal part of the

gene: stop-codons mutations in the C-terminal lead to a milder clinical picture compared to mutations in the catalytic domain (Bahi-Buisson et al., 2012).

To understand the mechanisms at the disorder basis, two mouse models have been generated. The first Cdkl5 KO mouse models a mutation site found in CDD and was generated in 2012 (Wang et al., 2012), deleting *Cdkl5* exon 6. This mutation generates a premature termination codon causing an early truncation of Cdkl5 in its N-terminal kinase domain, disrupting its functionality. As in RTT, the deriving genotypes are: homozygous females (-/-), heterozygous females (+/-) and hemizygous males (-/Y), which are until now, the most used. These mice displayed most of the symptomatology described in CDD patients, such as motor defects, sociability deficits, cognitive dysfunction. At the same time, another Cdkl5 KO mouse model was created by germline deletions of exon 4 of a Cdkl5 conditional KO allele produced by standard gene targeting in embryonic stem cells (Amendola et al., 2014) and displayed a wide range of CDD symptoms.

## 1.2 Serotoninergic system in neuropsychiatric disorders

### 1.2.1 General background

5-hydroxytryptamine (5-HT) or Serotonin is a monoamine neurotransmitter, conserved in many species (Marston et al., 2011), which it is found in many tissues: 95% of the body's serotonin is produced in the enterochromaffin (EC) cell, in the digestive tract (Gershon, 2004). In the CNS, serotonin synthesising cells are found in the dorsal and median raphe nuclei of the brain stem, giving rise to descending and ascending projections to every part of the brain (Fig. 11).
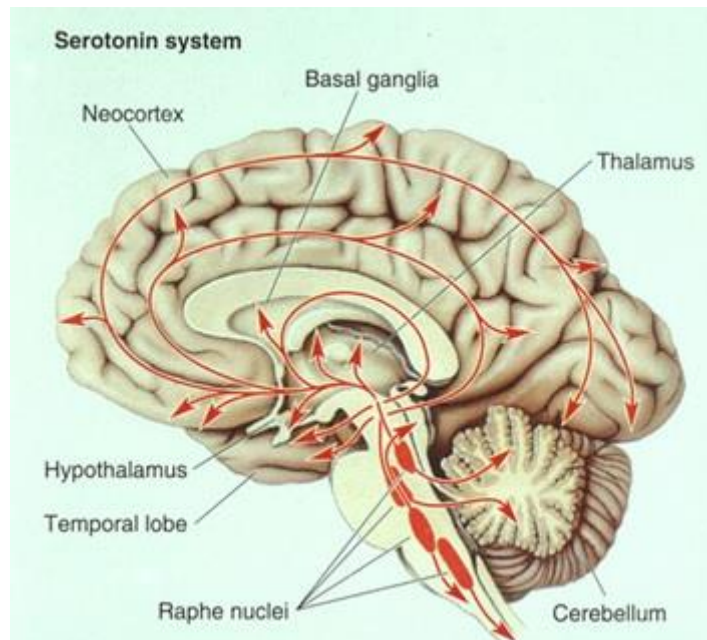


Fig. 11: **The neurons of the raphe nuclei are the main source of 5-HT in the brain, projecting to every part of the brain**

Serotonin is synthetized from tryptophan, which is introduced by diet in the organism (Fig. 12). The L-Tryptophan is converted to 5-hydroxy-L-Tryptophan (5-HTP) by tryptophan 5-hydroxylase (Tph). The two isoforms of the enzyme, Tph1 and Tph2, are located respectively in the EC cells and in the central and enteric neurons (Yu et al., 1999; Walther et al., 2003). The final step is the conversion of 5-HTP to serotonin by aromatic L-amino acid decarboxylase (Fig.11). Once formed, serotonin gets transported into vesicles by vesicular monoamine transporter (VMAT), which will release it via exocytosis into the synaptic cleft where serotonin can bind its receptors (Fig. 13). Serotonin receptors are divided into seven major classes ($5\text{-HT}_1$ to $5\text{-HT}_7$), which have multiple subtypes (e.g. $5\text{-HT}_{2A}$, $5\text{-HT}_{2B}$, and $5\text{-HT}_{2C}$). Except for $5\text{-HT}_3$, which is a ligand-gated ion-channel, the 5-HT receptors are G-protein-coupled, with signal transduction mediated by either stimulation or inhibition of cAMP synthesis (Gray and Roth, 2001). When the serotonin exerted its function in the synaptic cleft, the residual content goes through a reuptake process by $Na^+/Cl^-$ dependent transporter called Serotonin Reuptake Transporter (SERT) (Fuller and Wong, 1990). Moreover, serotonin can be degraded primarily by monoamine oxidase A ($MAO_A$) into 5-hydroxyindolacetic acid (5-HIAA) or metabolized into melatonin (Fig.12).

Dysfunction in serotoninergic system has been implicated in many neuropsychiatric conditions, as schizophrenia, major depression disorder, anxiety disorders, Alzheimer's and Parkinson's disease (Geldenhuys and Van der Schyf, 2011; Maron et al., 2012; Eggers, 2013; Andrews et al., 2015; Politis and Niccolini, 2015).
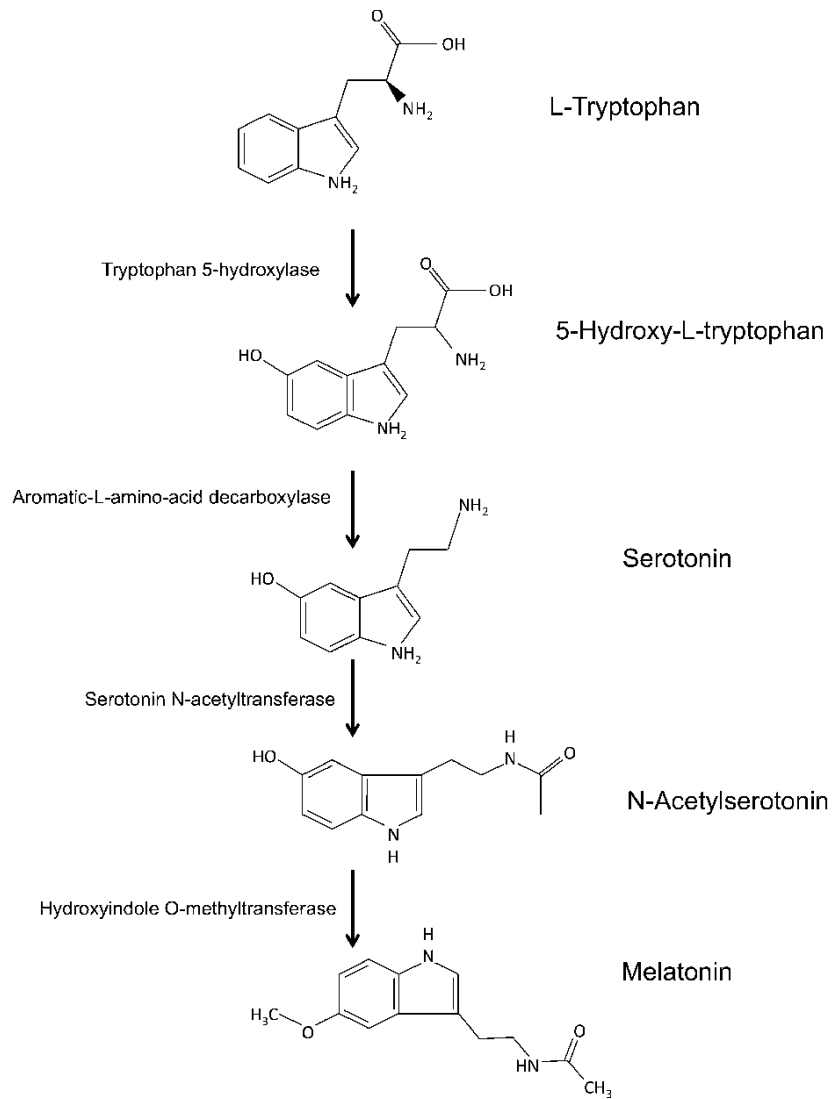
Fig. 12: **Serotonin synthesis from diet-introduced L-tryptophan** (Fidalgo et al., 2013)
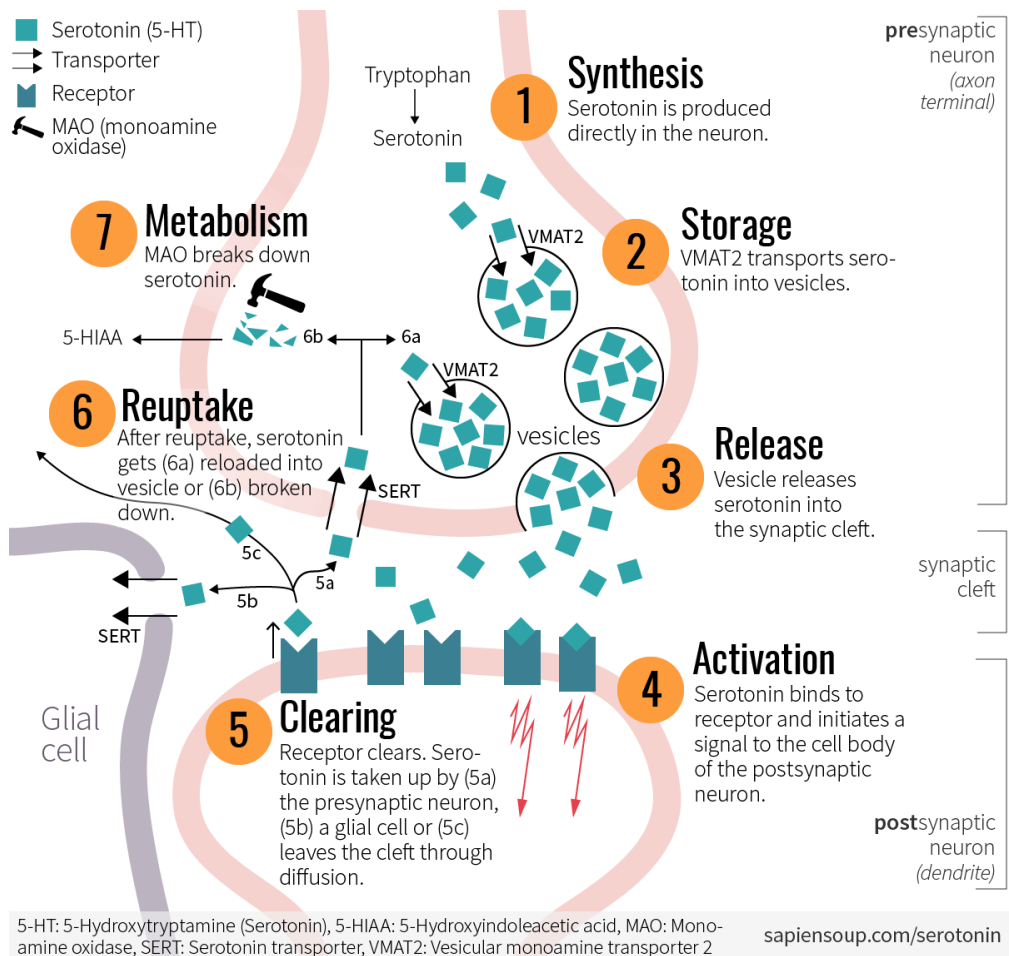
Fig. 13: **Representative scheme of the serotonin functions, from synthesis to metabolism.**

## 1.2.2 Serotonin receptor 7 (5-HT$_7$R): an innovative therapeutic target for RTT

Among the seven serotonin receptors family, the 5-HT$_7$R is one of the most recently discovered (Bard et al., 1993). The 5-HT$_7$R gene is located on human chromosome 10q23.3 – q24.3 and encodes for a protein of 445 amino acids (Bard et al., 1993). This receptor belongs to the family of G-protein coupled receptors (GPCRs), the largest and most diverse superfamily of transmembrane receptors, functioning as signal-transducer by translating extracellular stimuli into intracellular responses resulting in multiple physiological and pathophysiological responses (Thompson et al., 2008). All GPCRs contain an extracellular amino-terminus, seven membrane spanning α-helices and an intracellular carboxyl-terminus. The 5-HT$_7$R exerts this its function by two different signalling pathways. The canonical is the activation of Gs-protein which can activate different adenylyl cyclase (AC) isoforms (Shen et al., 1993). This activation leads to cAMP production which in turn activates protein kinase A (PKA), which induces phosphorylation of different target proteins. In this way, 5-HT$_7$R stimulation, will activates the neuroprotective extracellular signal-regulated kinases (ERK1/2) and Akt (protein kinase B) pathways (Errico et al., 2001; Johnson-Farley et al., 2005), involved in cytoskeleton formation and in gene transcription (Fig. 14). The secondary pathway concerns the activation of the Gα$_{12}$- protein, of which members of Rho GTPases (Rho, Rac and Cdc42) are the main downstream effectors. It has been demonstrated that Rho GTPase positive stimulation leads to activate gene transcription via transcription factor serum response factor (SRF) and to stimulate neurite outgrowth and synaptogenesis (Kvachnina et al., 2005; Kobe et al., 2012; Speranza et al., 2013) (Fig.14).

30
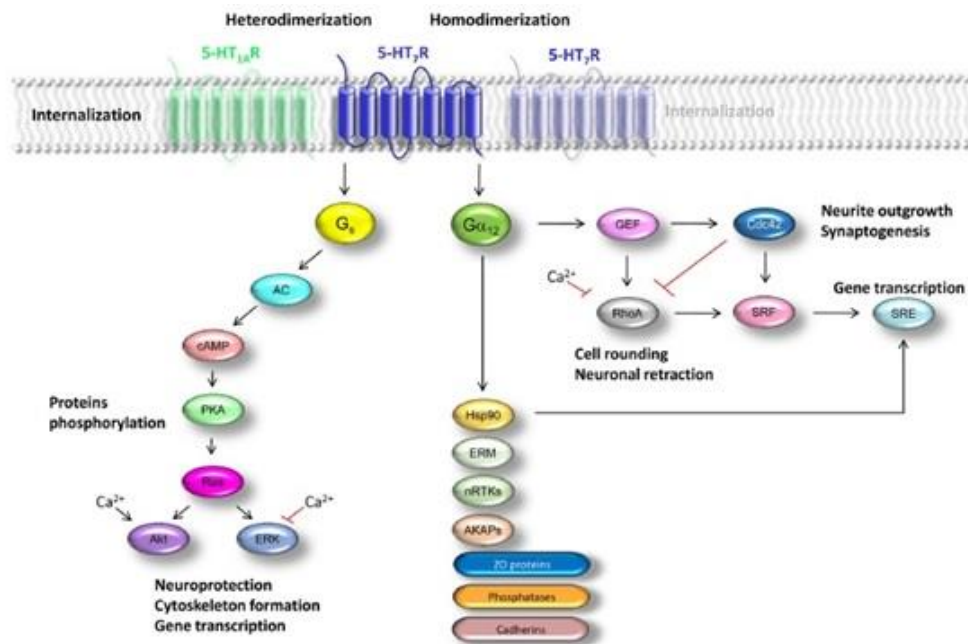
Fig. 14: **Schematic representation of signalling pathways regulated by the 5-HT₇R.** On the left part of the picture are represented effects mediated by Gs-protein. On the right part, are represented the effects mediated by Gα12- protein. Abbreviations: AC-Adenylyl cyclase; cAMP-cyclic adenosine monophosphate; PKA-protein kinase A; ERK-Extracellular signal-regulated kinases; Akt-Protein kinase B; Hsp90-Heat shot shock protein 90; GEF-Guanine nucleotide exchange factor; SRF-Serum response factor; SRE-Serum response element (Guseva et al., 2014).

The 5-HT₇R is widely express in all CNS (Hedlund and Sutcliffe, 2004) and it has been demonstrated its important role in the control of many physiological functions, such as circadian rhythms, thermoregulation, learning and memory, and its involvement in psychiatric disorders, such as Alzheimer's disease, depression, schizophrenia, anxiety, cognitive disturbances and pain (reviewed in Gellynck et al., 2013).

# 1.3 Endocannabinoid system in neuropsychiatric disorders

## 1.3.1 General background

The endocannabinoid system (ECS) is a complex neuromodulator system found in all vertebrate classes, involved in the regulation of numerous physiological functions (Kano et al., 2009). This "machine" is driven by endocannabinoids (eCBs), lipid mediators derived from arachidonic acid. The complexity of the system is due to the presence of many receptors, mediators and enzymes, which make this field not yet fully explored. Cannabinoid receptor type 1 (CB1), encoded by *CNR1,* was the first discovered guanine-nucleotide-binding-protein (G protein)-coupled receptor (GPCR) of the ECS (Devane et al., 1988). As the most of the GPCR, CB1 is formed by 473 amino acids, possessing seven transmembrane domains connected by three extracellular and three intracellular loops, an extracellular N-terminal tail, and an intracellular C-terminal tail (Shao et al., 2016). The second canonical ECS receptor is the CB2, encoded by *CNR2,* discovered for the first time in the immune cells (Munro et al., 1993), is formed by 360 amino acids and possesses the common structure of the GPCRs. The discoveries of these two receptors was due to the studies on the $\Delta^9$ – tetrahydrocannabinol (THC), the active principle of *Cannabis sativa,* which is fully and/or partial agonist of CB1 and CB2 receptors, gifted of psychostimulant effects on CNS, identified by (Gaoni and Mechoulam, 1964). Despite CB1 receptors are the most abundant receptors in the mammalian brain (Matsuda et al., 1990), they are also present in the peripheral tissues (Pagotto et al., 2006). CB2 are expressed mainly in the immune system cells, but recently was found to be present also in the brain and in the peripheral tissue (Gong et al., 2006; Juan-Pico et al., 2006; Ofek et al.,

2006). CB1 and CB2 couple with G protein type $G_{i/o}$ and their stimulation can activate mitogen activated protein kinases (MAPK), such as extracellular signal regulate kinase 1 and 2 (ERK1/2), and inhibit adelite cyclase (AC) and PKA signalling (Dalton et al., 2009).

The presence of these two receptors in the organisms suggested the existence of endogenous ligands, the endocannabinoids (eCBs). Starting from nineties, until now, the most active eCBs are Anandamide (arachidonoylethanolamide; AEA) and 2-arachidonoylglycerol (2-AG), which can mimic the action of $\Delta^9$ – tetrahydrocannabinol (THC), in several biological processes. eCBs, together with enzymes involved in their meta- and catabolism, and the two receptors, they form the ECS (Fig.15). eCBs are released "on demand" when intracellular $Ca^{2+}$ concentration is elevated through the action of different enzymes, actors of the ECS itself: N-acyl phosphatidylethanolamine-specific phospholipase D (NAPE-PLD), the main synthesizing enzyme of AEA (Okamoto et al., 2004) and diacylglycerol lipase (DAGL), responsible of 2-AG synthesis (Bisogno et al., 2003). Regarding the catabolism of eCBs, mainly two enzymes degraded AEA and 2-AG, Fatty acid amide hydrolase (FAAH)(Cravatt et al., 1996) and Monoacylglycerol lipase (MAGL)(Dinh et al., 2002) respectively (Fig. 15).

Recently, many works have provided evidences for the existence of additional receptors forming the ECS. The new receptors are: transient receptor potential (TRP) channels and G-coupled protein receptor GPR55, the leading candidate for the CB3 receptor name, receptors which can be bound by AEA and/or 2-AG.
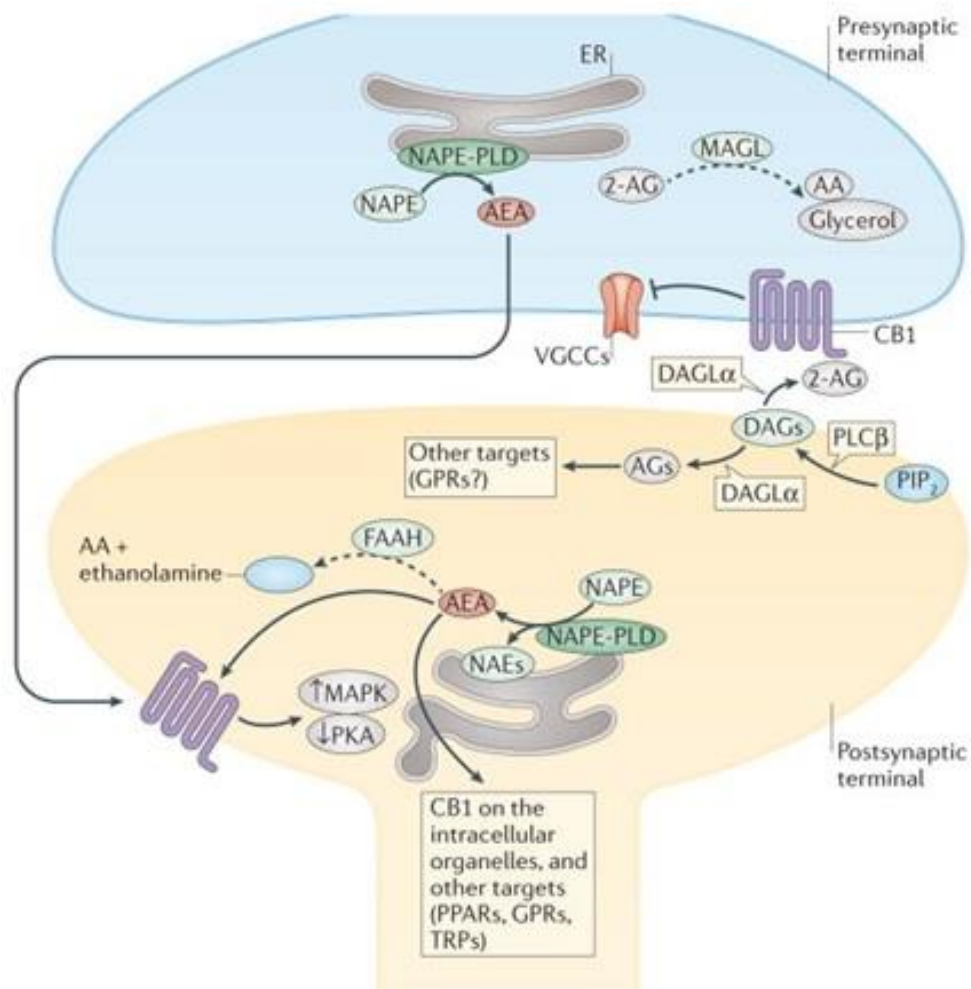
Fig. 15: **Schematic representation of the ECS**; eCBs derived from the arachidonic acid (AA). Anandamide (AEA) is produced from the hydrolysis of the corresponding N-acyl-phosphatidyl-ethanolamine (NAPE) by NAPE selective phospholipase D (NAPE-PLD) enzyme. After completing its task, it goes to degradation process mediated by fatty acid amide hydrolase 1 (FAAH). 2-Arachidonoyl-ethanolamine (2-AG) is produced from the hydrolysis of diacylglycerols (DAGs) by diacylglycerols-lipases (DAGL). 2-AG degradation process seems to be catalysed by monoacylglycerol lipase (MAGL). Solid arrows: transformation in active metabolites; dashed arrows: transformation in inactive metabolites. Abbreviation: AA, arachidonic

34

acids; AGs, 2-acylglycerols; DAGs, diacylglycerols, ER, endoplasmic reticulum; GPRs, orphan G-protein-coupled receptors; MAPK, mitogen-activated protein kinases; PIP2, phosphoinositide bisphosphate; PKA, protein kinase A; PLCβ, phospholipase Cβ; PPARs, peroxisome proliferator-activated receptors; TRPs, transient receptor potential channels; VGCCs, voltage-gated calcium channels (Di Marzo et al., 2015).

In the recent years, evidence of ECS involvement in numerous behavioural and physiological processes is constantly increasing. Moreover, ECS deregulation has been associated with many neuropsychiatric disorders particularly in affective disturbances such as anxiety and depression (Micale et al., 2013; Jenniches et al., 2016), mental disorder such as schizophrenia (Leweke et al., 2012; Clarke et al., 2017), neurodegenerative disorders associated with cognitive and motor dysfunctions such as Alzheimer's disease, Huntington's disease and Parkinson's disease (Dowie et al., 2009; Pisani et al., 2011; Maroof et al., 2014) and Autism Spectrum disorder (Chakrabarti et al., 2015; Servadio et al., 2016). Moreover, many of the symptoms correlated with the pathologies above mentioned, had been improved modulating the eCBs. Modulation can run through enzymes inhibitors or molecules directly acting on eCBs receptors; regarding FAAH inhibitors, in rodents, daily orally administered of ST4070, decreased anxious behaviour measured in elevated plus-maze and in the light/dark test (Marco et al., 2015) and still in rodents, once daily dose of URB597 elicits antidepressant effects, in chronically stressed animals (Bortolato et al., 2007); moreover, CB2 receptor agonist JWH-133 was tested in a genetic mouse model of Alzheimer's in which induced cognitive improvement (Aso et al., 2013). Of note, pathologies cited above have in common many symptoms characterizing RTT and detectable in available mouse models (Ricceri et al., 2013; De Filippis et al., 2014).

35

### 1.3.2 *Cannabis sativa* extracts as innovative therapeutic approaches

In the last twenty years, *Cannabis sativa* has been the subject of many debates, regarding its use as medical treatment, especially due to the psychotropic effect exerts on CNS. In 1964 THC, the main compound of *Cannabis*, was isolated from hashish (Gaoni and Mechoulam, 1964). Most THC psychotropic effects are mediated through agonistic actions at the cannabinoid receptors, especially CB1, which activation lead to the cascade events mentioned before. Pioneering studies tested THC treatment in order to increase the ECS response and ameliorates pathology symptoms (e.g. anxiety) (Berrendero and Maldonado, 2002). However, CB1 agonists may cause psychotropic side effects, like those reported with cannabis use in the recreational area. To avoid these undesirable effects, most recent preclinical studies focussed on the identification of molecules that modulates the ECS without the psychotropic effects of THC. The focus has shifted on non-psychotropic molecules contained in *Cannabis*; despite more of 120 substances, until now, few non-psychotropic phitocannabinoids (phCBs) had been tested as novel drugs (Morales et al., 2017). These phCBs are contained in *cannabis* in different percentages depending on the growing conditions, location and plant variety or chemotype. The most abundant phCBs in the plant are THC, cannabinol (CBN), cannabidiol (CBD), cannabigerol (CBG), cannabichromene (CBC), tetrahydrocannabivarin (THCV), cannabidivarin (CBDV) (Fig. 16)
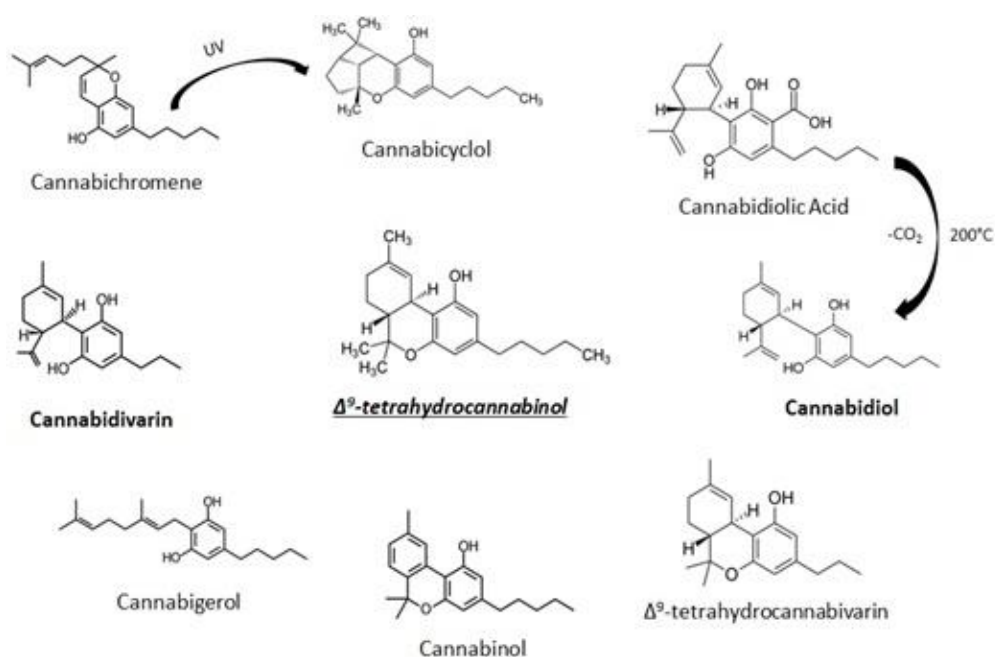
Fig. 16: **Most studied phytocannabinoids (phCBs)**

These compounds exerts multiple actions trough mechanisms which are only partially related to modulation of the ECS (Pertwee, 2008). Indeed, several studies elucidate the ability of phCBs to exerts pharmacological effects via different pathways such as TRP channels (De Petrocellis et al., 2008), peroxisome proliferator-activated receptor γ (PPARγ) (Vallee et al., 2017), GPR55 (Ryberg et al., 2007; Vigli et al., 2018), 5-HT$_{1A}$ (Espejo-Porras et al., 2013), the adenosine membrane transporter phospholipase A$_2$ (Evans et al., 1987), modulation of Ca$^{2+}$homeostasis (Drysdale et al., 2006; Ryan et al., 2009), often displaying weak affinity and/or real CB1 and CB2 antagonism (Thomas et al., 2005; Thomas et al., 2007).

Among the available phCBs, CBD has been more deeply studied. Several works highlighted the efficacy of CBD, in the treatment of muscular spasms and rigidity, combining it in 1:1 ratio with THC (GW pharmaceutical

Sativex is the first drug FDA approved for the symptomatologic treatment of Multiple Sclerosis) (Di Marzo, 2011), epilepsy (Gw pharmaceutical Epidiolex drug FDA approved for epilepsy treatment) (Gobira et al., 2015; Devinsky et al., 2018), mood disorders (Linge et al., 2016) and Alzheimer's disease (Cheng et al., 2014a; Cheng et al., 2014b); because of its numerous and different application diseases, the interest for CBD is constantly increasing. Interestingly CBD shows weak affinity for CB1 and CB2 receptors, but antagonistic properties on GPR55 receptor and agonistic properties on TRPV1 receptors in mice and rats (De Petrocellis et al., 2008; Iannotti et al., 2014; Kaplan et al., 2017).

## 1.4 Current pharmacological approaches for the treatment of Rett Syndrome and CDKL5 Deficiency Disorder

Despite numerous efforts have been made studying RTT and CDD etiopathogenesis, no cure for these disorders is available. In both the diseases, medical management is essentially symptomatic and supportive, also including psychosocial support for the families. Regarding RTT, there are many evidences/projections predicting that RTT patients will live into adult life. These data make it clear that it will be needed to plan an accurate therapeutic plan for RTT girls (Kirby et al., 2010). As we just mentioned, RTT patients, besides the severe mental retardation, suffer of many disturbs leading to a wide variety of symptoms.

Sleep is often disrupted in RTT girls, which can have difficult falling to sleep or frequent awakenings during night (Piazza et al., 1990). The causes of the disturb and be multiple. Indeed, gastrointestinal dysfunctions, such as constipation or gastroesophageal reflux disease (GERD), causing pain, are another of the disturbs present in RTT and it should be considered as causes of sleep disturbances. Sleep disturbances are treated using Trazodone, a serotonin receptor modulator, which is safe to initiate sleep. Moreover Melatonin, last metabolism product of serotonin (see 1.2.1) which is important to maintain circadian cycles, has been shown to be effective in the initial phase of sleep of RTT patients, increasing their sleep duration (McArthur and Budden, 1998). Beneficial effects for sleep maintenance have been showed using L-carnitine, amino acid required for energy metabolism (Ellaway et al., 2001). Instead, for the gastrointestinal dysfunctions, several drugs can be used in RTT. Laxatives (polyethylene glycol 3350 and magnesium hydroxide) can be used to treat and prevents constipation. For the GERD, which may cause pain due to

oesophageal mucosal damage, can be treated with antiacids (calcium carbonate) and proton-pump-inhibitor (PPIs).

RTT patients, due to lack of ambulation and inadequate diet, are victims of very frequent bone fractures and reduced bone mass. Osteopenia, the reduced bone mineralization, could be caused by low levels of vitamin D which was reported in RTT patients (Roende et al., 2011). When vitamin D is lacking, supplementation with diet is required. Moreover, to treat this disturb, bisphosphonates could be used to inhibit bone resorption and increasing the density of mineralized bone. However, these drugs have many side effects, including osteonecrosis and gastrointestinal pain.

Cardiac dysfunction and breathing abnormalities, are two characteristics symptoms in RTT. Cardiac prolonged QT interval, a delay of timing between ventricle depolarization and repolarization, is a prominent feature in RTT patients, which can increase the risk of sudden death, one of the problems reported in RTT (Sekul et al., 1994). For the management of this disturb, beta-blockers are recommended, but further studies are needed to clarify the real efficacy in RTT. The breathing dysfunctions, such as apnoea, hypoxia, hyperventilation, could be correlated with the prolonged QT interval and the cardiac disturbs. Unfortunately, no treatments for breathing irregularities was effective yet in RTT patients.

Majority of RTT individuals have some type of seizure disorder. Many options are available to alleviate seizures episodes, such as valproate, lamotrigine, carbamazepine. Levetiracetam is useful in RTT cases suffer of drug-resistant seizures (Specchio et al., 2010; Krajnc et al., 2011).

On the behavioural side, RTT girls suffer of mood disturbances including anxious and fearful behaviours. The most successful treatment for

anxiety and mood disturbances is the use of selective serotonin reuptake inhibitors (SSRIs), which increase serotonin levels in the synaptic cleft and are the elective therapy for this disturbs.

Most of the symptoms in CDD are similar to symptoms displayed in RTT, having in common the pharmacological treatments too. However, considering that the essential feature of CDD is the early onset of severe seizure episode, most of the disease management is for the treatment of epilepsy, having, unfortunately, limited effectiveness. Indeed, there is no single best anticonvulsant medication or combination for children with CDD. Besides the classical anticonvulsant drugs, already mentioned for RTT, other approaches have been tried to alleviate the seizures in CDD refractory epilepsy. Left cervical Vagus nerve stimulation (VNS) has been demonstrated being generally safe and effective treatment for CDD epilepsy. in addition, mood and behavioural improvements too have been described in CDD patients (Lim et al., 2018). The other innovative approach is the ketogenic diet (KD) introduced in the 1920s as a treatment option for refractory epilepsy in children. This diet brings elevated level of ketone bodies in the blood, a state known as ketosis, leads to a reduction in the frequency of epileptic seizures. It has been showed that in CDD this diet is a useful tool to control the seizures episodes (Lim et al., 2017).

Besides the approved pharmacological treatments, several preclinical studies have been carried to extend the possible pharmacological treatments to cure at least RTT and CDD symptomatology. In RTT, promising results have been obtained using molecules mimicking BDNF's effects. This idea has been formulated because BDNF protein levels were found to be lower in brain samples of MeCP2 mutant mice (Chang et al., 2006) The administration of BDNF is not useful, due to the low penetrant power through the blood-brain-

barrier (BBB). However, are available molecules able to mimic the effects of BDNF, such as BDNF-mimetics (LM22A-4) or increase its levels, such as AMPAkines. Mimicking the BDNF effects with LM22A-4 rescued breathing abnormalities in heterozygous female MeCP2 mutant mice (Schmid et al., 2012); instead systemic administration of AMPAkines improved breathing in *Mecp2* mutant mice by increasing BDNF in brain stem (Lauterborn et al., 2009). Unlike the BDNF, Insulin-like Growth factor-1 (IGF-1) crosses the BBB. It has been showed that daily administration of the active tri-peptide fragment of IGF-1 improved motor function, breathing abnormalities and cardiac irregularities in MeCP2 mutant mice (Tropea et al., 2009) and modulated the synaptic plasticity and morphology (Landi et al., 2011). A clinical trial is currently underway to determine administration to verify if administration of Mecasermin (synthetic analog of IGF-1) could improve RTT health and symptoms.

In CDD, few pharmacological preclinical studies are available in literature. One of this has reported an abnormal hippocampal development and neuronal maturation, accompanied by increased activity of GSK-3β, inhibitory regulator of many neurodevelopmental processes (Fuchs et al., 2014) Using the GSK-3β inhibitor SB216763 it has been showed a fully hippocampal development and behavioural deficits rescue in a CDD mouse model (Fuchs et al., 2014; Fuchs et al., 2015). In addition, considering the beneficial effects of IGF-1 administration in RTT mice, Della Sala and colleagues (2016) have tried IGF-1 administration in a CDD mouse model. Authors found that systemic administration of IGF-1 restored spine density and spine elimination rate and that this beneficial effect was detectable 20 days after the end of treatment (Della Sala et al., 2016).

### 1.4.1 5-HT₇R selective agonist LP-211

As mentioned above, 5-HT$_7$R, is the most recently discovered G-coupled serotonin receptor. This is involved in neurophysiological phenomena like regulation of circadian rhythm, mood, cognition, learning and synaptic plasticity. Moreover, it has been associated with different neuropsychiatric disorders like depression, anxious behaviour, schizophrenia and recently with Rett syndrome (De Filippis et al., 2014; De Filippis et al., 2015). After the receptor characterization, many studies tried to synthetize molecules able to selectively modulate the 5-HT$_7$R. One of the most interesting was LP-211 (Fig. 17), an arypiperazinic derivate that can bind and activate the 5-HT$_7$R which is, until now, the most powerful available agonist. This molecule was chosen because is characterized by high penetrant power through the BBB and high selectivity on the 5-HT$_7$R (Hedlund et al., 2010; Leopoldo et al., 2011). Like arypiperazinic derivatives in general, metabolism of LP-211 includes N-dealkylation of the aliphatic chain attached to the piperazine nitrogen, resulting in the formation of 1-(2-diphenyl) piperazine (RA-7). This potentially active metabolite rapidly enters the brain achieving higher concentrations than in plasma (Hedlund et al., 2010).
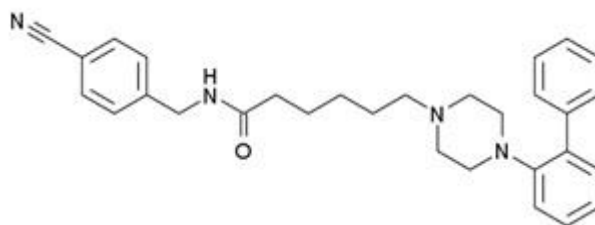


Fig. 17: **LP-211 chemical structure**

LP-211 showed a K$_i$ value of 15nM at human cloned 5-HT$_7$R. This affinity profile seems preferable compared to that of 8-OH-DPAT, which has

been reported to have $K_i = 467nM$ at the human cloned 5-HT$_7$R and $K_i = 3.8nM$ at human cloned 5-HT$_{1A}$R. The selectivity of LP-211 against 5-HT$_{1B}$R, 5-HT$_{2B}$R, 5-HT$_{2C}$R and 5-HT$_{5A}$R is modest, whereas significantly higher selectivity is observed for the subtypes 5-HT$_{1A}$R, 5-HT$_{1D}$R, 5-HT$_{2A}$R and 5-HT$_6$R. Finally, LP-211 does not significantly bind at 5-HT$_3$R and 5-HT$_{1E}$R receptors or at SERT. Interestingly, RA-7 appears to be a potent ligand for the human 5-HT$_7$R with a $K_i$ (1.4nM), approximately 10-fold lower than the corresponding value for LP-211 (Hedlund et al., 2010).

Efficacy of LP-211 rescuing RTT symptomatology in mouse model was previously demonstrated. In these previous experiments MeCP2-308 male mice (see 1.1.2) received 7 daily intraperitoneal injections of saline solution or LP-211 solution and then behavioural and molecular profile were evaluated. It has been demonstrated that LP-211 rescued anxiety like behaviour, improved motor coordination and increased novelty preference (De Filippis et al., 2014). The potential therapeutic efficacy of LP-211 emerged by molecular assays too, reversing RTT molecular alteration about cell cytoskeleton dynamic with reversion of abnormal activation of PAK and Cofilin, and about the protein synthesis, reversing abnormal activation of ribosomal protein S6, a downstream target of mTOR and S6 kinase, both in hippocampal tissue (De Filippis et al., 2014). Of note, these LP-211 beneficial effects were detectable until 2 months after the end of treatment in MeCP2-308 heterozygous female mice (De Filippis et al., 2015). Moreover, LP-211 treatment exerted beneficial effects on the mitochondrial dysfunction evaluated in two female RTT mice models (MeCP2-*null*(*Bird*) and MeCP2-308) (Valenti et al., 2017).

## 1.4.2  Phytocannabinoid Cannabidivarin (CBDV)

*Cannabis*, both *sativa* and *indica*, contains about 120 substance called phCBs (Morales et al., 2017). Besides THC and CBD, most of the phCBs are not well characterized and just few of them showed a potential as pharmacological treatment in preclinical studies. Another promising phCB is Cannabidivarin (CBDV) (Fig.18), the *n*-propyl analog of CBD. Recent evidences suggest that *in vitro* and *in vivo* treatment with CBDV in mouse and rat exerts anticonvulsant effects (Hill et al., 2012) and prevents neuronal hyperexcitability in cells (Iannotti et al., 2014). However, the studies focussed on this compound are still very limited and the mechanisms of action of CDBV have not been clarified so far. Current evidence suggest that CBDV may show weak affinity for CB1 and CB2 receptors, and presents both agonistic properties on transient receptor potential (TRP) channels receptors and antagonistic properties on the GPR55 receptor (Hagberg et al., 2002; Anavi-Goffer et al., 2012; Iannotti et al., 2014; Rosenthaler et al., 2014).
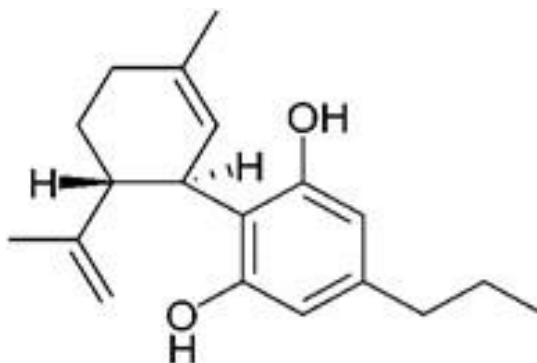


Fig. 18**: Cannabidivarin chemical structure**

# 1.5 Aims of the thesis

Considering previous evidences and lack of fully functional pharmacological treatment, the aim of this thesis was to evaluate two new drugs, LP-211 and CBDV, in highly validated MeCP2 and CDD mouse models.

The first aim of this thesis is to extend previous works evaluating LP-211 treatment in a female mouse model of RTT adding new behavioural task and new molecular analysis (Chapter 2); moreover, considering the analogies between RTT and CDD, for the first time we evaluated LP-211 treatment in a validated male mouse model of CDD (Chapter 3). To accomplish these aims, we followed the previous treatment experimental schedules (De Filippis et al., 2014; De Filippis et al., 2015) and then we evaluated the presence of behavioural and molecular deficits in both models and the LP-211 effects thereon. The second aim of this thesis is to identify for the first time the effects of three different daily intraperitoneal doses of CBDV treatment on a highly validated mouse model of RTT (hemizygous male MeCP2-308 mice) (Chapter 4). Of note, a clinical trial is currently in progress aimed at evaluating the potential efficacy of a treatment with CBDV on children affected by Autism Spectrum Disorder (clinicaltrial.gov, NCT03202303), giving to CBDV an highly translational power.

Despite LP-211 and CBDV, as well as their relative targets, are structurally different, recent evidence suggests a link between serotoninergic and endocannabinoid systems (Haj-Dahmane and Shen, 2011). Since both systems have been associated to the symptomatology of RTT, an evaluation of the effects of the above-mentioned drugs on RTT mouse models would be of great interest for this research field.

# 1.6    References

Adams, V. H., McBryant, S. J., Wade, P. A., Woodcock, C. L., Hansen, J. C., 2007. Intrinsic disorder and autonomous domain function in the multifunctional nuclear protein, MeCP2. J Biol Chem 282, 15057-15064.

Amendola, E., Zhan, Y., Mattucci, C., Castroflorio, E., Calcagno, E., Fuchs, C., Lonetti, G., Silingardi, D., Vyssotski, A. L., Farley, D., Ciani, E., Pizzorusso, T., Giustetto, M., Gross, C. T., 2014. Mapping pathological phenotypes in a mouse model of CDKL5 disorder. PLoS ONE 9, e91613.

Amir, R. E., Van den Veyver, I. B., Wan, M., Tran, C. Q., Francke, U., Zoghbi, H. Y., 1999. Rett syndrome is caused by mutations in X-linked MECP2, encoding methyl-CpG-binding protein 2. Nat Genet 23, 185-188.

Anavi-Goffer, S., Baillie, G., Irving, A. J., Gertsch, J., Greig, I. R., Pertwee, R. G., Ross, R. A., 2012. Modulation of L-alpha-lysophosphatidylinositol/GPR55 mitogen-activated protein kinase (MAPK) signaling by cannabinoids. J Biol Chem 287, 91-104.

Andrews, P. W., Bharwani, A., Lee, K. R., Fox, M., Thomson, J. A., Jr., 2015. Is serotonin an upper or a downer? The evolution of the serotonergic system and its role in depression and the antidepressant response. Neurosci Biobehav Rev 51, 164-188.

Ariani, F., Hayek, G., Rondinella, D., Artuso, R., Mencarelli, M. A., Spanhol-Rosseto, A., Pollazzon, M., Buoni, S., Spiga, O., Ricciardi, S., Meloni, I., Longo, I., Mari, F., Broccoli, V., Zappella, M., Renieri, A., 2008.

FOXG1 is responsible for the congenital variant of Rett syndrome. Am J Hum Genet 83, 89-93.

Armstrong, D., Dunn, J. K., Antalffy, B., Trivedi, R., 1995. Selective dendritic alterations in the cortex of Rett syndrome. J Neuropathol Exp Neurol 54, 195-201.

Armstrong, D. D., 2002. Neuropathology of Rett syndrome. Ment Retard Dev Disabil Res Rev 8, 72-76.

Armstrong, D. D., 2005. Neuropathology of Rett syndrome. J Child Neurol 20, 747-753.

Aso, E., Juves, S., Maldonado, R., Ferrer, I., 2013. CB2 cannabinoid receptor agonist ameliorates Alzheimer-like phenotype in AbetaPP/PS1 mice. J Alzheimers Dis 35, 847-858.

Ausio, J., Martinez de Paz, A., Esteller, M., 2014. MeCP2: the long trip from a chromatin protein to neurological disorders. Trends Mol Med 20, 487-498.

Bahi-Buisson, N., Villeneuve, N., Caietta, E., Jacquette, A., Maurey, H., Matthijs, G., Van Esch, H., Delahaye, A., Moncla, A., Milh, M., Zufferey, F., Diebold, B., Bienvenu, T., 2012. Recurrent mutations in the CDKL5 gene: genotype-phenotype relationships. Am J Med Genet A 158A, 1612-1619.

Baker, S. A., Chen, L., Wilkins, A. D., Yu, P., Lichtarge, O., Zoghbi, H. Y., 2013. An AT-hook domain in MeCP2 determines the clinical course of Rett syndrome and related disorders. Cell 152, 984-996.

Bard, J. A., Zgombick, J., Adham, N., Vaysse, P., Branchek, T. A., Weinshank, R. L., 1993. Cloning of a novel human serotonin receptor (5-HT7) positively linked to adenylate cyclase. J Biol Chem 268, 23422-23426.

Bebbington, A., Percy, A., Christodoulou, J., Ravine, D., Ho, G., Jacoby, P., Anderson, A., Pineda, M., Ben Zeev, B., Bahi-Buisson, N., Smeets, E., Leonard, H., 2010. Updating the profile of C-terminal MECP2 deletions in Rett syndrome. J Med Genet 47, 242-248.

Belichenko, P. V., Oldfors, A., Hagberg, B., Dahlstrom, A., 1994. Rett syndrome: 3-D confocal microscopy of cortical pyramidal dendrites and afferents. Neuroreport 5, 1509-1513.

Berrendero, F., Maldonado, R., 2002. Involvement of the opioid system in the anxiolytic-like effects induced by Delta(9)-tetrahydrocannabinol. Psychopharmacology (Berl) 163, 111-117.

Bertani, I., Rusconi, L., Bolognese, F., Forlani, G., Conca, B., De Monte, L., Badaracco, G., Landsberger, N., Kilstrup-Nielsen, C., 2006. Functional consequences of mutations in CDKL5, an X-linked gene involved in infantile spasms and mental retardation. J Biol Chem 281, 32048-32056.

Bienvenu, T., Chelly, J., 2006. Molecular genetics of Rett syndrome: when DNA methylation goes unrecognized. Nat Rev Genet 7, 415-426.

Bisogno, T., Howell, F., Williams, G., Minassi, A., Cascio, M. G., Ligresti, A., Matias, I., Schiano-Moriello, A., Paul, P., Williams, E. J., Gangadharan, U., Hobbs, C., Di Marzo, V., Doherty, P., 2003. Cloning of the first sn1-DAG lipases points to the spatial and temporal regulation of endocannabinoid signaling in the brain. J Cell Biol 163, 463-468.

Bortolato, M., Mangieri, R. A., Fu, J., Kim, J. H., Arguello, O., Duranti, A., Tontini, A., Mor, M., Tarzia, G., Piomelli, D., 2007. Antidepressant-like activity of the fatty acid amide hydrolase inhibitor URB597 in a rat model of chronic mild stress. Biol Psychiatry 62, 1103-1110.

Bourdon, V., Philippe, C., Bienvenu, T., Koenig, B., Tardieu, M., Chelly, J., Jonveaux, P., 2001. Evidence of somatic mosaicism for a MECP2 mutation in females with Rett syndrome: diagnostic implications. J Med Genet 38, 867-871.

Brucke, T., Sofic, E., Killian, W., Rett, A., Riederer, P., 1987. Reduced concentrations and increased metabolism of biogenic amines in a single case of Rett-syndrome: a postmortem brain study. J Neural Transm 68, 315-324.

Calamandrei, G., Aloe, L., Hajek, J., Zappella, M., 2001. Developmental profile of serum nerve growth factor levels in Rett complex. Ann Ist Super Sanita 37, 601-605.

Calfa, G., Percy, A. K., Pozzo-Miller, L., 2011. Experimental models of Rett syndrome based on Mecp2 dysfunction. Exp Biol Med (Maywood) 236, 3-19.

Chahrour, M., Jung, S. Y., Shaw, C., Zhou, X., Wong, S. T., Qin, J., Zoghbi, H. Y., 2008. MeCP2, a key contributor to neurological disease, activates and represses transcription. Science 320, 1224-1229.

Chahrour, M., Zoghbi, H. Y., 2007. The story of Rett syndrome: from clinic to neurobiology. Neuron 56, 422-437.

Chakrabarti, B., Persico, A., Battista, N., Maccarrone, M., 2015. Endocannabinoid Signaling in Autism. Neurotherapeutics 12, 837-847.

Chang, Q., Khare, G., Dani, V., Nelson, S., Jaenisch, R., 2006. The disease progression of Mecp2 mutant mice is affected by the level of BDNF expression. Neuron 49, 341-348.

Chapleau, C. A., Calfa, G. D., Lane, M. C., Albertson, A. J., Larimore, J. L., Kudo, S., Armstrong, D. L., Percy, A. K., Pozzo-Miller, L., 2009. Dendritic spine pathologies in hippocampal pyramidal neurons from Rett syndrome brain and after expression of Rett-associated MECP2 mutations. Neurobiol Dis 35, 219-233.

Chen, Q., Zhu, Y. C., Yu, J., Miao, S., Zheng, J., Xu, L., Zhou, Y., Li, D., Zhang, C., Tao, J., Xiong, Z. Q., 2010. CDKL5, a protein associated with rett syndrome, regulates neuronal morphogenesis via Rac1 signaling. J Neurosci 30, 12777-12786.

Chen, R. Z., Akbarian, S., Tudor, M., Jaenisch, R., 2001. Deficiency of methyl-CpG binding protein-2 in CNS neurons results in a Rett-like phenotype in mice. Nat Genet 27, 327-331.

Chen, W. G., Chang, Q., Lin, Y., Meissner, A., West, A. E., Griffith, E. C., Jaenisch, R., Greenberg, M. E., 2003. Derepression of BDNF transcription involves calcium-dependent phosphorylation of MeCP2. Science 302, 885-889.

Cheng, D., Low, J. K., Logge, W., Garner, B., Karl, T., 2014a. Chronic cannabidiol treatment improves social and object recognition in double transgenic APPswe/PS1E9 mice. Psychopharmacology (Berl) 231, 3009-3017.

Cheng, D., Spiro, A. S., Jenner, A. M., Garner, B., Karl, T., 2014b. Long-term cannabidiol treatment prevents the development of social recognition memory deficits in Alzheimer's disease transgenic mice. J Alzheimers Dis 42, 1383-1396.

Christodoulou, J., Weaving, L. S., 2003. MECP2 and beyond: phenotype-genotype correlations in Rett syndrome. J Child Neurol 18, 669-674.

Clarke, D. J., Stuart, J., McGregor, I. S., Arnold, J. C., 2017. Endocannabinoid dysregulation in cognitive and stress-related brain regions in the Nrg1 mouse model of schizophrenia. Prog Neuropsychopharmacol Biol Psychiatry 72, 9-15.

Cravatt, B. F., Giang, D. K., Mayfield, S. P., Boger, D. L., Lerner, R. A., Gilula, N. B., 1996. Molecular characterization of an enzyme that degrades neuromodulatory fatty-acid amides. Nature 384, 83-87.

Cuddapah, V. A., Pillai, R. B., Shekar, K. V., Lane, J. B., Motil, K. J., Skinner, S. A., Tarquinio, D. C., Glaze, D. G., McGwin, G., Kaufmann, W. E., Percy, A. K., Neul, J. L., Olsen, M. L., 2014. Methyl-CpG-binding protein 2 (MECP2) mutation type is associated with disease severity in Rett syndrome. J Med Genet 51, 152-158.

D'Esposito, M., Quaderi, N. A., Ciccodicola, A., Bruni, P., Esposito, T., D'Urso, M., Brown, S. D., 1996. Isolation, physical mapping, and northern analysis of the X-linked human gene encoding methyl CpG-binding protein, MECP2. Mamm Genome 7, 533-535.

Dalton, G. D., Bass, C. E., Van Horn, C. G., Howlett, A. C., 2009. Signal transduction via cannabinoid receptors. CNS Neurol Disord Drug Targets 8, 422-431.

De Filippis, B., Chiodi, V., Adriani, W., Lacivita, E., Mallozzi, C., Leopoldo, M., Domenici, M. R., Fuso, A., Laviola, G., 2015. Long-lasting beneficial effects of central serotonin receptor 7 stimulation in female mice modeling Rett syndrome. Front Behav Neurosci 9, 86.

De Filippis, B., Nativio, P., Fabbri, A., Ricceri, L., Adriani, W., Lacivita, E., Leopoldo, M., Passarelli, F., Fuso, A., Laviola, G., 2014. Pharmacological stimulation of the brain serotonin receptor 7 as a novel therapeutic approach for Rett syndrome. Neuropsychopharmacology 39, 2506-2518.

De Filippis, B., Ricceri, L., Laviola, G., 2010. Early postnatal behavioral changes in the Mecp2-308 truncation mouse model of Rett syndrome. Genes Brain Behav 9, 213-223.

De Petrocellis, L., Vellani, V., Schiano-Moriello, A., Marini, P., Magherini, P. C., Orlando, P., Di Marzo, V., 2008. Plant-derived cannabinoids modulate the activity of transient receptor potential channels of ankyrin type-1 and melastatin type-8. J Pharmacol Exp Ther 325, 1007-1015.

Della Sala, G., Putignano, E., Chelini, G., Melani, R., Calcagno, E., Michele Ratto, G., Amendola, E., Gross, C. T., Giustetto, M., Pizzorusso, T., 2016. Dendritic Spine Instability in a Mouse Model of CDKL5 Disorder Is Rescued by Insulin-like Growth Factor 1. Biol Psychiatry 80, 302-311.

Devane, W. A., Dysarz, F. A., 3rd, Johnson, M. R., Melvin, L. S., Howlett, A. C., 1988. Determination and characterization of a cannabinoid receptor in rat brain. Mol Pharmacol 34, 605-613.

Devinsky, O., Verducci, C., Thiele, E. A., Laux, L. C., Patel, A. D., Filloux, F., Szaflarski, J. P., Wilfong, A., Clark, G. D., Park, Y. D., Seltzer, L. E., Bebin, E. M., Flamini, R., Wechsler, R. T., Friedman, D., 2018. Open-label use of highly purified CBD (Epidiolex(R)) in patients with CDKL5 deficiency disorder and Aicardi, Dup15q, and Doose syndromes. Epilepsy Behav.

Di Marzo, V., 2011. Endocannabinoid pathways and their role in multiple sclerosis-related muscular dysfunction. Expert Rev Neurother 11, 9-14.

Di Marzo, V., Stella, N., Zimmer, A., 2015. Endocannabinoid signalling and the deteriorating brain. Nat Rev Neurosci 16, 30-42.

Dinh, T. P., Carpenter, D., Leslie, F. M., Freund, T. F., Katona, I., Sensi, S. L., Kathuria, S., Piomelli, D., 2002. Brain monoglyceride lipase participating in endocannabinoid inactivation. Proc Natl Acad Sci U S A 99, 10819-10824.

Dowie, M. J., Bradshaw, H. B., Howard, M. L., Nicholson, L. F., Faull, R. L., Hannan, A. J., Glass, M., 2009. Altered CB1 receptor and endocannabinoid levels precede motor symptom onset in a transgenic mouse model of Huntington's disease. Neuroscience 163, 456-465.

Drysdale, A. J., Ryan, D., Pertwee, R. G., Platt, B., 2006. Cannabidiol-induced intracellular Ca2+ elevations in hippocampal cells. Neuropharmacology 50, 621-631.

Ebert, D. H., Gabel, H. W., Robinson, N. D., Kastan, N. R., Hu, L. S., Cohen, S., Navarro, A. J., Lyst, M. J., Ekiert, R., Bird, A. P., Greenberg, M. E., 2013. Activity-dependent phosphorylation of MeCP2 threonine 308 regulates interaction with NCoR. Nature 499, 341-345.

Eggers, A. E., 2013. A serotonin hypothesis of schizophrenia. Med Hypotheses 80, 791-794.

Ellaway, C. J., Peat, J., Williams, K., Leonard, H., Christodoulou, J., 2001. Medium-term open label trial of L-carnitine in Rett syndrome. Brain Dev 23 Suppl 1, S85-89.

Errico, M., Crozier, R. A., Plummer, M. R., Cowen, D. S., 2001. 5-HT(7) receptors activate the mitogen activated protein kinase extracellular signal related kinase in cultured rat hippocampal neurons. Neuroscience 102, 361-367.

Espejo-Porras, F., Fernandez-Ruiz, J., Pertwee, R. G., Mechoulam, R., Garcia, C., 2013. Motor effects of the non-psychotropic phytocannabinoid cannabidiol that are mediated by 5-HT1A receptors. Neuropharmacology 75, 155-163.

Etienne-Manneville, S., Hall, A., 2002. Rho GTPases in cell biology. Nature 420, 629-635.

Evans, A. T., Formukong, E., Evans, F. J., 1987. Activation of phospholipase A2 by cannabinoids. Lack of correlation with CNS effects. FEBS Lett 211, 119-122.

Fehr, S., Wilson, M., Downs, J., Williams, S., Murgia, A., Sartori, S., Vecchi, M., Ho, G., Polli, R., Psoni, S., Bao, X., de Klerk, N., Leonard, H., Christodoulou, J., 2013. The CDKL5 disorder is an independent clinical entity associated with early-onset encephalopathy. Eur J Hum Genet 21, 266-273.

Fidalgo, S., Ivanov, D. K., Wood, S. H., 2013. Serotonin: from top to bottom. Biogerontology 14, 21-45.

Fuchs, C., Rimondini, R., Viggiano, R., Trazzi, S., De Franceschi, M., Bartesaghi, R., Ciani, E., 2015. Inhibition of GSK3beta rescues hippocampal development and learning in a mouse model of CDKL5 disorder. Neurobiol Dis 82, 298-310.

Fuchs, C., Trazzi, S., Torricella, R., Viggiano, R., De Franceschi, M., Amendola, E., Gross, C., Calza, L., Bartesaghi, R., Ciani, E., 2014. Loss of CDKL5 impairs survival and dendritic growth of newborn neurons by altering AKT/GSK-3beta signaling. Neurobiol Dis 70, 53-68.

Fuller, R. W., Wong, D. T., 1990. Serotonin uptake and serotonin uptake inhibition. Ann N Y Acad Sci 600, 68-78; discussion 79-80.

Gaoni, Y., Mechoulam, R., 1964. Isolation, Structure, and Partial Synthesis of an Active Constituent of Hashish. J Am Chem Soc 86, 1646-1647.

Geldenhuys, W. J., Van der Schyf, C. J., 2011. Role of serotonin in Alzheimer's disease: a new therapeutic target? CNS Drugs 25, 765-781.

Gellynck, E., Heyninck, K., Andressen, K. W., Haegeman, G., Levy, F. O., Vanhoenacker, P., Van Craenenbroeck, K., 2013. The serotonin 5-HT7 receptors: two decades of research. Exp Brain Res 230, 555-568.

Gershon, M. D., 2004. Review article: serotonin receptors and transporters -- roles in normal and abnormal gastrointestinal motility. Aliment Pharmacol Ther 20 Suppl 7, 3-14.

Ghosh, R. P., Nikitina, T., Horowitz-Scherer, R. A., Gierasch, L. M., Uversky, V. N., Hite, K., Hansen, J. C., Woodcock, C. L., 2010. Unique physical

properties and interactions of the domains of methylated DNA binding protein 2. Biochemistry 49, 4395-4410.

Gobira, P. H., Vilela, L. R., Goncalves, B. D., Santos, R. P., de Oliveira, A. C., Vieira, L. B., Aguiar, D. C., Crippa, J. A., Moreira, F. A., 2015. Cannabidiol, a Cannabis sativa constituent, inhibits cocaine-induced seizures in mice: Possible role of the mTOR pathway and reduction in glutamate release. Neurotoxicology 50, 116-121.

Gong, J. P., Onaivi, E. S., Ishiguro, H., Liu, Q. R., Tagliaferro, P. A., Brusco, A., Uhl, G. R., 2006. Cannabinoid CB2 receptors: immunohistochemical localization in rat brain. Brain Res 1071, 10-23.

Gray, J. A., Roth, B. L., 2001. Paradoxical trafficking and regulation of 5-HT(2A) receptors by agonists and antagonists. Brain Res Bull 56, 441-451.

Guerrini, R., Parrini, E., 2012. Epilepsy in Rett syndrome, and CDKL5- and FOXG1-gene-related encephalopathies. Epilepsia 53, 2067-2078.

Guseva, D., Wirth, A., Ponimaskin, E., 2014. Cellular mechanisms of the 5-HT7 receptor-mediated signaling. Front Behav Neurosci 8, 306.

Guy, J., Cheval, H., Selfridge, J., Bird, A., 2011. The role of MeCP2 in the brain. Annu Rev Cell Dev Biol 27, 631-652.

Guy, J., Hendrich, B., Holmes, M., Martin, J. E., Bird, A., 2001. A mouse Mecp2-null mutation causes neurological symptoms that mimic Rett syndrome. Nat Genet 27, 322-326.

Hagberg, B., 1985. Rett's syndrome: prevalence and impact on progressive severe mental retardation in girls. Acta Paediatr Scand 74, 405-408.

Hagberg, B., 2002. Clinical manifestations and stages of Rett syndrome. Ment Retard Dev Disabil Res Rev 8, 61-65.

Hagberg, B., Aicardi, J., Dias, K., Ramos, O., 1983. A progressive syndrome of autism, dementia, ataxia, and loss of purposeful hand use in girls: Rett's syndrome: report of 35 cases. Ann Neurol 14, 471-479.

Hagberg, B., Hanefeld, F., Percy, A., Skjeldal, O., 2002. An update on clinically applicable diagnostic criteria in Rett syndrome. Comments to Rett Syndrome Clinical Criteria Consensus Panel Satellite to European Paediatric Neurology Society Meeting, Baden Baden, Germany, 11 September 2001. Eur J Paediatr Neurol 6, 293-297.

Hanefeld, F., 1985a. The clinical pattern of the Rett syndrome. Brain Dev 7, 320-325.

Hanefeld, F., 1985b. [Epileptic attacks in childhood--myopathies in childhood]. Offentl Gesundheitswes 47, 357-360.

Hedlund, P. B., Leopoldo, M., Caccia, S., Sarkisyan, G., Fracasso, C., Martelli, G., Lacivita, E., Berardi, F., Perrone, R., 2010. LP-211 is a brain penetrant selective agonist for the serotonin 5-HT(7) receptor. Neurosci Lett 481, 12-16.

Hedlund, P. B., Sutcliffe, J. G., 2004. Functional, molecular and pharmacological advances in 5-HT7 receptor research. Trends Pharmacol Sci 25, 481-486.

Heinzel, T., Lavinsky, R. M., Mullen, T. M., Soderstrom, M., Laherty, C. D., Torchia, J., Yang, W. M., Brard, G., Ngo, S. D., Davie, J. R., Seto, E., Eisenman, R. N., Rose, D. W., Glass, C. K., Rosenfeld, M. G., 1997. A

complex containing N-CoR, mSin3 and histone deacetylase mediates transcriptional repression. Nature 387, 43-48.

Hill, A. J., Mercier, M. S., Hill, T. D., Glyn, S. E., Jones, N. A., Yamasaki, Y., Futamura, T., Duncan, M., Stott, C. G., Stephens, G. J., Williams, C. M., Whalley, B. J., 2012. Cannabidivarin is anticonvulsant in mouse and rat. Br J Pharmacol 167, 1629-1642.

Horike, S., Cai, S., Miyano, M., Cheng, J. F., Kohwi-Shigematsu, T., 2005. Loss of silent-chromatin looping and impaired imprinting of DLX5 in Rett syndrome. Nat Genet 37, 31-40.

Iannotti, F. A., Hill, C. L., Leo, A., Alhusaini, A., Soubrane, C., Mazzarella, E., Russo, E., Whalley, B. J., Di Marzo, V., Stephens, G. J., 2014. Nonpsychotropic plant cannabinoids, cannabidivarin (CBDV) and cannabidiol (CBD), activate and desensitize transient receptor potential vanilloid 1 (TRPV1) channels in vitro: potential for the treatment of neuronal hyperexcitability. ACS Chem Neurosci 5, 1131-1141.

Jenniches, I., Ternes, S., Albayram, O., Otte, D. M., Bach, K., Bindila, L., Michel, K., Lutz, B., Bilkei-Gorzo, A., Zimmer, A., 2016. Anxiety, Stress, and Fear Response in Mice With Reduced Endocannabinoid Levels. Biol Psychiatry 79, 858-868.

Johnson-Farley, N. N., Kertesy, S. B., Dubyak, G. R., Cowen, D. S., 2005. Enhanced activation of Akt and extracellular-regulated kinase pathways by simultaneous occupancy of Gq-coupled 5-HT2A receptors and Gs-coupled 5-HT7A receptors in PC12 cells. J Neurochem 92, 72-82.

Juan-Pico, P., Fuentes, E., Bermudez-Silva, F. J., Javier Diaz-Molina, F., Ripoll, C., Rodriguez de Fonseca, F., Nadal, A., 2006. Cannabinoid

receptors regulate Ca(2+) signals and insulin secretion in pancreatic beta-cell. Cell Calcium 39, 155-162.

Kalscheuer, V. M., Tao, J., Donnelly, A., Hollway, G., Schwinger, E., Kubart, S., Menzel, C., Hoeltzenbein, M., Tommerup, N., Eyre, H., Harbord, M., Haan, E., Sutherland, G. R., Ropers, H. H., Gecz, J., 2003. Disruption of the serine/threonine kinase 9 gene causes severe X-linked infantile spasms and mental retardation. Am J Hum Genet 72, 1401-1411.

Kameshita, I., Sekiguchi, M., Hamasaki, D., Sugiyama, Y., Hatano, N., Suetake, I., Tajima, S., Sueyoshi, N., 2008. Cyclin-dependent kinase-like 5 binds and phosphorylates DNA methyltransferase 1. Biochem Biophys Res Commun 377, 1162-1167.

Kano, M., Ohno-Shosaku, T., Hashimotodani, Y., Uchigashima, M., Watanabe, M., 2009. Endocannabinoid-mediated control of synaptic transmission. Physiol Rev 89, 309-380.

Kaplan, J. S., Stella, N., Catterall, W. A., Westenbroek, R. E., 2017. Cannabidiol attenuates seizures and social deficits in a mouse model of Dravet syndrome. Proc Natl Acad Sci U S A 114, 11229-11234.

Kilstrup-Nielsen, C., Rusconi, L., La Montanara, P., Ciceri, D., Bergo, A., Bedogni, F., Landsberger, N., 2012. What we know and would like to know about CDKL5 and its involvement in epileptic encephalopathy. Neural Plast 2012, 728267.

Kirby, R. S., Lane, J. B., Childers, J., Skinner, S. A., Annese, F., Barrish, J. O., Glaze, D. G., Macleod, P., Percy, A. K., 2010. Longevity in Rett

syndrome: analysis of the North American Database. J Pediatr 156, 135-138 e131.

Kobe, F., Guseva, D., Jensen, T. P., Wirth, A., Renner, U., Hess, D., Muller, M., Medrihan, L., Zhang, W., Zhang, M., Braun, K., Westerholz, S., Herzog, A., Radyushkin, K., El-Kordi, A., Ehrenreich, H., Richter, D. W., Rusakov, D. A., Ponimaskin, E., 2012. 5-HT7R/G12 signaling regulates neuronal morphology and function in an age-dependent manner. J Neurosci 32, 2915-2930.

Kokura, K., Kaul, S. C., Wadhwa, R., Nomura, T., Khan, M. M., Shinagawa, T., Yasukawa, T., Colmenares, C., Ishii, S., 2001. The Ski protein family is required for MeCP2-mediated transcriptional repression. J Biol Chem 276, 34115-34121.

Krajnc, N., Zupancic, N., Orazem, J., 2011. Epilepsy treatment in Rett syndrome. J Child Neurol 26, 1429-1433.

Kriaucionis, S., Bird, A., 2004. The major form of MeCP2 has a novel N-terminus generated by alternative splicing. Nucleic Acids Res 32, 1818-1823.

Kucukkal, T. G., Yang, Y., Uvarov, O., Cao, W., Alexov, E., 2015. Impact of Rett Syndrome Mutations on MeCP2 MBD Stability. Biochemistry 54, 6357-6368.

Kvachnina, E., Liu, G., Dityatev, A., Renner, U., Dumuis, A., Richter, D. W., Dityateva, G., Schachner, M., Voyno-Yasenetskaya, T. A., Ponimaskin, E. G., 2005. 5-HT7 receptor is coupled to G alpha subunits of heterotrimeric G12-protein to regulate gene transcription and neuronal morphology. J Neurosci 25, 7821-7830.

Landi, S., Putignano, E., Boggio, E. M., Giustetto, M., Pizzorusso, T., Ratto, G. M., 2011. The short-time structural plasticity of dendritic spines is altered in a model of Rett syndrome. Sci Rep 1, 45.

Lauterborn, J. C., Pineda, E., Chen, L. Y., Ramirez, E. A., Lynch, G., Gall, C. M., 2009. Ampakines cause sustained increases in brain-derived neurotrophic factor signaling at excitatory synapses without changes in AMPA receptor subunit expression. Neuroscience 159, 283-295.

Lekman, A., Witt-Engerstrom, I., Gottfries, J., Hagberg, B. A., Percy, A. K., Svennerholm, L., 1989. Rett syndrome: biogenic amines and metabolites in postmortem brain. Pediatr Neurol 5, 357-362.

Leontovich, T. A., Mukhina, J. K., Fedorov, A. A., Belichenko, P. V., 1999. Morphological study of the entorhinal cortex, hippocampal formation, and basal ganglia in Rett syndrome patients. Neurobiol Dis 6, 77-91.

Leopoldo, M., Lacivita, E., Berardi, F., Perrone, R., Hedlund, P. B., 2011. Serotonin 5-HT7 receptor agents: Structure-activity relationships and potential therapeutic applications in central nervous system disorders. Pharmacol Ther 129, 120-148.

Leweke, F. M., Piomelli, D., Pahlisch, F., Muhl, D., Gerth, C. W., Hoyer, C., Klosterkotter, J., Hellmich, M., Koethe, D., 2012. Cannabidiol enhances anandamide signaling and alleviates psychotic symptoms of schizophrenia. Transl Psychiatry 2, e94.

Lewis, J. D., Meehan, R. R., Henzel, W. J., Maurer-Fogy, I., Jeppesen, P., Klein, F., Bird, A., 1992. Purification, sequence, and cellular localization of a novel chromosomal protein that binds to methylated DNA. Cell 69, 905-914.

Lim, Z., Wong, K., Downs, J., Bebbington, K., Demarest, S., Leonard, H., 2018. Vagus nerve stimulation for the treatment of refractory epilepsy in the CDKL5 Deficiency Disorder. Epilepsy Res 146, 36-40.

Lim, Z., Wong, K., Olson, H. E., Bergin, A. M., Downs, J., Leonard, H., 2017. Use of the ketogenic diet to manage refractory epilepsy in CDKL5 disorder: Experience of >100 patients. Epilepsia 58, 1415-1422.

Linge, R., Jimenez-Sanchez, L., Campa, L., Pilar-Cuellar, F., Vidal, R., Pazos, A., Adell, A., Diaz, A., 2016. Cannabidiol induces rapid-acting antidepressant-like effects and enhances cortical 5-HT/glutamate neurotransmission: role of 5-HT1A receptors. Neuropharmacology 103, 16-26.

Liyanage, V. R., Rastegar, M., 2014. Rett syndrome and MeCP2. Neuromolecular Med 16, 231-264.

Lyst, M. J., Bird, A., 2015. Rett syndrome: a complex disorder with simple roots. Nat Rev Genet 16, 261-275.

Lyst, M. J., Ekiert, R., Ebert, D. H., Merusi, C., Nowak, J., Selfridge, J., Guy, J., Kastan, N. R., Robinson, N. D., de Lima Alves, F., Rappsilber, J., Greenberg, M. E., Bird, A., 2013. Rett syndrome mutations abolish the interaction of MeCP2 with the NCoR/SMRT co-repressor. Nat Neurosci 16, 898-902.

Marco, E. M., Rapino, C., Caprioli, A., Borsini, F., Laviola, G., Maccarrone, M., 2015. Potential Therapeutic Value of a Novel FAAH Inhibitor for the Treatment of Anxiety. PLoS ONE 10, e0137034.

Mari, F., Azimonti, S., Bertani, I., Bolognese, F., Colombo, E., Caselli, R., Scala, E., Longo, I., Grosso, S., Pescucci, C., Ariani, F., Hayek, G., Balestri, P., Bergo, A., Badaracco, G., Zappella, M., Broccoli, V., Renieri, A., Kilstrup-Nielsen, C., Landsberger, N., 2005. CDKL5 belongs to the same molecular pathway of MeCP2 and it is responsible for the early-onset seizure variant of Rett syndrome. Hum Mol Genet 14, 1935-1946.

Maron, E., Nutt, D., Shlik, J., 2012. Neuroimaging of serotonin system in anxiety disorders. Curr Pharm Des 18, 5699-5708.

Maroof, N., Ravipati, S., Pardon, M. C., Barrett, D. A., Kendall, D. A., 2014. Reductions in endocannabinoid levels and enhanced coupling of cannabinoid receptors in the striatum are accompanied by cognitive impairments in the AbetaPPswe/PS1DeltaE9 mouse model of Alzheimer's disease. J Alzheimers Dis 42, 227-245.

Marston, O. J., Garfield, A. S., Heisler, L. K., 2011. Role of central serotonin and melanocortin systems in the control of energy balance. Eur J Pharmacol 660, 70-79.

Martinowich, K., Hattori, D., Wu, H., Fouse, S., He, F., Hu, Y., Fan, G., Sun, Y. E., 2003. DNA methylation-related chromatin remodeling in activity-dependent BDNF gene regulation. Science 302, 890-893.

Matsuda, L. A., Lolait, S. J., Brownstein, M. J., Young, A. C., Bonner, T. I., 1990. Structure of a cannabinoid receptor and functional expression of the cloned cDNA. Nature 346, 561-564.

McArthur, A. J., Budden, S. S., 1998. Sleep dysfunction in Rett syndrome: a trial of exogenous melatonin treatment. Dev Med Child Neurol 40, 186-192.

Meehan, R. R., Lewis, J. D., Bird, A. P., 1992. Characterization of MeCP2, a vertebrate DNA binding protein with affinity for methylated DNA. Nucleic Acids Res 20, 5085-5092.

Micale, V., Di Marzo, V., Sulcova, A., Wotjak, C. T., Drago, F., 2013. Endocannabinoid system and mood disorders: priming a target for new therapies. Pharmacol Ther 138, 18-37.

Mnatzakanian, G. N., Lohi, H., Munteanu, I., Alfred, S. E., Yamada, T., MacLeod, P. J., Jones, J. R., Scherer, S. W., Schanen, N. C., Friez, M. J., Vincent, J. B., Minassian, B. A., 2004. A previously unidentified MECP2 open reading frame defines a new protein isoform relevant to Rett syndrome. Nat Genet 36, 339-341.

Montini, E., Andolfi, G., Caruso, A., Buchner, G., Walpole, S. M., Mariani, M., Consalez, G., Trump, D., Ballabio, A., Franco, B., 1998. Identification and characterization of a novel serine-threonine kinase gene from the Xp22 region. Genomics 51, 427-433.

Morales, P., Hurst, D. P., Reggio, P. H., 2017. Molecular Targets of the Phytocannabinoids: A Complex Picture. Prog Chem Org Nat Prod 103, 103-131.

Munro, S., Thomas, K. L., Abu-Shaar, M., 1993. Molecular characterization of a peripheral receptor for cannabinoids. Nature 365, 61-65.

Nan, X., Ng, H. H., Johnson, C. A., Laherty, C. D., Turner, B. M., Eisenman, R. N., Bird, A., 1998. Transcriptional repression by the methyl-CpG-binding protein MeCP2 involves a histone deacetylase complex. Nature 393, 386-389.

Nan, X., Tate, P., Li, E., Bird, A., 1996. DNA methylation specifies chromosomal localization of MeCP2. Mol Cell Biol 16, 414-421.

Neul, J. L., Kaufmann, W. E., Glaze, D. G., Christodoulou, J., Clarke, A. J., Bahi-Buisson, N., Leonard, H., Bailey, M. E., Schanen, N. C., Zappella, M., Renieri, A., Huppke, P., Percy, A. K., RettSearch, C., 2010. Rett syndrome: revised diagnostic criteria and nomenclature. Ann Neurol 68, 944-950.

Nikitina, T., Ghosh, R. P., Horowitz-Scherer, R. A., Hansen, J. C., Grigoryev, S. A., Woodcock, C. L., 2007. MeCP2-chromatin interactions include the formation of chromatosome-like structures and are altered in mutations causing Rett syndrome. J Biol Chem 282, 28237-28245.

Nomura, Y., Segawa, M., Higurashi, M., 1985. Rett syndrome--an early catecholamine and indolamine deficient disorder? Brain Dev 7, 334-341.

Ofek, O., Karsak, M., Leclerc, N., Fogel, M., Frenkel, B., Wright, K., Tam, J., Attar-Namdar, M., Kram, V., Shohami, E., Mechoulam, R., Zimmer, A., Bab, I., 2006. Peripheral cannabinoid receptor, CB2, regulates bone mass. Proc Natl Acad Sci U S A 103, 696-701.

Okamoto, Y., Morishita, J., Tsuboi, K., Tonai, T., Ueda, N., 2004. Molecular characterization of a phospholipase D generating anandamide and its congeners. J Biol Chem 279, 5298-5305.
66

Pagotto, U., Marsicano, G., Cota, D., Lutz, B., Pasquali, R., 2006. The emerging role of the endocannabinoid system in endocrine regulation and energy balance. Endocr Rev 27, 73-100.

Panayotis, N., Ghata, A., Villard, L., Roux, J. C., 2011. Biogenic amines and their metabolites are differentially affected in the Mecp2-deficient mouse brain. BMC Neurosci 12, 47.

Pelka, G. J., Watson, C. M., Christodoulou, J., Tam, P. P., 2005. Distinct expression profiles of Mecp2 transcripts with different lengths of 3'UTR in the brain and visceral organs during mouse development. Genomics 85, 441-452.

Pertwee, R. G., 2008. The diverse CB1 and CB2 receptor pharmacology of three plant cannabinoids: delta9-tetrahydrocannabinol, cannabidiol and delta9-tetrahydrocannabivarin. Br J Pharmacol 153, 199-215.

Piazza, C. C., Fisher, W., Kiesewetter, K., Bowman, L., Moser, H., 1990. Aberrant sleep patterns in children with the Rett syndrome. Brain Dev 12, 488-493.

Pisani, V., Madeo, G., Tassone, A., Sciamanna, G., Maccarrone, M., Stanzione, P., Pisani, A., 2011. Homeostatic changes of the endocannabinoid system in Parkinson's disease. Mov Disord 26, 216-222.

Politis, M., Niccolini, F., 2015. Serotonin in Parkinson's disease. Behav Brain Res 277, 136-145.

Quaderi, N. A., Meehan, R. R., Tate, P. H., Cross, S. H., Bird, A. P., Chatterjee, A., Herman, G. E., Brown, S. D., 1994. Genetic and physical mapping

of a gene encoding a methyl CpG binding protein, Mecp2, to the mouse X chromosome. Genomics 22, 648-651.

Rastegar, M., Hotta, A., Pasceri, P., Makarem, M., Cheung, A. Y., Elliott, S., Park, K. J., Adachi, M., Jones, F. S., Clarke, I. D., Dirks, P., Ellis, J., 2009. MECP2 isoform-specific vectors with regulated expression for Rett syndrome gene therapy. PLoS ONE 4, e6810.

Reiss, A. L., Faruque, F., Naidu, S., Abrams, M., Beaty, T., Bryan, R. N., Moser, H., 1993. Neuroanatomy of Rett syndrome: a volumetric imaging study. Ann Neurol 34, 227-234.

Renieri, A., Meloni, I., Longo, I., Ariani, F., Mari, F., Pescucci, C., Cambi, F., 2003. Rett syndrome: the complex nature of a monogenic disease. J Mol Med (Berl) 81, 346-354.

Rett, A., 1966. On a unusual brain atrophy syndrome in hyperammonemia in childhood. Wiener Medizinische Wochenschrift 116, 723-726.

Ricceri, L., De Filippis, B., Laviola, G., 2012. Rett syndrome treatment in mouse models: searching for effective targets and strategies. Neuropharmacology 68, 106-115.

Ricceri, L., De Filippis, B., Laviola, G., 2013. Rett syndrome treatment in mouse models: searching for effective targets and strategies. Neuropharmacology 68, 106-115.

Ricciardi, S., Ungaro, F., Hambrock, M., Rademacher, N., Stefanelli, G., Brambilla, D., Sessa, A., Magagnotti, C., Bachi, A., Giarda, E., Verpelli, C., Kilstrup-Nielsen, C., Sala, C., Kalscheuer, V. M., Broccoli, V., 2012. CDKL5 ensures excitatory synapse stability by reinforcing NGL-1-

68

PSD95 interaction in the postsynaptic compartment and is impaired in patient iPSC-derived neurons. Nat Cell Biol 14, 911-923.

Riikonen, R., 2003. Neurotrophic factors in the pathogenesis of Rett syndrome. J Child Neurol 18, 693-697.

Roende, G., Ravn, K., Fuglsang, K., Andersen, H., Nielsen, J. B., Brondum-Nielsen, K., Jensen, J. E., 2011. DXA measurements in Rett syndrome reveal small bones with low bone mass. J Bone Miner Res 26, 2280-2286.

Rosenthaler, S., Pohn, B., Kolmanz, C., Huu, C. N., Krewenka, C., Huber, A., Kranner, B., Rausch, W. D., Moldzio, R., 2014. Differences in receptor binding affinity of several phytocannabinoids do not explain their effects on neural cell cultures. Neurotoxicol Teratol 46, 49-56.

Rusconi, L., Salvatoni, L., Giudici, L., Bertani, I., Kilstrup-Nielsen, C., Broccoli, V., Landsberger, N., 2008. CDKL5 expression is modulated during neuronal development and its subcellular distribution is tightly regulated by the C-terminal tail. J Biol Chem 283, 30101-30111.

Ryan, D., Drysdale, A. J., Lafourcade, C., Pertwee, R. G., Platt, B., 2009. Cannabidiol targets mitochondria to regulate intracellular Ca2+ levels. J Neurosci 29, 2053-2063.

Ryberg, E., Larsson, N., Sjogren, S., Hjorth, S., Hermansson, N. O., Leonova, J., Elebring, T., Nilsson, K., Drmota, T., Greasley, P. J., 2007. The orphan receptor GPR55 is a novel cannabinoid receptor. Br J Pharmacol 152, 1092-1101.

Samaco, R. C., Neul, J. L., 2011. Complexities of Rett syndrome and MeCP2. J Neurosci 31, 7951-7959.

Schmid, D. A., Yang, T., Ogier, M., Adams, I., Mirakhur, Y., Wang, Q., Massa, S. M., Longo, F. M., Katz, D. M., 2012. A TrkB small molecule partial agonist rescues TrkB phosphorylation deficits and improves respiratory function in a mouse model of Rett syndrome. J Neurosci 32, 1803-1810.

Sekiguchi, M., Katayama, S., Hatano, N., Shigeri, Y., Sueyoshi, N., Kameshita, I., 2013. Identification of amphiphysin 1 as an endogenous substrate for CDKL5, a protein kinase associated with X-linked neurodevelopmental disorder. Arch Biochem Biophys 535, 257-267.

Sekul, E. A., Moak, J. P., Schultz, R. J., Glaze, D. G., Dunn, J. K., Percy, A. K., 1994. Electrocardiographic findings in Rett syndrome: an explanation for sudden death? J Pediatr 125, 80-82.

Servadio, M., Melancia, F., Manduca, A., di Masi, A., Schiavi, S., Cartocci, V., Pallottini, V., Campolongo, P., Ascenzi, P., Trezza, V., 2016. Targeting anandamide metabolism rescues core and associated autistic-like symptoms in rats prenatally exposed to valproic acid. Transl Psychiatry 6, e902.

Shahbazian, M. D., Young, J. I., Yuva-Paylor, L. A., Spencer, C. M., Antalffy, B. A., Noebels, J. L., Armstrong, D. L., Paylor, R., Zoghbi, H. Y., 2002. Mice with Truncated MeCP2 Recapitulate Many Rett Syndrome Features and Display Hyperacetylation of Histone H3. Neuron 35, 243-254.

Shao, Z., Yin, J., Chapman, K., Grzemska, M., Clark, L., Wang, J., Rosenbaum, D. M., 2016. High-resolution crystal structure of the human CB1 cannabinoid receptor. Nature.

Shen, Y., Monsma, F. J., Jr., Metcalf, M. A., Jose, P. A., Hamblin, M. W., Sibley, D. R., 1993. Molecular cloning and expression of a 5-hydroxytryptamine7 serotonin receptor subtype. J Biol Chem 268, 18200-18204.

Smeets, E., Terhal, P., Casaer, P., Peters, A., Midro, A., Schollen, E., van Roozendaal, K., Moog, U., Matthijs, G., Herbergs, J., Smeets, H., Curfs, L., Schrander-Stumpel, C., Fryns, J. P., 2005. Rett syndrome in females with CTS hot spot deletions: a disorder profile. Am J Med Genet A 132A, 117-120.

Specchio, N., Balestri, M., Striano, P., Cilio, M. R., Nardello, R., Patane, S., Margiotta, M. L., D'Orsi, G., Striano, S., Russo, S., Specchio, L. M., Cusmai, R., Fusco, L., Vigevano, F., 2010. Efficacy of levetiracetam in the treatment of drug-resistant Rett syndrome. Epilepsy Res 88, 112-117.

Speranza, L., Chambery, A., Di Domenico, M., Crispino, M., Severino, V., Volpicelli, F., Leopoldo, M., Bellenchi, G. C., di Porzio, U., Perrone-Capano, C., 2013. The serotonin receptor 7 promotes neurite outgrowth via ERK and Cdk5 signaling pathways. Neuropharmacology 67, 155-167.

Szulwach, K. E., Li, X., Li, Y., Song, C. X., Han, J. W., Kim, S., Namburi, S., Hermetz, K., Kim, J. J., Rudd, M. K., Yoon, Y. S., Ren, B., He, C., Jin,

P., 2011. Integrating 5-hydroxymethylcytosine into the epigenomic landscape of human embryonic stem cells. PLoS Genet 7, e1002154.

Thambirajah, A. A., Eubanks, J. H., Ausio, J., 2009. MeCP2 post-translational regulation through PEST domains: two novel hypotheses: potential relevance and implications for Rett syndrome. Bioessays 31, 561-569.

Thomas, A., Baillie, G. L., Phillips, A. M., Razdan, R. K., Ross, R. A., Pertwee, R. G., 2007. Cannabidiol displays unexpectedly high potency as an antagonist of CB1 and CB2 receptor agonists in vitro. Br J Pharmacol 150, 613-623.

Thomas, A., Stevenson, L. A., Wease, K. N., Price, M. R., Baillie, G., Ross, R. A., Pertwee, R. G., 2005. Evidence that the plant cannabinoid Delta9-tetrahydrocannabivarin is a cannabinoid CB1 and CB2 receptor antagonist. Br J Pharmacol 146, 917-926.

Thompson, M. D., Cole, D. E., Jose, P. A., 2008. Pharmacogenomics of G protein-coupled receptor signaling: insights from health and disease. Methods Mol Biol 448, 77-107.

Tolias, K. F., Duman, J. G., Um, K., 2011. Control of synapse development and plasticity by Rho GTPase regulatory proteins. Prog Neurobiol 94, 133-148.

Trappe, R., Laccone, F., Cobilanschi, J., Meins, M., Huppke, P., Hanefeld, F., Engel, W., 2001. MECP2 mutations in sporadic cases of Rett syndrome are almost exclusively of paternal origin. Am J Hum Genet 68, 1093-1101.

Tropea, D., Giacometti, E., Wilson, N. R., Beard, C., McCurry, C., Fu, D. D., Flannery, R., Jaenisch, R., Sur, M., 2009. Partial reversal of Rett Syndrome-like symptoms in MeCP2 mutant mice. Proc Natl Acad Sci U S A 106, 2029-2034.

Valenti, D., de Bari, L., Vigli, D., Lacivita, E., Leopoldo, M., Laviola, G., Vacca, R. A., De Filippis, B., 2017. Stimulation of the brain serotonin receptor 7 rescues mitochondrial dysfunction in female mice from two models of Rett syndrome. Neuropharmacology.

Vallee, A., Lecarpentier, Y., Guillevin, R., Vallee, J. N., 2017. Effects of cannabidiol interactions with Wnt/beta-catenin pathway and PPARgamma on oxidative stress and neuroinflammation in Alzheimer's disease. Acta Biochim Biophys Sin (Shanghai) 49, 853-866.

Viemari, J. C., Roux, J. C., Tryba, A. K., Saywell, V., Burnet, H., Pena, F., Zanella, S., Bevengut, M., Barthelemy-Requin, M., Herzing, L. B., Moncla, A., Mancini, J., Ramirez, J. M., Villard, L., Hilaire, G., 2005. Mecp2 deficiency disrupts norepinephrine and respiratory systems in mice. J Neurosci 25, 11521-11530.

Vigli, D., Cosentino, L., Raggi, C., Laviola, G., Woolley-Roberts, M., De Filippis, B., 2018a. Chronic treatment with the phytocannabinoid Cannabidivarin (CBDV) rescues behavioural alterations and brain atrophy in a mouse model of Rett syndrome. Neuropharmacology, **140**, 121-129.

Walther, D. J., Peter, J. U., Bashammakh, S., Hortnagl, H., Voits, M., Fink, H., Bader, M., 2003. Synthesis of serotonin by a second tryptophan hydroxylase isoform. Science 299, 76.

73

Wang, I. T., Allen, M., Goffin, D., Zhu, X., Fairless, A. H., Brodkin, E. S., Siegel, S. J., Marsh, E. D., Blendy, J. A., Zhou, Z., 2012. Loss of CDKL5 disrupts kinome profile and event-related potentials leading to autistic-like phenotypes in mice. Proc Natl Acad Sci U S A 109, 21516-21521.

Weaving, L. S., Christodoulou, J., Williamson, S. L., Friend, K. L., McKenzie, O. L., Archer, H., Evans, J., Clarke, A., Pelka, G. J., Tam, P. P., Watson, C., Lahooti, H., Ellaway, C. J., Bennetts, B., Leonard, H., Gecz, J., 2004. Mutations of CDKL5 cause a severe neurodevelopmental disorder with infantile spasms and mental retardation. Am J Hum Genet 75, 1079-1093.

Weaving, L. S., Ellaway, C. J., Gecz, J., Christodoulou, J., 2005. Rett syndrome: clinical review and genetic update. J Med Genet 42, 1-7.

Wenk, G. L., O'Leary, M., Nemeroff, C. B., Bissette, G., Moser, H., Naidu, S., 1993. Neurochemical alterations in Rett syndrome. Brain Res Dev Brain Res 74, 67-72.

Williamson, S. L., Giudici, L., Kilstrup-Nielsen, C., Gold, W., Pelka, G. J., Tam, P. P., Grimm, A., Prodi, D., Landsberger, N., Christodoulou, J., 2012. A novel transcript of cyclin-dependent kinase-like 5 (CDKL5) has an alternative C-terminus and is the predominant transcript in brain. Hum Genet 131, 187-200.

Young, J. I., Hong, E. P., Castle, J. C., Crespo-Barreto, J., Bowman, A. B., Rose, M. F., Kang, D., Richman, R., Johnson, J. M., Berget, S., Zoghbi, H. Y., 2005. Regulation of RNA splicing by the methylation-dependent

transcriptional repressor methyl-CpG binding protein 2. Proc Natl Acad Sci U S A 102, 17551-17558.

Yu, P. L., Fujimura, M., Okumiya, K., Kinoshita, M., Hasegawa, H., Fujimiya, M., 1999. Immunohistochemical localization of tryptophan hydroxylase in the human and rat gastrointestinal tracts. J Comp Neurol 411, 654-665.

Zappella, M., Meloni, I., Longo, I., Hayek, G., Renieri, A., 2001. Preserved speech variants of the Rett syndrome: molecular and clinical analysis. Am J Med Genet 104, 14-22.

# Chapter 2

## 2. Targeting serotonin receptor 7 rescues physiological alterations and restores brain histone H3 acetylation and MeCP2 co-repressors proteins levels in a female mouse model of RTT syndrome

Daniele Vigli[1,2*], Giorgia Napolitani[2*], Livia Cosentino[1], Maria Cristina Talamo[1], Maddalena Grieco[2], Enza Lacivita[3], Marcello Leopoldo[3], Giovanni Laviola[1], Andrea Fuso[4], Maria d'Erme[2], Bianca De Filippis[1]

[1]*Center for Behavioral Sciences and Mental Health, Istituto Superiore di Sanità, Rome, Italy;* [2]*Department of Biochemical Sciences, Sapienza University of Roma, Italy;* [3]*Dept. Pharmacy, University of Bari "Aldo Moro", Bari, Italy;* [4]*Department of Surgery "Pietro Valdoni", Sapienza University of Rome, Italy.*

*equally contributed

## 2.1   Abstract

Rett syndrome (RTT) is a rare neurodevelopmental disorder caused by mutations in the MECP2 gene in about 95% of cases and no cure is available for this disorder. MECP2 mainly exerts transcriptional regulatory functions, directly interacting with nucleosomes or acting as a platform for recruitment of recruit histone deacetylase (HDAC)-containing co repressor complexes. How mutations in the MeCP2 gene lead to the neurobehavioural features of RTT is still not clear and there is no cure for this devastating disorder. In the present study we demonstrate that stimulation of the serotonin receptor 7 (5-HT7R) with the agonist molecule LP-211 (0.25 mg/kg once/day for 7 days) rescues the altered histone H3 acetylation levels in the cortex and hippocampus of heterozygous MeCP2-308 female mice, a RTT mouse model bearing a C-terminal truncating mutation on the MeCP2 gene (RTT mice). Moreover, the LP-211 treatment restored the abnormal protein levels of NCoR and HDAC3 in RTT mouse cortex. A normalization of the carotid pulse distension and a rescue of the aberrant sociability in RTT female mice treated with LP-211 were also uncovered, thus extending previous findings and adding further support to the translational value of this promising pharmacological approach for RTT.

## 2.2    Introduction

The serotonin receptor 7 (5-HT$_7$R) is one of the most recently discovered serotonin receptor (Bard et al., 1993). The 5-HT$_7$R is widely expressed throughout the central nervous system (Hedlund and Sutcliffe, 2004; Romano et al., 2014) and plays an important role in the control of many physiological functions, such as circadian rhythms, thermoregulation, learning and memory (Canese et al., 2014; Meneses, 2014; Volpicelli et al., 2014). The receptor belongs to the family of G-protein coupled receptors (GPCRs), functioning as signal-transducer by translating extracellular stimuli into intracellular responses resulting in multiple physiological and pathophysiological responses (Thompson et al., 2008). In particular, the 5-HT$_7$R stimulation activates several pathways involved in synaptic plasticity and cognition (Ciranna and Catania, 2014; Stiedl et al., 2015; Zareifopoulos and Papatheodoropoulos, 2016), such as protein kinase A (PKA), which induces activation of the neuroprotective extracellular signal-regulated kinases (ERK1/2) and cyclin-dependent kinase 5 (Cdk5) pathways (Guseva et al., 2014; Volpicelli et al., 2014; Costa et al., 2018). Aberrant 5-HT$_7$R signalling has been involved in a number of psychiatric disorders, such as Alzheimer's disease, depression, schizophrenia and anxiety disorders (Gellynck et al., 2013; Naumenko et al., 2014; Ivachtchenko et al., 2016). Moreover, recent evidence suggest that the stimulation of the central 5-HT$_7$R signalling as a new therapeutic strategy in X-linked neurodevelopmental disorders characterized by intellectual disability such as Fragile X syndrome (Costa et al., 2018) and CDKL5 Deficiency Disorder (Vigli et al., 2018b).

In this context, we have demonstrated that repeated systemic treatment with LP-211, a brain penetrant selective agonist which binds with high affinity at the human cloned 5-HT$_7$R (Leopoldo et al., 2008; Hedlund et al., 2010;

Leopoldo et al., 2011), substantially rescues the neurobehavioral phenotype of a mouse model of Rett Syndrome (RTT; OMIM 312750) (De Filippis et al., 2014; De Filippis et al., 2015a). RTT is a rare neurodevelopmental disorder characterized by severe behavioural and physiological symptoms (Rett, 1966; Hagberg et al., 2002; Ricceri et al., 2012). RTT almost exclusively affects females with an incidence of 1 in every 10,000 births. Patients present a wide variety of symptoms including autistic features, social interaction deficit, mental retardation, stereotyped hand movements, seizures and breath impairments.

Classic RTT is caused in about 90–95% of cases by mutations in the X-linked *MECP2* gene located on Xq28 (Amir et al., 1999), which encodes the methyl CpG-binding protein 2 (MECP2), a multifunctional protein that binds to methylated DNA and mainly acts as a key transcriptional regulator (Guy et al., 2011). MECP2 mainly exerts transcriptional regulatory functions, directly interacting with nucleosomes via its methyl-CpG–binding domain (MBD) or acting as a platform for recruitment of numerous protein partners via its a transcriptional repression domain (TRD), leading to chromatin compaction and transcriptional repression (Lyst et al., 2013). Historically, the repressive MeCP2 activity was thought to be primarily promoted through the recruitment of SIN3α/HDACs complex and the consequent de-acetylation of histones (Jones et al., 1998; Nan et al., 1998). Major interest in the last few years has been however attracted by the histone deacetylase (HDAC)-containing co-repressor complex NCoR/SMRT/HDACs, which binds the TRD terminal residues (285-319) of MeCP2 (Lyst et al., 2013). Despite numerous efforts have been made in this field, how mutations in the MeCP2 gene lead to the neurobehavioural features of RTT is still not clear and there is no cure for this devastating disorder. Indeed, most of the MeCP2 mutations in RTT patients

occurs in the MDB, disrupting the MeCP2 binding with DNA leading to severe phenotype (Amir et al., 1999). Mutations in TRD also occur in RTT patients, that could compromise the repression function of NCoR/SMRT/HDACs on MeCP2-regulated genes (Kokura et al., 2001; Lyst et al., 2013), suggesting a pathogenic role in RTT (Shahbazian et al., 2002; Guy et al., 2011). In this line, an hyperacetylation of the histone H3 was found in the brain of MeCP2-308 male mice bearing a truncating mutation on the *MeCP2* gene, leading to the expression of a protein truncated in the TRD at amino acid 308 (Shahbazian et al., 2002). Alterations in chromatin accessibility for transcriptional regulators and consequent alterations in gene transcription may thus occur in the brain of this RTT mouse model, explaining at least in part the altered RTT phenotype (Shahbazian et al., 2002).

In the present study we have further explored the therapeutic efficacy of repeated systemic treatment with the 5HT7R agonist LP-211 in MeCP2-308 mice (Shahbazian et al., 2002). Our previous studies have demonstrated that repeated systemic treatment with LP-211 (0.25 mg/kg once/day for 7 days) rescues several RTT-related behavioural alterations in MeCP2-308 mouse model restoring motor deficits, cognitive impairments and anxious profile and restoring altered proteins synthesis and synaptic plasticity (De Filippis et al., 2014; De Filippis et al., 2015a). Treatment efficacy was confirmed in symptomatic MeCP2-308 heterozygous female mice, the genetic and hormonal milieus that more closely resemble those of RTT patients. Moreover, we demonstrated that the LP-211 treatment restores mitochondria functions in the brain of heterozygous female mice from two highly validated mouse models of RTT (MeCP2-308 and MeCP2-Bird mice) (Valenti et al., 2017). Notably, the beneficial effects of LP-211 treatment on behavioural, molecular and brain mitochondrial defects were evident out up to 2 months after the last

83

injection, thus suggesting long-lasting effects of LP211 exposure on RTT-related impairments (De Filippis et al., 2015a).

Considering the wide variety of beneficial effect which LP-211 exerted in RTT mice (De Filippis et al., 2014; De Filippis et al., 2015a; Valenti et al., 2017), we reasoned that LP-211 treatment may have restored abnormal histone acetylation in RTT mouse brain (Shahbazian et al., 2002). To test this hypothesis, in the present study heterozygous fully symptomatic female MeCP2-308 female mice and wt littermates were treated with LP-211 (0.25 mg/kg once/day intraperitoneal (i.p.) injection for 7 days) or control (veh) solution, following previous treatment schedules (De Filippis et al., 2014; De Filippis et al., 2015a). The histones acetylation and the level of co-repressors proteins were evaluated in mouse brain to verify whether they are altered in RTT and LP-211 treatment effects thereon. In addition, to extend and support our previous results demonstrating widespread behavioural effects of the LP-211 treatment, physiological parameters, such as carotid distension, breath frequency and hearth rate, and sociability were evaluated in experimental mice, considering that in human RTT patients breath impairments and aberrant social behavior are present (Katz et al., 2009; Kaufmann et al., 2012).

## 2.3　Materials and methods

### 2.3.1　Subjects

The experimental subjects were 1-year old MeCP2-308 heterozygous female mice (RTT) [B6.129S-MeCP2tm1Heto/J, stock number: 005439; backcrossed to C57BL/6J mice for at least 12 generations from the Jackson Laboratories (USA)] and wild-type (wt) littermates. The MeCP2-308 model bears a truncating mutation, leading to the expression of a protein truncated at amino acid 308(Shahbazian et al., 2002; De Filippis et al., 2014; De Filippis et al., 2015a).

Mice were housed in 2-3 groups in polycarbonate transparent cages (33X13X14 cm) with sawdust bedding and kept on a 12-h light-dark schedule (lights off at 8:00 am). Temperature was maintained at 21 ±1 C° and relative humidity at 60± 10%. Animals were provided ad libitum with tap water and a complete pellet diet (Altromin, Germany). All experimental procedures were conducted in conformity with the European Directive 2010/63/EU and the Italian legislation on animal experimentation, D.Lgs. 26/2014 and formally approved by Italian Ministry of Health.

### 2.3.2　Genotyping

DNA has been prepared from a small tail-tip biopsy taken at 21–28 days of age, as previously described De Filippis et al., 2010). The MeCP2 alleles have been identified by PCR using two sets of primers. Primer set 1 (5′ primer: 5′-AAC GGG GTA GAA AGC CTG-3′ and 3′ primer: 5′-ATG CTC CAG ACT GCC TTG -3′) yields a product of 396 bp identifying the wildtype allele. Primer set 2 (5′ primer same as for primer set 1 and 3′ primer: 5′- TGA TGG GGT CCTCAG AGC -3′) yields a product of apparent size 318 bp identifying the null allele. PCR products were electrophoresed through a 2%

NuSieve 3:1 agarose gel (Cambrex Bio Science, Rockland, ME, USA) containing 0.5 µg/mL ethidium bromide, and examined under UV light.

### 2.3.3 Drug and Treatment

LP-211 was prepared following the same synthetic procedure described in(Leopoldo et al., 2008). The compound was dissolved in a vehicle solution of 1% dimethyl sulfoxide (DMSO) in saline (0.9% NaCl). RTT mice and wt littermate controls were randomly assigned to be daily intra-peritoneally (ip) injected (between 9.00 and 11.00 am) for 7 consecutive days with either LP-211 (0.25 mg/kg) or vehicle (1% of DMSO in saline) (veh). The following sample size was used for the behavioural tasks: MouseOx: wt, veh = 11; wt, LP-211 = 10; Het, veh = 6; Het, LP-211 = 8; Three chamber: wt, veh = 9; wt, LP-211 = 8; Het, veh = 5; Het, LP-211 = 7.

To test whether LP-211 can counteract RTT related abnormalities when they are fully manifested, RTT mice were treated at about 12 months of age, in which RTT mice are fully symptomatic (De Filippis et al., 2014; De Filippis et al., 2015a).

### 2.3.4 In vivo testing

Mice were experimentally naïve at the start of the test battery. All in vivo testing took place during the dark phase of the L/D cycle and was carried out by experimenters blind to mouse genotypes and treatments. Behavioural testing started 1 month after the end of the i.p. treatment, according to the schedule described in (De Filippis et al., 2015a). In particular, physiological parameters were evaluated on the day 35 of the schedule; the Three-Chamber Social test was performed on day 41 of the schedule (see Figure 1A for experimental design and treatment schedule). The brains of the experimental mice were collected two months after the last i.p. injection, based on previous

data suggesting long-term effects of a seven-day-long treatment with LP-211 (De Filippis et al., 2015a).
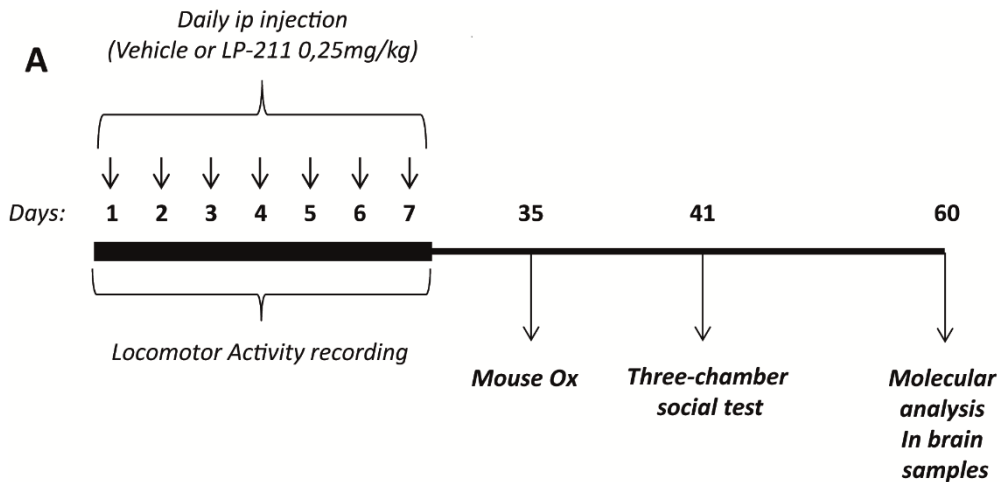


**Fig. 1: (A)** Experimental schedule

## 2.3.4.1 Three chambered social test

Sociability and social recognition were assessed in the three-chambered test, as previously described (Smith et al., 2007; Vigli et al., 2018a). The test consists of 4 consecutive phases of 10 minutes during which each mouse is individually placed in the apparatus: Phase 1 (S1): mice can freely explore the central chamber of the apparatus; Phase 2 (S2): mice can explore the three empty chambers; Phase 3 (S3): mice can explore either the chamber containing an empty small wire cage or the other one containing a conspecific kept under an identical small wire cage; Phase 4 (S4): an unfamiliar mouse is located under the cage wire which was empty during S3. Allocation of mouse partners to specific chambers was counterbalanced within each experimental group. Time spent exploring the mouse versus the empty wire cage during S3 is considered as an index of sociability. Time spent exploring the unfamiliar mouse versus the familiar one during S4 is considered as an index of memory

87

of the social stimuli. Naïve C57 adult male mice were used as partners in this test. They were first habituated to the small wire cages in the test environment for 2 consecutive days before the testing day. After each animal was tested, the three-chamber apparatus and the wire cages were thoroughly cleaned with 70% ethanol.

### 2.3.4.2 Physiological parameters measurement

The non-invasive MouseOx Apparatus (STARR Life Sciences, Holliston, Ma, USA) allows the measure of the Oxygen Saturation (% = percentage of hemoglobin saturated by O2), Heart rate (bpm = number of beats per minute) and Breath Rate (brpm = number of breaths per minute) and the Pulse Distention (μm = distention of the blood carotid artery due to a cardiac pulse). Experimental subjects were habituated to the collar clip placing a blank collar on the neck for 12h the day before the test. On the testing day, blank collar was removed from the neck of the animal and substituted with the infrared pulse oximeter clip connected to the instrument. Physiological parameters were recorded for 10 minutes as reported in previous studies (Bittolo et al., 2016).

### 2.3.5   Molecular analysis

### 2.3.5.1 Protein extraction

Histone proteins from mice cortex and hippocampus were extracted using the EpiQuik™ Total Histone Extraction Kit (EpiGentek), according to the manufacturer's instructions, in presence of Proteases Inhibitor Cocktail (PIC 1X, Sigma) and 1mM Phenyl methyl sulfonyl fluoride (PMSF). Total histone proteins were collected and quantified by Bradford Assay (Bio-Rad) at 595 nm with a microplate-reader Appliskan TM (Thermofisher). Total Histone extracts were aliquoted and stored the at –80°C until use.

To analyse endogenous proteins, cortex and hippocampus samples were lysed in RIPA buffer (50 mM pH 7,4 Tris HCl, 150 mM NaCl, 1.0% NP-40, 0.5% deoxycholic acid (NaDOC), 0.1% SDS, 1 mM EDTA, 5mM NaF, 1 mM Na3VO4) supplemented with 1X PIC and 1 mM PMSF. Briefly, small tissue pieces resuspended in RIPA buffer were homogenized through at least 20-30 strokes in a Dounce homogenizer and incubated on ice for 30 min with gentle stirring. Protein extracts were obtained by centrifugation at 14000 rpm for 10 min at 4°C. The supernatants were collected and the proteins concentration was determined by Bradford Assay, as described above. The extracts were aliquoted and stored the at –80°C.

## 2.3.5.2 Western Blot (WB)

Histone and endogenous protein extracts were resolved by gel electrophoresis on a 4–20% polyacrylamide gradient PROTEAN® TGX Stain-Free™ protein gel (Bio-Rad) and transferred onto a PVDF membrane (Biorad) by Trans-Blot® Turbo™ Transfer System (Bio-Rad). Membranes were blocked in 5% milk in TBST for 1 hour at room temperature, and then incubated with indicated antibodies: polyclonal anti-Di-Methyl Histone H3 (Lys9) (1:1000) (Cell Signaling), polyclonal anti-acetyl-Histone H3 (1:500-1:1000) (Millipore), polyclonal anti-H3 (1:1500), polyclonal anti-SIN3α (1:500), monoclonal anti-MeCP2 (1:500) (Sigma)or polyclonal anti-MeCP2 (1:500), polyclonal anti-NCoR (1:500) (abcam®), monoclonal anti-HDAC1 (1:500), monoclonal anti-HDAC3 (1:500), monoclonal anti-GAPDH (1:5000), monoclonal anti-actin (1:5000) (Santa Cruz Biotechnology). The proteins were visualized by chemiluminescence detection with LuminataCrescendo Western HRP substrate (Millipore) using ChemiDoc™ MP System (Bio-Rad), and densitometric analyses were performed with ImageLab software (Bio-Rad) and normalized to a reference protein.

### 2.3.6    Statistical analysis

Behavioural data were analysed with two-way ANOVA models, using statistical software (Statview v 5.0) including genotype and treatment as between-subject factors and repeated measurements as within-subject factor. The alpha level was set to 5%. The Levene test was applied to confirm the equality of variance. The presence of outliers was verified using Grubbs method. Post-hoc comparisons were performed by Tukey HSD, even in the absence of statistically significant interactions (Wilcox, 1987).  For the western blot analyses, data were analysed with one-way ANOVA models, using statistical software (Graphpad Prism v. 6.0) Experiments were repeated at least three times. Post-hoc comparisons were performed by Bonferroni post hoc test; p values <0.05 were regarded as significant.

# 2.4    Results

## 2.4.1    In vivo testing results

### 2.4.1.1 Three chambered social test

The three chambered social test was performed to evaluate sociability skill in RTT mice and LP-211 effects thereon. The analysis of the S3 phase highlighted a statistically significant genotype difference, with RTT mice showing an aberrant hyper preference for the social stimulus (versus the empty cage) in comparison to wt controls [Fig. 1B; $p < 0.05$ after *post-hoc* comparison on Genotype*Treatment interaction $F_{(1,25)}= 9.888$ $p = 0.004$]. Importantly, the LP-211 treatment rescued this social deficit in RTT mice, restoring wt-like levels of the social preference [Fig. 1B; $p < 0.05$ after *post-hoc* comparison on Genotype*Treatment interaction]. From the S4 analysis, no genotype or treatment effects were highlighted (*data not shown*).

**B**
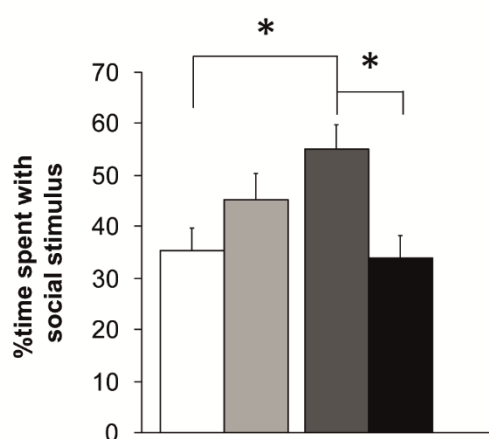


**Fig. 1:** *LP-211 treatment rescues social defects in RTT female mice*. (**B**) The three-

chamber social task highlighted aberrant sociability in RTT mice, measured as % of time spent with the social stimulus, in comparison to wt controls. This abnormal behaviour was restored by LP-211 treatment, that restored to wt-like levels the % of time spent with social stimulus in RTT mice. Data are mean ± SEM. Statistical significance was calculated by two-way ANOVA with Tukey's post hoc test. $p < 0.01$; **, $p < 0.05$, *

### 2.4.1.2 Physiological parameters

The MouseOx was applied to evaluate the presence of cardiac and breath impairments in RTT mice. A genotype difference was found on Pulse distention parameter, with RTT mice showing a lower carotid artery distention in comparison with wt controls [Fig. 1C; $p < 0.05$ after *post-hoc* comparison on Genotype*Treatment interaction $F_{(1,31)}= 4.506$ $p = 0.042$]. Furthermore, LP-211 treatment increased pulse distention dysfunction in RTT mice, restoring carotid artery distention at the same level of wt controls [Fig. 1C; $p < 0.05$ after *post-hoc* comparison on Genotype*Treatment interaction]. No genotype differences were found as for SpO2, Hearth rate and Breath rate and the LP-211 treatment did not affect these parameters.

**C**
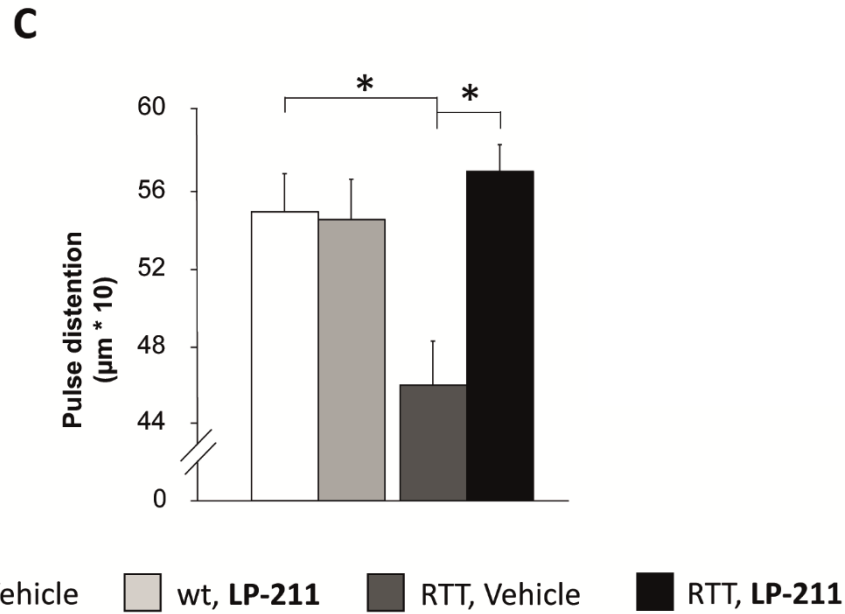
**Fig. 1:** *LP-211 treatment rescues pulse distention in RTT female mice*. (**C**) it has been possible to detect a defective pulse distention in RTT mice compared to wt littermates was found through the MouseOx apparatus. LP-211 treatment rescued this defective parameter in RTT mice, increasing levels of pulse distention. Data are mean ± SEM. Statistical significance was calculated by two-way ANOVA with Tukey's post hoc test. $p < 0.01$; **, $p < 0.05$, *

## 2.4.2 Molecular results

### 2.4.2.1 LP-211 treatment normalizes the abnormal acetylation level of histone H3 in RTT mouse cortex and hippocampus

To clarify the possible relationship between MeCP2 and alterations in histone H3 modifications in RTT, we analyzed acetylation of the lysine 9 on the histone H3 (K9H3) in cortex and in hippocampus of RTT mice. We found that RTT mice showed lower levels of cortical histone H3 acetylation compared to wt mice (Fig.2A $p < 0.01$ after *post-hoc* comparison),whereas the hippocampus of RTT mice was characterized by hyperacetylation of histone

93

H3 (Fig.2B; p < 0.01 after *post-hoc* comparison). LP-211 treatment normalized histone H3 acetylation levels in both brain areas of RTT mice in comparison to veh treated RTT mice (Fig.2A,B; p < 0.01 and p < 0.05 for LP-211 effect in cortex and hippocampus respectively, after *post-hoc* comparison).
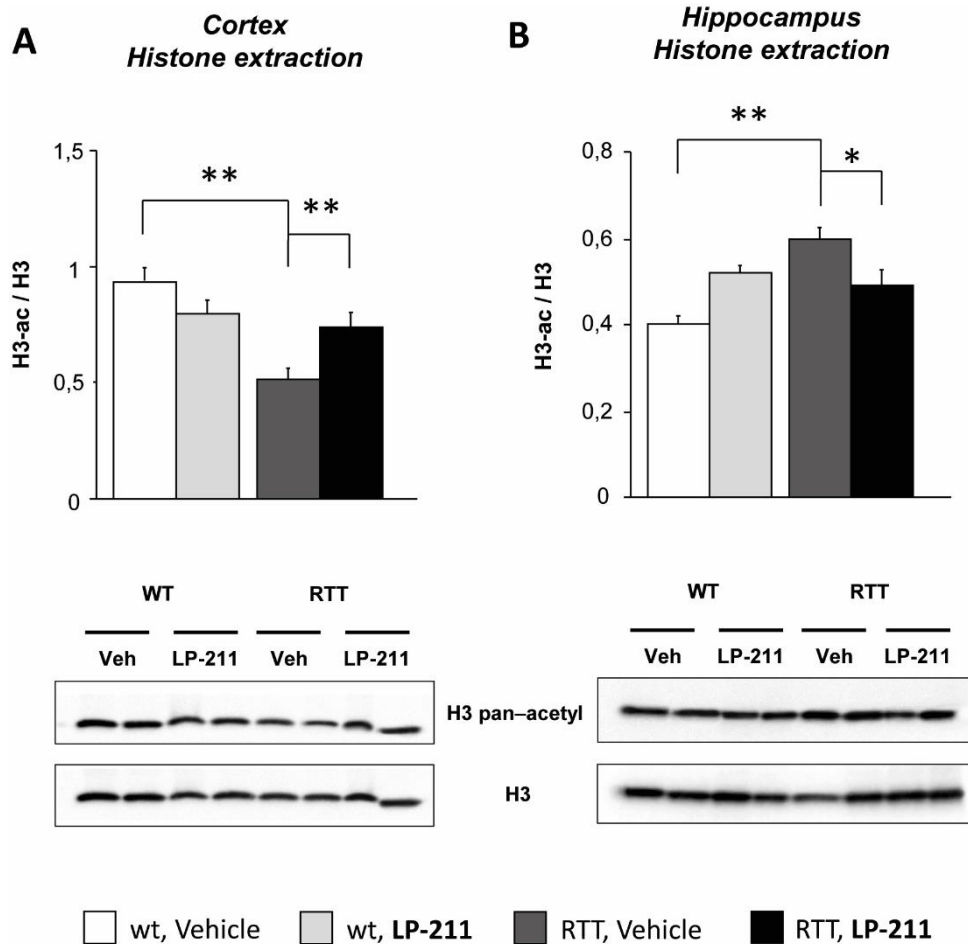


**Fig. 2:** *LP-211 treatment normalizes cortical and hippocampal histone H3 acetylation level in RTT female mice*. Cortical and hippocampal histone H3 acetylation levels were evaluated by western blot analysis. RTT mice showed a histone H3 hyperacetylation in cortex **(A)** and a histone H3 hypoacetylation in the hippocampus compared to wt **(B)**; in both brain regions, LP-211 treatment normalizes histone H3 acetylation levels, restoring them to wt levels **(A-B)**. Data are mean ± SEM. Statistical

significance was calculated by one-way ANOVA with Bonferroni post hoc test. $p < 0.01$; **, $p < 0.05$, *

## 2.4.2.2 LP-211 treatment influences cortical and hippocampal levels of MeCP2 complexes proteins in RTT mouse model

We assessed whether NCoR/HDAC3 and SIN3α/HDAC1 have different protein levels in the cortex and in the hippocampus of RTT mice and whether LP-211 was able to modulate them.

In the cortex of RTT mice we found a significant increase of NCoR and HDAC3 protein level up to 50% compared with WT mice (Fig.3A,B; NCoR: $p < 0.05$ and HDAC3: $p < 0.05$ after *post-hoc* comparison). LP-211 administration markedly reduced the levels of both proteins in comparison with RTT mice, thus restoring wt-like levels (Fig.3A,B ; $p < 0.05$ and $p < 0.05$ for LP-211 effect in cortical levels of NCoR and HDAC3 respectively, after *post-hoc* comparison).

On the contrary, no genotype difference was highlighted for SIN3α levels (Fig. 3D); HDAC1 showed a slight decrease, just missing statistical significance (Fig. 3C). LP-211 treatment increased HDAC1 and SIN3α protein levels selectively in RTT mouse cortex (Fig.3C,D ; $p < 0.05$ and $p < 0.01$ for LP-211 effect in cortical levels of HDAC1 and SIN3α respectively, after *post-hoc* comparison).
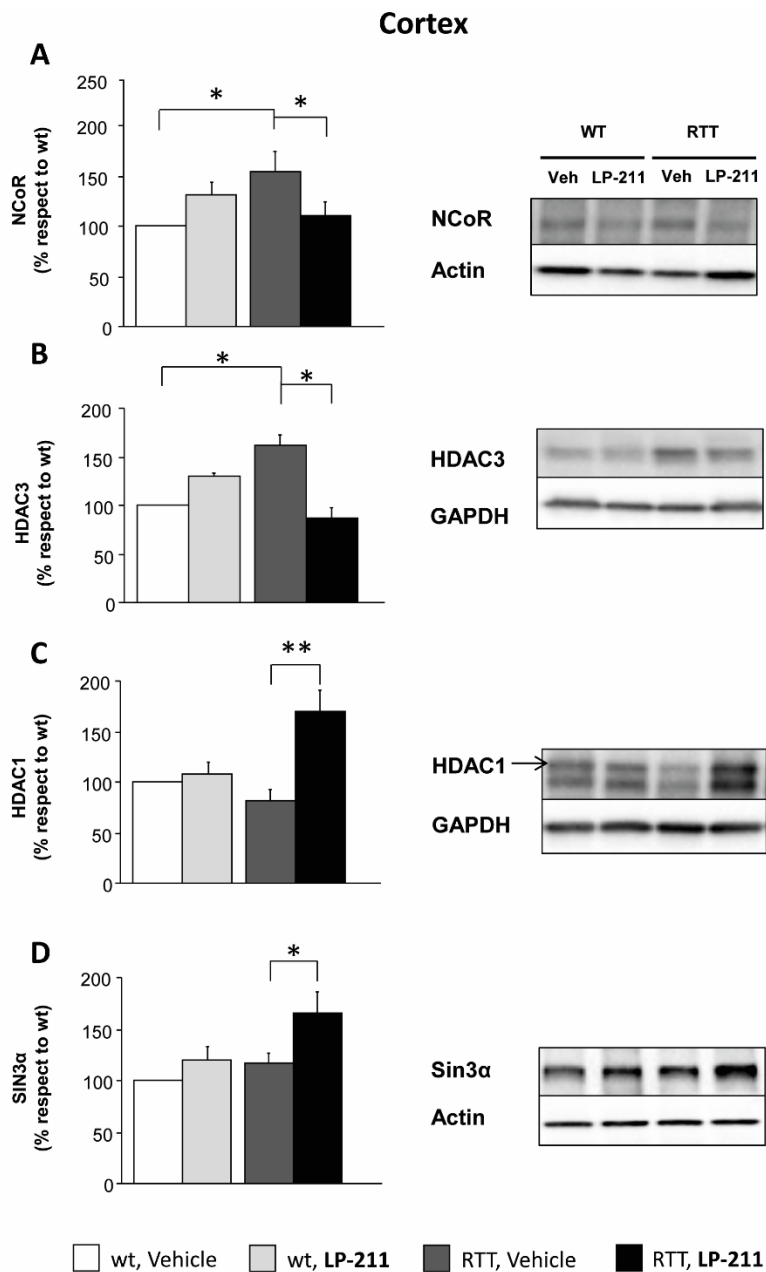
**Fig. 3:** *LP-211 treatment normalizes altered cortical levels of NCoR and HDAC3 and increases levels of SIN3α and HDAC1 in RTT female mice.* Western blot analyses highlighted increased levels of the NCoR **(A)** and HDAC3 **(B)** in the cortex of RTT mice compared to wt littermates. No genotype differences emerged analyzing HDAC

1 and SIN3α levels **(C-D)**; in the cortex of RTT female mice LP-211 treatment restored normal levels of NCoR **(A)** and HDAC3 **(B),** in comparison to veh treated RTT mice and increased levels of HDAC 1 and SIN3α **(C-D)**. Data are mean ± SEM. Statistical significance was calculated by one-way ANOVA with Bonferroni post hoc test. $p < 0.01$; **, $p < 0.05$, *

In the hippocampus of RTT mice we found a significant decrease of NCoR protein levels (Fig.4A; $p < 0.01$ after *post-hoc* comparison). LP-211 treatment did not rescue this alteration. No alterations in RTT mice were found considering the levels of HDAC3, HDAC1 and SIN3α levels. However, in RTT mice, LP-211 treatment increased HDAC3 and SIN3α levels (Fig.4B,D; HDAC3: $p < 0.05$ and SIN3α: $p < 0.05$ after *post-hoc* comparison).
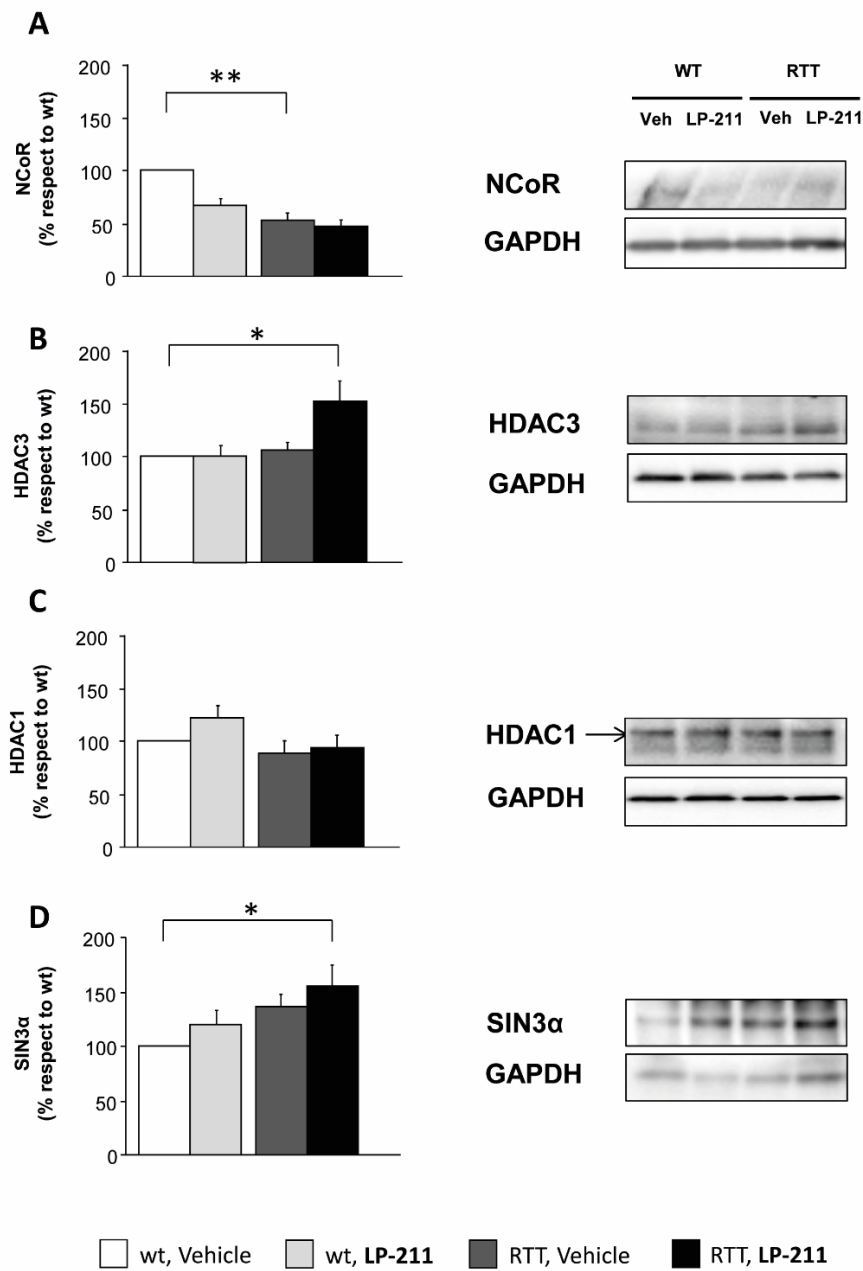
**Fig. 4:** *LP-211 treatment modulates hippocampal levels of SIN3α and HDAC3 in RTT female mice*. Western blot analyses highlighted lower levels of the NCoR **(A)** in the hippocampus of RTT mice compared to wt littermates. No genotype differences

emerged analyzing HDAC3, HDAC 1 and SIN3α, levels **(B-C-D)**; in the hippocampus of RTT female mice LP-211 treatment increase levels of SIN3α **(B)** and HDAC3 **(D),** in comparison to veh treated wt mice. Data are mean ± SEM. Statistical significance was calculated by one-way ANOVA with Bonferroni post hoc test. $p < 0.01$; **, $p < 0.05$, *

## 2.5 Discussion

The present study extends previous results about the treatment effects of the 5-HT$_7$R agonist LP-211 in a fully symptomatic mouse model of RTT syndrome (12 months of age) (De Filippis et al., 2014; De Filippis et al., 2015a), showing a normalization of the carotid pulse distension and a rescue of the aberrant sociability in female RTT mice. Moreover, we found for the first time a normalization of the altered histone H3 acetylation and NCoR and HDAC3 levels in the cortex of LP-211 treated RTT mice. Present results provide further support on the therapeutic efficacy of the LP-211 treatment for RTT and shed some light on the molecular mechanisms underlying the reported beneficial effects of LP-211.

Social impairments are a common symptom characterizing RTT. Alterations in social behaviors have been widely studied, reporting mild to severe impairments that are consistent with reports in RTT girls (Ricceri et al., 2012). Contrary to what expected, we found an aberrant sociability in fully symptomatic MeCP2-308 female mouse model at 9-12 months of age, showing an increase social preference, that was completely rescued by LP-211 treatment. Indeed, previous studies demonstrated the presence of defective sociability in MeCP2-308 female and male mice respectively at 2 or 5 months of age, showing low social preference (Woods et al., 2012; Vigli et al., 2018a). However, another work reported an increase social behaviour displayed by 3 months old MeCP2-308 male mice measured in the same task using a slightly

different protocol (Pearson et al., 2012). Even though several studies have reported the presence of sex and/or age difference when measuring the sociability (Greenberg et al., 2013; Shoji et al., 2016), altogether these results suggest that the old age of the experimental mice or the sex of the animals may not sufficient to explain the hyper-sociability we uncovered in the present study. Further studies are thus needed to clarify the mechanisms leading to social deficit in RTT.

Cardiorespiratory dysfunctions occurring in RTT patients in the late stage of the disorder, are responsible for 26% of deaths (Rohdin et al., 2007) and these alterations are also detectable in mouse models (Johnson et al., 2015; Bittolo et al., 2016). Using the MouseOx, we recorded, for the first time in this RTT mouse model, several cardio circulatory parameters. We found a severe pulse distention impairment in RTT mice. This alteration suggests that carotid stenosis may occur in this RTT mouse model, possibly as a result of a sort of occlusion or vasculopathy leading to a decrease in the oxygenated blood flow rate and a consequent decrease in brain oxygen levels (Olivera et al., 2010; Nayak et al., 2014). In present study we demonstrate that LP-211 treatment rescues the pulse distention deficit in RTT mice, restoring it to wt levels. These data are in agreement with previous work suggesting that the 5-HT7 receptor mediates 5-HT induced dilation of the carotid artery (Villalon et al., 1997; Terron and Martinez-Garcia, 2007). Carotid stenosis is an important risk factor for stroke and it was associated with the presence of cognitive dysfunction and psychiatric symptomatology in humans (Sours, 1964; Kim et al., 2007) and mice (Jiwa et al., 2010). In this line, restoration of pulse distention impairment by LP-211 treatment was accompanied by a substantial rescue of behavioural alterations in RTT mice (Table 1, in bold the new results). Even though further studies are necessary to elucidate the correlation between the effects of

possible carotid stenosis and the severity of RTT symptomatology, present results provide further support to the therapeutic value of this pharmacological approach.

Given the promising behavioural results so far obtained (Table 1), we have further explored the molecular mechanisms underlying the reported beneficial effects of the LP-211 treatment in RTT mouse brain. Notably, we found that the LP-211 treatment was able to counterbalance histone H3 acetylation abnormalities in RTT mouse brain in comparison to veh treated RTT mice, suggesting H3 acetylation modulation as a good target to ameliorate RTT phenotype. Indeed, compelling evidence demonstrate a tight link between histone acetylation abnormalities and poor synaptic plasticity and memory (Alarcon et al., 2004; Levenson et al., 2004; Yeh et al., 2004; Fischer et al., 2007; Vecsey et al., 2007; Stefanko et al., 2009). Moreover, epigenetic modifications play a fundamental role in the pathogenesis of different neurocognitive and neurodegenerative disorders, including autism spectrum disorders, intellectual disability disorders, schizophrenia, and epilepsy (Koshibu et al., 2009; Miller et al., 2010; Graff et al., 2012). Of note, several evidences also suggest that the histone acetylation is important for the control of lipid homeostasis and mitochondria activity (Shen et al., 2015), both of which are altered in RTT (Kyle et al., 2016; Valenti et al., 2017).

Interestingly, however, different brain areas presented opposite profiles, with the RTT hippocampus presenting the expected hyperacetylation of H3, while the cortex showing lower levels of histone acetylation in RTT mice compared to wt mice.

The decrease in global acetylation levels of the histone H3 we found in the cortex of RTT mice was in fact surprising, as previous work reported a

cortical histone H3 hyperacetylation in the same RTT mouse model (Shahbazian et al., 2002). One possible explanation for this discrepancy may derive from the sex of the animals. Indeed, in the present study, we quantified for the first time the histone H3 acetylation level in two different brain regions of MeCP2-308 heterozygous female mice. Differences between male and female in the modulation of gene expression involving histone methylation and acetylation have been hypothesized in previous studies, suggesting a key role of the sex-hormones in the regulation of epigenetic modification in complex diseases, such as autism and depression (Kaminsky et al., 2006). Another important difference from the study of Shahbazian and colleagues was the age of the mice (3-5 months vs 12 months of age in the present study) which could explain, at least in part, the different H3 acetylation levels in cortical brain areas. Indeed, previous works showed differences of acetylation levels of H3 and H4 in the visual cortex of 1 month of age mice compared to adult mice (about 3 months of age), demonstrating the impact of visual experience on acetylation (Vierci et al., 2016). In addition, in previous studies no cortical hyperacetylation of histone H3 and H4 was found on 2 months old female RTT-*null* mice (Urdinguio et al., 2007), suggesting that acetylation process may be dependent, beside the age, also on the type of *MeCP2* mutation occurring in RTT mouse models.

To understand the causes leading to this unexpected acetylation profile in RTT mouse brain and LP-211 treatment thereon, we verified whether brain-area specific differences in the levels of SIN3α, NCoR, HDAC1 and 3 might be found in RTT mouse brain. In fact, all these proteins are able to directly or indirectly associate with an array of DNA binding repressors, beyond MeCP2 (Guenther et al., 2001). Interestingly, we found a hyper-expression of the NCoR and HDAC3 proteins in RTT mouse cortex, that was completely

normalized by LP-211 treatment. These results are consistent with the possibility that NCoR/HDAC3 complex in this brain area might be responsible for the H3 histone hypo-acetylation. Indeed, HDAC3 regulates many biological processes in a variety of tissues, such as lipid metabolism in liver and heart and the cell cycle progression of fibroblasts (Sun et al., 2013), which may be relevant for RTT. Moreover, neuronal deletion of *Hdac3* in mice elicits abnormal locomotor coordination, defective sociability, and cognition (Nott et al., 2016). The observation that lower levels of histone acetylation are accompanied by the overexpression of HDAC3 in RTT mouse cortex thus suggests that MeCP2-independent catalytic activity of NCoR/HDAC3 may be abnormal in this brain areas and that the LP-211-induced restoration of HDAC3 may at least partially account for the beneficial effects exerted by the pharmacological treatment under investigation on behavioural parameters. Considering the complexity of the epigenetic regulation of gene expression and the involvement of numerous actors in this process, such as the histones acetyltransferase (HAT), the Acetyl-CoA, NAD+ and HDACs (Shen et al., 2015), we cannot exclude that LP-211 treatment may exert its beneficial effects on histone H3 acetylation in the brain of RTT mice by modulating the levels and the functionality of other proteins.

A different profile was found in the hippocampus of RTT mice, in which lower levels of NCoR protein, in the absence of changes in HDAC3, were found. Present molecular results, together with the observation that cortical and hippocampal brain areas present opposite H3 acetylation levels in RTT mice compared to wt controls, are consistent with the idea that MeCP2 function differs between cell types and that the lack of fully functional MeCP2 may differentially impact the complex regulation of gene transcription in a brain-area specific manner (Lyst and Bird, 2015).

103

Even though no alterations in SIN3α and HDAC1 protein levels were found in the hippocampus or the cortex of RTT mice, we found that the LP-211 treatment significantly increased SIN3α and HDAC1 level in both brain areas selectively in RTT mice. These results suggest that the LP-211 treatment may have boosted MeCP2-independent catalytic activity of SIN3α in RTT mouse brain. In fact, SIN3α plays a key role in regulation of lifespan and health maintenance (Barnes et al., 2014) as well as in mitochondrial function regulation (Pile et al., 2003; Barnes et al., 2010; Barnes et al., 2014), thus representing an intriguing therapeutic target. Dysfunction in the bioenergetic metabolism and in brain mitochondria functionality has been consistently demonstrated in RTT mice (Valenti et al., 2014; De Filippis et al., 2015b) , that was completely normalized by the LP-211 treatment (Valenti et al., 2017). Further exploring LP-211 effects on Sin3a functionality could thus provide interesting results.

In conclusion, the present study provides evidence that the LP-211 treatment can rescue histone acetylation abnormalities, even though they are present in opposite directions in different brain areas. Moreover, present data extend previous behavioural results demonstrating the beneficial effects of LP-211 treatment also on alterations in the social sphere and on the cardiocirculatory impairments detected in a female mouse model of RTT. Even though further studies are needed to understand the importance of histone acetylation in different brain area behaviourally relevant for RTT and to clarify whether LP-211 treatment can repristinate the MeCP2 functionality, present results shed some light on the molecular mechanisms underlying the beneficial effects of the LP-211 treatment and add further support to the translational value of this promising pharmacological approach.

# 2.6    References

Alarcon, J. M., Malleret, G., Touzani, K., Vronskaya, S., Ishii, S., Kandel, E. R., Barco, A., 2004. Chromatin acetylation, memory, and LTP are impaired in CBP+/- mice: a model for the cognitive deficit in Rubinstein-Taybi syndrome and its amelioration. Neuron 42, 947-959.

Amir, R. E., Van den Veyver, I. B., Wan, M., Tran, C. Q., Francke, U., Zoghbi, H. Y., 1999. Rett syndrome is caused by mutations in X-linked MECP2, encoding methyl-CpG-binding protein 2. Nat Genet 23, 185-188.

Bard, J. A., Zgombick, J., Adham, N., Vaysse, P., Branchek, T. A., Weinshank, R. L., 1993. Cloning of a novel human serotonin receptor (5-HT7) positively linked to adenylate cyclase. J Biol Chem 268, 23422-23426.

Barnes, V. L., Bhat, A., Unnikrishnan, A., Heydari, A. R., Arking, R., Pile, L. A., 2014. SIN3 is critical for stress resistance and modulates adult lifespan. Aging (Albany NY) 6, 645-660.

Barnes, V. L., Strunk, B. S., Lee, I., Huttemann, M., Pile, L. A., 2010. Loss of the SIN3 transcriptional corepressor results in aberrant mitochondrial function. BMC Biochem 11, 26.

Bittolo, T., Raminelli, C. A., Deiana, C., Baj, G., Vaghi, V., Ferrazzo, S., Bernareggi, A., Tongiorgi, E., 2016. Pharmacological treatment with mirtazapine rescues cortical atrophy and respiratory deficits in MeCP2 null mice. Scientific Reports 6, 19796.

Canese, R., Zoratto, F., Altabella, L., Porcari, P., Mercurio, L., de Pasquale, F., Butti, E., Martino, G., Lacivita, E., Leopoldo, M., Laviola, G., Adriani, W., 2014. Persistent modification of forebrain networks and

metabolism in rats following adolescent exposure to a 5-HT7 receptor agonist. Psychopharmacology (Berl) 232, 75-89.

Ciranna, L., Catania, M. V., 2014. 5-HT7 receptors as modulators of neuronal excitability, synaptic transmission and plasticity: physiological role and possible implications in autism spectrum disorders. Front Cell Neurosci 8, 250.

Costa, L., Sardone, L. M., Bonaccorso, C. M., D'Antoni, S., Spatuzza, M., Gulisano, W., Tropea, M. R., Puzzo, D., Leopoldo, M., Lacivita, E., Catania, M. V., Ciranna, L., 2018. Activation of Serotonin 5-HT7 Receptors Modulates Hippocampal Synaptic Plasticity by Stimulation of Adenylate Cyclases and Rescues Learning and Behavior in a Mouse Model of Fragile X Syndrome. Frontiers in Molecular Neuroscience 11.

De Filippis, B., Chiodi, V., Adriani, W., Lacivita, E., Mallozzi, C., Leopoldo, M., Domenici, M. R., Fuso, A., Laviola, G., 2015a. Long-lasting beneficial effects of central serotonin receptor 7 stimulation in female mice modeling Rett syndrome. Front Behav Neurosci 9, 86.

De Filippis, B., Nativio, P., Fabbri, A., Ricceri, L., Adriani, W., Lacivita, E., Leopoldo, M., Passarelli, F., Fuso, A., Laviola, G., 2014. Pharmacological stimulation of the brain serotonin receptor 7 as a novel therapeutic approach for Rett syndrome. Neuropsychopharmacology 39, 2506-2518.

De Filippis, B., Ricceri, L., Laviola, G., 2010. Early postnatal behavioral changes in the Mecp2-308 truncation mouse model of Rett syndrome. Genes Brain Behav 9, 213-223.

De Filippis, B., Valenti, D., de Bari, L., De Rasmo, D., Musto, M., Fabbri, A., Ricceri, L., Fiorentini, C., Laviola, G., Vacca, R. A., 2015b. Mitochondrial free radical overproduction due to respiratory chain impairment in the brain of a mouse model of Rett syndrome: protective effect of CNF1. Free Radic Biol Med 83, 167-177.

Fischer, A., Sananbenesi, F., Wang, X., Dobbin, M., Tsai, L. H., 2007. Recovery of learning and memory is associated with chromatin remodelling. Nature 447, 178-182.

Gellynck, E., Heyninck, K., Andressen, K. W., Haegeman, G., Levy, F. O., Vanhoenacker, P., Van Craenenbroeck, K., 2013. The serotonin 5-HT7 receptors: two decades of research. Exp Brain Res 230, 555-568.

Graff, J., Woldemichael, B. T., Berchtold, D., Dewarrat, G., Mansuy, I. M., 2012. Dynamic histone marks in the hippocampus and cortex facilitate memory consolidation. Nat Commun 3, 991.

Greenberg, G. D., Laman-Maharg, A., Campi, K. L., Voigt, H., Orr, V. N., Schaal, L., Trainor, B. C., 2013. Sex differences in stress-induced social withdrawal: role of brain derived neurotrophic factor in the bed nucleus of the stria terminalis. Front Behav Neurosci 7, 223.

Guenther, M. G., Barak, O., Lazar, M. A., 2001. The SMRT and N-CoR corepressors are activating cofactors for histone deacetylase 3. Mol Cell Biol 21, 6091-6101.

Guseva, D., Wirth, A., Ponimaskin, E., 2014. Cellular mechanisms of the 5-HT7 receptor-mediated signaling. Front Behav Neurosci 8, 306.

Guy, J., Cheval, H., Selfridge, J., Bird, A., 2011. The role of MeCP2 in the brain. Annu Rev Cell Dev Biol 27, 631-652.

Hagberg, B., Hanefeld, F., Percy, A., Skjeldal, O., 2002. An update on clinically applicable diagnostic criteria in Rett syndrome. Comments to Rett Syndrome Clinical Criteria Consensus Panel Satellite to European Paediatric Neurology Society Meeting, Baden Baden, Germany, 11 September 2001. Eur J Paediatr Neurol 6, 293-297.

Hedlund, P. B., Leopoldo, M., Caccia, S., Sarkisyan, G., Fracasso, C., Martelli, G., Lacivita, E., Berardi, F., Perrone, R., 2010. LP-211 is a brain penetrant selective agonist for the serotonin 5-HT(7) receptor. Neurosci Lett 481, 12-16.

Hedlund, P. B., Sutcliffe, J. G., 2004. Functional, molecular and pharmacological advances in 5-HT7 receptor research. Trends Pharmacol Sci 25, 481-486.

Ivachtchenko, A. V., Lavrovsky, Y., Okun, I., 2016. AVN-101: A Multi-Target Drug Candidate for the Treatment of CNS Disorders. J Alzheimers Dis 53, 583-620.

Jiwa, N. S., Garrard, P., Hainsworth, A. H., 2010. Experimental models of vascular dementia and vascular cognitive impairment: a systematic review. J Neurochem 115, 814-828.

Johnson, C. M., Cui, N., Zhong, W., Oginsky, M. F., Jiang, C., 2015. Breathing abnormalities in a female mouse model of Rett syndrome. J Physiol Sci 65, 451-459.

Jones, P. L., Veenstra, G. J., Wade, P. A., Vermaak, D., Kass, S. U., Landsberger, N., Strouboulis, J., Wolffe, A. P., 1998. Methylated DNA and MeCP2 recruit histone deacetylase to repress transcription. Nat Genet 19, 187-191.

Kaminsky, Z., Wang, S. C., Petronis, A., 2006. Complex disease, gender and epigenetics. Ann Med 38, 530-544.

Katz, D. M., Dutschmann, M., Ramirez, J. M., Hilaire, G., 2009. Breathing disorders in Rett syndrome: progressive neurochemical dysfunction in the respiratory network after birth. Respir Physiol Neurobiol 168, 101-108.

Kaufmann, W. E., Tierney, E., Rohde, C. A., Suarez-Pedraza, M. C., Clarke, M. A., Salorio, C. F., Bibat, G., Bukelis, I., Naram, D., Lanham, D. C., Naidu, S., 2012. Social impairments in Rett syndrome: characteristics and relationship with clinical severity. J Intellect Disabil Res 56, 233-247.

Kim, J. E., Lee, B. R., Chun, J. E., Lee, S. J., Lee, B. H., Yu, I. K., Kim, S., 2007. Cognitive dysfunction in 16 patients with carotid stenosis: detailed neuropsychological findings. J Clin Neurol 3, 9-17.

Kokura, K., Kaul, S. C., Wadhwa, R., Nomura, T., Khan, M. M., Shinagawa, T., Yasukawa, T., Colmenares, C., Ishii, S., 2001. The Ski protein family is required for MeCP2-mediated transcriptional repression. J Biol Chem 276, 34115-34121.

Koshibu, K., Graff, J., Beullens, M., Heitz, F. D., Berchtold, D., Russig, H., Farinelli, M., Bollen, M., Mansuy, I. M., 2009. Protein phosphatase 1

regulates the histone code for long-term memory. J Neurosci 29, 13079-13089.

Kyle, S. M., Saha, P. K., Brown, H. M., Chan, L. C., Justice, M. J., 2016. MeCP2 co-ordinates liver lipid metabolism with the NCoR1/HDAC3 corepressor complex. Hum Mol Genet 25, 3029-3041.

Leopoldo, M., Lacivita, E., Berardi, F., Perrone, R., Hedlund, P. B., 2011. Serotonin 5-HT7 receptor agents: Structure-activity relationships and potential therapeutic applications in central nervous system disorders. Pharmacol Ther 129, 120-148.

Leopoldo, M., Lacivita, E., De Giorgio, P., Fracasso, C., Guzzetti, S., Caccia, S., Contino, M., Colabufo, N. A., Berardi, F., Perrone, R., 2008. Structural modifications of N-(1,2,3,4-tetrahydronaphthalen-1-yl)-4-aryl-1-piperazinehexanamides: influence on lipophilicity and 5-HT7 receptor activity. Part III. J Med Chem 51, 5813-5822.

Levenson, J. M., O'Riordan, K. J., Brown, K. D., Trinh, M. A., Molfese, D. L., Sweatt, J. D., 2004. Regulation of histone acetylation during memory formation in the hippocampus. J Biol Chem 279, 40545-40559.

Lyst, M. J., Ekiert, R., Ebert, D. H., Merusi, C., Nowak, J., Selfridge, J., Guy, J., Kastan, N. R., Robinson, N. D., de Lima Alves, F., Rappsilber, J., Greenberg, M. E., Bird, A., 2013. Rett syndrome mutations abolish the interaction of MeCP2 with the NCoR/SMRT co-repressor. Nat Neurosci 16, 898-902.

Meneses, A., 2014. Memory formation and memory alterations: 5-HT6 and 5-HT7 receptors, novel alternative. Rev Neurosci 25, 325-356.

Miller, S., Razvi, S., Russell, A., 2010. Reading epilepsy. Pract Neurol 10, 278-281.

Nan, X., Ng, H. H., Johnson, C. A., Laherty, C. D., Turner, B. M., Eisenman, R. N., Bird, A., 1998. Transcriptional repression by the methyl-CpG-binding protein MeCP2 involves a histone deacetylase complex. Nature 393, 386-389.

Naumenko, V. S., Popova, N. K., Lacivita, E., Leopoldo, M., Ponimaskin, E. G., 2014. Interplay between serotonin 5-HT1A and 5-HT7 receptors in depressive disorders. CNS Neurosci Ther 20, 582-590.

Nayak, S., Doerfler, P. A., Porvasnik, S. L., Cloutier, D. D., Khanna, R., Valenzano, K. J., Herzog, R. W., Byrne, B. J., 2014. Immune responses and hypercoagulation in ERT for Pompe disease are mutation and rhGAA dose dependent. PLoS ONE 9, e98336.

Nott, A., Cheng, J., Gao, F., Lin, Y. T., Gjoneska, E., Ko, T., Minhas, P., Zamudio, A. V., Meng, J., Zhang, F., Jin, P., Tsai, L. H., 2016. Histone deacetylase 3 associates with MeCP2 to regulate FOXO and social behavior. Nat Neurosci 19, 1497-1505.

Olivera, A., Eisner, C., Kitamura, Y., Dillahunt, S., Allende, L., Tuymetova, G., Watford, W., Meylan, F., Diesner, S. C., Li, L., Schnermann, J., Proia, R. L., Rivera, J., 2010. Sphingosine kinase 1 and sphingosine-1-phosphate receptor 2 are vital to recovery from anaphylactic shock in mice. J Clin Invest 120, 1429-1440.

Pearson, B. L., Defensor, E. B., Pobbe, R. L., Yamamoto, L. H., Bolivar, V. J., Blanchard, D. C., Blanchard, R. J., 2012. Mecp2 truncation in male mice promotes affiliative social behavior. Behav Genet 42, 299-312.

Pile, L. A., Spellman, P. T., Katzenberger, R. J., Wassarman, D. A., 2003. The SIN3 deacetylase complex represses genes encoding mitochondrial proteins: implications for the regulation of energy metabolism. J Biol Chem 278, 37840-37848.

Rett, A., 1966. On a unusual brain atrophy syndrome in hyperammonemia in childhood. Wiener Medizinische Wochenschrift 116, 723-726.

Ricceri, L., De Filippis, B., Laviola, G., 2012. Rett syndrome treatment in mouse models: searching for effective targets and strategies. Neuropharmacology 68, 106-115.

Rohdin, M., Fernell, E., Eriksson, M., Albage, M., Lagercrantz, H., Katz-Salamon, M., 2007. Disturbances in cardiorespiratory function during day and night in Rett syndrome. Pediatr Neurol 37, 338-344.

Romano, E., Ruocco, L. A., Nativio, P., Lacivita, E., Ajmone-Cat, M. A., Boatto, G., Nieddu, M., Tino, A., Sadile, A. G., Minghetti, L., Passarelli, F., Leopoldo, M., Laviola, G., Adriani, W., 2014. Modulatory effects following subchronic stimulation of brain 5-HT7-R system in mice and rats. Rev Neurosci 25, 383-400.

Shahbazian, M. D., Young, J. I., Yuva-Paylor, L. A., Spencer, C. M., Antalffy, B. A., Noebels, J. L., Armstrong, D. L., Paylor, R., Zoghbi, H. Y., 2002. Mice with Truncated MeCP2 Recapitulate Many Rett Syndrome Features and Display Hyperacetylation of Histone H3. Neuron 35, 243-254.

Shen, Y., Wei, W., Zhou, D. X., 2015. Histone Acetylation Enzymes Coordinate Metabolism and Gene Expression. Trends Plant Sci 20, 614-621.

Shoji, H., Takao, K., Hattori, S., Miyakawa, T., 2016. Age-related changes in behavior in C57BL/6J mice from young adulthood to middle age. Mol Brain 9, 11.

Smith, S. E., Li, J., Garbett, K., Mirnics, K., Patterson, P. H., 2007. Maternal immune activation alters fetal brain development through interleukin-6. J Neurosci 27, 10695-10702.

Sours, J. A., 1964. Neuropsychiatric Findings in Internal Carotid Artery Occlusive Disease with Cerebrovascular Damage. Report of Nine Cases and Review of the Literature. Psychiatr Q 38, 405-423.

Stefanko, D. P., Barrett, R. M., Ly, A. R., Reolon, G. K., Wood, M. A., 2009. Modulation of long-term memory for object recognition via HDAC inhibition. Proc Natl Acad Sci U S A 106, 9447-9452.

Stiedl, O., Pappa, E., Konradsson-Geuken, A., Ogren, S. O., 2015. The role of the serotonin receptor subtypes 5-HT1A and 5-HT7 and its interaction in emotional learning and memory. Front Pharmacol 6, 162.

Sun, Z., Feng, D., Fang, B., Mullican, S. E., You, S. H., Lim, H. W., Everett, L. J., Nabel, C. S., Li, Y., Selvakumaran, V., Won, K. J., Lazar, M. A., 2013. Deacetylase-independent function of HDAC3 in transcription and metabolism requires nuclear receptor corepressor. Mol Cell 52, 769-782.

Terron, J. A., Martinez-Garcia, E., 2007. 5-HT7 receptor-mediated dilatation in the middle meningeal artery of anesthetized rats. Eur J Pharmacol 560, 56-60.

Thompson, M. D., Cole, D. E., Jose, P. A., 2008. Pharmacogenomics of G protein-coupled receptor signaling: insights from health and disease. Methods Mol Biol 448, 77-107.

Urdinguio, R. G., Pino, I., Ropero, S., Fraga, M. F., Esteller, M., 2007. Histone H3 and H4 modification profiles in a Rett syndrome mouse model. Epigenetics 2, 11-14.

Valenti, D., de Bari, L., De Filippis, B., Henrion-Caude, A., Vacca, R. A., 2014. Mitochondrial dysfunction as a central actor in intellectual disability-related diseases: an overview of Down syndrome, autism, Fragile X and Rett syndrome. Neurosci Biobehav Rev 46 Pt 2, 202-217.

Valenti, D., de Bari, L., Vigli, D., Lacivita, E., Leopoldo, M., Laviola, G., Vacca, R. A., De Filippis, B., 2017. Stimulation of the brain serotonin receptor 7 rescues mitochondrial dysfunction in female mice from two models of Rett syndrome. Neuropharmacology 121, 79-88.

Vecsey, C. G., Hawk, J. D., Lattal, K. M., Stein, J. M., Fabian, S. A., Attner, M. A., Cabrera, S. M., McDonough, C. B., Brindle, P. K., Abel, T., Wood, M. A., 2007. Histone deacetylase inhibitors enhance memory and synaptic plasticity via CREB:CBP-dependent transcriptional activation. J Neurosci 27, 6128-6140.

Vierci, G., Pannunzio, B., Bornia, N., Rossi, F. M., 2016. H3 and H4 Lysine Acetylation Correlates with Developmental and Experimentally Induced Adult Experience-Dependent Plasticity in the Mouse Visual Cortex. J Exp Neurosci 10, 49-64.

Vigli, D., Cosentino, L., Raggi, C., Laviola, G., Woolley-Roberts, M., De Filippis, B., 2018a. Chronic treatment with the phytocannabinoid

Cannabidivarin (CBDV) rescues behavioural alterations and brain atrophy in a mouse model of Rett syndrome. Neuropharmacology 140, 121-129.

Villalon, C. M., Centurion, D., Lujan-Estrada, M., Terron, J. A., Sanchez-Lopez, A., 1997. Mediation of 5-HT-induced external carotid vasodilatation in GR 127935-pretreated vagosympathectomized dogs by the putative 5-HT7 receptor. Br J Pharmacol 120, 1319-1327.

Volpicelli, F., Speranza, L., di Porzio, U., Crispino, M., Perrone-Capano, C., 2014. The serotonin receptor 7 and the structural plasticity of brain circuits. Front Behav Neurosci 8, 318.

Wilcox, R. R., 1987. New designs in analysis of variance. Annual Review of Psychology 38, 29-60.

Woods, R., Vallero, R. O., Golub, M. S., Suarez, J. K., Ta, T. A., Yasui, D. H., Chi, L. H., Kostyniak, P. J., Pessah, I. N., Berman, R. F., LaSalle, J. M., 2012. Long-lived epigenetic interactions between perinatal PBDE exposure and Mecp2308 mutation. Hum Mol Genet 21, 2399-2411.

Yeh, S. H., Lin, C. H., Gean, P. W., 2004. Acetylation of nuclear factor-kappaB in rat amygdala improves long-term but not short-term retention of fear memory. Mol Pharmacol 65, 1286-1292.

Zareifopoulos, N., Papatheodoropoulos, C., 2016. Effects of 5-HT-7 receptor ligands on memory and cognition. Neurobiol Learn Mem 136, 204-209.

# Chapter 3

# 3. Rescue of prepulse inhibition deficit and brain mitochondrial dysfunction by pharmacological stimulation of the central serotonin receptor 7 in a mouse model of CDKL5 Deficiency Disorder

Daniele Vigli[1], Laura Rusconi[2], Daniela Valenti[3], Paolo La Montanara[2], Livia Cosentino[1], Enza Lacivita[4], Marcello Leopoldo[4], Elena Amendola[5], Cornelius Gross[6], Nicoletta Landsberger[7], Giovanni Laviola[1], Charlotte Kilstrup-Nielsen[2], Rosa A. Vacca[3], Bianca De Filippis[1]

*[1]Center for Behavioral Sciences and Mental Health, Istituto Superiore di Sanità, 00161 Rome, Italy; [2]Department of Biotechnology and Life Sciences and Center of Neuroscience, University of Insubria, 21052 Busto Arsizio, Italy; [3]Institute of Biomembranes, Bioenergetics and Molecular Biotechnologies, National Council of Research, 70126 Bari, Italy; [4]Dept. Pharmacy, University of Bari "Aldo Moro", 70125 Bari, Italy; [5]Molecular Medicine and Medical Biotechnologies, University of Naples "Federico II", 80131 Napoli, Italy; [6]Mouse Biology Unit, European Molecular Biology Laboratory (EMBL) 00015 Monterotondo, Italy; [7]Department of Medical Biotechnology and Translational Medicine, University of Milan, 20090 Segrate, Italy.*

# 3.1 Abstract

Mutations in the X-linked *cyclin-dependent kinase-like 5* (*CDKL5*) gene cause CDKL5 Deficiency Disorder (CDD), a rare neurodevelopmental syndrome characterized by severe behavioural and physiological symptoms. No cure is available for CDD. CDKL5 is a kinase that is abundantly expressed in the brain and plays a critical role in neurodevelopmental processes, such as neuronal morphogenesis and plasticity. This study provides the first characterization of the neurobehavioural phenotype of 1-year old *Cdkl5*-null mice and demonstrates that stimulation of the serotonin receptor 7 (5-HT$_7$R) with the agonist molecule LP-211 (0.25 mg/kg once/day for 7 days) partially rescues the abnormal phenotype and brain molecular alterations in *Cdkl5*-null male mice. In particular, LP-211 treatment completely normalizes the prepulse inhibition defects observed in *Cdkl5*-null mice and, at a molecular level, restores the abnormal cortical phosphorylation of rpS6, a downstream target of mTOR and S6 kinase, which plays a direct role in regulating protein synthesis. Moreover, we demonstrate for the first time that mitochondria show prominent functional abnormalities in *Cdkl5*-null mouse brains that can be restored by pharmacological stimulation of brain 5-HT$_7$R.

## 3.2   Introduction

CDKL5 Deficiency Disorder (CDD) (OMIM #300672) is a rare neuropathological condition that is caused by mutations in the X-linked *cyclin-dependent kinase-like 5* (*CDKL5*) gene (Kalscheuer et al., 2003). This disorder is characterized by a variety of behavioural and physiological symptoms that include the onset of seizures in the first months of life, severe global developmental delay resulting in intellectual disability (ID) and poor motor control, and the presence of peculiar hand stereotypies (Bahi-Buisson et al., 2008; Fehr et al., 2016). No cure exists for patients affected by CDD.

*CDKL5* encodes a serine/threonine kinase expressed in various tissues, with the brain showing the highest levels of expression (Rusconi et al., 2008; Kilstrup-Nielsen et al., 2012). Available data point to a crucial role of Cdkl5 in fundamental neurodevelopmental processes such as activity-dependent regulation of neuronal morphogenesis and plasticity (Fuchs et al., 2014; Zhou et al., 2017). These processes require a fine-tune regulation of Cdkl5 localization in neurons, with the shuttling between the cytoplasm and the nucleus being regulated by the activation of extra-synaptic NMDA receptors (Rusconi et al., 2011), and protein localization on the post-synaptic side of excitatory synapses being regulated by the association of the kinase with PSD-95 (Ricciardi et al., 2012). These neuronal alterations are accompanied by a number of behavioural deficits in mice lacking Cdkl5, including motor dysfunction, autistic-like behaviours and memory deficits (Jhang et al., 2017; Okuda et al., 2018).

The serotonin receptor 7 (5-HT$_7$R) is a G protein-coupled receptor broadly expressed in the central nervous system that is involved in a variety of neurophysiological phenomena relevant for CDD, such as sleep, cognitive processes and synaptic plasticity (Hedlund et al., 2003; Cifariello et al., 2008;

Matthys et al., 2011). Pharmacological stimulation of the 5-HT$_7$R by the brain penetrant agonist LP-211 has provided promising results in preclinical studies for disorders associated with syndromic IDs, such as Fragile X syndrome and Rett syndrome (RTT) (Costa et al., 2012; De Filippis et al., 2014a; De Filippis et al., 2015b). Of note, the beneficial effects of LP-211 treatment extend beyond intellectual deficits and impact other domains, such as motor function and autistic-like behaviours in a mouse model of RTT (De Filippis et al., 2014a; De Filippis et al., 2015b), a syndrome that presents several symptoms in common with CDD (Fehr et al., 2013). Moreover, 5-HT$_7$R stimulation by LP-211 impacts a number of behavioural domains and molecular pathways that have been demonstrated to be altered in *Cdkl5*-null mouse brain and in induced-pluripotent stem cell (iPSCs)-derived neurons from CDKL5 patients (Ricciardi et al., 2012; Amendola et al., 2014), as it promotes a rearrangement of neuronal morphology, facilitates synaptogenesis and modulates the activation of the Akt/mTOR/S6 pathway (De Filippis et al., 2014a; Speranza et al., 2017).

Based on these pieces of evidence, in the present study we evaluated whether the stimulation of 5-HT$_7$R might represent a potential therapeutic approach for CDD. To test this hypothesis, 9-12-months old *Cdkl5*-null male mice and wild-type littermate controls received a repeated systemic intraperitoneal (i.p.) treatment with LP-211 (0.25 mg/kg once/day for 7 days) (De Filippis et al., 2015b). We reasoned that the translational relevance of the treatment under investigation might be increased if the relief of symptoms was demonstrated at an advanced and more severely affected stage of the disease (1-year-old mice). Male mice were used based on clinical evidences of CDD in males (Elia et al., 2008) and on the effects of mosaic CDKL5 expression due to random X-chromosome inactivation in females. To evaluate therapeutic

122

efficacy, a battery of behavioural analyses was carried out at the end of the treatment specifically tailored to detect CDD-related behavioural alterations. Behavioural testing started at least 7 days after the end of the i.p. treatment and the brains of the experimental mice were collected two months after the last i.p. injection, based on previous data suggesting long-term effects of a seven-day-long treatment with LP-211 (De Filippis et al., 2015b).

In the brain of *Cdkl5*-null mice treated with either LP-211 or vehicle, Rac1 activation and mitochondrial functionality were evaluated, since recent data suggest a role for 5-HT$_7$R in the activation of brain Rho GTPases and in the regulation of the oxidative phosphorylation (OXPHOS) apparatus, the mitochondrial molecular machinery responsible for the majority of cell energy production (De Filippis et al., 2015c; De Filippis et al., 2015d; Valenti et al., 2017), central players in several pathological conditions associated with ID (De Filippis et al., 2014b; Valenti et al., 2014). We also verified whether the expression and the activation of Rho GTPase-dependent pathways are abnormal in *Cdkl5*-null mouse brain and LP-211 treatment effects thereon, based on previous data pointing to a pathogenic role of a disrupted interaction between Cdkl5 and the Rho GTPases Rac1 (Chen et al., 2010; Barbiero et al., 2017). In particular, we explored whether the LP-211 treatment impacts group I PAKs, the leading molecules by which Rho GTPases affect actin cytoskeleton dynamics (De Filippis et al., 2014b), and the activation of the rpS6 and its upstream regulator Akt, a pathway that is modulated by Rho GTPases and is involved in protein synthesis (Ricciardi et al., 2011; De Filippis et al., 2014a).

## 3.3 Materials and methods

### 3.3.1 Subjects

The experimental subjects were 9-12-months old *Cdkl5*-null male mice and wild-type littermates (wt) backcrossed to C57BL/6N mice for at least 10 generations (Amendola et al., 2014). Experimental mice were obtained by crossing *Cdkl5* heterozygous (-/+) female mice and wt male mice and weaned at postnatal day 25. After weaning, mice were housed according to sex in groups of two or three in polycarbonate transparent cages (33 x 13 x 14 cm) with sawdust bedding and kept on a 12-h light-dark schedule (lights off at 8:00 a.m.). Temperature was maintained at 21 $\pm 1$ °C and relative humidity at 60$\pm$10%. Animals were provided *ad libitum* with tap water and a complete pellet diet (Altromin, 1324 - 10mm pellets, Germany). All experimental procedures were conducted in conformity with the European Directive 2010/63/EU and the Italian legislation on animal experimentation, D.Lgs. 26/2014.

### 3.3.2 Genotyping

DNA has been prepared from a small tail-tip biopsy taken at weaning, as previously described (De Filippis et al., 2014a). The *Cdkl5* alleles have been identified by PCR using two sets of primers (for further details see Supplementary materials). PCR products were electrophoresed through a 2% NuSieve 3:1 agarose gel (Cambrex Bio Science, Rockland, ME, USA) containing 0.1 µl/ml GelRed™ and examined under UV light.

### 3.3.3 Drug and Treatment

LP-211 was prepared following the same synthetic procedure described in (Leopoldo et al., 2008). The compound, which has a half-life 65 minutes,

was dissolved in a vehicle solution of 1% dimethyl sulfoxide (DMSO) in saline (0.9% NaCl). *Cdkl5*-null mice and wt littermate controls were randomly assigned to be daily i.p. injected (between 9.00 and 11.00 am) for 7 consecutive days with either LP-211 (0.25 mg/kg) or vehicle (1% of DMSO in saline).

### 3.3.4  Behavioural testing

A comprehensive test battery was carried out aimed at assessing treatment effects on the behavioural domains that are compromised in CDD. The selection of the tests to be performed was based on previous literature addressing the neurobehavioural phenotype of Cdkl5-*null* mice (Amendola et al., 2014; Okuda et al., 2018) and on our lasting experience on the study of mouse models of RTT, a syndrome that has many symptoms in common with CDD (De Filippis et al., 2010; De Filippis et al., 2015a). Mice were experimentally naïve at the start of the behavioural test battery. All behavioural testing took place during the dark phase of the L/D cycle, between 9.00 am and 3.00 pm, and was carried out by experimenters blind to the mouse genotypes. A minimum of 24 h was left between tests.

### 3.3.4.1 Prepulse inhibition (PPI) paradigm

Sensorimotor gating was evaluated 7 days after the last i.p. with the prepulse inhibition (PPI) paradigm (Swerdlow et al., 2001). The apparatus consisted of two Plexiglas rectangular boxes (startle cages) (9 x 7 cm), placed in sound-attenuated chambers with a red light and a fan ventilator (Med associates inc. St Albans, VT, United States of America). Background white (62 db) noise and acoustic bursts were conveyed by two separate speakers, properly spaced from the startle cage so as to produce a fine-tuned regulation of sound. Both speakers and startle cages were connected to a main PC computer, which detected and analyzed all chamber variables by means of a

specific software. Two slightly different protocols were adopted on two cohorts of mice, that differed in the range of prepulse intensities under investigation. On the first cohort of mice, prepulse intensities were as follows: 67, 70, 73 or 76 db (Macri et al., 2015). On the second cohort, 78, 82 or 84 dB pre-pulse intensities were applied (Chao et al., 2010). To evaluate sensorimotor gating capabilities in Cdkl5-*null* mice, the % PPI was calculated as follows: (100-[(mean startle amplitude for prepulse + pulse trials/mean startle amplitude for pulse-alone trials) x 100]) (for further details see Supplementary materials).

### 3.3.4.2 General health score

The general health of the experimental mice was qualitatively evaluated 1 and 28 days after the last injection, by a trained observer, blind to the genotype of the experimental mice, according to a method that has been developed to assess the health status of RTT mice (Guy et al., 2007; De Filippis et al., 2014a). Briefly, mice received a score (ranging from 0 – normal appearance- to 4- highly compromised) for each of the following parameters: gait, mobility, breathing, kyphosis, fur, hind limb clasping, tremors and general conditions. The individual scores for each category were subsequently averaged to obtain a semi-quantitative measure of the general health status.

### 3.3.4.3 Nest Building evaluation

Nest building ability was scored 21 days from the last i.p. injection to assess purposeful and coordinated forepaw use to unravel whether *Cdkl5*-null mice display alterations and LP-211 effects thereon, as previously described (De Filippis et al., 2015a). The quality of the nests was evaluated 24 h after nest material provision (for further details see Supplementary materials).

### 3.3.4.4 Home cage locomotor activity

To verify whether LP-211 treatment affects the daily locomotor activity in *Cdkl5*-null mice, spontaneous locomotor activity in the home-cages was evaluated 33 days after the last i.p. injection. Levels of activity were monitored continuously by means of an automatic device using small passive infrared sensors positioned on the top of each cage (ACTIVISCOPE system, NewBehaviour Inc., Zurich, Switzerland) as previously described (De Filippis et al., 2013) (for further details see Supplementary materials). To avoid confounding effects due to cage clean procedures and/or room entrances, the analysis was performed during two 6-hours intervals, during the dark and the light phase, in which animals were left undisturbed.

### 3.3.4.5 Open Field test

Locomotor activity was assessed in the Open Field test 30 days after the last i.p injection, to complement the home-cage recording (Ricceri et al., 2011) (for further details see Supplementary materials).

### 3.3.4.6 Fear conditioning task

The fear conditioning task was carried out 14 days after the last i.p. injection to evaluate cognitive abilities in *Cdkl5*-null mice and LP-211 effect thereon (Wang et al., 2012). An automated system was used (UgoBasile S.R.L.), which consisted in a soundproof cubic apparatus with inside a mouse cage (21(d) x 24(w) x 30(h) cm) with electrified grid floor. The task consisted of a two-days-long protocol in which freezing frequency and duration were measured with an automatic freezing detector (UgoBasile S.R.L.). Throughout the task, mice were exposed to a white noise (WN- 60db, 2000 Hz). On the first day (training), animals were placed in the fear conditioning apparatus for 180s (baseline, BL) and then exposed for three times to the acoustic

conditioned stimulus (CS; 2000 Hz – 68db, 30s). Each CS on the first day was paired with a 0.7 mA shock released during the last 2s (unconditioned stimulus; US). A 95s inter trial interval (ITI) was used. On the second day(test), mice were placed in the same chamber and, after a 180s BL, were exposed to fifteen trials consisting in 30s of CS plus 10s of ITI. Contextual fear memory was established by measuring the time spent in freezing behaviour during the baseline on the testing day compared to levels shown during the baseline on the training day. Freezing behaviour in response to the CSs on the test day was also evaluated. Before the starting of each session the grid floor of the apparatus was cleaned with 70% ethanol.

### 3.3.5 Neurobiological analyses

Two months after the last i.p. injection, the brains of the experimental mice were dissected and cortices, a behaviourally relevant brain area in which 5-HT$_7$R (Hedlund, 2009) and Cdkl5 (Wang et al., 2012) are highly expressed, were immediately frozen in dry ice for G-LISA Assay and western blot analyses (De Filippis et al., 2015b).

For mitochondrial analyses, the hemispheres from additional subjects were cryopreserved, as previously described (Valenti et al., 2017). Previous data in fact demonstrate that cryopreserved brain tissues show mitochondrial membrane potential, outer and inner membrane integrity and mitochondrial ATP production capacity comparable to mitochondria isolated from fresh brains (Valenti et al., 2014b).

### 3.3.5.1 RAC-1 G-LISA Assay

Rac1 G-Lisa Activation Assay BiochemkitTM (Cytoskeleton, Denver, CO) (n = 4-5) was used to measure Rac1 activity in mouse cortices according to the manufacturer's recommendations.

### 3.3.5.2 Western blot analysis

Cortices were homogenized in lysis buffer and centrifuged. Then the supernatant was collected and the protein content was quantified by bicinchonic acid assay. For western blotting analysis, 20 μg of total proteins were separated on a 12% SDS-PAGE and membranes incubated with the appropriate primary and secondary antibodies. Images of the membranes were acquired by a CCD camera (Syngene, G-Box Chemi XRQ) and optical densities (O.D.) of the protein signals calculated for each sample with Image J software and normalized with the corresponding housekeeping signal (Fig. 4 A, C); the O.D. ratios were then compared and expressed as the average fold increase, with 1 (wt control) as baseline (for further details see Supplementary materials).

### 3.3.5.3 Mitochondrial analysis

*Measurement of mitochondrial respiratory chain complex (MRC) activities.* MRC activities were evaluated in mitochondrial membrane-enriched fractions obtained from isolated mitochondria. Measurement of MRC complex activities were performed essentially as in (Manente et al., 2013), by three assays which rely on the sequential addition of reagents to measure the activities of: i) NADH: ubiquinone oxidoreductase (complex I) followed by ATP synthase (complex V), ii) succinate: ubiquinone oxidoreductase (complex II) and iii) cytochrome c oxidase (complex IV) followed by cytochrome c oxidoreductase (complex III) (for further details see Supplementary materials).

*Measurement of mitochondrial ATP production rate.* The rate of ATP production by OXPHOS was determined in isolated mitochondria, as previously described in (Valenti et al., 2010) (for further details see Supplementary materials).

*Measurement of mouse brain ATP levels.* Half brain was weighted (approx. 20 mg) and subjected to perchloric acid extraction as described in (Khan, 2003) (for further details see Supplementary materials). The amount of tissue ATP was determined enzymatically in KOH neutralized extracts, as described in (Valenti et al., 2010).

### 3.3.6 Statistical analysis

Data were analyzed using the two-way ANOVA model, including genotype and treatment as between-subjects factors, or applying repeated measures ANOVAs if there was a within-subjects factor, using Statview vers. 5.0 (Sas, Institute Inc., Cary, NC). The alpha level was set to 5%. To unravel the presence of outliers, the Grubbs' test was applied. *Post-hoc* comparisons were performed using Tukey HSD (Wilcox, 1987).

## 3.4 Results

### 3.4.1 LP-211 treatment selectively rescues PPI deficit in mice lacking Cdkl5 at an advanced stage of the disease

To evaluate the efficacy of the LP-211 treatment for CDD, a broad test battery was carried out.

*Prepulse inhibition (PPI).* The evaluation of the sensorimotor gating showed significant deficits in PPI capacity in *Cdkl5*-null mice compared to wild–type (wt) controls, in the absence of changes in the acoustic startle response (see Fig.S1A-B). This genotype effect was replicated on two cohorts of animals using protocols adopting different ranges of prepulse intensities [Fig.1A cohort 1: Genotype*Treatment interaction: $F_{(1,22)} = 12.2$, $p = 0.021$; *post-hoc:* $p < 0.01$; Fig.1B cohort 2: Genotype*Treatment interaction: $F_{(1,33)} = 7.3$, $p = 0.011$; *post-hoc*: $p < 0.01$].The LP-211 treatment significantly improved this abnormal behaviour in *Cdkl5*-null mice compared to vehicle (veh)-treated *Cdkl5*-null mice in both cohorts of animals [Fig.1A, Genotype*Treatment; *post-hoc*: $p < 0.01$; Fig.1B; Genotype*Treatment; *post-hoc:* $p < 0.05$]. No significant prepulse intensities*genotype*treatment interactions were found (Fig.S1C-D).
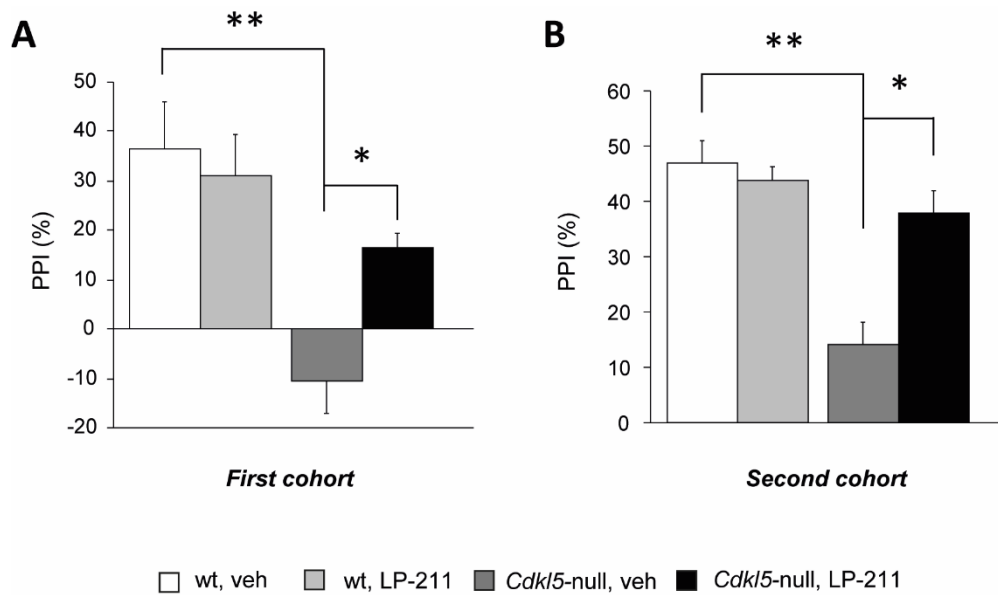
**Fig.1***: LP-211 treatment selectively rescues prepulse inhibition (PPI) deficit in Cdkl5-null mice at an advanced stage of the disease*. PPI evaluation was carried out on two cohorts of animals using protocols adopting different ranges of prepulse intensities; (**A-B**) *Cdkl5*-null mice show a severe impairment in PPI compared to wt mice. LP-211 treatment rescues the abnormal sensory motor gating in *Cdkl5*-null mice (cohort 1: wt, Veh = 4; wt, LP-211 =7; *Cdkl5*-null, Veh = 8; *Cdkl5*-null, LP-211 = 9; cohort 2: wt, Veh = 11; wt, LP-211 =12; *Cdkl5*-null, Veh = 7; *Cdkl5*-null, LP-211 = 7). The histograms show the average of all prepulse intensities. Data are mean ± SEM. Statistical significance was calculated by two-way ANOVA. **p<0,01; *p<0,05 after Tukey's *post-hoc* tests.

*General health status.* We found that fully symptomatic *Cdkl5*-null mice showed worse general health conditions in comparison to wt mice [Fig.2A; Genotype: $F_{(1,35)} = 7.8$; p = 0.008]. The LP-211 treatment did not significantly improve general health status in *Cdkl5*-null mice (Fig.2A). No differences between the first and the second evaluation (1 and 28 days from the last i.p.), and no interaction of the repeated measures with genotype and treatment were found. Figure 2A represents the genotype*treatment interaction, in which the

132

general health scores obtained at 1 and 28 days after the last i.p. injections were averaged.
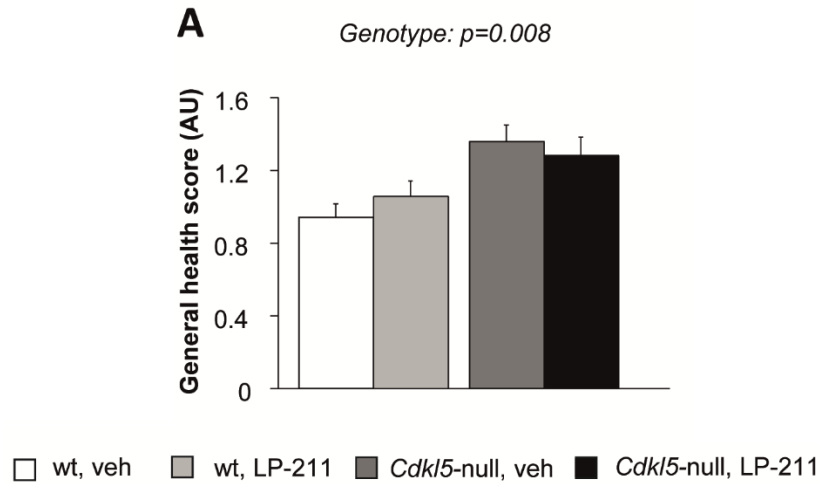


**Fig.2:** *Cdkl5-null mice show severe general health status at an advanced stage of the disease.* (**A**) *Cdkl5*-null mice present a higher general health score compared to wt controls, thus confirming a worse general health status (score= 0-4). No treatment effects are found (wt, Veh = 11; wt, LP-211 = 12; *Cdkl5*-null, Veh = 8; *Cdkl5*-null, LP-211 = 8). Data are mean ± SEM. Statistical significance was calculated by two-way ANOVA. **p < 0.01; *p < 0.05 after Tukey's *post-hoc* tests.

*Nest building ability.* Nest building ability was slightly, but significantly impaired in *Cdkl5*-null mice in comparison to wt controls [Genotype: $F_{(1,35)}$ = 4.9; p = 0.032], thus confirming defective coordination of forepaws (De Filippis et al., 2015a; Fuchs et al., 2018b). The LP-211 treatment did not affect the quality of the nests built by *Cdkl5*-null mice (wt veh: 2.3 ± 1.2; *Cdkl5*-null veh: 1.8 ± 1.4; wt LP-211: 2.5 ± 1.2; *Cdkl5*-null LP-211: 1.3 ± 1.0).

*Home cage locomotor activity.* The evaluation of spontaneous home cage locomotor activity highlighted a hypoactive profile in *Cdkl5*-null mice

133

compared to wt controls, as demonstrated by the lower number of beam breaks they performed during the dark/active phase of the Light/Dark cycle [Fig.2B; Phase*Genotype*Treatment interaction: $F_{(1,28)} = 3.3$; p =n0.082; *post-hoc:* p < 0.05]. The LP-211 treatment did not affect the abnormal locomotor profile shown by *Cdkl5*-null mice in the home cage.



**Fig.2:** *Cdkl5-null mice show hypo-active profile during the dark phase of the circadian rhythm at an advanced stage of the disease* (**B**) *Cdkl5*-null mice show hypoactivity in the home cage in comparison to wt mice during the dark/active phase of the circadian cycle. The LP-211 treatment does not affect this parameter. The infrared sensors detect any movement of mice with a frequency of 20 events per second (20 Hz). Scores are obtained as counts per hour (cph) expressed during 1-hour periods, and the profile of daily activity is obtained by averaging 6-hours of continuous registration per phase (Dark vs Light; 1-6pm - 2-8am) (wt, Veh = 8; wt, LP-211 = 10; *Cdkl5*-null, Veh = 7; *Cdkl5*-null, LP-211 = 7). Data are mean ± SEM. Statistical significance was calculated by two-way ANOVA. **p < 0.01; *p < 0.05 after Tukey's*post-hoc* tests.

134

*Open field test.* We found that *Cdkl5*-null mice show hyperactivity when exposed to a novel environment compared to wt controls, as demonstrated by the increased distance they moved in the open field [Fig.2C; Genotype: $F_{(1,33)}$ = 13.6; p < 0.001] as well as the number of entrances in the central zone of the arena [Genotype: $F_{(1,33)}$ = 5.9, p < 0.021]. Increased locomotion was confirmed throughout the 60-min Open Field test, with no differences between the initial and the last 5-min blocks (Fig.S2). LP-211 treatment did not exert any effects on the total distance moved (Fig.2C) as well as the number of entrances in the central zone of the arena (wt veh:191.5 ± 65.1; *Cdkl5*-null mice veh: 222.4 ± 83.9; wt LP-211: 176.6 ± 55.2; *Cdkl5*-null mice LP-211: 252.6 ± 60.7). No difference between *Cdkl5*-null mice and wt controls was found in time spent in the central/intimidating zone of the arena, an index of anxiety-like behaviours (*data not shown*).



**Fig.2:** *Cdkl5-null mice show hyper-active profile in the open field task at an advanced stage of the disease* (**C**) A hyperactive profile is evident in the open field task, with *Cdkl5*-null mice moving more than wt controls, that is not affected by the

LP-211 treatment. (wt, Veh = 11; wt, LP-211 = 12; *Cdkl5*-null, Veh = 8; *Cdkl5*-null, LP-211 = 8). Data are mean ± SEM. Statistical significance was calculated by two-way ANOVA. **p<0,01; *p<0,05 after Tukey's *post-hoc* tests.

*Fear conditioning test.* Defective contextual fear memory was found in *Cdkl5*-null mice, as demonstrated by the reduced freezing levels they displayed compared to wt controls when exposed to the context in which they received the footshock on the previous day [Fig.2D; Day*Genotype*Treatment interaction: $F_{(1,35)} = 3.1$; p = 0.086; *post-hoc:* p < 0.01]; no significant LP-211 treatment effect was highlighted on this hippocampus-dependent cognitive deficit. Reduced freezing in response to the presentation of the 15 CSs on the second day of testing compared to wt controls was also evident in *Cdkl5*-null mice [Genotype: $F_{(1,35)} = 11.6$; p < 0.001]. The LP-211 treatment did not improve this abnormal freezing response shown by *Cdkl5*-null mice (wt veh:27.9 ± 10.2; *Cdkl5*-null mice veh: 16.3 ± 12.0; wt LP-211: 24.1 ± 11.8; *Cdkl5*-null mice LP-211: 16.5 ± 12.8).

**Fig.2:** *Cdkl5-null mice show reduced freezing behaviour in the fear conditioning paradigm at an advanced stage of the disease* (**D**) *Cdkl5*-null mice show reduced freezing behaviour in comparison to wt mice in the fear conditioning task, suggesting defective contextual fear memory. The LP-211 treatment does not affect the performance in this cognitive test (wt, Veh = 11; wt, LP-211 = 12; *Cdkl5*-null, Veh = 8; *Cdkl5*-null, LP-211 = 8). Data are mean ± SEM. Statistical significance was calculated by two-way ANOVA. **p < 0.01; *p < 0.05 after Tukey's *post-hoc* tests.

### 3.4.2 The LP-211 treatment activates Rac1 and rescues the abnormal activation of rpS6 in the cortex of Cdkl5-null mice

Based on available data suggesting that Rac1 signaling may be defective in CDD (Chen et al., 2010), the activation of Rac1 and of the Rho GTPases downstream molecules PAKs and rpS6 was evaluated in *Cdkl5*-null mouse cortex, to verify whether they are abnormal and whether pharmacological stimulation of the 5-HT$_7$R may recover them.

137

*Rac1 activation.* No genotype difference was found in the activation of Rac1 in *Cdkl5*-null mouse cortex. The LP-211 treatment significantly increased Rac1 activation in both genotypes [Fig.3, Treatment: $F_{(1,15)} = 5.8$; p = 0.028].



**Fig.3**: *The LP-211 treatment significantly increases Rac1 activation in both genotypes*. The activation of Rac1 protein was evaluated in mouse cortical brain areas by G-Lisa Activation Assay. No differences were found between *Cdkl5*-null mice and wt littermates. LP-211 treatment increases Rac1 activation levels in both genotypes (wt, Veh = 5; wt, LP-211 = 5; *Cdkl5*-null, Veh = 5; *Cdkl5*-null, LP-211 = 4). Data are mean ± SEM. Statistical significance was calculated by two-way ANOVA.

*Expression and activation of RhoGTPase-dependent signaling pathways.* We found that phospho-PAK(p-PAK)/total PAK ratio, which provides an index of the net functionality of the kinase, was shifted toward increased activation in *Cdkl5*-null mouse cortex compared to wt controls [Fig.4A,B; Genotype: $F_{(1,17)} = 15.7$; $p < 0.001$]. The LP-211 treatment

increased PAK activation in the cortex of both genotypes, as demonstrated by increased p-PAK/total PAK ratio [Fig.4B, Treatment: $F_{(1,17)} = 11.7$; $p = 0.003$].



**Fig.4**: *The LP-211 treatment increases the activation of PAK in the cortex of Cdkl5-null mice.* Representative Western blot analysis (summarized view corresponding to one or three animals per group) of (**A**) phospho-PAK (p-PAK) and PAK tot in cortical brain areas. (**B**) The LP-211 treatment increases the activation of group I PAKs, measured as p-PAK/PAK tot ratio in the cortex of *Cdkl5*-null and wt mice. This leads to an exacerbation of the overactivation of PAK in *Cdkl5*-null mouse cortex (wt, Veh = 4; wt, LP-211 = 6; *Cdkl5*-null, Veh = 6; *Cdkl5*-null, LP-211 = 6). Data are expressed as percentage of wt veh controls (100). Data are mean ± SEM. Statistical significance was calculated by two-way ANOVA. \*\*p < 0.01; \*p < 0.05 after Tukey's *post-hoc* tests.

In *Cdkl5*-null mouse cortex, we also observed increased ribosomal protein S6 (rpS6) activation (Fig. 4C representative blots), as demonstrated by increased phospho-rpS6 (240/244)(p-rpS6)/total rpS6 ratio, which was normalized by the LP-211 treatment [Fig.4D; Genotype\*Treatment interaction: $F_{(1,18)} = 3.2$, $p = 0.089$; *post-hoc:* $p < 0.05$]. No genotype or treatment effects were found on the phosphorylation levels of the rpS6 at Ser235/236 in the cortex (Fig.4E).
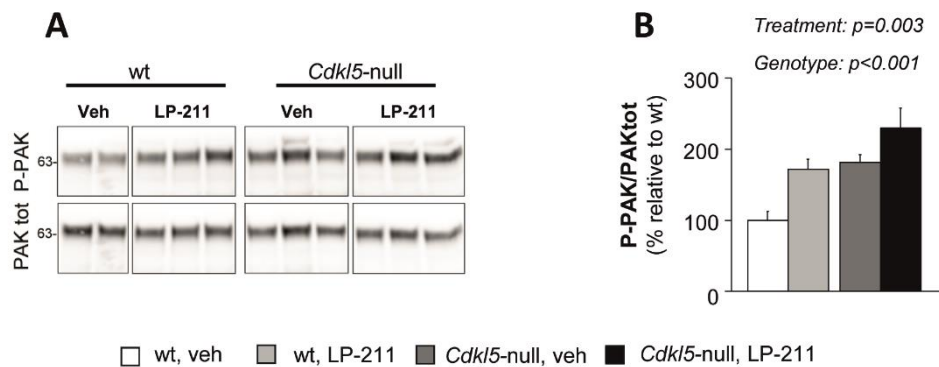
139

**Fig.4**: *The LP-211 treatment rescues the abnormal activation of rpS6 in the cortex of Cdkl5-null mice.* Representative Western blot analysis (summarized view corresponding to one or three animals per group) (**C**) rpS6 p240/244, rpS6 p235/236 and rpS6 tot proteins in cortical brain areas. (**D**) The LP-211 treatment normalizes the abnormal level of the p-rpS6(240/244)/ rpS6tot ratio in*Cdkl5*-null mouse cortex. The LP-211 treatment does not affect cortical levels of the p-rpS6(235/236)/ rpS6 tot ratio (**E**) (wt, Veh = 4; wt, LP-211 = 6; *Cdkl5*-null, Veh = 6; *Cdkl5*-null, LP-211 = 6). Data are expressed as percentage of wt veh controls (100). Data are mean ± SEM. Statistical significance was calculated by two-way ANOVA. **p < 0.01; *p < 0.05 after Tukey's *post-hoc* tests.

*Akt activation levels.* In the cortex of *Cdkl5*-null mice, no genotype difference and no LP-211 treatment was detected for the activation of Akt quantified as the ratio phospho-Akt (p-Akt)/Akt total (Fig.S3).

*Cdkl5 levels.* Interestingly, the LP-211 treatment slightly, but significantly increased Cdkl5 protein levels in the cortex of LP-211-treated wt mice, in comparison to wt controls [Genotype*Treatment interaction: $F_{(1,18)} = 11.6$, p = 0.003; *post-hoc*: p < 0.01; wt, veh: 100±0.2 and wt, LP-211: 140±0.2

(% relative to wt)]. As expected, Cdkl5 was not detected in the brain of mutant mice.

*5-HT₇R levels*. We also evaluated whether the levels of the $5\text{-HT}_7\text{R}$ differ in the brain of *Cdkl5*-null mice compared to wt controls and LP-211 effects thereon. No significant genotype or treatment effects were found in cortex (Fig.S4).

### 3.4.3 Cdkl5-null mouse brain shows defective mitochondrial functionality that is rescued by the LP-211 treatment

Based on recent evidence suggesting a role for $5\text{-HT}_7\text{R}$ and Rho GTPases in the regulation of brain mitochondrial functionality (De Filippis et al., 2015a; De Filippis et al., 2015b; Valenti et al., 2017), we analyzed mitochondrial functionality in *Cdkl5*-null mouse brains.

*Activity of Mitochondrial Respiratory Chain (MRC) complexes.* We found reduced activity of the MRC complexes III, IV and V in *Cdkl5*-null mouse brains compared to wt controls [Fig.5A; Repeated measure*Genotype*Treatment interaction: $F_{(4,32)} = 13.4$; $p < 0.001$; *post-hoc*: $p < 0.01$]. No difference was found in the activity of complexes I and II (Fig.5A). A complete restoration in the activity of the defective MRC complexes in LP-211-treated *Cdkl5*-null mice was found [Fig.5A; Repeated measure*Genotype*Treatment interaction; *post-hoc:* $p < 0.01$ compared to vehicle-treated *Cdkl5*-null mice for complexes IV and V and $p < 0.05$ compared to vehicle-treated *Cdkl5*-null mice for complex III].

**Fig.5**: *Cdkl5-null mouse brain shows defective mitochondrial functionality that is rescued by the LP-211 treatment.* (**A**) Reduced activity of mitochondrial respiratory chain (MRC) complexes III, IV, V is evident in *Cdkl5*-null mouse brain compared to wt controls. LP-211 treatment rescues these alterations (wt, Veh = 3; wt, LP-211 = 3; *Cdkl5*-null, Veh = 3; *Cdkl5*-null, LP-211 = 3). Data are mean ± SEM. Statistical significance was calculated by two-way ANOVA. **$p < 0.01$; *$p < 0.05$ after Tukey's *post-hoc* test.

*Brain energy status evaluation*. To evaluate if normalization of the activity of MRC complexes was associated with a normalization of their bioenergetic efficiency, the ATP production rate and ATP whole brain levels were measured (Fig.5B,C). In line with the results on complexes activity, *Cdkl5*-null mouse mitochondria showed a significant reduction in mitochondrial ATP production rate when supplied with the substrate for complex IV

(ascorbate/TMDP), as energy source [Fig. 5B; Repeated measure*Genotype*Treatment interaction: $F_{(2,16)} = 3.2$; $p = 0.066$; *post-hoc:* $p < 0.05$]. No changes were found when substrates for complexes I and II were used (Fig.5B). Importantly, whole brain ATP levels were also reduced in *Cdkl5*-null mouse brain in comparison to wt controls [Fig.5C; Genotype*Treatment interaction: $F_{(1,12)} = 20.2$; $p < 0.001$; *post-hoc*: $p < 0.01$]. LP-211 treatment completely rescued the defective mitochondrial ATP production and the reduced brain ATP levels in *Cdkl5*-null mice [Fig.5B; ATP production: Repeated measure*Genotype*Treatment interaction; *post-hoc:* $p < 0.05$; Fig.5C; whole brain ATP level: Genotype*Treatment interaction; *post-hoc*: $p < 0.01$].



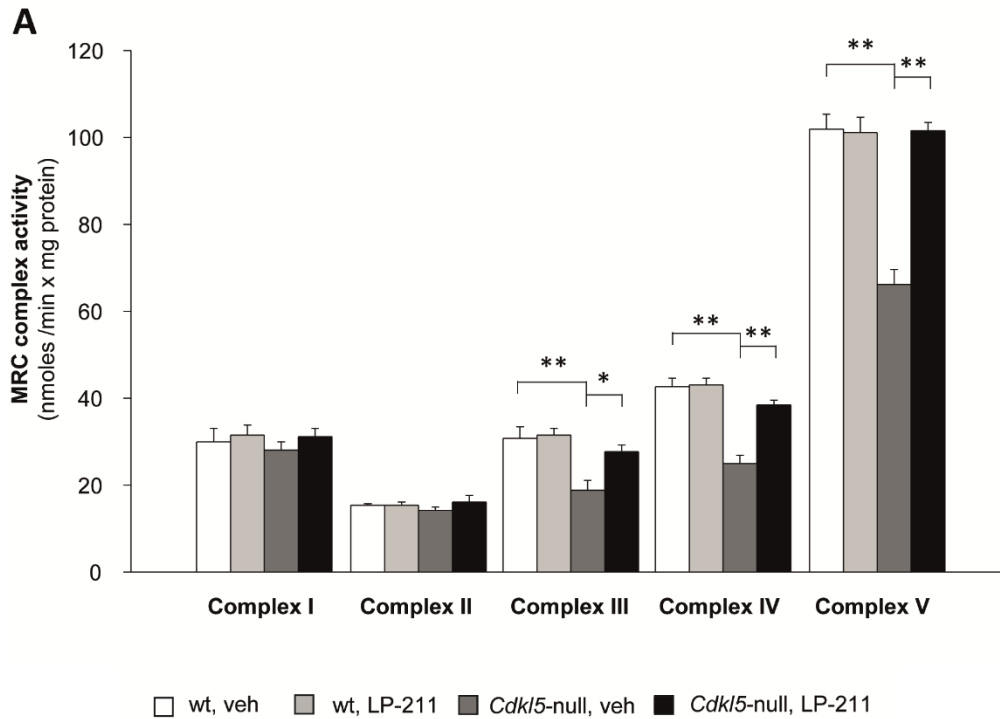**Fig.5**: *Cdkl5-null mouse brain shows defective mitochondrial functionality that is rescued by the LP-211 treatment.* (**B**) Mitochondrial ATP production rate and (**C**) ATP level are lower in the brain of *Cdkl5*-null mice. The LP-211 rescues the defective energy status in the brain of *Cdkl5*-null mice (**B, C**) (wt, Veh = 3; wt, LP-211 = 3; *Cdkl5*-null, Veh = 3; *Cdkl5*-null, LP-211 = 3). Data are mean ± SEM. Statistical

significance was calculated by two-way ANOVA. \*\*p <0.01; \*p < 0.05 after Tukey's *post-hoc* test.

## 3.5 Discussion

This study provides the first characterization of the behavioural phenotype of *Cdkl5*-null mice at an advanced stage of the disease and demonstrates that 5-HT$_7$R modulation, with the 5-HT$_7$R agonist LP-211, partially rescues the abnormal neurobehavioural phenotype of fully symptomatic *Cdkl5*-null male mice. In particular, in *Cdkl5*-null mice receiving the LP-211 treatment we found a normalization of PPI deficits and a complete restoration of rpS6 activation in cortical brain areas. Moreover, we demonstrate for the first time that mitochondria, the powerhouses of the cells, show important abnormalities at the functional level in *Cdkl5*-null brain and that such functional alterations can be persistently restored by modulation of brain 5-HT$_7$R.

In spite of the progressive nature of CDD, mouse studies have been so far focused on young animals (i.e. 2-4 months of age) and no information is available on behavioural as well as brain molecular alterations in *Cdkl5*-null mice at an advanced stage of the disease. The present study provides the first comprehensive characterization of the behavioural phenotype displayed by 9-12-months old *Cdkl5*-null male mice. In particular, we found marked alterations in the general health status and in the locomotor profile, with *Cdkl5*-null mice showing an hypo-locomotor profile in the home cage and hyperlocomotion in the open field, thus confirming previous data in young animals (Amendola et al., 2014; Jhang et al., 2017). An abnormal profile was also observed in the fear conditioning task, suggestive of a profound cognitive impairment in fully symptomatic *Cdkl5*-null mice. We cannot however exclude that the hyperactive profile shown by *Cdkl5*-null mice when exposed to novel contexts may account for the reduced freezing behavior in this cognitive task (Amendola et al., 2014; Jhang et al., 2017).

145

Furthermore, the comprehensive battery of behavioural tests we carried out allowed us to identify the presence of severe PPI deficits in fully symptomatic *Cdkl5*-null mice, a measure of sensorimotor gating of the startle reflex (Swerdlow et al., 2001) that is known to be affected in patients with several neuropsychiatric disorders including schizophrenia (Braff et al., 2001), and in rodent models (Schwabe and Krauss, 2017). As PPI can be easily assessed in patients (Braff et al., 2001), present results provide to the clinical setting an innovative, non-invasive tool to test the efficacy of potential treatments for CDD. Further studies are however needed to uncover the developmental course of this behavioural alteration as a reduction in PPI was previously reported in two-months old *Cdkl5*-null mice, that just missed statistical significance (Okuda et al., 2018).

Of note, the LP-211 treatment rescued this behavioural alteration in *Cdkl5*-null mice. A link between PPI deficits and abnormal serotonin signalling has been clearly established, with either an increase or a decrease in serotonin signalling leading to PPI disruption (Fletcher et al., 2001). Moreover, based on human studies demonstrating that 5-HT$_7$R mRNA is downregulated in the dorsolateral prefrontal cortex of schizophrenics (East et al., 2002), several works have addressed and demonstrated the involvement of 5-HT$_7$R in regulation of the PPI response in rodents (Pouzet et al., 2002b; Semenova et al., 2008). Our results similarly suggest that 5-HT$_7$R may be critically involved in serotonin-dependent regulation of the sensorimotor gating processing. Since we did not observe any change in the levels of the 5-HT$_7$R in *Cdkl5*-null mouse brain, our results suggest that stimulation of the 5-HT$_7$R might have indirectly rescued 5-HT$_7$R-independent defects in *Cdkl5*-null mouse brain. Indeed, several serotonin receptors have been found to be involved in the regulation of PPI (Pouzet et al., 2002a; Mitchell and Neumaier, 2008; Pogorelov et al.,

2017). Moreover, other neurotransmitter systems including glutamate and dopamine play a role in regulating sensorimotor gating (reviewed in (Geyer et al., 2001)).

Another important finding of the present study concerns the demonstration that *Cdkl5*-null mouse brains display impaired mitochondrial OXPHOS and a consequent decrease in brain energy status. We found reduced activity of the complexes III, IV, V and decreased ATP production and whole brain levels. How the lack of Cdkl5 produces such a mitochondrial dysfunction in mouse brain is not yet clear. Both transcriptional and post-translational mechanisms may be involved (De Filippis et al., 2015b). Of note, high levels of oxidative stress markers have been found in CDKL5 patients (Pecorelli et al., 2011), that have been proposed to be due to mitochondrial dysfunction (Pecorelli et al., 2015). We clearly demonstrate here the occurrence of multilevel dysfunctions of brain mitochondria in *Cdkl5*-null mice, thus providing support to this hypothesis.

Interestingly, reactivation of mitochondrial respiratory chain complexes in *Cdkl5*-null mouse brain by the LP-211 treatment rescued the defective brain energy status. Present results are in line with previous studies reporting the beneficial effect of the LP-211 treatment on brain mitochondrial function of two mouse models of RTT (Valenti et al., 2017). Taken together, these data strengthen the suggested link between 5-HT$_7$R and mitochondria in mouse brain and add relevant information to previous studies demonstrating a role for the serotonergic system in the regulation of mitochondria homeostasis (Chen et al., 2007; de Oliveira, 2016).

In the present study, we focused on RhoGTPases signaling, based on previous evidence suggesting that these pathways may be altered in CDD (Chen et al., 2010). Contrary to our expectation, we found normal activation

levels of Rac1 in *Cdkl5*-null mouse cortex at the tested age. These results are in contrast with previous *in vitro* studies suggesting that defective Rac1 activation may play a role in CDD pathogenesis (Chen et al., 2010; Barbiero et al., 2017). Since no data on younger animals are currently available we cannot however exclude that such inconsistency may be due to the advanced age of the experimental mice. Indeed, a recent study aimed at evaluating Rac1 signaling in the brain of Fragile X mouse model has uncovered an age-dependent effect, with the observed Rac1 overactivation disappearing in older animals (Pyronneau et al., 2017).

Evidence that CDKL5 pathogenesis changes as the disease progresses is in fact provided by the increased activation of rpS6 (p 240/244) and the lack of genotype differences in Akt activation we found in *Cdkl5*-null mouse cortex at an advanced stage of the disease, which are in contrast with the previously reported reductions in younger animals (9-12 months of age vs postnatal day 27 and 60) (Amendola et al., 2014; Della Sala et al., 2016). Moreover, recent evidence demonstrated age-dependent efficacy of pharmacological treatment strategies in *Cdkl5*-null mice, with drugs exerting promising beneficial effects in two-month old *Cdkl5*-null mice losing their effectiveness at an advanced stage of the disease (Fuchs et al., 2018a). Altogether, these data highlight the need for studies aimed at evaluating the developmental progression of the disease and for innovative therapeutic strategies to be applied at an advanced stage of the disease, when previously efficacious therapies may lose their effectiveness.

We found that the LP-211 treatment normalized the unexpected overactivation of rpS6 in *Cdkl5*-null cortex, in addition to PPI deficits and mitochondrial dysfunction. Given that Rac1 and AkT activation were found to be normal and were not affected by the LP-211 treatment, present results

148

suggest that different upstream molecules of rpS6 are altered in *Cdkl5*-null mouse brain at an advanced stage of the disease, that may account for the beneficial effects of the treatment under investigation (Bokoch, 2003; Biever et al., 2015). Indeed, the 5-HT$_7$R activation is known to stimulate several signalling cascades (Speranza et al., 2013; Guseva et al., 2014). Interestingly, among them, PKA activation has been intriguingly linked to de-phosphorylation of rpS6 at Ser240/244 (Bonito-Oliva et al., 2013) and to regulation of PPI (Kelly et al., 2007).

Besides the overactivation of rpS6, increased activation of group I PAKs was also evident in *Cdkl5*-null mouse brain, that was exacerbated by the LP-211 treatment. This family of proteins is crucially involved in several neuronal processes potentially relevant for CDD. In fact, group I PAKs play a crucial role in modulating ultrastructural neuronal morphology *in vivo* and in regulating activity-dependent actin dynamics, underlying synaptic plasticity (Hayashi-Takagi et al., 2010; De Filippis et al., 2014b; Duffney et al., 2015). Moreover, overactivation of the Rac/Pak pathway affects fear memory (Das et al., 2017), social learning (Molosh et al., 2014) and synaptic plasticity (Hayashi et al., 2004; Hayashi et al., 2007; Martinez and Tejada-Simon, 2011). Taken together, these results highlight the overactivation of Group I PAKs as a potential innovative target for the treatment of CDD at an advanced stage of the disease. Group I PAKs inhibitors are in fact increasingly recognized as promising candidates for the treatment of Fragile X and schizophrenia (Dolan et al., 2013; Hayashi-Takagi et al., 2014).

In conclusion, the present study provides the first evidence that the LP-211 treatment partially rescues the abnormal neurobehavioural phenotype of clearly symptomatic *Cdkl5*-null male mice. Abnormal PPI and reduced brain energy status due to mitochondrial dysfunction were also uncovered, for the

first time, in *Cdkl5*-null mice at an advanced stage of the disease, thus providing innovative endophenotypes for CDD. Moreover, we provide here the first *in vivo* evidence that Cdkl5 in mouse cortex is involved in regulation of group I PAKs, a family of proteins that are crucially involved in several neuronal processes potentially relevant for CDD. Altogether, the present data highlight innovative endophenotypes and druggable molecular targets for this devastating disorder.

### *Disclosure/Conflicts of interest*

None of the authors declare financial interests or potential conflict of interests.

# 3.6 References

Amendola, E., Zhan, Y., Mattucci, C., Castroflorio, E., Calcagno, E., Fuchs, C., Lonetti, G., Silingardi, D., Vyssotski, A. L., Farley, D., Ciani, E., Pizzorusso, T., Giustetto, M., Gross, C. T., 2014. Mapping pathological phenotypes in a mouse model of CDKL5 disorder. PLoS ONE 9, e91613.

Bahi-Buisson, N., Nectoux, J., Rosas-Vargas, H., Milh, M., Boddaert, N., Girard, B., Cances, C., Ville, D., Afenjar, A., Rio, M., Heron, D., N'Guyen Morel, M. A., Arzimanoglou, A., Philippe, C., Jonveaux, P., Chelly, J., Bienvenu, T., 2008. Key clinical features to identify girls with CDKL5 mutations. Brain 131, 2647-2661.

Barbiero, I., Peroni, D., Tramarin, M., Chandola, C., Rusconi, L., Landsberger, N., Kilstrup-Nielsen, C., 2017. The neurosteroid pregnenolone reverts microtubule derangement induced by the loss of a functional CDKL5-IQGAP1 complex. Hum Mol Genet 26, 3520-3530.

Biever, A., Valjent, E., Puighermanal, E., 2015. Ribosomal Protein S6 Phosphorylation in the Nervous System: From Regulation to Function. Front Mol Neurosci 8, 75.

Bokoch, G. M., 2003. Biology of the p21-activated kinases. Annu Rev Biochem 72, 743-781.

Bonito-Oliva, A., Pallottino, S., Bertran-Gonzalez, J., Girault, J. A., Valjent, E., Fisone, G., 2013. Haloperidol promotes mTORC1-dependent phosphorylation of ribosomal protein S6 via dopamine- and cAMP-regulated phosphoprotein of 32 kDa and inhibition of protein phosphatase-1. Neuropharmacology 72, 197-203.

151

Braff, D. L., Geyer, M. A., Swerdlow, N. R., 2001. Human studies of prepulse inhibition of startle: normal subjects, patient groups, and pharmacological studies. Psychopharmacology (Berl) 156, 234-258.

Chao, H. T., Chen, H., Samaco, R. C., Xue, M., Chahrour, M., Yoo, J., Neul, J. L., Gong, S., Lu, H. C., Heintz, N., Ekker, M., Rubenstein, J. L., Noebels, J. L., Rosenmund, C., Zoghbi, H. Y., 2010. Dysfunction in GABA signalling mediates autism-like stereotypies and Rett syndrome phenotypes. Nature 468, 263-269.

Chen, Q., Zhu, Y. C., Yu, J., Miao, S., Zheng, J., Xu, L., Zhou, Y., Li, D., Zhang, C., Tao, J., Xiong, Z. Q., 2010. CDKL5, a protein associated with rett syndrome, regulates neuronal morphogenesis via Rac1 signaling. J Neurosci 30, 12777-12786.

Chen, S., Owens, G. C., Crossin, K. L., Edelman, D. B., 2007. Serotonin stimulates mitochondrial transport in hippocampal neurons. Mol Cell Neurosci 36, 472-483.

Cifariello, A., Pompili, A., Gasbarri, A., 2008. 5-HT(7) receptors in the modulation of cognitive processes. Behav Brain Res 195, 171-179.

Costa, L., Spatuzza, M., D'Antoni, S., Bonaccorso, C. M., Trovato, C., Musumeci, S. A., Leopoldo, M., Lacivita, E., Catania, M. V., Ciranna, L., 2012. Activation of 5-HT7 serotonin receptors reverses metabotropic glutamate receptor-mediated synaptic plasticity in wild-type and Fmr1 knockout mice, a model of Fragile X syndrome. Biol Psychiatry 72, 924-933.

Das, A., Dines, M., Alapin, J. M., Lamprecht, R., 2017. Affecting long-term fear memory formation through optical control of Rac1 GTPase and PAK activity in lateral amygdala. Sci Rep 7, 13930.

De Filippis, B., Chiodi, V., Adriani, W., Lacivita, E., Mallozzi, C., Leopoldo, M., Domenici, M. R., Fuso, A., Laviola, G., 2015b. Long-lasting beneficial effects of central serotonin receptor 7 stimulation in female mice modeling Rett syndrome. Front Behav Neurosci 9, 86.

De Filippis, B., Musto, M., Altabella, L., Romano, E., Canese, R., Laviola, G., 2015a. Deficient Purposeful Use of Forepaws in Female Mice Modelling Rett Syndrome. Neural Plast 2015a, 326184.

De Filippis, B., Nativio, P., Fabbri, A., Ricceri, L., Adriani, W., Lacivita, E., Leopoldo, M., Passarelli, F., Fuso, A., Laviola, G., 2014a. Pharmacological stimulation of the brain serotonin receptor 7 as a novel therapeutic approach for Rett syndrome. Neuropsychopharmacology 39, 2506-2518.

De Filippis, B., Ricceri, L., Fuso, A., Laviola, G., 2013. Neonatal exposure to low dose corticosterone persistently modulates hippocampal mineralocorticoid receptor expression and improves locomotor/exploratory behaviour in a mouse model of Rett syndrome. Neuropharmacology 68, 174-183.

De Filippis, B., Ricceri, L., Laviola, G., 2010. Early postnatal behavioral changes in the Mecp2-308 truncation mouse model of Rett syndrome. Genes Brain Behav 9, 213-223.

De Filippis, B., Romano, E., Laviola, G., 2014b. Aberrant Rho GTPases signaling and cognitive dysfunction: in vivo evidence for a compelling molecular relationship. Neurosci Biobehav Rev 46 Pt 2, 285-301.

De Filippis, B., Valenti, D., Chiodi, V., Ferrante, A., de Bari, L., Fiorentini, C., Domenici, M. R., Ricceri, L., Vacca, R. A., Fabbri, A., Laviola, G., 2015c. Modulation of Rho GTPases rescues brain mitochondrial

dysfunction, cognitive deficits and aberrant synaptic plasticity in female mice modeling Rett syndrome. Eur Neuropsychopharmacol 25, 889-901.

De Filippis, B., Valenti, D., de Bari, L., De Rasmo, D., Musto, M., Fabbri, A., Ricceri, L., Fiorentini, C., Laviola, G., Vacca, R. A., 2015d. Mitochondrial free radical overproduction due to respiratory chain impairment in the brain of a mouse model of Rett syndrome: protective effect of CNF1. Free Radic Biol Med 83, 167-177.

de Oliveira, M. R., 2016. Fluoxetine and the mitochondria: A review of the toxicological aspects. Toxicol Lett 258, 185-191.

Della Sala, G., Putignano, E., Chelini, G., Melani, R., Calcagno, E., Michele Ratto, G., Amendola, E., Gross, C. T., Giustetto, M., Pizzorusso, T., 2016. Dendritic Spine Instability in a Mouse Model of CDKL5 Disorder Is Rescued by Insulin-like Growth Factor 1. Biol Psychiatry 80, 302-311.

Dolan, B. M., Duron, S. G., Campbell, D. A., Vollrath, B., Shankaranarayana Rao, B. S., Ko, H. Y., Lin, G. G., Govindarajan, A., Choi, S. Y., Tonegawa, S., 2013. Rescue of fragile X syndrome phenotypes in Fmr1 KO mice by the small-molecule PAK inhibitor FRAX486. Proc Natl Acad Sci U S A 110, 5671-5676.

Duffney, L. J., Zhong, P., Wei, J., Matas, E., Cheng, J., Qin, L., Ma, K., Dietz, D. M., Kajiwara, Y., Buxbaum, J. D., Yan, Z., 2015. Autism-like Deficits in Shank3-Deficient Mice Are Rescued by Targeting Actin Regulators. Cell Rep 11, 1400-1413.

East, S. Z., Burnet, P. W., Kerwin, R. W., Harrison, P. J., 2002. An RT-PCR study of 5-HT(6) and 5-HT(7) receptor mRNAs in the hippocampal

formation and prefrontal cortex in schizophrenia. Schizophr Res 57, 15-26.

Elia, M., Falco, M., Ferri, R., Spalletta, A., Bottitta, M., Calabrese, G., Carotenuto, M., Musumeci, S. A., Lo Giudice, M., Fichera, M., 2008. CDKL5 mutations in boys with severe encephalopathy and early-onset intractable epilepsy. Neurology 71, 997-999.

Fehr, S., Downs, J., Ho, G., de Klerk, N., Forbes, D., Christodoulou, J., Williams, S., Leonard, H., 2016. Functional abilities in children and adults with the CDKL5 disorder. Am J Med Genet A 170, 2860-2869.

Fehr, S., Wilson, M., Downs, J., Williams, S., Murgia, A., Sartori, S., Vecchi, M., Ho, G., Polli, R., Psoni, S., Bao, X., de Klerk, N., Leonard, H., Christodoulou, J., 2013. The CDKL5 disorder is an independent clinical entity associated with early-onset encephalopathy. Eur J Hum Genet 21, 266-273.

Fletcher, P. J., Selhi, Z. F., Azampanah, A., Sills, T. L., 2001. Reduced brain serotonin activity disrupts prepulse inhibition of the acoustic startle reflex. Effects of 5,7-dihydroxytryptamine and p-chlorophenylalanine. Neuropsychopharmacology 24, 399-409.

Fuchs, C., Fustini, N., Trazzi, S., Gennaccaro, L., Rimondini, R., Ciani, E., 2018a. Treatment with the GSK3-beta inhibitor Tideglusib improves hippocampal development and memory performance in juvenile, but not adult, Cdkl5 knockout mice. Eur J Neurosci 47, 1054-1066.

Fuchs, C., Gennaccaro, L., Trazzi, S., Bastianini, S., Bettini, S., Martire, V. L., Ren, E., Medici, G., Zoccoli, G., Rimondini, R., Ciani, E., 2018b. Heterozygous CDKL5 Knockout Female Mice Are a Valuable Animal Model for CDKL5 Disorder. Neural Plast 2018, 9726950.

Fuchs, C., Trazzi, S., Torricella, R., Viggiano, R., De Franceschi, M., Amendola, E., Gross, C., Calza, L., Bartesaghi, R., Ciani, E., 2014. Loss of CDKL5 impairs survival and dendritic growth of newborn neurons by altering AKT/GSK-3beta signaling. Neurobiol Dis 70, 53-68.

Geyer, M. A., Krebs-Thomson, K., Braff, D. L., Swerdlow, N. R., 2001. Pharmacological studies of prepulse inhibition models of sensorimotor gating deficits in schizophrenia: a decade in review. Psychopharmacology (Berl) 156, 117-154.

Guseva, D., Wirth, A., Ponimaskin, E., 2014. Cellular mechanisms of the 5-HT7 receptor-mediated signaling. Front Behav Neurosci 8, 306.

Guy, J., Gan, J., Selfridge, J., Cobb, S., Bird, A., 2007. Reversal of neurological defects in a mouse model of Rett syndrome. Science 315, 1143-1147.

Hayashi-Takagi, A., Araki, Y., Nakamura, M., Vollrath, B., Duron, S. G., Yan, Z., Kasai, H., Huganir, R. L., Campbell, D. A., Sawa, A., 2014. PAKs inhibitors ameliorate schizophrenia-associated dendritic spine deterioration in vitro and in vivo during late adolescence. Proc Natl Acad Sci U S A 111, 6461-6466.

Hayashi-Takagi, A., Takaki, M., Graziane, N., Seshadri, S., Murdoch, H., Dunlop, A. J., Makino, Y., Seshadri, A. J., Ishizuka, K., Srivastava, D. P., Xie, Z., Baraban, J. M., Houslay, M. D., Tomoda, T., Brandon, N. J., Kamiya, A., Yan, Z., Penzes, P., Sawa, A., 2010. Disrupted-in-Schizophrenia 1 (DISC1) regulates spines of the glutamate synapse via Rac1. Nat Neurosci 13, 327-332.

Hayashi, M. L., Choi, S. Y., Rao, B. S., Jung, H. Y., Lee, H. K., Zhang, D., Chattarji, S., Kirkwood, A., Tonegawa, S., 2004. Altered cortical

synaptic morphology and impaired memory consolidation in forebrain-specific dominant-negative PAK transgenic mice. Neuron 42, 773-787.

Hayashi, M. L., Rao, B. S., Seo, J. S., Choi, H. S., Dolan, B. M., Choi, S. Y., Chattarji, S., Tonegawa, S., 2007. Inhibition of p21-activated kinase rescues symptoms of fragile X syndrome in mice. Proc Natl Acad Sci U S A 104, 11489-11494.

Hedlund, P. B., 2009. The 5-HT7 receptor and disorders of the nervous system: an overview. Psychopharmacology (Berl) 206, 345-354.

Hedlund, P. B., Danielson, P. E., Thomas, E. A., Slanina, K., Carson, M. J., Sutcliffe, J. G., 2003. No hypothermic response to serotonin in 5-HT7 receptor knockout mice. Proc Natl Acad Sci U S A 100, 1375-1380.

Jhang, C. L., Huang, T. N., Hsueh, Y. P., Liao, W., 2017. Mice lacking cyclin-dependent kinase-like 5 manifest autistic and ADHD-like behaviors. Hum Mol Genet 26, 3922-3934.

Kalscheuer, V. M., Tao, J., Donnelly, A., Hollway, G., Schwinger, E., Kubart, S., Menzel, C., Hoeltzenbein, M., Tommerup, N., Eyre, H., Harbord, M., Haan, E., Sutherland, G. R., Ropers, H. H., Gecz, J., 2003. Disruption of the serine/threonine kinase 9 gene causes severe X-linked infantile spasms and mental retardation. Am J Hum Genet 72, 1401-1411.

Kelly, M. P., Isiegas, C., Cheung, Y. F., Tokarczyk, J., Yang, X., Esposito, M. F., Rapoport, D. A., Fabian, S. A., Siegel, S. J., Wand, G., Houslay, M. D., Kanes, S. J., Abel, T., 2007. Constitutive activation of Galphas within forebrain neurons causes deficits in sensorimotor gating because of PKA-dependent decreases in cAMP. Neuropsychopharmacology 32, 577-588.

Khan, H. A., 2003. Bioluminometric assay of ATP in mouse brain: Determinant factors for enhanced test sensitivity. J Biosci 28, 379-382.

Kilstrup-Nielsen, C., Rusconi, L., La Montanara, P., Ciceri, D., Bergo, A., Bedogni, F., Landsberger, N., 2012. What we know and would like to know about CDKL5 and its involvement in epileptic encephalopathy. Neural Plast 2012, 728267.

Leopoldo, M., Lacivita, E., De Giorgio, P., Fracasso, C., Guzzetti, S., Caccia, S., Contino, M., Colabufo, N. A., Berardi, F., Perrone, R., 2008. Structural modifications of N-(1,2,3,4-tetrahydronaphthalen-1-yl)-4-aryl-1-piperazinehexanamides: influence on lipophilicity and 5-HT7 receptor activity. Part III. J Med Chem 51, 5813-5822.

Macri, S., Ceci, C., Onori, M. P., Invernizzi, R. W., Bartolini, E., Altabella, L., Canese, R., Imperi, M., Orefici, G., Creti, R., Margarit, I., Magliozzi, R., Laviola, G., 2015. Mice repeatedly exposed to Group-A beta-Haemolytic Streptococcus show perseverative behaviors, impaired sensorimotor gating, and immune activation in rostral diencephalon. Sci Rep 5, 13257.

Manente, A. G., Valenti, D., Pinton, G., Jithesh, P. V., Daga, A., Rossi, L., Gray, S. G., O'Byrne, K. J., Fennell, D. A., Vacca, R. A., Nilsson, S., Mutti, L., Moro, L., 2013. Estrogen receptor beta activation impairs mitochondrial oxidative metabolism and affects malignant mesothelioma cell growth in vitro and in vivo. Oncogenesis 2, e72.

Martinez, L. A., Tejada-Simon, M. V., 2011. Pharmacological inactivation of the small GTPase Rac1 impairs long-term plasticity in the mouse hippocampus. Neuropharmacology 61, 305-312.

Matthys, A., Haegeman, G., Van Craenenbroeck, K., Vanhoenacker, P., 2011. Role of the 5-HT7 receptor in the central nervous system: from current status to future perspectives. Mol Neurobiol 43, 228-253.

Mitchell, E. S., Neumaier, J. F., 2008. 5-HT6 receptor antagonist reversal of emotional learning and prepulse inhibition deficits induced by apomorphine or scopolamine. Pharmacol Biochem Behav 88, 291-298.

Molosh, A. I., Johnson, P. L., Spence, J. P., Arendt, D., Federici, L. M., Bernabe, C., Janasik, S. P., Segu, Z. M., Khanna, R., Goswami, C., Zhu, W., Park, S. J., Li, L., Mechref, Y. S., Clapp, D. W., Shekhar, A., 2014. Social learning and amygdala disruptions in Nf1 mice are rescued by blocking p21-activated kinase. Nat Neurosci 17, 1583-1590.

Okuda, K., Takao, K., Watanabe, A., Miyakawa, T., Mizuguchi, M., Tanaka, T., 2018. Comprehensive behavioral analysis of the Cdkl5 knockout mice revealed significant enhancement in anxiety- and fear-related behaviors and impairment in both acquisition and long-term retention of spatial reference memory. PLoS ONE 13, e0196587.

Pecorelli, A., Belmonte, G., Meloni, I., Cervellati, F., Gardi, C., Sticozzi, C., De Felice, C., Signorini, C., Cortelazzo, A., Leoncini, S., Ciccoli, L., Renieri, A., Jay Forman, H., Hayek, J., Valacchi, G., 2015. Alteration of serum lipid profile, SRB1 loss, and impaired Nrf2 activation in CDKL5 disorder. Free Radic Biol Med 86, 156-165.

Pecorelli, A., Ciccoli, L., Signorini, C., Leoncini, S., Giardini, A., D'Esposito, M., Filosa, S., Hayek, J., De Felice, C., Valacchi, G., 2011. Increased levels of 4HNE-protein plasma adducts in Rett syndrome. Clin Biochem 44, 368-371.

Pogorelov, V. M., Rodriguiz, R. M., Cheng, J., Huang, M., Schmerberg, C. M., Meltzer, H. Y., Roth, B. L., Kozikowski, A. P., Wetsel, W. C., 2017. 5-HT2C Agonists Modulate Schizophrenia-Like Behaviors in Mice. Neuropsychopharmacology 42, 2163-2177.

Pouzet, B., Didriksen, M., Arnt, J., 2002a. Effects of the 5-HT(6) receptor antagonist, SB-271046, in animal models for schizophrenia. Pharmacol Biochem Behav 71, 635-643.

Pouzet, B., Didriksen, M., Arnt, J., 2002b. Effects of the 5-HT(7) receptor antagonist SB-258741 in animal models for schizophrenia. Pharmacol Biochem Behav 71, 655-665.

Pyronneau, A., He, Q., Hwang, J. Y., Porch, M., Contractor, A., Zukin, R. S., 2017. Aberrant Rac1-cofilin signaling mediates defects in dendritic spines, synaptic function, and sensory perception in fragile X syndrome. Sci Signal 10.

Ricceri, L., De Filippis, B., Fuso, A., Laviola, G., 2011. Cholinergic hypofunction in MeCP2-308 mice: beneficial neurobehavioural effects of neonatal choline supplementation. Behav Brain Res 221, 623-629.

Ricciardi, S., Boggio, E. M., Grosso, S., Lonetti, G., Forlani, G., Stefanelli, G., Calcagno, E., Morello, N., Landsberger, N., Biffo, S., Pizzorusso, T., Giustetto, M., Broccoli, V., 2011. Reduced AKT/mTOR signaling and protein synthesis dysregulation in a Rett syndrome animal model. Hum Mol Genet 20, 1182-1196.

Ricciardi, S., Ungaro, F., Hambrock, M., Rademacher, N., Stefanelli, G., Brambilla, D., Sessa, A., Magagnotti, C., Bachi, A., Giarda, E., Verpelli, C., Kilstrup-Nielsen, C., Sala, C., Kalscheuer, V. M., Broccoli, V., 2012. CDKL5 ensures excitatory synapse stability by reinforcing NGL-1-

PSD95 interaction in the postsynaptic compartment and is impaired in patient iPSC-derived neurons. Nat Cell Biol 14, 911-923.

Rusconi, L., Kilstrup-Nielsen, C., Landsberger, N., 2011. Extrasynaptic N-methyl-D-aspartate (NMDA) receptor stimulation induces cytoplasmic translocation of the CDKL5 kinase and its proteasomal degradation. J Biol Chem 286, 36550-36558.

Rusconi, L., Salvatoni, L., Giudici, L., Bertani, I., Kilstrup-Nielsen, C., Broccoli, V., Landsberger, N., 2008. CDKL5 expression is modulated during neuronal development and its subcellular distribution is tightly regulated by the C-terminal tail. J Biol Chem 283, 30101-30111.

Schwabe, K., Krauss, J. K., 2017. What rodent models of deep brain stimulation can teach us about the neural circuit regulation of prepulse inhibition in neuropsychiatric disorders. Schizophr Res.

Semenova, S., Geyer, M. A., Sutcliffe, J. G., Markou, A., Hedlund, P. B., 2008. Inactivation of the 5-HT(7) receptor partially blocks phencyclidine-induced disruption of prepulse inhibition. Biol Psychiatry 63, 98-105.

Speranza, L., Chambery, A., Di Domenico, M., Crispino, M., Severino, V., Volpicelli, F., Leopoldo, M., Bellenchi, G. C., di Porzio, U., Perrone-Capano, C., 2013. The serotonin receptor 7 promotes neurite outgrowth via ERK and Cdk5 signaling pathways. Neuropharmacology 67, 155-167.

Speranza, L., Labus, J., Volpicelli, F., Guseva, D., Lacivita, E., Leopoldo, M., Bellenchi, G. C., di Porzio, U., Bijata, M., Perrone-Capano, C., Ponimaskin, E., 2017. Serotonin 5-HT7 receptor increases the density of dendritic spines and facilitates synaptogenesis in forebrain neurons. J Neurochem 141, 647-661.

Swerdlow, N. R., Geyer, M. A., Braff, D. L., 2001. Neural circuit regulation of prepulse inhibition of startle in the rat: current knowledge and future challenges. Psychopharmacology (Berl) 156, 194-215.

Valenti, D., de Bari, L., De Filippis, B., Henrion-Caude, A., Vacca, R. A., 2014. Mitochondrial dysfunction as a central actor in intellectual disability-related diseases: an overview of Down syndrome, autism, Fragile X and Rett syndrome. Neurosci Biobehav Rev 46 Pt 2, 202-217.

Valenti, D., de Bari, L., Vigli, D., Lacivita, E., Leopoldo, M., Laviola, G., Vacca, R. A., De Filippis, B., 2017. Stimulation of the brain serotonin receptor 7 rescues mitochondrial dysfunction in female mice from two models of Rett syndrome. Neuropharmacology 121, 79-88.

Valenti, D., Tullo, A., Caratozzolo, M. F., Merafina, R. S., Scartezzini, P., Marra, E., Vacca, R. A., 2010. Impairment of F1F0-ATPase, adenine nucleotide translocator and adenylate kinase causes mitochondrial energy deficit in human skin fibroblasts with chromosome 21 trisomy. Biochem J 431, 299-310.

Wang, I. T., Allen, M., Goffin, D., Zhu, X., Fairless, A. H., Brodkin, E. S., Siegel, S. J., Marsh, E. D., Blendy, J. A., Zhou, Z., 2012. Loss of CDKL5 disrupts kinome profile and event-related potentials leading to autistic-like phenotypes in mice. Proc Natl Acad Sci U S A 109, 21516-21521.

Wilcox, R. R., 1987. New Designs in Analysis of Variance. Annual Review of Psychology 38, 29-60.

Zhou, A., Han, S., Zhou, Z. J., 2017. Molecular and genetic insights into an infantile epileptic encephalopathy - CDKL5 disorder. Front Biol (Beijing) 12, 1-6.

*Supplementary materials*

## Genotyping

DNA has been prepared from a small tail-tip biopsy taken at weaning, as previously described (De Filippis et al., 2010). The *Cdkl5* alleles have been identified by PCR using two sets of primers. Primer set 1 (5′ primer: 5'- ACG-ATA-GAA-ATA-GAG-GAT-CAA-CCC-3′ and 3′ primer: 5'-CCC-AAG-TAT-ACC-CCT-TTC-CA-3') yields a product of 240 bp identifying the wild type allele. Primer set 2 (5′ primer same as for primer set 1 and 3′ primer: 5'-CTG-TGA-CTA-GGG-GCT-AGA-GA 3') yields a product of apparent size 344 bp identifying the null allele. PCR products were electrophoresed through a 2% NuSieve 3:1 agarose gel (Cambrex Bio Science, Rockland, ME, USA) containing 0.1 µl/ml GelRed™ and examined under UV light.

## Behavioural testing

*Prepulse Inhibition*

Sensorimotor gating was evaluated 7 days after the last i.p. with the prepulse inhibition (PPI) paradigm (Swerdlow et al., 2001). The apparatus consisted of two Plexiglas rectangular boxes (startle cages) (9 x 7 cm), placed in sound-attenuated chambers with a red light and a fan ventilator (Med associates inc. St Albans, VT, United States of America). Background white noise and acoustic bursts were conveyed by two separate speakers, properly spaced from the startle cage so as to produce a fine-tuned regulation of sound. Both speakers and startle cages were connected to a main PC computer, which detected and analyzed all chamber variables by means of a specific software. Before every testing session, acoustic stimuli and mechanical responses were calibrated via specific devices supplied by Med Associates. One day before the

experiment, all mice were left undisturbed in the apparatus in the presence of the background noise for 5 minutes (habituation). On the following day (test), mice were positioned inside the startle chamber and exposed to a continuous white noise (62 db) for 5 min, followed by three blocks of trials. The first and third blocks consisted of 10 pulses (40ms, 120 db) interspaced by an average inter-trial interval of 15s. The second block of trials displayed a pseudorandom sequence of 28 trials. Each trial started with a 50ms null period, followed by a 20ms pre-pulse noise bursts. The delay between the pre-pulses and the startle was 100ms. Two slightly different protocols were adopted on two cohorts of mice, that differed in the range of prepulse intensities under investigation. On the first cohort of mice, prepulse intensities were as follows: 67, 70, 73 or 76 db and the following types of trials were entailed: prepulse plus startle (four trials per prepulse intensity), prepulse alone (four trials per prepulse intensity), startle alone (four trials) and no stimulation (four trials) (Macri et al., 2015). On the second cohort, 78, 82 or 84 dB pre-pulse intensities were applied (Chao et al., 2010), with the following trials: prepulse plus startle (eight trials per prepulse intensity), prepulse alone (eight trials per prepulse intensity), startle alone (eight trials) and no stimulation (eight trials). To prevent habituation, the inter-trial interval randomly varied between 10s and 20s. Before each animal testing the apparatus was cleaned with 70% ethanol solution. To evaluate sensorimotor gating capabilities in Cdkl5-*null* mice, the % PPI was calculated as follows: (100-[(mean startle amplitude for prepulse +pulse trials/mean startle amplitude for pulse-alone trials) x100]).

*Nest building evaluation*

One piece of filter paper (5 cm × 5 cm) was provided to each singly housed mouse. Mice were singly housed on the day before nest material provision. The quality of the nests was scored by a trained observer, according

164

to the following five-point qualitative scale: 0: nest material untouched; 1: nest material nearly untouched; 2: nest material scattered, no clear shape evident; 3: nest of intermediate quality; 4: nest round and well built.

*Home cage locomotor activity*

To verify whether LP-211 treatment affects the daily locomotor activity in *Cdkl5*-null mice, spontaneous locomotor activity in the home cages was evaluated. Levels of activity were monitored continuously by means of an automatic device using small passive infrared sensors positioned on the top of each cage (ACTIVISCOPE system, NewBehaviour Inc., Zurich, Switzerland). The sensors (20 Hz) detected any movement of mice with a frequency of 20 events per second. Data were recorded by a computer with dedicated software. No movements were detected by the sensors when mice were sleeping, inactive, or performing moderate self-grooming. Scores were obtained during 60 min intervals and expressed as counts per hour. The position of cages in the rack was such that mice of each group were equally distributed in rows and columns.

*Open field test*

The apparatus consisted of a black plastic cubical arena ($40 \times 40 \times 40$ cm) with a grey floor subdivided by black line into $8 \times 8$ cm squares. The session started by placing the animal in one corner of the arena and lasted 60 min. Activity was recorded by a suspended video camera and analyzed using Ethovision software (Noldus, Netherlands). A central square zone (30 x 30 cm) was defined to evaluate anxiety-related responses. Total distance moved, speed and number of entries into the central zone of the arena were automatically scored throughout the 60-min session. The floor of the apparatus was cleaned with 70% ethanol before each testing session.

**Neurobiological analyses**

*Western blot analysis*

Tissues, hippocampi and cortices, from 4 mice for WT-Vehicle group and from 6 mice for the other groups were collected 2 months after the last i.p. and immediately frozen in dry ice. To prepare the lysate, tissue were defrosted in ice and soon after homogenized with a glass-glass ice-cold dounce homogenizer in lysis buffer (Tris-HCl pH 8, 50 mM; NaCl, 150 mM; EDTA, 2 mM) supplemented with protease and phosphatase inhibitor cocktails (PIC, cod. P8340, Sigma Aldrich and PhosSTOP, cod. 04 906 837 001, Roche, respectively). To the homogenized tissues, a final concentration of 1% NP40 and 0,1% SDS were added to promote membrane solubilization. After a 30-minute incubation in ice, samples were sonicated to fragment nucleic acids and centrifuged at 16000g for 15' at 4°C. Cellular debris were discarded and the supernatants collected, dosed with the bicinchonic acid assay (Pierce) and stored in laemmli buffer. For western blotting analysis, 20 mg of total proteins were separated on a 12% SDS-PAGE and blotted to nitrocellulose membrane. The following primary antibodies were used: rabbit polyconal anti-rpS6 (1:1000, cod. 2217, Cell Signaling), rabbit polyclonal anti-phospho-rpS6 (1:1000, cod. 2211 (Ser 235/236) and cod. 2215 (Ser 240/244), Cell Signaling), rabbit polyclonal anti phospho S473 Akt (1:1000, cod. 9271, Cell Signaling), rabbit polyclonal anti Akt total (1:1000, cod. 9272, Cell Signaling), rabbit polyclonal anti-phospho PAK Ser 141 (1:500, cod. 44940G, Invitrogen), rabbit polyclonal anti-PAK (C-19) (1:1000, cod. sc-881, Santa Cruz), rabbit polyclonal anti-CDKL5 (1:1000, cod. HPA002847) and mouse monoclonal anti-neuronal class III b-tubulin (clone TUJ1, cod. MMS-435P, Covance). Images of the membranes were acquired by a CCD camera (Syngene, G-Box Chemi XRQ) and optical densities (O.D.) of the protein signals calculated for

each sample with Image J software and normalized with the corresponding TUJ1 signal; the O.D. ratios were then compared and expressed as the average fold increase, with 1 (wt control) as baseline.

## *Mitochondrial analysis*

*Brain tissue cryopreservation*. Brains were submerged in a dry-ice-cold cryopreservation solution consisting of 50 mM K-MES (pH 7.1), 3 mM $K_2HPO_4$, 9.5 mM $MgCl_2$, 3 mM ATP plus 20% glycerol and 10 mg/ml BSA and stored at -80°C until assayed.

*Measurement of mitochondrial ATP production rate.* Mitochondria isolated from total brain were incubated at 37°C in 2 ml of respiratory medium consisting of 210 mM mannitol, 70 mM sucrose, 20 mM Tris/HCl, 5 mM $KH_2PO_4$/$K_2HPO_4$, (pH 7.4) plus 5 mg/ml BSA, 3 mM $MgCl_2$, in the presence of the ATP detecting system consisting of glucose (2.5 mM), hexokinase (HK, 2 e.u.), glucose 6-phosphate dehydrogenase (G6P-DH, 1 e.u.) and $NADP^+$ (0.25 mM) in the presence of glutamate (GLU) plus malate (MAL) (5 mM each) or succinate (SUCC, 5 mM) plus rotenone (ROT, 3 µM), or ascorbate (ASC, 0.5 mM) plus N,N,N',N'- tetramethyl-p-phenylenediamine (TMPD, 0.25 mM), as energy sources. The reduction of $NADP^+$ in the extramitochondrial phase, which reveals ATP formation from externally added ADP (0.5 mM), was monitored as an increase in absorbance at 340 nm. Care was taken to use enough HK/G6P-DH coupled enzymes to ensure a non-limiting ADP-regenerating system for the measurement of ATP production.

*Measurement of mouse brain ATP levels.* Half brain was weighted (approx. 20 mg) and subjected to perchloric acid extraction: tissues were homogenized in 600 µl of pre-cooled 10% perchloric acid neutralized with 2.5 M KOH and then centrifuged at 14000 rpm for 10 min, 4°C. The amount of

tissue ATP was determined enzymatically in KOH neutralized extracts, as described in (Valenti et al., 2010).

*Measurement of mitochondrial respiratory chain complex (MRC) activities*. For isolation of mitochondrial membrane-enriched fractions, mitochondrial pellets were first frozen at -80° C, then thawed at 2-4°C, suspended in 1 ml of 10 mM Tris-HCl (pH 7.5) plus 1mg/ml BSA and exposed to ultrasound energy for 8s at 0°C (11 pulse 0.7 sec on, 0.7 sec off) at 20 kHz, intensity 2. The ultrasound-treated mitochondria were centrifuged at 600 rpm for 10 min, 4°C. The supernatant was centrifuged again at 14000 rpm for 10 min, 4°C and the resulting pellet was kept at -80°C until use. Measurement of MRC complex activities were performed essentially as in (Manente et al., 2013), by three assays which rely on the sequential addition of reagents to measure the activities of: i) NADH: ubiquinone oxidoreductase (complex I) followed by ATP synthase (complex V), ii) succinate: ubiquinone oxidoreductase (complex II) and iii) cytochrome *c* oxidase (complex IV) followed by cytochrome *c* oxidoreductase (complex III).
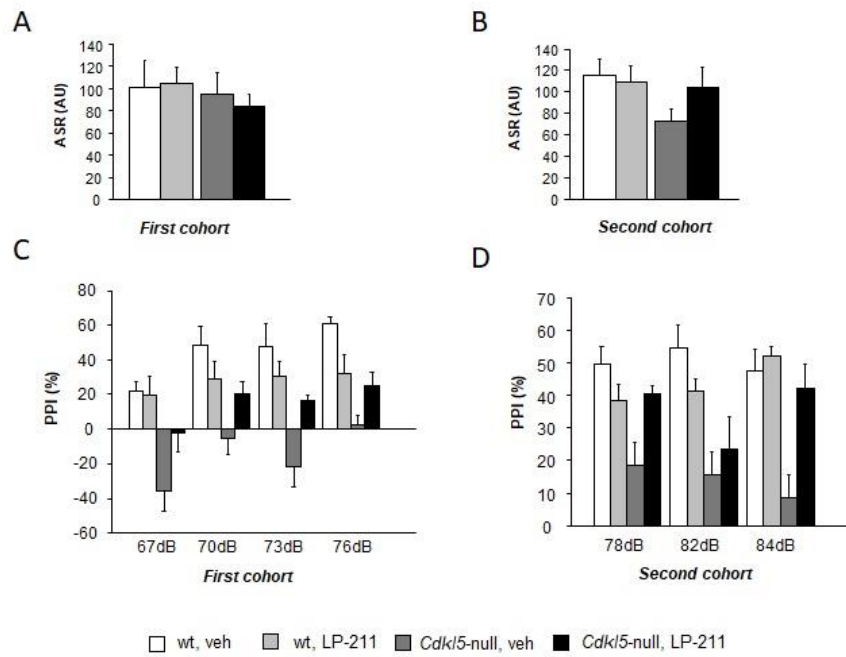
**Figure S1**: *Prepulse inhibition (PPI) paradigm.* **(A-B)** No genotype or treatment effect was found in the Acoustic Startle Response (ASR) on the two cohorts of animals; **(C-D)** the graphs show the % PPI in the not significant prepulses intensities*genotype*treatment interactions of the two experiments. Data are mean±SEM. Statistical significance was calculated by two-way ANOVA with Tukey's post hoc tests.
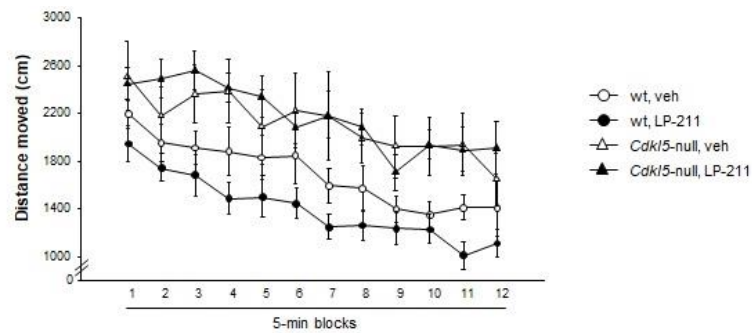


**Figure S2**: *Open Field task.* The graph shows the distance moved in the 5 minutes-blocks*genotype*treatment interaction. Data are mean±SEM. Statistical significance was calculated by two-way ANOVA with Tukey's post hoc tests.
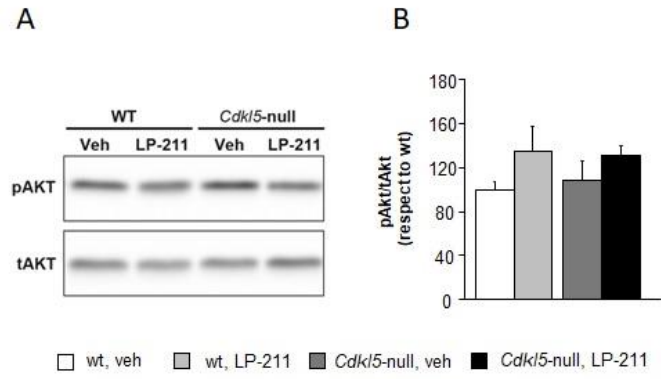
**Figure S3**: *Cortical Akt activity.* **(A)** Representative Western blot analysis (summarized view corresponding to one animal per group). **(B)** No genotype or treatment effects were found. Data are mean±SEM. Statistical significance was calculated by two-way ANOVA with Tukey's post hoc tests. pAKT: phopsho-AKT; tAKT: AKT total
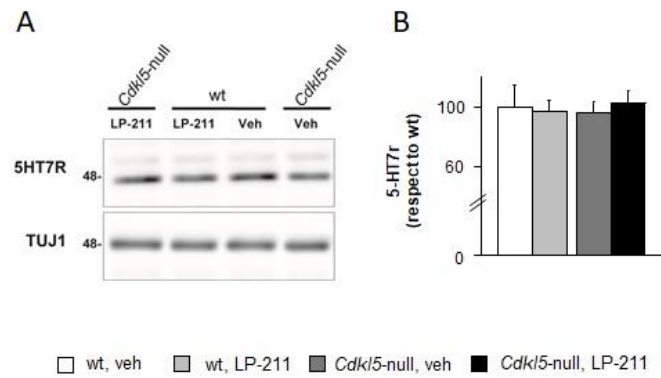


**Figure S4**: *Cortical 5-HT$_7$ receptors (5-HT$_7$ r) levels.* **(A)** Representative Western blot analysis (summarized view corresponding to one animal per group). **(B)** No genotype or treatment effects were found. Data are mean±SEM. Statistical significance was calculated by two-way ANOVA with Tukey's post hoc tests.

170

*Chapter 4*

# 4.    Chronic treatment with the phytocannabinoid Cannabidivarin (CBDV) rescues behavioural alterations and brain atrophy in a mouse model of Rett syndrome

[1]Daniele Vigli, [1]Livia Cosentino, [2]Carla Raggi, [1]Giovanni Laviola, [3]Marie Woolley-Roberts, [1]Bianca De Filippis.

[1]*Center for Behavioral Sciences and Mental Health, Istituto Superiore di Sanità, Rome, Italy;* [2]*National Center for Control and Evaluation of Medicines, Istituto Superiore di Sanità, Rome, Italy;* [3]*GW Research Ltd, Cambridge, UK.*

# 4.1 Abstract

Rett syndrome (RTT) is a rare neurodevelopmental disorder, characterized by severe behavioural and physiological symptoms. RTT is caused by mutations in the *MECP2* gene in about 95% of cases and to date no cure is available. The endocannabinoid system modulates several physiological processes and behavioural responses that are impaired in RTT and its deregulation has been associated with neuropsychiatric disorders which have symptoms in common with RTT. The present study evaluated the potential therapeutic efficacy for RTT of cannabidivarin (CBDV), a non-psychotropic phytocannabinoid from *Cannabis sativa* that presents antagonistic properties on the G protein-coupled receptor 55 (GPR55), the most recently identified cannabinoid receptor. Present results demonstrate that systemic treatment with CBDV (2, 20, 100 mg/Kg ip for 14 days) rescues behavioural and brain alterations in MeCP2-308 male mice, a validated RTT model. The CBDV treatment restored the compromised general health status, the sociability and the brain weight in RTT mice. A partial restoration of motor coordination was also observed. Moreover, increased levels of GPR55 were found in RTT mouse hippocampus, suggesting this G protein-coupled receptor as new potential target for the treatment of this disorder. Present findings highlight for the first time for RTT the translational relevance of CBDV, an innovative therapeutic agent that is under active investigation in the clinical setting.

## 4.2   Introduction

Rett syndrome (RTT) is a rare neurodevelopmental disorder, characterized by severe behavioural and physiological symptoms (Hagberg et al., 2002; Rett, 1966; Ricceri et al., 2012). One essential feature of RTT is the apparently normal perinatal development until about 6-18 months of age, when RTT patients start losing their acquired cognitive, social, and motor skills and develop a wide variety of symptoms (Hagberg, 2002). Classic RTT is caused in about 90–95% of cases by *de novo* mutations in the X-linked *MECP2* gene, which encodes the methyl CpG-binding protein 2 (MECP2), a multifunctional protein that binds to methylated DNA and mainly acts as a key transcriptional regulator (Guy et al., 2011). Despite extensive effort in this research field, how mutations in *MECP2* lead to the symptomatology of RTT is still unknown and no effective therapy is currently available for this devastating syndrome.

The endocannabinoid system (ECS) is a complex neuromodulatory system found in all vertebrate classes, involved in the regulation of numerous physiological functions (Kano et al., 2009). At the central level, ECS modulates several physiological processes and behavioural responses that are impaired in RTT (Di Marzo et al., 2015), such as social behaviour (Wei et al., 2017), anxiety and stress response (Jenniches et al., 2016) and motor control (El Manira and Kyriakatos, 2010). Moreover, ECS deregulation has been associated with many neuropsychiatric disorders such as anxiety and depression (Jenniches et al., 2016; Micale et al., 2013), Fragile X syndrome (Jung et al., 2012), schizophrenia (Clarke et al., 2017) and with neurodegenerative disorders characterized by cognitive and motor dysfunctions such as Alzheimer's, Huntington's and Parkinson's disease (Dowie et al., 2009; Maroof et al., 2014; Pisani et al., 2011). Recent data also

suggest an involvement of the ECS in Autism Spectrum disorders (Chakrabarti et al., 2015).

A growing number of molecules able to directly or indirectly modulate the ECS have been identified to date. Pioneering studies increased the ECS response using agonists of the CB1 receptor, one of the two well characterized G-coupled receptors for endocannabinoids (Berrendero and Maldonado, 2002; Jiang et al., 2005; Patel et al., 2003). However, CB1 agonists may cause psychotropic side effects, similar to those reported with cannabis use in recreational settings. Such effects are now known to be due to the assimilation of $\Delta^9$-tetrahydrocannabinol (THC), the main compound of *Cannabis sativa*. To avoid these undesirable effects, most recent preclinical studies focussed on the identification of molecules that modulate the ECS without the psychotropic effects of THC, such as Rimonabant and URB597 (see e.g.(Griebel et al., 2005; Marco et al., 2015)). In addition, much attention has been devoted to non-psychotropic molecules from *Cannabis sativa*, which contains more than 120 substances (Morales et al., 2017). This has led to the identification of few non-psychotropic phytocannabinoids (phCBs) with a potential as novel drugs. These include Cannabigerol (CBG) and Cannabidiol (CBD), the second and the third most abundant chemical class types contained in *Cannabis sativa* respectively. In particular CBD bears a high potential in the treatment of muscular spasms and rigidity (Di Marzo, 2011), epilepsy (Chiu et al., 1979; Devinsky et al., 2017), mood disorders (Linge et al., 2016) and Alzheimer's disease (Cheng et al., 2014). Moreover, recent evidences suggest a potential application for CBD in paediatric conditions such as autistic-related syndromes (Kaplan et al., 2017) and in children with refractory epilepsy (Brodie and Ben-Menachem, 2018; Geffrey et al., 2015).

Another promising phCB is Cannabidivarin (CBDV), the *n*-propyl analog of CBD. Recent evidence proves that *in vitro* and *in vivo* treatment with CBDV in mouse and rat exerts anticonvulsant effects (Hill et al., 2012) and prevents neuronal hyperexcitability (Iannotti et al., 2014). However, the studies focussed on this compound are still very limited and the mechanisms of action of CDBV have not been clarified so far. Current evidences suggest that at physiologically relevant concentrations of CBDV show no affinity for CB1 and CB2 receptors (Hill et al., 2012) and presents antagonistic properties on the G protein-coupled receptor 55 (GPR55) receptor, the leading candidate for the CB3 receptor name (Anavi-Goffer et al., 2012; Iannotti et al., 2014; Marichal-Cancino et al., 2017; Turner et al., 2017). This lipid-activated G protein-coupled receptor has been suggested to regulate motor function, spatial memory and sociability (Bjursell et al., 2016; Kramar et al., 2017; Marichal-Cancino et al., 2018), behavioural domains that are compromised in RTT (De Filippis et al., 2014; Moretti et al., 2006). Moreover, antagonism of GPR55 has been recently suggested as a potential therapeutic approach for Dravet syndrome (Kaplan et al., 2017), an autistic-like syndrome with several symptoms in common with RTT.

Importantly, a clinical trial is currently listed aimed at evaluating the potential efficacy of a treatment with CBDV on children affected by Autism Spectrum Disorder (clinicaltrial.gov, NCT03202303). Based on the high translational potentiality of CBDV as an innovative therapeutic agent, in the present study MeCP2-308 hemizygous male mice, a highly validated mouse model of RTT (De Filippis et al., 2010), and wild-type littermate controls received a repeated systemic intraperitoneal (ip) treatment with CBDV (2, 20, 100 mg/Kg ip for 14 days). Mice were treated at 5 months of age, an early symptomatic stage at which MeCP2-308 mice already present reduced

spontaneous home-cage motor activity, motor coordination impairments, and a more marked profile of D-amphetamine-released stereotyped behavioural syndrome than WT controls (De Filippis et al., 2010). A battery of behavioural analyses was carried out to evaluate treatment effects. Given CBDV antagonistic action on GPR55 (Marichal-Cancino et al., 2017), levels of this receptor were evaluated, to verify whether they are abnormal in RTT and CBDV treatment effects thereon. As markers of efficacy we also explored whether the CBDV treatment impacts the abnormal activation of the ribosomal protein (rp) S6, a downstream target of mTOR, in the brain of MeCP2-308 mice (De Filippis et al., 2014; Ricciardi et al., 2011), and the alterations in brain neurotrophins levels (Chang et al., 2006; Ricceri et al., 2011). Indeed, based on previous reports suggesting that ECS modulation in mouse brain can impact mTOR signalling (Busquets-Garcia et al., 2013; Puighermanal et al., 2012) and neurotrophins levels (Keimpema et al., 2014), we hypothesised that the CBDV treatment may normalize these RTT-related brain molecular alterations. A focus was made on the hippocampus, a brain region critically involved in regulation of relevant behavioural domains (Kaplan et al., 2017; De Filippis et al., 2014).

# 4.3 Materials and methods

## 4.3.1 Animals

The experimental subjects were 5 month-old MeCP2-308 hemizygous male mice (RTT) and wild-type (WT) littermates (B6.129S-MeCP2tm1Heto/J from the Jackson Laboratories (USA), stock number: 005439) (De Filippis et al., 2010; Shahbazian et al., 2002), bred in our facility. Mice were weaned at postnatal day 25 and maintained in groups of 2-3 (according to sex) until 5 months of age. Temperature was maintained at $21 \pm 1$ °C and relative humidity at $60 \pm 10\%$. Animals were provided *ad libitum* with tap water and a complete pellet diet (Altromin, 1324 - 10mm pellets, Germany). All experimental procedures were conducted in conformity with the European Directive 2010/63/EU and the Italian legislation on animal experimentation, D.Lgs. 26/2014.

## 4.3.2 Genotyping

DNA has been prepared from a small tail-tip biopsy taken at weaning, as previously described (De Filippis et al., 2010). The MeCP2 alleles have been identified by PCR using two sets of primers. Primer set 1 (5′ primer: 5′-AAC GGG GTA GAA AGC CTG-3′ and 3′ primer: 5′-ATG CTC CAG ACT GCC TTG - 3′) yields a product of 396 bp identifying the wildtype allele. Primer set 2 (5′ primer same as for primer set 1 and 3′ primer: 5′- TGA TGG GGT CCTCAG AGC -3′) yields a product of apparent size 318 bp identifying the null allele. PCR products were electrophoresed through a 2% NuSieve 3:1 agarose gel (Cambrex Bio Science, Rockland, ME, USA) containing 0.5 µg/mL ethidium bromide, and examined under UV light.

### 4.3.3   Drug and treatment

CBDV (purity by HPLC: 95.9%) was supplied by GW Research Limited (Salisbury, UK) and stored in a freezer (at approximately −20°C), protected from light and freshly prepared immediately prior to injection. Given that CBDV is a nonpolar molecule with very low solubility in water solution, the emulsion was prepared using Cremophor® mixed with EtOH and saline. RTT mice and WT littermate controls were injected daily i.p. (between 9.00 and 11.00 am) for 14 consecutive days with CBDV (2, 20 or 100 mg/kg) or vehicle (veh) (Cremophor® EL:EtOH:saline in a ratio of 1:2:17). After a 24-hour washout period from the 14th i.p. injection, mice were sacrificed by decapitation. Before the regions collection, whole brains (including olfactory bulbs) of experimental animals were rapidly weighted. Subsequently, brains were dissected and hippocampi were collected and rapidly frozen for biochemical analyses.

### 4.3.4   Behavioural tests

To unravel the effects of the CBDV treatment on RTT-related behavioural alterations, mice were subjected to a battery of behavioural tests (Figure 1). The following numerosity for each experimental group has been achieved in the behavioural analyses: WT, veh: 9; WT, CBDV 2 mg/Kg: 9; WT, CBDV 20 mg/Kg: 9; WT, CBDV 100 mg/Kg: 9; Hz, veh: 7; Hz, CBDV 2 mg/Kg: 8; Hz, CBDV 20 mg/Kg: 8; Hz, CBDV 100 mg/Kg: 9. A total of 70 animals were used for the study.
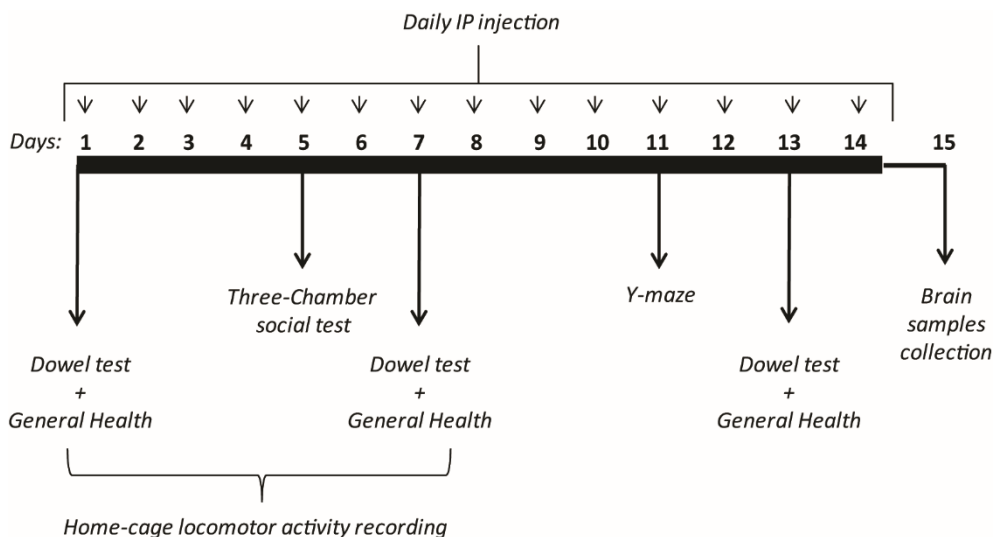
**Fig. 1:** Experimental schedule

## 4.3.4.1 General health score

The general health of the experimental mice was qualitatively evaluated by a trained observer, blind to the genotype of the experimental mice, at the end of behavioural testing after the 1st, the 7th and the 13th injection, as previously described (De Filippis et al., 2014; Guy et al., 2001). Briefly, mice received a score (ranging from 0 – normal appearance- to 4- highly compromised) for each of the following symptoms: gait, mobility, breathing, kyphosis, fur, hind limb clasping, tremors and general conditions. The individual scores for each category have been subsequently analysed to obtain a semi-quantitative measure of the general health status. Body weight was also recorded at each scoring session.

## 4.3.4.2 Dowel Test

To evaluate the effects of the treatment on motor learning capacities, the dowel test has been performed 1.5 hours after the 1st, the 7th i.p. and the 13th injections as previously described (De Filippis et al., 2015a). The

181

hardwood round dowel is 9.0 mm in diameter and 35 cm long. The dowel has been mounted horizontally 50 cm above a 5 cm depth bedding of sawdust. At the beginning of the testing, each mouse has been placed in the middle of the dowel so that the length of its body was parallel to the dowel. Latency to fall from the dowel into a cage of bedding has been recorded (30-second criterion) and used as a measure of motor coordination abilities. Each mouse has repeated the test twice per each testing day, with an inter-trial interval of at least 15 minutes.

### 4.3.4.3 Home-cage spontaneous activity and its circadian variation

Spontaneous locomotor activity in the home-cages has been monitored by means of an automatic device using small passive infrared sensors positioned on the top of each cage, as previously described (De Filippis et al., 2012; De Filippis et al., 2010). Data presented in the Results section are referred to a selection of 5 hours per phase (dark: 2-6 pm; light: 2-6 am) recorded on the first and the seventh day of the treatment schedule. We in fact hypothesised that the arousal state of the experimental animals is highly influenced by the number and type of experiments that are performed on a particular day and may affect the locomotor activity in the home cages. We therefore selected two days of the treatment schedule on which mice were subjected to a comparable battery of behavioural evaluations which included a motor coordination test and the general health score evaluation (see Fig. 1)

### 4.3.4.4 Three-chamber social test

Sociability and social recognition were assessed in the three-chambered test, as previously described (Smith et al., 2007). The test started 1 hour after the 5th i.p. injection. The test consists of 4 consecutive phases of 10 minutes during which each mouse is individually placed in the apparatus: Phase 1 (S1): mice can freely explore the central chamber of the apparatus; Phase 2 (S2):

mice can explore the three empty chambers; Phase 3 (S3): mice can explore either the chamber containing an empty small wire cage or the other one containing a conspecific kept under an identical small wire cage; Phase 4 (S4): an unfamiliar mouse is located under the cage wire which was empty during S3. Allocation of mouse partners to specific chambers was counterbalanced within each experimental group. Time spent exploring the mouse versus the empty wire cage during S3 is considered as an index of sociability. Time spent exploring the unfamiliar mouse versus the familiar one during S4 is considered as an index of memory of the social stimuli. Naïve C57 adult male mice were used as partners in this test. They were first habituated to the small wire cages in the test environment for 2 consecutive days before the testing day. After each animal was tested, the three-chamber apparatus and the wire cages were thoroughly cleaned with 70% ethanol.

### 4.3.4.5 Y-Maze test

The effects of the treatment on short-term spatial memory were assessed on the cognitive, exploratory driven, spatial novelty preference task. This task was carried out 1 hour after the 11th i.p. injection, as previously described (De Filippis et al., 2015a; De Filippis et al., 2014). Mice were tested on a spontaneous, spatial novelty preference task as previously described (Lyon et al., 2011; Sanderson et al., 2007). The Y-maze was made from transparent Perspex, and consisted of three 30 cm long, 8 cm wide arms with 20 cm high walls, connected by a central junction. A thin layer of sawdust covered the floor of the maze. The test was carried out as previously described (Lyon et al., 2011; Sanderson et al., 2007). Each mouse was assigned two arms (the 'start arm' and the 'other arm') to which they were exposed during the first phase of the task (the 'exposure phase'). Allocation of arms to specific spatial locations was counterbalanced within each experimental group. During

183

the 5-min 'exposure' phase, the entrance to the third, 'novel', arm was closed off by the presence of a large Perspex white block. The mouse was placed at the end of the start arm, facing the experimenter, and allowed to explore the start arm and the other arm freely for 5 min, beginning as soon as the mouse left the start arm. At the end of 5min exposure phase, the mouse was removed from the maze and returned to the home cage for 1 min. During this time, the Perspex block closing off the novel arm was removed and the sawdust redistributed throughout the maze to minimize the use of odour cues. The mouse was then returned to the start arm, facing the experimenter, for the 2-min 'test phase'. This consisted of 2-min free exploration during which the mouse could enter all the three arms, beginning as soon as the mouse left the start arm. The test was video-recorded and the number of entries and the length of time spent into each arm, during both the exposure and the test phase, were subsequently scored by means of the Noldus Observer XT. For the test phase, a discrimination ratio [novel arm/(novel+other arm)]*100 was calculated for time spent in each arm.

### 4.3.5 Neurobiological analyses

### 4.3.5.1 Western Blot Analyses

Hippocampal tissues were suspended in buffer containing 50 mM Tris–HCl, pH 8.0, 150 mM NaCl, 1% Triton-X100, 2mM $MgCl_2$ and phosphatase and protease inhibitors cocktail (PhosSTOP, Complete Mini, Roche) and then sonicated on ice. Lysates were centrifuged at $10000 \times g$ for 15 min at 4 °C. Protein concentration was determined by Bradford assay (BioRad). Samples containing 30µg of proteins were resolved by 7,5% SDS-PAGE under reducing and denaturing conditions and transferred to nitrocellulose membrane (Amersham Protran Premium). Membranes were blocked in TBST (10 mM Tris-HCl pH 8.0, 150 mM NaCl, 0.05% Tween 20) with 5% non-fat dry milk

for 45 min at room temperature, and then incubated with rabbit anti-rpS6 (1:1000,Cell Signaling), rabbit anti-phospho-rpS6 (Ser 240/244) (1:1000, Cell Signaling), rabbit anti-GPR55 (Abcam, 1:1000) and rabbit anti-beta actin (Cell Signaling, 1:1000) overnight at 4 °C. After washing, membranes were incubated with secondary anti- rabbit IgG HRP-conjugated antibodies (1:3000, Amersham) for 45 min at room temperature. Detection was performed by Immobilon Western Chemiluminescent HRP substrate (Millipore). Quantification of protein expression was performed by densitometry analysis using ImageLab software V.6.0 (Chemidoc, Biorad). Optical Density (OD) from at least 4 different experimental mice per group were calculated for each sample and normalized with the corresponding actin signal OD; the OD ratios were then compared and expressed as the average fold increase, with 100 (WT control) as the control value.

### 4.3.5.2 Enzyme-Linked Immunosorbent Assay (ELISA)

ELISA was performed to quantify levels of different neurotrophins in the hippocampus of the experimental mice. Levels of BDNF, NGF, and IGF-1 were analysed by using microtiter wells plates coated with anti-mouse neurotrophins antibodies (BDNF rapid, NGF rapid, Biosensis, Australia; IGF-1 Elisa kit, Abcam, UK) according to the manufacturer's instructions. The absorbance was read on a spectro-photometer (Bio-Rad) using 450 nm as the primary wave length, with a sub-wave length of 650 nm. The quantity of neurotrophins was expressed as percentage average fold increase of WT control values (100).

### 4.3.6 Statistical analyses

Data were analyzed with two-way ANOVA models including genotype and treatment as between-subject factors and repeated measurements as within-subject factor. The alpha level was set to 5%. The Levene test was

applied to confirm the equality of variance. The presence of outliers was verified using ROUT method. *Post-hoc* comparisons were performed by Tukey HSD, even in the absence of statistically significant interactions (Wilcox, 1987).

# 4.4 Results

## 4.4.1 Behavioural analyses

### 4.4.1.1 General health score

The evaluation of the general health status of the experimental mice confirmed that consistent gross phenotypic alterations can be detected in 5-month-old RTT mice (Fig.2a, RTT, veh vs WT, veh, $p < 0.01$ after *post-hoc* comparison on Genotype*treatment interaction: $F_{(3,60)} = 2.906$; $p = 0.042$). We found that 14 injections of CBDV at the doses of 20 and 100 mg/Kg can improve the general health status of RTT mice (Fig.2a, RTT, veh vs RTT, CBDV 20 mg/Kg, p<0.01 and RTT, veh vs RTT, CBDV, 100 mg/Kg, $p < 0.01$ after *post-hoc* comparison on Genotype*treatment interaction). The ANOVA highlights significant effect of repeated measures (Days of the schedule number 1, 7 ,13: $F_{(2,120)} = 5.350$; $p < 0.006$) and interaction of this factor with Genotype ($F_{(2,120)} = 3.930$; $p < 0.022$) but no interaction with Treatment ($F_{(2,120)} = 0.839$; $p < 0.542$). All these results are contained in Figure 2a which graphically shows the significant genotype*treatment interaction, thus the average of all time points (for further information on the profile of repeated measures see *Supplementary Figure 1a*). RTT mice weighed less compared to WT littermates (Genotype: $F_{(1,60)} = 12.048$; $p < 0.001$). No treatment effects were found on this parameter *(data not shown).*
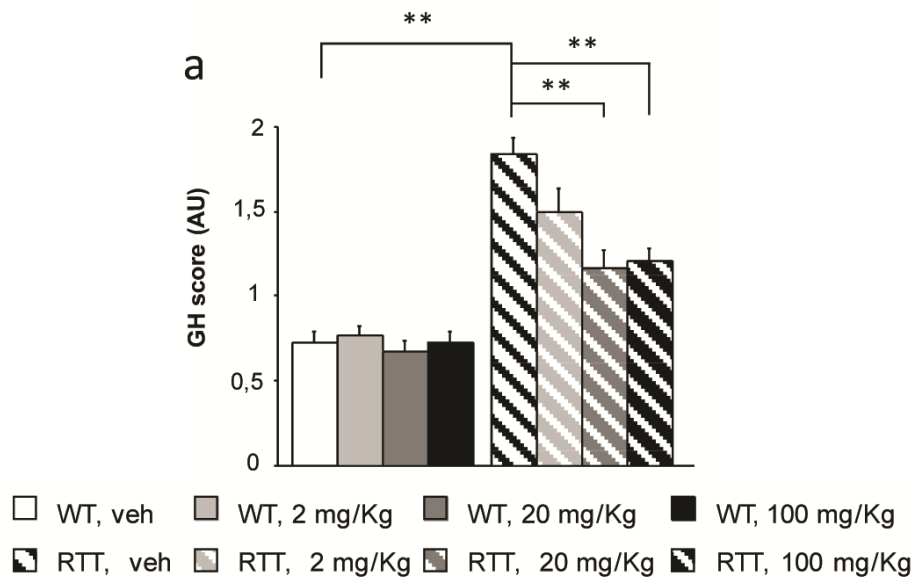
**Figure 2**: *Cannabidivarin (CBDV) treatment rescues general health status in 5-month-old RTT male mice;* Vehicle-injected RTT mice (RTT, veh) showed worse health conditions compared to WT controls (WT, veh). Treatment with Cannabidivarin (CBDV) at 20 and 100 mg/Kg ameliorates the general health status of RTT mice; GH scores (AU: Arbitrary units) are mean values of the three time points in which the evaluation was carried out (Days of the schedule number 1, 7 ,13). Data are mean±SEM. Statistical significance was calculated by two-way ANOVA with Tukey's *post-hoc* test. **p < 0.01; *p < 0.05.

### 4.4.1.2 Dowel test

Motor learning ability was assessed in the Dowel test (Fig.2b). In line with previous data, RTT mice showed shorter latency to fall from the bar compared to WT controls (RTT, veh vs WT, veh, p < 0.01 after *post-hoc* comparison on Day*trial*genotype*treatment interaction: $F_{(6,120)} = 2.512$; p = 0.025). A worse performance of RTT mice was thus confirmed in this test (De Filippis et al., 2012; De Filippis et al., 2010). Treatment with CBDV at the dose of 20 mg/kg significantly improved the motor learning ability of RTT mice and restored

WT-like levels of performance on the second testing day (the seventh of the experimental schedule). This profile was evident on both the first and the second trials ($p < 0.01$ and $p < 0.05$ after *post-hoc* comparisons on the Day*trial*genotype*treatment interaction, respectively). However, this treatment effect was no more evident on the 13th day of the treatment schedule. By contrast, at this latest time point, the dose of 100 mg/Kg significantly improved the motor learning ability of RTT mice ($p < 0.05$ after *post-hoc* comparison on the Day*trial* genotype*treatment interaction).



**Figure 2**: *Cannabidivarin (CBDV) treatment rescues motor alterations in 5-month-old RTT male mice;* **(b)** in the Dowel test, RTT mice displayed significantly shorter latencies to fall from a dowel compared to WT controls, confirming impaired motor learning capacities. CBDV at the dose of 20 mg/Kg improved the performance of RTT mice on day 7 and the 100mg/Kg dose improved the performance of RTT mice in the second trial of day 13; Mice were tested twice per day, with an inter-trial interval of

189

at least 15 minutes. Data are mean±SEM. Statistical significance was calculated by two-way ANOVA with Tukey's *post-hoc* test. **p < 0.01; *p < 0.05.

### 4.4.1.3 Spontaneous locomotor activity

In line with previous reports, the evaluation of spontaneous locomotor activity in home cage revealed that RTT mice are generally less active than WT controls (Genotype*treatment interaction: $F_{(3, 46)} = 5.032$; $p = 0.004$). This profile was mainly evident during the dark/active phase (Fig. 2c, $p < 0.01$ after *post-hoc* comparison on the Phase*genotype*treatment interaction: $F_{(3,46)} = 4.757$; $p = 0.001$). Levels of activity exhibited by RTT mice treated with CBDV at 2 mg/kg tended to be increased compared to those shown by vehicle-injected ones. However, such a trend did not reach statistical significance. The ANOVA did not highlight any significant effect of repeated measures (Days of the schedule number 1 and 7: $F_{(1,46)} = 3.147$; $p < 0.083$) or interaction of this factor with Genotype ($F_{(1,46)} = 1.432$; $p < 0.238$) or Treatment ($F_{(3,46)} = 0.818$; $p < 0.490$). Figure 2c graphically shows the significant Phase*genotype*treatment interaction, thus the average of both days (for further information on the effects of repeated measures see *Supplementary Figure1b*).
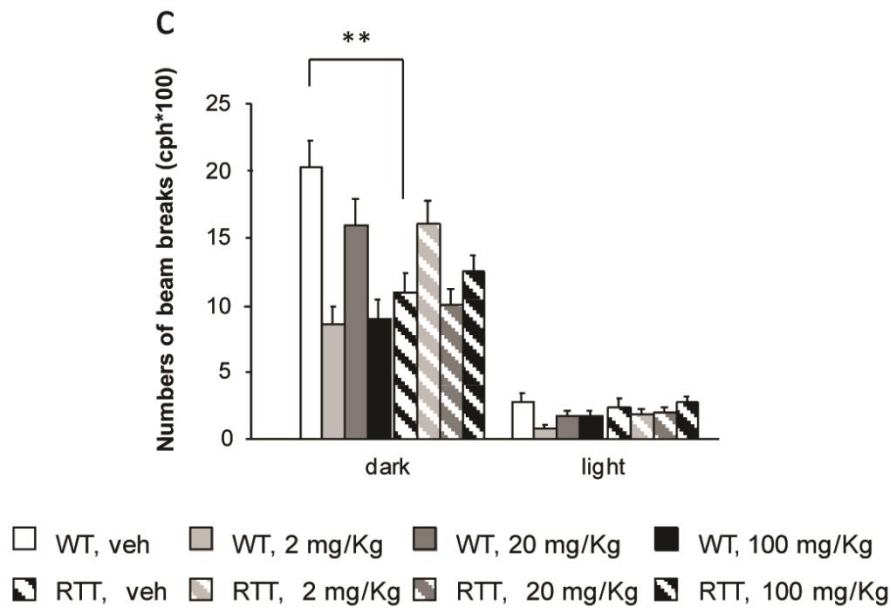
**Figure 2**: *Cannabidivarin (CBDV) treatment did not rescue spontaneous locomotor activity in 5-month-old RTT male mice;* **(c)** RTT, veh mice are generally less active than WT controls in the home cages. This profile was mainly evident during the dark/active phase. CBDV treatment did not affect the hypoactive profile of RTT mice, despite a trend for the 2mg/kg dose of CBDV treatment; Activity was automatically monitored by passive infrared sensors. Number of beam breaks (cph: counts per hour) are referred to a selection of 5 hours per phase (dark: 2-6 pm; light: 2-6 am) recorded on the first and the seventh day of the treatment schedule. Data are mean±SEM. Statistical significance was calculated by two-way ANOVA with Tukey's *post-hoc* test. **p < 0.01; *p < 0.05.

### 4.4.1.4 Three-chamber social test

The test was carried out in order to evaluate CBDV effect on social behaviour. As expected, the analysis of the S3 phase revealed a statistically significant difference between genotypes, with veh-injected RTT mice showing a reduced preference for the social stimulus (versus the inanimate

191

one) in comparison to veh-injected WT controls (Fig.2d, p < 0.01 after *post-hoc* comparison on the Genotype\*treatment interaction: $F_{(3,58)} = 3.527$; $p = 0.020$). Importantly, the CBDV treatment at the dose of 2 and 20 mg/Kg rescued this social deficit in RTT mice, restoring WT-like levels of social preference (Fig.2d, p < 0.05 after *post-hoc* comparison on the Genotype\*treatment interaction). The analysis of the S4 phase did not highlight significant genotype or treatment effects in the recognition of a novel social stimulus (versus the familiar one) (*Supplementary Figure 1c*).



**Figure 2**: *Cannabidivarin (CBDV) treatment rescues social impairment in 5-month-old RTT male mice;* (**d**) in the three-chamber social test, RTT mice spent less time exploring the mouse versus the empty wire cage during sociability phase (S3) in comparison to WT controls. CBDV at the doses of 2 and 20 mg/Kg rescued this aberrant behaviour restoring normal level of sociability. Data are mean±SEM. Statistical significance was calculated by two-way ANOVA with Tukey's *post-hoc* test. \*\*p < 0.01; \*p < 0.05.

### 4.4.1.5 Y-maze test

No genotype effects were found in the discrimination ratio index at this early symptomatic age (Fig.2e); all the experimental mice recognized the novel arm versus the familiar one (discrimination ratio > 50). No treatment effects were evident.
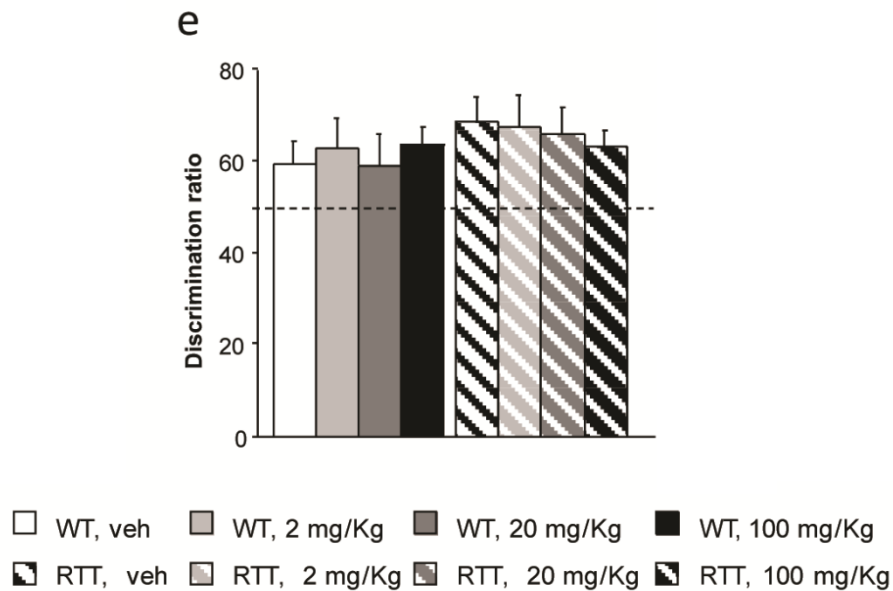


**Figure 2**: *Cannabidivarin (CBDV) treatment rescues behavioural alterations in 5-month-old RTT male mice;* **(e)** in the Y-maze task, no genotype differences were found in the discrimination ratio index [time spent in novel arm/(novel+other arm)]*100 and no treatment effect was evident. Data are mean±SEM. Statistical significance was calculated by two-way ANOVA with Tukey's *post-hoc* test. \*\*p<0.01; \*p<0.05.

### 4.4.2  Neurobiological analyses

### 4.4.2.1 Brain weight

We found that the whole brain of veh-injected RTT mice weighted less compared to those of WT littermate controls (Fig.3, p < 0.05 after *post-hoc*

comparison on Genotype*treatment interaction: $F_{(3,60)} = 1.714$; $p = 0.174$). Interestingly, the whole brain of RTT mice was increased at levels comparable to those of WT animals by 14 injections of CBDV at the doses of 2 and 100 mg/Kg (Fig.3, RTT, veh vs RTT, CBDV 2 and 100 mg/Kg, $p < 0.05$ after *post-hoc* comparisons on Genotype*treatment interaction).
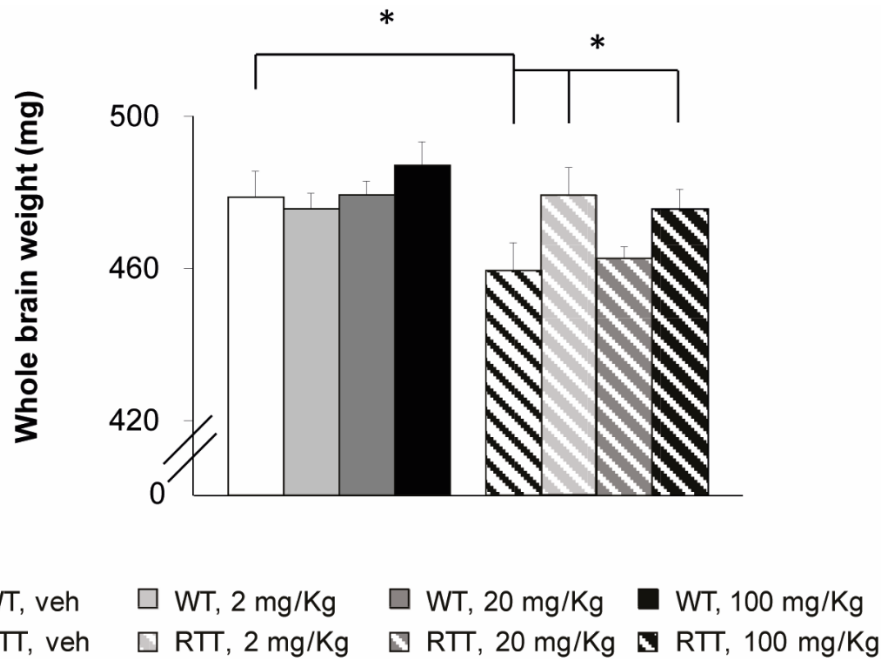


**Figure 3**: *Cannabidivarin (CBDV) treatment normalizes the reduced brain weight of 5 month-old RTT male mice*; after sacrifice, the brain of experimental animals was collected and weighted before the hippocampal dissection; the brain of vehicle-injected RTT mice (RTT, veh) weighted less in comparison to WT controls (WT, Veh); CBDV at the doses of 2mg/kg and 100 mg/Kg rescues the reduced brain weight of RTT mice. Data are mean±SEM. Statistical significance was calculated by two-way ANOVA with Tukey's *post-hoc* test. **$p < 0.01$; *$p < 0.05$.

## 4.4.2.2 Western Blot

GPR55 has been described as a major target of CBDV (Anavi-Goffer et al., 2012; Marichal-Cancino et al., 2017). Based on this evidence, hippocampal levels of GPR55 were evaluated (Fig4a, Representative blots). We found a two-fold increase in GPR55 levels in RTT mice compared to WT littermates (Fig.4a-b, Genotype: $F_{(1,24)} = 18.880$; $p = 0.001$). CBDV treatment did not exert significant effects on GPR55 level (Fig.4a-b, Genotype*treatment interaction: $F_{(3,24)} = 1.253$; $p = 0.313$).
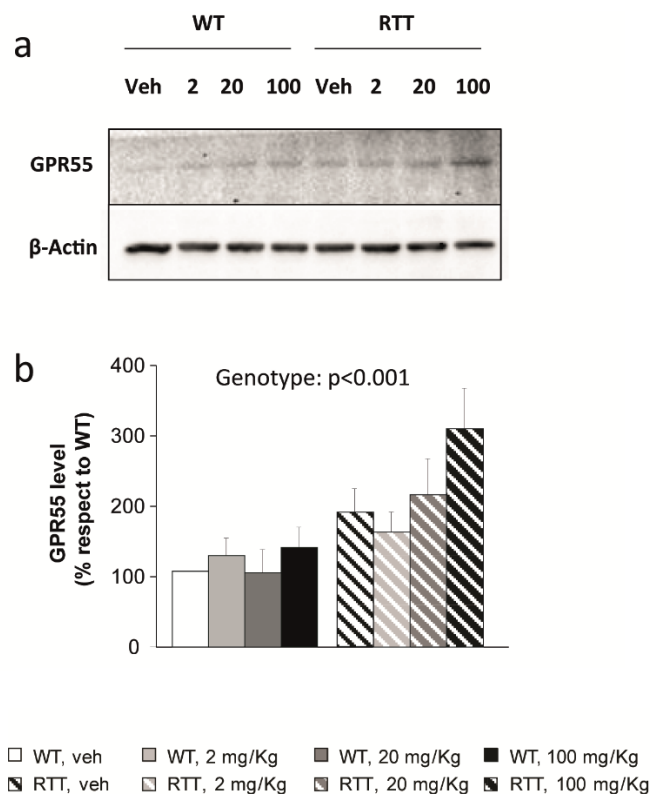


**Figure 4**: *5-month-old RTT male mice present enhanced hippocampal levels of GPR55.* **(a)** Representative Western blot analysis (summarized view corresponding to one animal per group) of GPR55 and actin. **(b)** Western blot analysis highlighted higher GPR55 level in hippocampus of RTT mice compared to WT mice. CBDV did

not alter GPR55 levels in both genotypes. (Data are mean±SEM. Statistical significance was calculated by two-way ANOVA with Tukey's *post-hoc* test. \*\*p < 0.01; \*p < 0.05.

We explored whether the chronic treatment with CBDV affects the activation of the ribosomal protein (rp) S6 in the hippocampus of RTT mice. Neither genotype nor treatment effects were found as for total rpS6 protein level (S6tot) and no differences between genotypes were found as for the ratio between phospho-S6 (phS6) and S6tot, which expresses the functionality of the kinase. The CBDV treatment did not affect this parameter (Table 1).

***Table 1. Levels of BDNF, IGF-1 and Ribosomal protein S6 activity in hippocampus***

| Genotype | Treatment | BDNF | IGF-1 | phS6/S6tot |
|---|---|---|---|---|
| **WT** | vehicle | 100 ±58.0 | 100±11.7 | 100±0.0 |
| **WT** | CBDV 2mg/Kg | 149.7±50.6 | 108.4±6.7 | 96.2±31.5 |
| **WT** | CBDV 20mg/Kg | 89.5±59.3 | 92.3±43.9 | 103.9±44.6 |
| **WT** | CBDV 100mg/Kg | 132.6±77.0 | 94.088±5.2 | 117.9±41.6 |
| **RTT** | vehicle | 133.0±28.0 | 106.1±13.9 | 100.4±51.6 |
| **RTT** | CBDV 2mg/Kg | 173.8±63.4 | 101.996±8.3 | 95.8±26.6 |
| **RTT** | CBDV 20mg/Kg | 109.1±36.3 | 82.207±17.1 | 76.6±23.3 |
| **RTT** | CBDV 100mg/Kg | 89.8±24.2 | 96.0±3.7 | 85.8±48.2 |

Data are mean±SEM. Hippocampal BDNF an IGF-1 levels were calculated performing ELISA assays and were expressed respect to WT=100. Western blot assay was used to quantify hippocampal levels of Ribosomal protein S6 (S6tot) and its phosphorylated form (phS6). rpS6 activity was expressed as ratio phS6/S6tot levels, respect to WT=100. MeCP2-308 hemizygous male mice (RTT); wild-type littermates (WT); Cannabidivarin (CBDV).

### 4.4.2.3 ELISA

The hippocampal levels of the neurotrophins BDNF, NGF and IGF-1 were measured as markers of treatment efficacy. We found that hippocampal levels of BDNF and IGF1 did not significantly differ between RTT mice and WT controls at this testing age (Table 1), even though BDNF levels tended to be higher in RTT mouse brain. Conversely, NGF was significantly reduced in RTT mice (Fig.4c, $p < 0.05$ after *post-hoc* comparison on Genotype*treatment interaction: $F_{(3,22)} = 5.663$; $p = 0.005$). CBDV did not produce any significant effect on neurotrophins levels in the hippocampus of RTT mice. However, the treatment with CBDV at the 100 mg/kg dose significantly increased NGF levels selectively in the hippocampus of WT mice (about 160% of veh-injected WT mice, Fig.4c, $p < 0.01$ after *post-hoc* comparison on Genotype*treatment interaction).



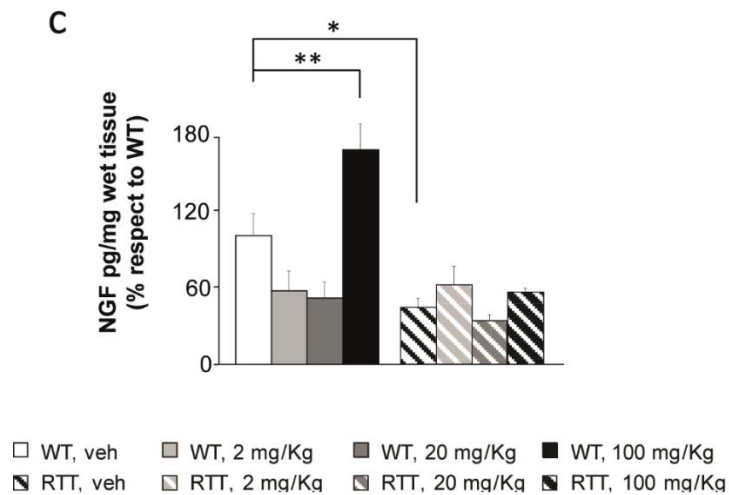**Figure 4**: *5-month-old RTT male mice present low hippocampal levels of NFG did not normalize by LP-211 treatment.* **(c)** ELISA assays revealed that RTT mice display lower NGF levels in comparison to WT controls; CBDV did not rescue this alteration;

Data are mean±SEM. Statistical significance was calculated by two-way ANOVA with Tukey's *post-hoc* test. **p < 0.01; *p < 0.05.

## 4.5    Discussion

The present study demonstrates, for the first time, that 14 days of treatment with CBDV, a phCB extracted from *Cannabis sativa*, improves important aspects of the aberrant phenotype in a validated mouse model of RTT. The positive effects of CBDV treatment on RTT mice were specifically related to the general health status, the social sphere and the motor skills, phenotypic domains which are highly compromised in RTT patients (Morel and Demily, 2017; Stahlhut et al., 2017). Of note, the reduced brain weight of RTT mice was also normalized by the repeated CBDV treatment. Furthermore, the present study provides the first evidence of abnormal hippocampal levels of lipid-activated G protein-coupled receptor GPR55, a recently identified cannabinoid receptor, in a RTT mouse model.

Present data provide convincing evidence that the CBDV treatment rescues a number of behavioural and phenotypic alterations in a validated RTT mouse model. In line with previous reports (Woods et al., 2012), we found that RTT mice show abnormal sociability in the three-chamber social test. These results are consistent with the increasing literature providing evidence of a link between cannabinoids and social behaviour in humans (Wei et al., 2017) and in animal models (Kaplan et al., 2017; Kramar et al., 2017; Marco et al., 2015). In particular, the ECS is suggested to control the molecular mechanisms underpinning social anxiety (Viveros et al., 2005; Wei et al., 2017). In this line, we found that RTT mice exhibited avoidance of the social stimulus, rather than a lack of preference for the social vs the inanimate one. This abnormal behavioural profile was largely attenuated by the CBDV treatment.

Of note, a normalization of the compromised general health status in RTT mice was also observed. This effect was attributable to improvements in

a number of parameters which are relevant for this disorder such as mobility, gait, kyphosis and tremors. Moreover, these beneficial effects of the CBDV treatment were accompanied by a partial restoration of motor coordination and spontaneous locomotor activity in the home cage. Increasing evidence suggests the potential therapeutic efficacy of phCBs in a number of disorders characterized by motor dysfunctions, such as Alzheimer's, Huntington's and Parkinson's disease (Dowie et al., 2009; Maroof et al., 2014; Pisani et al., 2011). Taken together, present findings suggest that CBDV may provide significant beneficial effects on RTT-related motor defects. Further studies specifically tailored to confirm this hypothesis are however needed (De Filippis et al., 2015b).

Another important finding of the present study concerns the normalization of brain atrophy in CBDV-treated RTT mice. Microcephaly is a peculiar feature of RTT and several studies have reported reduced brain weight in the mouse models (Zhou et al., 2017). It is generally acknowledged that such reduction is attributable to cell atrophy due to abnormalities in the cytoskeleton, rather than cell death (neurodegeneration is not observed in RTT mice or patients) (Guy et al., 2007). Given that the ECS is known to modulate the actin cytoskeleton (Njoo et al., 2015; Roland et al., 2014), one intriguing hypothesis concerns the possibility that the CBDV treatment may have restored the structural integrity of neurons and astrocytes or the cytoarchitecture of the cortex, which are abnormal in RTT mouse brain (Bittolo et al., 2016; Fukuda et al., 2005; Maezawa et al., 2009).

In the present study, we provide the first evidence that GPR55 levels are increased in the hippocampus of early symptomatic RTT mice. Considering previous studies linking GPR55 with social behaviour (Kaplan et al., 2017; Kramar et al., 2017), motor function (Bjursell et al., 2016) and spatial memory

(Marichal-Cancino et al., 2018), it is conceivable that CBDV-mediated antagonism of GPR55 may account for the rescue of RTT-related alterations we report in the present study. Although further studies are needed to verify this possibility, our results provide a new pharmacological target for the treatment of RTT. In this line, it is worth noting that GPR55 has been suggested to be involved in the regulation of energetic metabolism (Simcocks et al., 2014). Given that mitochondrial dysfunction is emerging as crucial in the pathogenesis of RTT (De Filippis et al., 2015c; Valenti et al., 2017), we suggest that further studies aimed at verifying whether abnormal GPR55 levels may account for defective mitochondrial energy production in RTT mouse brain should be performed.

Interestingly, the CBDV treatment provided different effects in different paradigms depending on the dose used. The social defect was in fact contrasted by the low and the intermediate dose of CBDV (2 and 20 mg/kg), whereas the defective general health status and motor coordination appeared more efficaciously contrasted by the high and the intermediate dose (20 and 100 mg/kg). Present results support the intermediate dose of 20 mg/kg as the most efficacious and highlight the need for further studies aimed at clarifying the molecular mechanisms underlying CBDV beneficial effects on RTT symptomatology. In fact, similar differential effects of low and high doses have been already reported for other molecules, including CBD, that were explained by actions on different molecular pathways (Han et al., 2014; Kaplan et al., 2017).

In the present study, using early symptomatic RTT mice we were not able to detect some behavioural and molecular alterations in veh-injected RTT mice that were previously reported in this RTT mouse model (De Filippis et al., 2012; De Filippis et al., 2014). One explanation for such discrepancies may

reside in the age of the experimental animals which were younger compared to previous experiments (5 months vs at least 7 months of age) (De Filippis et al., 2014). This is the case for the cognitive abilities of RTT mice in the Y maze test as well as brain neurotrophins levels and the phosphorylation level of rpS6. Indeed, these cognitive and molecular deficits have been reported at 7-8 months of age in this RTT mouse model compared to WT controls (De Filippis et al., 2014), but they have never been assessed at 5 months of age. In fact, most of the studies carried out so far in such RTT mouse model have focussed on clearly symptomatic mice (Moretti et al., 2006; Shahbazian et al., 2002) and only one study has addressed the progression of symptoms (De Filippis et al., 2010). Present results provide new relevant information regarding the progression of RTT-related behavioural and molecular abnormalities in MeCP2-308 mice (De Filippis et al., 2010) and highlight the importance of studies aimed at testing the potential value of innovative therapeutic strategies for RTT at different stages of the disease.

Increasing evidence suggests that modulation of neurotrophins, such as BDNF and IGF1, can improve RTT symptomatology and neuropathological signs in mouse models (Castro et al., 2014) and in patients (Katz, 2014; Pini et al., 2012). Besides this, numerous findings argue for a role of ECS in modulation of brain neurotrophin levels (Keimpema et al., 2014). Based on these evidences, we aimed at evaluating the effect of CBDV on the altered levels of relevant neurotrophins in the brain of RTT mice (Katz, 2014). In contrast to previous studies on older mice, in this study we could only identify abnormalities in the hippocampus of RTT mice concerning reduced NGF levels, which were not modulated by the CBDV treatment. Furthermore, no effects of the treatment on BDNF and IGF1 levels were evidenced. Even though we cannot exclude that the CBDV treatment might impact a defective

BDNF/IGF1 signalling at an advanced stage of the disease, present results suggest that the reported phenotypic improvement by CBDV treatment in RTT mice at the tested age involves different signalling pathways.

We also evaluated CBDV treatment effects on the defects in mTOR/S6 activation known to be characteristic of RTT mouse brain (De Filippis et al., 2014; Ricciardi et al., 2011). Indeed, even though no studies have so far addressed CBDV effects on mTOR activation, this signalling pathway plays a crucial role in a number of neurodevelopmental disorders (Troca-Marín et al., 2012) and is critically involved in regulation of synaptic plasticity and memory processes (Costa-Mattioli et al., 2009). Moreover, previous reports suggest that ECS modulation can impact mTOR signalling (Busquets-Garcia et al., 2013; Puighermanal et al., 2012). Based on these evidences, we reasoned that the CBDV treatment may normalize the defective activation of the mTOR pathway in RTT mouse brain. Unfortunately, at this early symptomatic stage of the disease we did not find any defect in the phosphorylation level of the rpS6, a downstream target of mTOR and S6 kinase, in the brain of MeCP2-308 mice. This is consistent with the lack of cognitive defects in 5-month-old RTT mice we report in the present study. Present results do not allow us to exclude that the CBDV treatment might impact the defective mTOR pathway at a more advanced stage of the disease in the brain of RTT mice, thus restoring cognitive deficits.

### *Conclusions*

No cure is currently available for patients suffering from RTT, a devastating neurodevelopmental disorder with a huge burden for families. Present data provide evidence that the CBDV treatment rescues several behavioural and phenotypic defects in a mouse model of RTT, thus

representing a potential therapeutic approach for this disorder. Moreover, GPR55 was herein for the first time suggested to be a potential target for the treatment of RTT. Even though further studies are needed to clarify the mechanisms of action of CBDV, present data highlight for the first time the potential therapeutic efficacy of a molecule which bears a high translational value. CBDV is in fact currently under investigation in the clinical setting and is involved in a clinical trial in children affected by Autism Spectrum Disorders.

## Founding and disclosure

## Acknowledgements

# 4.6    References

Anavi-Goffer, S., Baillie, G., Irving, A. J., Gertsch, J., Greig, I. R., Pertwee, R. G., Ross, R. A., 2012. Modulation of L-alpha-lysophosphatidylinositol/GPR55 mitogen-activated protein kinase (MAPK) signaling by cannabinoids. J Biol Chem 287, 91-104.

Berrendero, F., Maldonado, R., 2002. Involvement of the opioid system in the anxiolytic-like effects induced by Delta(9)-tetrahydrocannabinol. Psychopharmacology (Berl) 163, 111-117.

Bittolo, T., Raminelli, C. A., Deiana, C., Baj, G., Vaghi, V., Ferrazzo, S., Bernareggi, A., Tongiorgi, E., 2016. Pharmacological treatment with mirtazapine rescues cortical atrophy and respiratory deficits in MeCP2 null mice. Scientific Reports 6, 19796.

Bjursell, M., Ryberg, E., Wu, T., Greasley, P. J., Bohlooly, Y. M., Hjorth, S., 2016. Deletion of Gpr55 Results in Subtle Effects on Energy Metabolism, Motor Activity and Thermal Pain Sensation. PLoS ONE 11, e0167965.

Brodie, M. J., Ben-Menachem, E., 2018. Cannabinoids for epilepsy: What do we know and where do we go? Epilepsia 59, 291-296.

Busquets-Garcia, A., Gomis-Gonzalez, M., Guegan, T., Agustin-Pavon, C., Pastor, A., Mato, S., Perez-Samartin, A., Matute, C., de la Torre, R., Dierssen, M., Maldonado, R., Ozaita, A., 2013. Targeting the endocannabinoid system in the treatment of fragile X syndrome. Nat Med 19, 603-607.

Castro, J., Garcia, R. I., Kwok, S., Banerjee, A., Petravicz, J., Woodson, J., Mellios, N., Tropea, D., Sur, M., 2014. Functional recovery with recombinant human IGF1 treatment in a mouse model of Rett Syndrome. Proc Natl Acad Sci U S A 111, 9941-9946.

Chakrabarti, B., Persico, A., Battista, N., Maccarrone, M., 2015. Endocannabinoid Signaling in Autism. Neurotherapeutics 12, 837-847.

Chang, Q., Khare, G., Dani, V., Nelson, S., Jaenisch, R., 2006. The disease progression of Mecp2 mutant mice is affected by the level of BDNF expression. Neuron 49, 341-348.

Cheng, D., Low, J. K., Logge, W., Garner, B., Karl, T., 2014. Chronic cannabidiol treatment improves social and object recognition in double transgenic APPswe/PS1E9 mice. Psychopharmacology (Berl) 231, 3009-3017.

Chiu, P., Olsen, D. M., Borys, H. K., Karler, R., Turkanis, S. A., 1979. The influence of cannabidiol and delta 9-tetrahydrocannabinol on cobalt epilepsy in rats. Epilepsia 20, 365-375.

Clarke, D. J., Stuart, J., McGregor, I. S., Arnold, J. C., 2017. Endocannabinoid dysregulation in cognitive and stress-related brain regions in the Nrg1 mouse model of schizophrenia. Prog Neuropsychopharmacol Biol Psychiatry 72, 9-15.

Costa-Mattioli, M., Sossin, W. S., Klann, E., Sonenberg, N., 2009. Translational control of long-lasting synaptic plasticity and memory. Neuron 61, 10-26.

De Filippis, B., Fabbri, A., Simone, D., Canese, R., Ricceri, L., Malchiodi-Albedi, F., Laviola, G., Fiorentini, C., 2012. Modulation of RhoGTPases improves the behavioral phenotype and reverses astrocytic deficits in a mouse model of Rett syndrome. Neuropsychopharmacology 37, 1152-1163.

De Filippis, B., Lyon, L., Taylor, A., Lane, T., Burnet, P. W., Harrison, P. J., Bannerman, D. M., 2015a. The role of group II metabotropic glutamate receptors in cognition and anxiety: comparative studies in GRM2(-/-), GRM3(-/-) and GRM2/3(-/-) knockout mice. Neuropharmacology 89, 19-32.

De Filippis, B., Musto, M., Altabella, L., Romano, E., Canese, R., Laviola, G., 2015b. Deficient Purposeful Use of Forepaws in Female Mice Modelling Rett Syndrome. Neural Plast 2015, 326184.

De Filippis, B., Nativio, P., Fabbri, A., Ricceri, L., Adriani, W., Lacivita, E., Leopoldo, M., Passarelli, F., Fuso, A., Laviola, G., 2014. Pharmacological stimulation of the brain serotonin receptor 7 as a novel therapeutic approach for Rett syndrome. Neuropsychopharmacology 39, 2506-2518.

De Filippis, B., Ricceri, L., Laviola, G., 2010. Early postnatal behavioral changes in the Mecp2-308 truncation mouse model of Rett syndrome. Genes Brain Behav 9, 213-223.

De Filippis, B., Valenti, D., Chiodi, V., Ferrante, A., de Bari, L., Fiorentini, C., Domenici, M. R., Ricceri, L., Vacca, R. A., Fabbri, A., Laviola, G., 2015c. Modulation of Rho GTPases rescues brain mitochondrial dysfunction, cognitive deficits and aberrant synaptic plasticity in female

mice modeling Rett syndrome. Eur Neuropsychopharmacol 25, 889-901.

Devinsky, O., Cross, J. H., Laux, L., Marsh, E., Miller, I., Nabbout, R., Scheffer, I. E., Thiele, E. A., Wright, S., Cannabidiol in Dravet Syndrome Study, G., 2017. Trial of Cannabidiol for Drug-Resistant Seizures in the Dravet Syndrome. N Engl J Med 376, 2011-2020.

Di Marzo, V., 2011. Endocannabinoid pathways and their role in multiple sclerosis-related muscular dysfunction. Expert Rev Neurother 11, 9-14.

Di Marzo, V., Stella, N., Zimmer, A., 2015. Endocannabinoid signalling and the deteriorating brain. Nat Rev Neurosci 16, 30-42.

Dowie, M. J., Bradshaw, H. B., Howard, M. L., Nicholson, L. F., Faull, R. L., Hannan, A. J., Glass, M., 2009. Altered CB1 receptor and endocannabinoid levels precede motor symptom onset in a transgenic mouse model of Huntington's disease. Neuroscience 163, 456-465.

El Manira, A., Kyriakatos, A., 2010. The role of endocannabinoid signaling in motor control. Physiology (Bethesda) 25, 230-238.

Fukuda, T., Itoh, M., Ichikawa, T., Washiyama, K., Goto, Y., 2005. Delayed maturation of neuronal architecture and synaptogenesis in cerebral cortex of Mecp2-deficient mice. J Neuropathol Exp Neurol 64, 537-544.

Geffrey, A. L., Pollack, S. F., Bruno, P. L., Thiele, E. A., 2015. Drug-drug interaction between clobazam and cannabidiol in children with refractory epilepsy. Epilepsia 56, 1246-1251.

Griebel, G., Stemmelin, J., Scatton, B., 2005. Effects of the cannabinoid CB1 receptor antagonist rimonabant in models of emotional reactivity in rodents. Biol Psychiatry 57, 261-267.

Guy, J., Cheval, H., Selfridge, J., Bird, A., 2011. The role of MeCP2 in the brain. Annu Rev Cell Dev Biol 27, 631-652.

Guy, J., Gan, J., Selfridge, J., Cobb, S., Bird, A., 2007. Reversal of neurological defects in a mouse model of Rett syndrome. Science 315, 1143-1147.

Guy, J., Hendrich, B., Holmes, M., Martin, J. E., Bird, A., 2001. A mouse Mecp2-null mutation causes neurological symptoms that mimic Rett syndrome. Nat Genet 27, 322-326.

Hagberg, B., 2002. Clinical manifestations and stages of Rett syndrome. Ment Retard Dev Disabil Res Rev 8, 61-65.

Hagberg, B., Hanefeld, F., Percy, A., Skjeldal, O., 2002. An update on clinically applicable diagnostic criteria in Rett syndrome. Comments to Rett Syndrome Clinical Criteria Consensus Panel Satellite to European Paediatric Neurology Society Meeting, Baden Baden, Germany, 11 September 2001. Eur J Paediatr Neurol 6, 293-297.

Han, S., Tai, C., Jones, C. J., Scheuer, T., Catterall, W. A., 2014. Enhancement of inhibitory neurotransmission by GABAA receptors having alpha2,3-subunits ameliorates behavioral deficits in a mouse model of autism. Neuron 81, 1282-1289.

Hill, A. J., Mercier, M. S., Hill, T. D., Glyn, S. E., Jones, N. A., Yamasaki, Y., Futamura, T., Duncan, M., Stott, C. G., Stephens, G. J., Williams, C.

M., Whalley, B. J., 2012. Cannabidivarin is anticonvulsant in mouse and rat. Br J Pharmacol 167, 1629-1642.

Iannotti, F. A., Hill, C. L., Leo, A., Alhusaini, A., Soubrane, C., Mazzarella, E., Russo, E., Whalley, B. J., Di Marzo, V., Stephens, G. J., 2014. Nonpsychotropic plant cannabinoids, cannabidivarin (CBDV) and cannabidiol (CBD), activate and desensitize transient receptor potential vanilloid 1 (TRPV1) channels in vitro: potential for the treatment of neuronal hyperexcitability. ACS Chem Neurosci 5, 1131-1141.

Jenniches, I., Ternes, S., Albayram, O., Otte, D. M., Bach, K., Bindila, L., Michel, K., Lutz, B., Bilkei-Gorzo, A., Zimmer, A., 2016. Anxiety, Stress, and Fear Response in Mice With Reduced Endocannabinoid Levels. Biol Psychiatry 79, 858-868.

Jiang, W., Zhang, Y., Xiao, L., Van Cleemput, J., Ji, S. P., Bai, G., Zhang, X., 2005. Cannabinoids promote embryonic and adult hippocampus neurogenesis and produce anxiolytic- and antidepressant-like effects. J Clin Invest 115, 3104-3116.

Jung, K. M., Sepers, M., Henstridge, C. M., Lassalle, O., Neuhofer, D., Martin, H., Ginger, M., Frick, A., DiPatrizio, N. V., Mackie, K., Katona, I., Piomelli, D., Manzoni, O. J., 2012. Uncoupling of the endocannabinoid signalling complex in a mouse model of fragile X syndrome. Nat Commun 3, 1080.

Kano, M., Ohno-Shosaku, T., Hashimotodani, Y., Uchigashima, M., Watanabe, M., 2009. Endocannabinoid-Mediated Control of Synaptic Transmission. Physiological Reviews 89, 309-380.

Kaplan, J. S., Stella, N., Catterall, W. A., Westenbroek, R. E., 2017. Cannabidiol attenuates seizures and social deficits in a mouse model of Dravet syndrome. Proc Natl Acad Sci U S A 114, 11229-11234.

Katz, D. M., 2014. Brain-derived neurotrophic factor and Rett syndrome. Handb Exp Pharmacol 220, 481-495.

Keimpema, E., Hokfelt, T., Harkany, T., Doherty, P., 2014. The molecular interplay between endocannabinoid and neurotrophin signals in the nervous system and beyond. Eur J Neurosci 39, 334-343.

Kramar, C., Loureiro, M., Renard, J., Laviolette, S. R., 2017. Palmitoylethanolamide Modulates GPR55 Receptor Signaling in the Ventral Hippocampus to Regulate Mesolimbic Dopamine Activity, Social Interaction, and Memory Processing. Cannabis Cannabinoid Res 2, 8-20.

Linge, R., Jimenez-Sanchez, L., Campa, L., Pilar-Cuellar, F., Vidal, R., Pazos, A., Adell, A., Diaz, A., 2016. Cannabidiol induces rapid-acting antidepressant-like effects and enhances cortical 5-HT/glutamate neurotransmission: role of 5-HT1A receptors. Neuropharmacology 103, 16-26.

Lyon, L., Burnet, P. W., Kew, J. N., Corti, C., Rawlins, J. N., Lane, T., De Filippis, B., Harrison, P. J., Bannerman, D. M., 2011. Fractionation of spatial memory in GRM2/3 (mGlu2/mGlu3) double knockout mice reveals a role for group II metabotropic glutamate receptors at the interface between arousal and cognition. Neuropsychopharmacology 36, 2616-2628.

Maezawa, I., Swanberg, S., Harvey, D., LaSalle, J. M., Jin, L. W., 2009. Rett syndrome astrocytes are abnormal and spread MeCP2 deficiency through gap junctions. J Neurosci 29, 5051-5061.

Marco, E. M., Rapino, C., Caprioli, A., Borsini, F., Laviola, G., Maccarrone, M., 2015. Potential Therapeutic Value of a Novel FAAH Inhibitor for the Treatment of Anxiety. PLoS ONE 10, e0137034.

Marichal-Cancino, B. A., Fajardo-Valdez, A., Ruiz-Contreras, A. E., Mendez-Diaz, M., Prospero-Garcia, O., 2017. Advances in the Physiology of GPR55 in the Central Nervous System. Curr Neuropharmacol 15, 771-778.

Marichal-Cancino, B. A., Fajardo-Valdez, A., Ruiz-Contreras, A. E., Mendez-Diaz, M., Prospero-Garcia, O., 2018. Possible role of hippocampal GPR55 in spatial learning and memory in rats. Acta Neurobiol Exp (Wars) 78, 41-50.

Maroof, N., Ravipati, S., Pardon, M. C., Barrett, D. A., Kendall, D. A., 2014. Reductions in endocannabinoid levels and enhanced coupling of cannabinoid receptors in the striatum are accompanied by cognitive impairments in the AbetaPPswe/PS1DeltaE9 mouse model of Alzheimer's disease. J Alzheimers Dis 42, 227-245.

Micale, V., Di Marzo, V., Sulcova, A., Wotjak, C. T., Drago, F., 2013. Endocannabinoid system and mood disorders: priming a target for new therapies. Pharmacol Ther 138, 18-37.

Morales, P., Hurst, D. P., Reggio, P. H., 2017. Molecular Targets of the Phytocannabinoids: A Complex Picture. Prog Chem Org Nat Prod 103, 103-131.

Morel, A., Demily, C., 2017. [Social cognition in children with neurogenetic syndromes: A literature review]. Arch Pediatr.

Moretti, P., Levenson, J. M., Battaglia, F., Atkinson, R., Teague, R., Antalffy, B., Armstrong, D., Arancio, O., Sweatt, J. D., Zoghbi, H. Y., 2006. Learning and Memory and Synaptic Plasticity Are Impaired in a Mouse Model of Rett Syndrome. The Journal of Neuroscience 26, 319.

Njoo, C., Agarwal, N., Lutz, B., Kuner, R., 2015. The Cannabinoid Receptor CB1 Interacts with the WAVE1 Complex and Plays a Role in Actin Dynamics and Structural Plasticity in Neurons. PLoS Biol 13, e1002286.

Patel, S., Rademacher, D. J., Hillard, C. J., 2003. Differential regulation of the endocannabinoids anandamide and 2-arachidonylglycerol within the limbic forebrain by dopamine receptor activity. J Pharmacol Exp Ther 306, 880-888.

Pini, G., Scusa, M. F., Congiu, L., Benincasa, A., Morescalchi, P., Bottiglioni, I., Di Marco, P., Borelli, P., Bonuccelli, U., Della-Chiesa, A., Prina-Mello, A., Tropea, D., 2012. IGF1 as a Potential Treatment for Rett Syndrome: Safety Assessment in Six Rett Patients. Autism Res Treat 2012, 679801.

Pisani, V., Madeo, G., Tassone, A., Sciamanna, G., Maccarrone, M., Stanzione, P., Pisani, A., 2011. Homeostatic changes of the endocannabinoid system in Parkinson's disease. Mov Disord 26, 216-222.

Puighermanal, E., Busquets-Garcia, A., Maldonado, R., Ozaita, A., 2012. Cellular and intracellular mechanisms involved in the cognitive

impairment of cannabinoids. Philos Trans R Soc Lond B Biol Sci 367, 3254-3263.

Rett, A., 1966. On a unusual brain atrophy syndrome in hyperammonemia in childhood. Wiener Medizinische Wochenschrift 116, 723-726.

Ricceri, L., De Filippis, B., Fuso, A., Laviola, G., 2011. Cholinergic hypofunction in MeCP2-308 mice: beneficial neurobehavioural effects of neonatal choline supplementation. Behav Brain Res 221, 623-629.

Ricceri, L., De Filippis, B., Laviola, G., 2012. Rett syndrome treatment in mouse models: searching for effective targets and strategies. Neuropharmacology 68, 106-115.

Ricciardi, S., Boggio, E. M., Grosso, S., Lonetti, G., Forlani, G., Stefanelli, G., Calcagno, E., Morello, N., Landsberger, N., Biffo, S., Pizzorusso, T., Giustetto, M., Broccoli, V., 2011. Reduced AKT/mTOR signaling and protein synthesis dysregulation in a Rett syndrome animal model. Hum Mol Genet 20, 1182-1196.

Roland, A. B., Ricobaraza, A., Carrel, D., Jordan, B. M., Rico, F., Simon, A., Humbert-Claude, M., Ferrier, J., McFadden, M. H., Scheuring, S., Lenkei, Z., 2014. Cannabinoid-induced actomyosin contractility shapes neuronal morphology and growth. Elife 3, e03159.

Sanderson, D. J., Gray, A., Simon, A., Taylor, A. M., Deacon, R. M., Seeburg, P. H., Sprengel, R., Good, M. A., Rawlins, J. N., Bannerman, D. M., 2007. Deletion of glutamate receptor-A (GluR-A) AMPA receptor subunits impairs one-trial spatial memory. Behav Neurosci 121, 559-569.

Shahbazian, M. D., Young, J. I., Yuva-Paylor, L. A., Spencer, C. M., Antalffy, B. A., Noebels, J. L., Armstrong, D. L., Paylor, R., Zoghbi, H. Y., 2002. Mice with Truncated MeCP2 Recapitulate Many Rett Syndrome Features and Display Hyperacetylation of Histone H3. Neuron 35, 243-254.

Simcocks, A. C., O'Keefe, L., Jenkin, K. A., Mathai, M. L., Hryciw, D. H., McAinch, A. J., 2014. A potential role for GPR55 in the regulation of energy homeostasis. Drug Discov Today 19, 1145-1151.

Smith, S. E., Li, J., Garbett, K., Mirnics, K., Patterson, P. H., 2007. Maternal immune activation alters fetal brain development through interleukin-6. J Neurosci 27, 10695-10702.

Stahlhut, M., Downs, J., Leonard, H., Bisgaard, A. M., Nordmark, E., 2017. Building the repertoire of measures of walking in Rett syndrome. Disabil Rehabil 39, 1926-1931.

Troca-Marín, J. A., Alves-Sampaio, A., Montesinos, M. L., 2012. Deregulated mTOR-mediated translation in intellectual disability. Prog Neurobiol 96, 268-282.

Turner, S. E., Williams, C. M., Iversen, L., Whalley, B. J., 2017. Molecular Pharmacology of Phytocannabinoids. Prog Chem Org Nat Prod 103, 61-101.

Valenti, D., de Bari, L., Vigli, D., Lacivita, E., Leopoldo, M., Laviola, G., Vacca, R. A., De Filippis, B., 2017. Stimulation of the brain serotonin receptor 7 rescues mitochondrial dysfunction in female mice from two models of Rett syndrome. Neuropharmacology 121, 79-88.

Viveros, M. P., Marco, E. M., File, S. E., 2005. Endocannabinoid system and stress and anxiety responses. Pharmacol Biochem Behav 81, 331-342.

Wei, D., Allsop, S., Tye, K., Piomelli, D., 2017. Endocannabinoid Signaling in the Control of Social Behavior. Trends Neurosci 40, 385-396.

Wilcox, R. R., 1987. New designs in analysis of variance. Annual Review of Psychology 38, 29-60.

Woods, R., Vallero, R. O., Golub, M. S., Suarez, J. K., Ta, T. A., Yasui, D. H., Chi, L. H., Kostyniak, P. J., Pessah, I. N., Berman, R. F., LaSalle, J. M., 2012. Long-lived epigenetic interactions between perinatal PBDE exposure and Mecp2308 mutation. Hum Mol Genet 21, 2399-2411.

Zhou, H., Wu, W., Zhang, Y., He, H., Yuan, Z., Zhu, Z., Zhao, Z., 2017. Selective preservation of cholinergic MeCP2 rescues specific Rett-syndrome-like phenotypes in MeCP2stop mice. Behavioural Brain Research 322, Part A, 51-59.
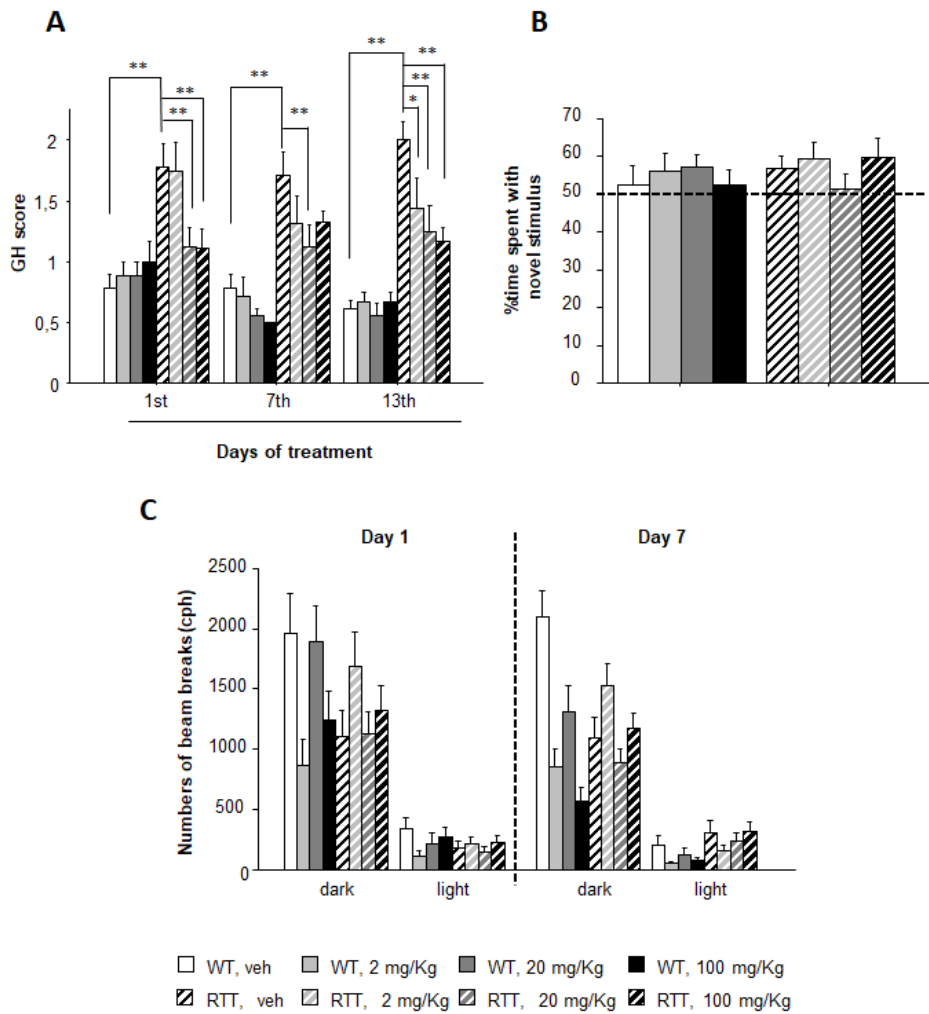
**Figure 1s**: **(a)** Vehicle-injected RTT mice (RTT, Veh) showed worse health conditions compared to wt controls (WT, Veh) in all testing days (day 1, 7 and 13 of the schedule). Cannabidivarin treatment (CBDV) at 20 and 100 mg/Kg ameliorates the general health status of RTT mice. This effect was remarkable especially on day 1 and 13; of note, after 14 IP injections, CBDV 2mg/kg too exerted the same positive effect on RTT mice; **(b)** in the three-chamber social test, during the 10 minutes of social novelty phase (S4), no genotype or treatment effects were highlighted; **(c)** RTT veh mice are less active than wt controls in the home cages (cph: count per hour). This profile was evident during the dark/active phase on both testing days (day 1 and day 7 of the schedule). CBDV treatment did not affect the hypoactive profile of RTT mice. Data are mean±SEM. Statistical significance was calculated by two-way ANOVA with Tukey's post hoc test. **p<0.01; *p<0.05.

*Chapter 5*

# 5.    Conclusion

The present thesis aimed to search new pharmacological approaches for the cure of RTT and its variant CDD. No cure for these devastating disorders is in fact available and no completely efficacious pharmacological treatment is able to ameliorate full symptomatology characteristic of both RTT and CDD. For these reasons, the research in this field is focused on the identification of new therapeutic targets and new pharmacological approaches in order to at least ameliorate disorders symptoms and improve the quality of patient life.

We propose two receptors as innovative pharmacological targets for the cure of RTT: the 5-HT$_7$R, the most recently discovered serotonin receptor (Leopoldo et al., 2011), and the GPR55 (Ryberg et al., 2007), the leading candidate to be called cannabinoid receptor 3 (CB3) for its affinity with endocannabinoids and phytocannabinoids. To "hit" the two innovative targets, we used two different molecules: LP-211, a synthetic drug agonist of the 5-HT$_7$R, and CBDV, a non-psychotropic phytocannabinoid extracts from *Cannabis sativa,* antagonist of GPR55.

In the present work we extended previous results obtained on MeCP2-308 male and female mouse models (De Filippis et al., 2014; De Filippis et al., 2015; Valenti et al., 2017) demonstrating that sub-chronic treatment with LP-211 was able to rescue physiological and behavioural deficits (pulse distension and social impairments) and to normalize altered brain histone H3 acetylation and the levels of proteins forming a complex with MeCP2, the gene whose mutations are responsible for 95% of classical RTT cases (Vigli et al., in preparation); moreover, in CDD mouse model at an advanced stage of disease (12 months of age) the effects of LP-211 treatment were characterized for the first time, demonstrating that LP-211 treatment was able to normalize Prepulse

Inhibition deficit (proposing it as new tool for diagnosis of this pathology and to evaluate the drug efficacy) and to normalize cortical ribosomal protein S6 and mitochondrial functionality (Vigli et al., 2018b), alterations previously detected also in RTT mouse models, suggesting the straight correlation between the two disorders.

Regarding the use of phytocannabinoids extracts as new drugs, we demonstrated for the first time the positive effects of chronic treatment with CBDV on RTT male mouse model (MeCP2-308), showing CBDV wide beneficial effects on altered behavioural domains, such as worst general health status, motor impairments and social deficit. The reduced brain weight was also normalized. In addition, we demonstrated for the first time the higher expression of GPR55 in the hippocampus of RTT mice, proposing it as new pharmacological targets for the treatment of RTT (Vigli et al., 2018a).

In conclusion, the present thesis provides compelling evidence that two pharmacological treatments targeting either the serotoninergic or endocannabinoid system ameliorate the symptomatology displayed by RTT and CDD mouse models, both on behavioural and molecular point of view, suggesting two innovative therapeutic approaches for the cure/treatment of two severe disorders for which no cure is available.

# LIST OF PUBLICATIONS

PUBLICATIONS WITHIN THE Ph.D. RESEARCH PROJECT

*Publications in peer-reviewed journals*

**Vigli D., Rusconi L, Valenti D., La Montanara P., Cosentino L., Lacivita E., Leopoldo M., Amendola E., Gross C., Landsberger N., Laviola G., Kilstrup-Nielsen C., Vacca R.A., De Filippis B**. 2018 Rescue of prepulse inhibition deficit and brain mitochondrial dysfunction by pharmacological stimulation of the central serotonin receptor 7 in a mouse model of CDKL5 Deficiency Disorder, *Neuropharmacology*, **144**, 104-114.

**Vigli, D., Cosentino, L., Raggi, C., Laviola, G., Woolley-Roberts, M., De Filippis, B.,** 2018. Chronic treatment with the phytocannabinoid Cannabidivarin (CBDV) rescues behavioural alterations and brain atrophy in a mouse model of Rett syndrome. *Neuropharmacology*, **140**, 121-129.

**Valenti, D., de Bari, L., Vigli, D., Lacivita, E., Leopoldo, M., Laviola, G., Vacca, R. A., De Filippis, B**., 2017. Stimulation of the brain serotonin receptor 7 rescues mitochondrial dysfunction in female mice from two models of Rett syndrome. *Neuropharmacology*, **121**, 79-88.

*Manuscript in preparation*

**Vigli D.[*], Napolitani G.[*], Cosentino L., Talamo M.C., Lacivita E., Leopoldo M., Laviola G., Fuso A., d'Erme M., De Filippis B.** Targeting serotonin receptor 7 rescues physiological alterations and restores brain histone H3 acetylation and MeCP2 co-repressors proteins levels in a female mouse model of RTT syndrome (in preparation).

PUBLICATIONS WITHIN OTHER PROJECTS

*Publications in peer-reviewed journals*

**Francioso A., Fanelli S., <u>Vigli D.</u>, Ricceri R., Cavallaro R.A., Baseggio Conrado A., Fontana M., d'Erme M., Mosca L**., 2017. HPLC determination of bioactive sulfur compounds, amino acids and biogenic amines in biological specimens. *Advances in Experimental medicine and Biology*, **975 pt 1**, 535-549.

**Cosentino L., <u>Vigli D.</u>, Medici V., Flor H., Lucarelli M., Fuso A., De Filippis B.,** Trauma-exposed methyl-CpG binding protein 2 mutant mice: a new animal model for post-traumatic stress disorder (submitted)

**Cosentino L., <u>Vigli D.</u>, Franchi F., Laviola G., De Filippis B.,** Rett syndrome before regression: a time window of overlooked opportunities for diagnosis and intervention (submitted)

# APPENDIX: THESIS' PUBBLICATIONS

# Chronic treatment with the phytocannabinoid Cannabidivarin (CBDV) rescues behavioural alterations and brain atrophy in a mouse model of Rett syndrome

Daniele Vigli [a], Livia Cosentino [a], Carla Raggi [b], Giovanni Laviola [a], Marie Woolley-Roberts [c], Bianca De Filippis [a, *]

[a] Center for Behavioral Sciences and Mental Health, Istituto Superiore di Sanità, Rome, Italy
[b] National Center for Control and Evaluation of Medicines, Istituto Superiore di Sanità, Rome, Italy
[c] GW Research Ltd, Cambridge, UK

## ABSTRACT

Rett syndrome (RTT) is a rare neurodevelopmental disorder, characterized by severe behavioural and physiological symptoms. RTT is caused by mutations in the *MECP2* gene in about 95% of cases and to date no cure is available. The endocannabinoid system modulates several physiological processes and behavioural responses that are impaired in RTT and its deregulation has been associated with neuro-psychiatric disorders which have symptoms in common with RTT. The present study evaluated the potential therapeutic efficacy for RTT of cannabidivarin (CBDV), a non-psychotropic phytocannabinoid from *Cannabis sativa* that presents antagonistic properties on the G protein-coupled receptor 55 (GPR55), the most recently identified cannabinoid receptor. Present results demonstrate that systemic treatment with CBDV (2, 20, 100 mg/Kg ip for 14 days) rescues behavioural and brain alterations in MeCP2-308 male mice, a validated RTT model. The CBDV treatment restored the compromised general health status, the sociability and the brain weight in RTT mice. A partial restoration of motor coordination was also observed. Moreover, increased levels of GPR55 were found in RTT mouse hippocampus, suggesting this G protein-coupled receptor as new potential target for the treatment of this disorder. Present findings highlight for the first time for RTT the translational relevance of CBDV, an innovative therapeutic agent that is under active investigation in the clinical setting.

© 2018 Elsevier Ltd. All rights reserved.

## 1. Introduction

Rett syndrome (RTT) is a rare neurodevelopmental disorder, characterized by severe behavioural and physiological symptoms (Hagberg et al., 2002; Rett, 1966; Ricceri et al., 2012). One essential feature of RTT is the apparently normal perinatal development until about 6–18 months of age, when RTT patients start losing their acquired cognitive, social, and motor skills and develop a wide variety of symptoms (Hagberg, 2002). Classic RTT is caused in about 90–95% of cases by *de novo* mutations in the X-linked *MECP2* gene, which encodes the methyl CpG-binding protein 2 (MECP2), a multifunctional protein that binds to methylated DNA and mainly

acts as a key transcriptional regulator (Guy et al., 2011). Despite extensive effort in this research field, how mutations in *MECP2* lead to the symptomatology of RTT is still unknown and no effective therapy is currently available for this devastating syndrome.

The endocannabinoid system (ECS) is a complex neuro-modulatory system found in all vertebrate classes, involved in the regulation of numerous physiological functions (Kano et al., 2009). At the central level, ECS modulates several physiological processes and behavioural responses that are impaired in RTT (Di Marzo et al., 2015), such as social behaviour (Wei et al., 2017), anxiety and stress response (Jenniches et al., 2016) and motor control (El Manira and Kyriakatos, 2010). Moreover, ECS deregulation has been associated with many neuropsychiatric disorders such as anxiety and depression (Jenniches et al., 2016; Micale et al., 2013), Fragile X syndrome (Jung et al., 2012), schizophrenia (Clarke et al., 2017) and with neurodegenerative disorders characterized by cognitive and motor dysfunctions such as Alzheimer's, Huntington's and

Parkinson's disease (Dowie et al., 2009; Maroof et al., 2014; Pisani et al., 2011). Recent data also suggest an involvement of the ECS in Autism Spectrum disorders (Chakrabarti et al., 2015).

A growing number of molecules able to directly or indirectly modulate the ECS have been identified to date. Pioneering studies increased the ECS response using agonists of the CB1 receptor, one of the two well characterized G-coupled receptors for endocannabinoids (Berrendero and Maldonado, 2002; Jiang et al., 2005; Patel et al., 2003). However, CB1 agonists may cause psychotropic side effects, similar to those reported with cannabis use in recreational settings. Such effects are now known to be due to the assimilation of $\Delta^9$-tetrahydrocannabinol (THC), the main compound of *Cannabis sativa*. To avoid these undesirable effects, most recent preclinical studies focussed on the identification of molecules that modulate the ECS without the psychotropic effects of THC, such as Rimonabant and URB597 (see e.g.(Griebel et al., 2005; Marco et al., 2015)). In addition, much attention has been devoted to non-psychotropic molecules from *Cannabis sativa*, which contains more than 120 substances (Morales et al., 2017). This has led to the identification of few non-psychotropic phytocannabinoids (phCBs) with a potential as novel drugs. These include Cannabigerol (CBG) and Cannabidiol (CBD), the second and the third most abundant chemical class types contained in *Cannabis sativa* respectively. In particular CBD bears a high potential in the treatment of muscular spasms and rigidity (Di Marzo, 2011), epilepsy (Chiu et al., 1979; Devinsky et al., 2017), mood disorders (Linge et al., 2016) and Alzheimer's disease (Cheng et al., 2014). Moreover, recent evidences suggest a potential application for CBD in pediatric conditions such as autistic-related syndromes (Kaplan et al., 2017) and in children with refractory epilepsy (Brodie and Ben-Menachem, 2018; Geffrey et al., 2015).

Another promising phCB is Cannabidivarin (CBDV), the *n*-propyl analog of CBD. Recent evidence proves that *in vitro* and *in vivo* treatment with CBDV in mouse and rat exerts anticonvulsant effects (Hill et al., 2012) and prevents neuronal hyperexcitability (Iannotti et al., 2014). However, the studies focussed on this compound are still very limited and the mechanisms of action of CDBV have not been clarified so far. Current evidences suggest that at physiologically relevant concentrations of CBDV show no affinity for CB1 and CB2 receptors (Hill et al., 2012) and presents antagonistic properties on the G protein-coupled receptor 55 (GPR55) receptor, the leading candidate for the CB3 receptor name (Anavi-Goffer et al., 2012; Iannotti et al., 2014; Marichal-Cancino et al., 2017; Turner et al., 2017). This lipid-activated G protein-coupled receptor has been suggested to regulate motor function, spatial memory and sociability (Bjursell et al., 2016; Kramar et al., 2017; Marichal-Cancino et al., 2018), behavioural domains that are compromised in RTT (De Filippis et al., 2014; Moretti et al., 2006). Moreover, antagonism of GPR55 has been recently suggested as a potential therapeutic approach for Dravet syndrome (Kaplan et al., 2017), an autistic-like syndrome with several symptoms in common with RTT.

Importantly, a clinical trial is currently listed aimed at evaluating the potential efficacy of a treatment with CBDV on children affected by Autism Spectrum Disorder (clinicaltrial.gov, NCT03202303). Based on the high translational potentiality of CBDV as an innovative therapeutic agent, in the present study MeCP2-308 hemizygous male mice, a highly validated mouse model of RTT (De Filippis et al., 2010), and wild-type littermate controls received a repeated systemic intraperitoneal (i.p.) treatment with CBDV (2, 20, 100 mg/Kg ip for 14 days). Mice were treated at 5 months of age, an early symptomatic stage at which MeCP2-308 mice already present reduced spontaneous home-cage motor activity, motor coordination impairments, and a more marked profile of D-amphetamine-released stereotyped behavioural syndrome than WT controls (De Filippis et al., 2010). A battery of behavioural analyses was carried out to evaluate treatment effects. Given CBDV antagonistic action

on GPR55 (Marichal-Cancino et al., 2017), levels of this receptor were evaluated, to verify whether they are abnormal in RTT and CBDV treatment effects thereon. As markers of efficacy we also explored whether the CBDV treatment impacts the abnormal activation of the ribosomal protein (rp) S6, a downstream target of mTOR, in the brain of MeCP2-308 mice (De Filippis et al., 2014; Ricciardi et al., 2011), and the alterations in brain neurotrophins levels (Chang et al., 2006; Ricceri et al., 2011). Indeed, based on previous reports suggesting that ECS modulation in mouse brain can impact mTOR signalling (Busquets-Garcia et al., 2013; Puighermanal et al., 2012) and neurotrophins levels (Keimpema et al., 2014), we hypothesised that the CBDV treatment may normalize these RTT-related brain molecular alterations. A focus was made on the hippocampus, a brain region critically involved in regulation of relevant behavioural domains (Kaplan et al., 2017; De Filippis et al., 2014).

## 2. Experimental procedures

### 2.1. Animals

The experimental subjects were 5 month-old MeCP2-308 hemizygous male mice (RTT) and wild-type (WT) littermates (B6.129S-MeCP2tm1Heto/J from the Jackson Laboratories (USA), stock number: 005439) (De Filippis et al., 2010; Shahbazian et al., 2002), bred in our facility. Mice were weaned at postnatal day 25 and maintained in groups of 2–3 (according to sex) until 5 months of age. Temperature was maintained at $21 \pm 1\,°C$ and relative humidity at $60 \pm 10\%$. Animals were provided *ad libitum* with tap water and a complete pellet diet (Altromin, 1324 - 10 mm pellets, Germany). All experimental procedures were conducted in conformity with the European Directive 2010/63/EU and the Italian legislation on animal experimentation, D.Lgs. 26/2014.

### 2.2. Genotyping

DNA has been prepared from a small tail-tip biopsy taken at weaning, as previously described (De Filippis et al., 2010). The MeCP2 alleles have been identified by PCR using two sets of primers. Primer set 1 (5′ primer: 5′-AAC GGG GTA GAA AGC CTG-3′ and 3′ primer: 5′-ATG CTC CAG ACT GCC TTG -3′) yields a product of 396 bp identifying the wildtype allele. Primer set 2 (5′ primer same as for primer set 1 and 3′ primer: 5′- TGA TGG GGT CCTCAG AGC -3′) yields a product of apparent size 318 bp identifying the null allele. PCR products were electrophoresed through a 2% NuSieve 3:1 agarose gel (Cambrex Bio Science, Rockland, ME, USA) containing $0.5\,\mu g/mL$ ethidium bromide, and examined under UV light.

### 2.3. Drug and treatment

CBDV (purity by HPLC: 95.9%) was supplied by GW Research Limited (Salisbury, UK) and stored in a freezer (at approximately $-20\,°C$), protected from light and freshly prepared immediately prior to injection. Given that CBDV is a nonpolar molecule with very low solubility in water solution, the emulsion was prepared using Cremophor® mixed with EtOH and saline. RTT mice and WT littermate controls were injected daily i.p. (between 9.00 and 11.00 a.m.) for 14 consecutive days with CBDV (2, 20 or 100 mg/kg) or vehicle (veh) (Cremophor® EL:EtOH:saline in a ratio of 1:2:17). After a 24-h washout period from the 14th i.p. injection, mice were sacrificed by decapitation. Before the regions collection, whole brains (including olfactory bulbs) of experimental animals were rapidly weighted. Subsequently, brains were dissected and hippocampi were collected and rapidly frozen for biochemical analyses.

## 2.4. Behavioural tests

To unravel the effects of the CBDV treatment on RTT-related behavioural alterations, mice were subjected to a battery of behavioural tests (Fig. 1). The following numerosity for each experimental group has been achieved in the behavioural analyses: WT, veh: 9; WT, CBDV 2 mg/Kg: 9; WT, CBDV 20 mg/Kg: 9; WT, CBDV 100 mg/Kg: 9; Hz, veh: 7; Hz, CBDV 2 mg/Kg: 8; Hz, CBDV 20 mg/Kg: 8; Hz, CBDV 100 mg/Kg: 9. A total of 70 animals were used for the study.

### 2.4.1. General health score

The general health of the experimental mice was qualitatively evaluated by a trained observer, blind to the genotype of the experimental mice, at the end of behavioural testing after the 1st, the 7th and the 13th injection, as previously described (De Filippis et al., 2014; Guy et al., 2001). Briefly, mice received a score (ranging from 0 − normal appearance-to 4- highly compromised) for each of the following symptoms: gait, mobility, breathing, kyphosis, fur, hind limb clasping, tremors and general conditions The individual scores for each category have been subsequently analysed to obtain a semi-quantitative measure of the general health status. Body weight was also recorded at each scoring session.

### 2.4.2. Dowel test

To evaluate the effects of the treatment on motor learning capacities, the dowel test has been performed 1.5 h after the 1st, the 7th i.p. and the 13th injections as previously described (De Filippis et al., 2015a). The hardwood round dowel is 9.0 mm in diameter and 35 cm long. The dowel has been mounted horizontally 50 cm above a 5 cm depth bedding of sawdust. At the beginning of the testing, each mouse has been placed in the middle of the dowel so that the length of its body was parallel to the dowel. Latency to fall from the dowel into a cage of bedding has been recorded (30-s criterion) and used as a measure of motor coordination abilities. Each mouse has repeated the test twice per each testing day, with an inter-trial interval of at least 15 min.

### 2.4.3. Home-cage spontaneous activity and its circadian variation

Spontaneous locomotor activity in the home-cages has been monitored by means of an automatic device using small passive infrared sensors positioned on the top of each cage, as previously described (De Filippis et al., 2010, 2012). Data presented in the Results section are referred to a selection of 5 h per phase (dark: 2−6 pm; light: 2−6 am) recorded on the first and the seventh day of the treatment schedule. We in fact hypothesised that the arousal state of the experimental animals is highly influenced by the number and type of experiments that are performed on a particular day and may affect the locomotor activity in the home cages. We therefore selected two days of the treatment schedule on which mice were subjected to a comparable battery of behavioural evaluations which included a motor coordination test and the general health score evaluation (see Fig. 1).

### 2.4.4. Three-chamber social test

Sociability and social recognition were assessed in the three-chambered test, as previously described (Smith et al., 2007). The test started 1 h after the 5th i.p. injection. The test consists of 4 consecutive phases of 10 min during which each mouse is individually placed in the apparatus: Phase 1 (S1): mice can freely explore the central chamber of the apparatus; Phase 2 (S2): mice can explore the three empty chambers; Phase 3 (S3): mice can explore either the chamber containing an empty small wire cage or the other one containing a conspecific kept under an identical small wire cage; Phase 4 (S4): an unfamiliar mouse is located under the cage wire which was empty during S3. Allocation of mouse partners to specific chambers was counterbalanced within each experimental group. Time spent exploring the mouse versus the empty wire cage during S3 is considered as an index of sociability. Time spent exploring the unfamiliar mouse versus the familiar one during S4 is considered as an index of memory of the social stimuli. Naïve C57 adult male mice were used as partners in this test. They were first habituated to the small wire cages in the test environment for 2 consecutive days before the testing day. After each animal was tested, the three-chamber apparatus and the wire cages were thoroughly cleaned with 70% ethanol.

### 2.4.5. Y-maze test

The effects of the treatment on short-term spatial memory were assessed on the cognitive, exploratory driven, spatial novelty preference task. This task was carried out 1 h after the 11th i.p. injection, as previously described (De Filippis et al., 2014, 2015a). Mice were tested on a spontaneous, spatial novelty preference task as previously described (Lyon et al., 2011; Sanderson et al., 2007). The Y-maze was made from transparent Perspex, and consisted of three 30 cm long, 8 cm wide arms with 20 cm high walls, connected by a central junction. A thin layer of sawdust covered the floor of the maze. The test was carried out as previously described (Lyon et al., 2011; Sanderson et al., 2007). Each mouse was assigned two arms (the 'start arm' and the 'other arm') to which they were
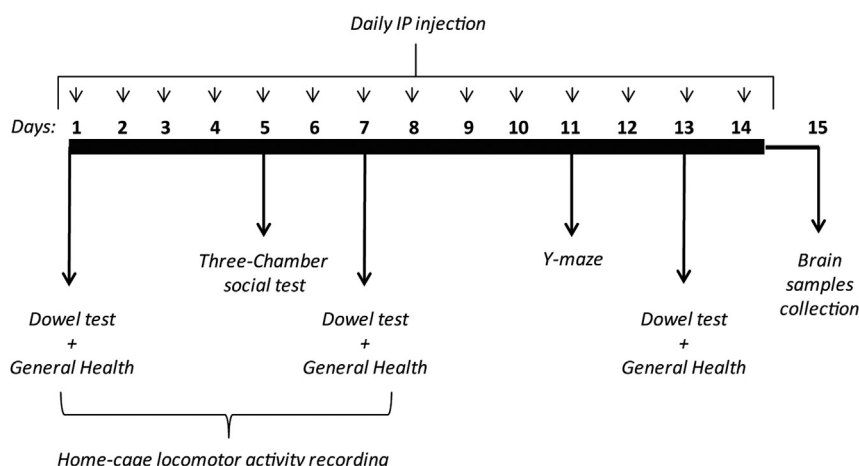


Fig. 1. Experimental schedule; IP: intra-peritoneal.

exposed during the first phase of the task (the 'exposure phase'). Allocation of arms to specific spatial locations was counterbalanced within each experimental group. During the 5-min 'exposure' phase, the entrance to the third, 'novel', arm was closed off by the presence of a large Perspex white block. The mouse was placed at the end of the start arm, facing the experimenter, and allowed to explore the start arm and the other arm freely for 5 min, beginning as soon as the mouse left the start arm. At the end of 5min exposure phase, the mouse was removed from the maze and returned to the home cage for 1 min. During this time, the Perspex block closing off the novel arm was removed and the sawdust redistributed throughout the maze to minimize the use of odor cues. The mouse was then returned to the start arm, facing the experimenter, for the 2-min 'test phase'. This consisted of 2-min free exploration during which the mouse could enter all the three arms, beginning as soon as the mouse left the start arm. The test was video-recorded and the number of entries and the length of time spent into each arm, during both the exposure and the test phase, were subsequently scored by means of the Noldus Observer XT. For the test phase, a discrimination ratio [novel arm/(novel + other arm)]*100 was calculated for time spent in each arm.

## 2.5. Neurobiological analyses

### 2.5.1. Western blot analyses

Hippocampal tissues were suspended in buffer containing 50 mM Tris—HCl, pH 8.0, 150 mM NaCl, 1% Triton-X100, 2 mM MgCl2 and phosphatase and protease inhibitors cocktail (PhosSTOP, Complete Mini, Roche) and then sonicated on ice. Lysates were centrifuged at $10000 \times g$ for 15 min at 4 °C. Protein concentration was determined by Bradford assay (BioRad). Samples containing 30 μg of proteins were resolved by 7,5% SDS-PAGE under reducing and denaturing conditions and transferred to nitrocellulose membrane (Amersham Protran Premium). Membranes were blocked in TBST (10 mM Tris-HCl pH 8.0, 150 mM NaCl, 0.05% Tween 20) with 5% non-fat dry milk for 45 min at room temperature, and then incubated with rabbit anti-rpS6 (1:1000, Cell Signalling), rabbit anti-phospho-rpS6 (Ser 240/244) (1:1000, Cell Signaling), rabbit anti-GPR55 (Abcam, 1:1000) and rabbit anti-beta actin (Cell Signaling, 1:1000) overnight at 4 °C. After washing, membranes were incubated with secondary anti-rabbit IgG HRP-conjugated antibodies (1:3000, Amersham) for 45 min at room temperature. Detection was performed by Immobilon Western Chemiluminescent HRP substrate (Millipore). Quantification of protein expression was performed by densitometry analysis using ImageLab software V.6.0 (Chemidoc, Biorad). Optical Density (OD) from at least 4 different experimental mice per group were calculated for each sample and normalized with the corresponding actin signal OD; the OD ratios were then compared and expressed as the average fold increase, with 100 (WT control) as the control value.

### 2.5.2. Enzyme-linked immunosorbent assay (ELISA)

ELISA was performed to quantify levels of different neurotrophins in the hippocampus of the experimental mice. Levels of BDNF, NGF, and IGF-1 were analysed by using microtiter wells plates coated with anti-mouse neurotrophins antibodies (BDNF rapid, NGF rapid, Biosensis, Australia; IGF-1 Elisa kit, Abcam, UK) according to the manufacturer's instructions. The absorbance was read on a spectro-photometer (Bio-Rad) using 450 nm as the primary wave length, with a sub-wave length of 650 nm. The quantity of neurotrophins was expressed as percentage average fold increase of WT control values (100).

### 2.5.3. Statistical analyses

Data were analysed with ANOVA models including genotype and treatment as between-subject factors and repeated measurements as within-subject factor. The alpha level was set to 5%. The Levene test was applied to confirm the equality of variance. The presence of outliers was verified using ROUT method. *Post-hoc* comparisons were performed by Tukey HSD, even in the absence of statistically significant interactions (Wilcox, 1987).

## 3. Results

### 3.1. Behavioural analyses

#### 3.1.1. General health score

The evaluation of the general health status of the experimental mice confirmed that consistent gross phenotypic alterations can be detected in 5 month old RTT mice (Fig. 2a, RTT, veh vs WT, veh, $p < 0.01$ after *post-hoc* comparison on Genotype*Treatment interaction: $F_{(3,60)} = 2.906$; $p = 0.042$). We found that 14 injections of CBDV at the doses of 20 and 100 mg/Kg can improve the general health status of RTT mice (Fig. 2a, RTT, veh vs RTT, CBDV 20 mg/Kg, $p < 0.01$ and RTT, veh vs RTT, CBDV, 100 mg/Kg, $p < 0.01$ after *post-hoc* comparison on Genotype*Treatment interaction). The ANOVA highlights significant effect of repeated measures (Days of the schedule number 1, 7, 13: $F_{(2,120)} = 5.350$; $p < 0.006$) and interaction of this factor with Genotype ($F_{(2,120)} = 3.930$; $p < 0.022$) but no interaction with Treatment. Fig. 2a graphically shows the significant Genotype*Treatment interaction, thus the average of all time points (for further information on the effects of repeated measures see Supplementary Fig. 1a). RTT mice weighed less compared to WT littermates (Genotype: $F_{(1,60)} = 12.048$; $p < 0.001$). No treatment effects were found on this parameter *(data not shown).*

#### 3.1.2. Dowel test

Motor learning ability was assessed in the Dowel test (Fig. 2b). In line with previous data, RTT mice showed shorter latency to fall down from the bar compared to WT controls (RTT, veh vs WT, veh, $p < 0.01$ after *post-hoc* comparison on Day*Trial*Genotype*Treatment interaction: $F_{(6,120)} = 2.512$; $p = 0.025$). A worse performance of RTT mice was thus confirmed in this test (De Filippis et al., 2010, 2012). Treatment with CBDV at the dose of 20 mg/kg significantly improved the motor learning ability of RTT mice and restored WT-like levels of performance on the second testing day (the seventh of the experimental schedule). This profile was evident on both the first and the second trials ($p < 0.01$ and $p < 0.05$ after *post-hoc* comparisons on the Day*Trial*Genotype*Treatment interaction, respectively). However, this treatment effect was no more evident on the 13th day of the treatment schedule. By contrast, at this latest time point, the dose of 100 mg/Kg significantly improved the motor learning ability of RTT mice ($p < 0.05$ after *post-hoc* comparison on the Day*Trial* Genotype*Treatment interaction).

#### 3.1.3. Spontaneous locomotor activity

In line with previous reports, the evaluation of spontaneous locomotor activity in home cage revealed that RTT mice are generally less active than WT controls (Genotype*Treatment interaction: $F_{(3,46)} = 5.032$; $p = 0.004$). This profile was mainly evident during the dark/active phase (Fig. 2c, $p < 0.01$ after *post-hoc* comparison on the Phase*Genotype*Treatment interaction: $F_{(3,46)} = 4.757$; $p = 0.001$). Levels of activity exhibited by RTT mice treated with CBDV at 2 mg/kg tended to be increased compared to those shown by vehicle-injected ones. However, such a trend did not reach statistical significance. The ANOVA did not highlight any significant effect of repeated measures (Days of the schedule number 1 and 7: $F_{(1,46)} = 3.147$; $p < 0.083$) or interaction of this factor with Genotype or Treatment. Fig. 2c graphically shows the significant Phase*Genotype*Treatment interaction, thus the
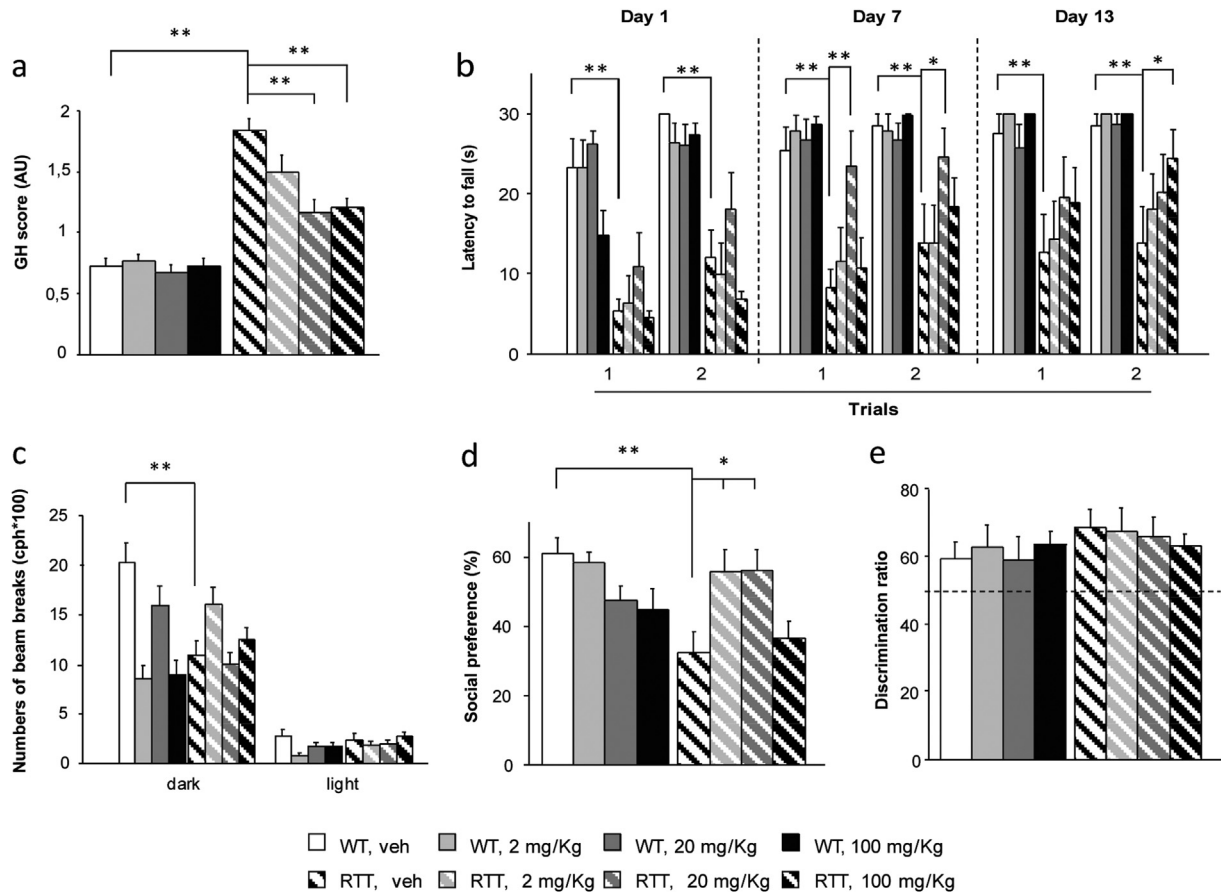
**Fig. 2.** *Cannabidivarin (CBDV) treatment rescues behavioural alterations in* 5 *month-old RTT male mice;* Vehicle-injected RTT mice (RTT, veh) showed worse health conditions compared to WT controls (WT, veh). Treatment with Cannabidivarin (CBDV) at 20 and 100 mg/Kg ameliorates the general health status of RTT mice; GH scores (AU: Arbitrary units) are mean values of the three time points in which the evaluation was carried out (Days of the schedule number 1, 7, 13). **(b)** in the Dowel test, RTT mice displayed significantly shorter latencies to fall from a dowel compared to WT controls, confirming impaired motor learning capacities. CBDV at the dose of 20 mg/Kg improved the performance of RTT mice on day 7 and the 100 mg/Kg dose improved the performance of RTT mice in the second trial of day 13; Mice were tested twice per day, with an inter-trial interval of at least 15 min **(c)** RTT, veh mice are generally less active than WT controls in the home cages. This profile was mainly evident during the dark/active phase. CBDV treatment did not affect the hypoactive profile of RTT mice, despite a trend for the 2 mg/kg dose of CBDV treatment; activity was automatically monitored by passive infrared sensors. Number of beam breaks (cph: counts per hour) are referred to a selection of 5 h per phase (dark: 2—6 pm; light: 2—6 am) recorded on the first and the seventh day of the treatment schedule. **(d)** in the three-chamber social test, RTT mice spent less time exploring the mouse versus the empty wire cage during sociability phase (S3) in comparison to WT controls. CBDV at the doses of 2 and 20 mg/Kg rescued this aberrant behaviour restoring normal level of sociability; **(e)** in the Y-maze task, no genotype differences were found in the discrimination ratio index [time spent in novel arm/(novel + other arm)]*100 and no treatment effect was evident. Data are mean ± SEM. Statistical significance was calculated by two-way ANOVA with Tukey's *post-hoc* test. **p < 0.01; *p < 0.05.

average of both days (for further information on the effects of repeated measures see Supplementary Figure 1b).

### 3.1.4. Three-chamber social test

The test was carried out in order to evaluate CBDV effect on social behaviour. As expected, the analysis of the S3 phase revealed a statistically significant difference between genotypes, with veh-injected RTT mice showing a reduced preference for the social stimulus (versus the inanimate one) in comparison to veh-injected WT controls (Fig. 2d, p < 0.01 after *post-hoc* comparison on the Genotype*Treatment interaction: F $_{(3,58)} = 3.527$; p = 0.020). Importantly, the CBDV treatment at the dose of 2 and 20 mg/Kg rescued this social deficit in RTT mice, restoring WT-like levels of social preference (Fig. 2d, p < 0.05 after *post-hoc* comparison on the Genotype*Treatment interaction). The analysis of the S4 phase did not highlight significant genotype or treatment effects in the recognition of a novel social stimulus (versus the familiar one) (Supplementary Figure 1c).

### 3.1.5. Y-maze test

No genotype effects were found in the discrimination ratio

index at this early symptomatic age (Fig. 2e); all the experimental mice recognized the novel arm versus the familiar one (discrimination ratio > 50). No treatment effects were evident.

### 3.2. Neurobiological analyses

### 3.2.1. Brain weight

We found that the whole brain of veh-injected RTT mice weighted less compared to those of WT littermate controls (Fig. 3, p < 0.05 after *post-hoc* comparison on Genotype*Treatment interaction: $F_{(3,60)} = 1.714$; p = 0.174). Interestingly, the whole brain of RTT mice was increased at levels comparable to those of WT animals by 14 injections of CBDV at the doses of 2 and 100 mg/Kg (Fig. 3, RTT, veh vs RTT, CBDV 2 and 100 mg/Kg, p < 0.05 after *post-hoc* comparisons on Genotype*Treatment interaction).

### 3.2.2. Western blot

GPR55 has been described as a major target of CBDV (Anavi-Goffer et al., 2012; Marichal-Cancino et al., 2017). Based on this evidence, hippocampal levels of GPR55 were evaluated (Fig. 4a, Representative blots). We found a two-fold increase in GPR55 levels
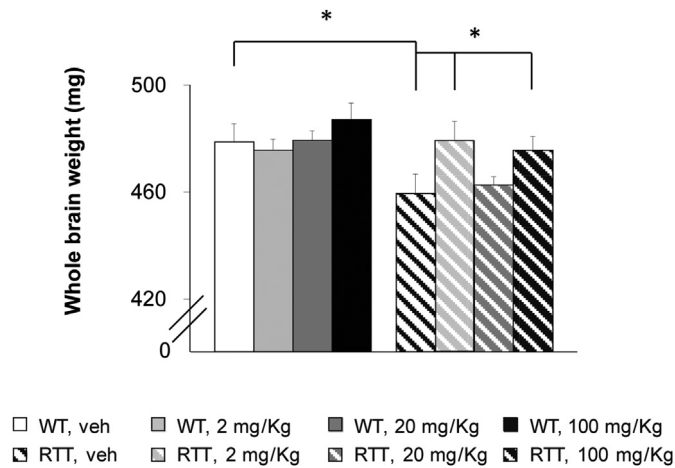
**Fig. 3.** *Cannabidivarin (CBDV) treatment normalizes the reduced brain weight of* 5 month-*old RTT male mice*; after sacrifice, the brain of experimental animals was collected and weighted before the hippocampal dissection; the brain of vehicle-injected RTT mice (RTT, veh) weighted less in comparison to WT controls (WT, Veh); CBDV at the doses of 2 mg/kg and 100 mg/Kg rescues the reduced brain weight of RTT mice. Data are mean $\pm$ SEM. Statistical significance was calculated by two-way ANOVA with Tukey's *post-hoc* test. *$p < 0.05$.

in RTT mice compared to WT littermates (Fig. 4a—b, Genotype: $F_{(1,24)} = 18.880$; $p = 0.001$). CBDV treatment did not exert significant effects on GPR55 level (Fig. 4a—b, Genotype*Treatment interaction: $F_{(3,24)} = 1.253$; $p = 0.313$).

We explored whether the chronic treatment with CBDV affects the activation of the ribosomal protein (rp) S6 in the hippocampus of RTT mice. Neither genotype nor treatment effects were found as for total rpS6 protein level (S6tot) and no differences between genotypes were found as for the ratio between phospho-S6 (phS6) and S6tot, which expresses the functionality of the kinase. The CBDV treatment did not affect this parameter (Table 1).

### 3.2.3. ELISA

The hippocampal levels of the neurotrophins BDNF, NGF and IGF-1 were measured as markers of treatment efficacy. We found that hippocampal levels of BDNF and IGF1 did not significantly differ between RTT mice and WT controls at this testing age (Table 1), even though BDNF levels tended to be higher in RTT mouse brain. Conversely, NGF was significantly reduced in RTT mice (Fig. 4c, $p < 0.05$ after *post-hoc* comparison on Genotype*-Treatment interaction: $F_{(3,22)} = 5.663$; $p = 0.005$). CBDV did not produce any significant effect on neurotrophins levels in the hippocampus of RTT mice. However, the treatment with CBDV at the 100 mg/kg dose significantly increased NGF levels selectively in the hippocampus of WT mice (about 160% of veh-injected WT mice, Fig. 4c, $p < 0.01$ after *post-hoc* comparison on Genotype*Treatment interaction).

## 4. Discussion

The present study demonstrates, for the first time, that 14 days of treatment with CBDV, a phCB extracted from *Cannabis sativa*, improves important aspects of the aberrant phenotype in a validated mouse model of RTT. The positive effects of CBDV treatment on RTT mice were specifically related to the general health status, the social sphere and the motor skills, phenotypic domains which are highly compromised in RTT patients (Morel and Demily, 2017; Stahlhut et al., 2017). Of note, the reduced brain weight of RTT mice was also normalized by the repeated CBDV treatment. Furthermore, the present study provides the first evidence of abnormal
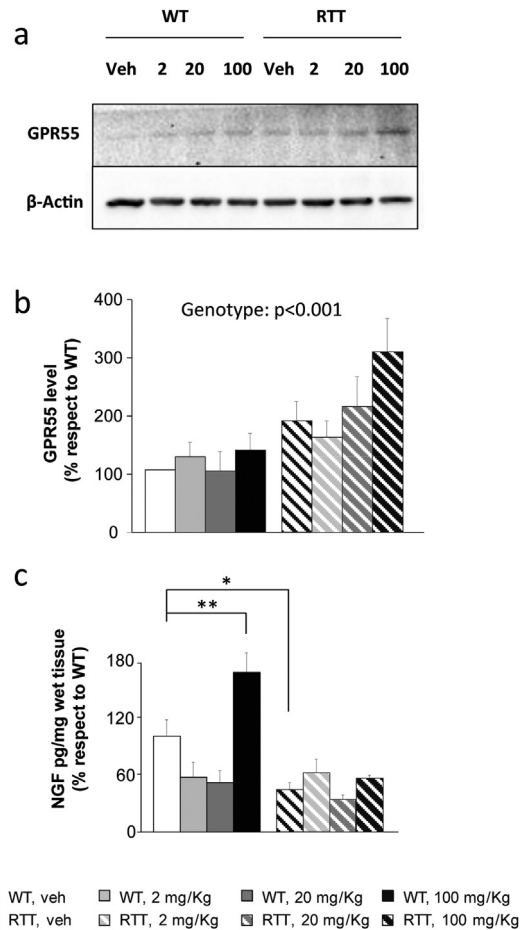


**Fig. 4.** 5 month-*old RTT male mice present enhanced hippocampal levels of GPR55.* **(a)** Representative Western blot analysis (summarized view corresponding to one animal per group) of GPR55 and actin. **(b)** Western blot analysis highlighted higher GPR55 level in hippocampus of RTT mice compared to WT mice. CBDV did not alter GPR55 levels in both genotypes. **(c)** ELISA assays revealed that RTT mice display lower NGF levels in comparison to WT controls; CBDV did not rescue this alteration; Data are mean $\pm$ SEM. Statistical significance was calculated by two-way ANOVA with Tukey's *post-hoc* test. **$p < 0.01$; *$p < 0.05$.

**Table 1**
Levels of BDNF, IGF-1 and Ribosomal protein S6 activity in hippocampus.

| Genotype | Treatment | BDNF | IGF-1 | phS6/S6tot |
|---|---|---|---|---|
| WT | vehicle | $100 \pm 58.0$ | $100 \pm 11.7$ | $100 \pm 0.0$ |
| WT | CBDV 2mg/Kg | $149.7 \pm 50.6$ | $108.4 \pm 6.7$ | $96.2 \pm 31.5$ |
| WT | CBDV 20mg/Kg | $89.5 \pm 59.3$ | $92.3 \pm 43.9$ | $103.9 \pm 44.6$ |
| WT | CBDV 100mg/Kg | $132.6 \pm 77.0$ | $94.088 \pm 5.2$ | $117.9 \pm 41.6$ |
| RTT | vehicle | $133.0 \pm 28.0$ | $106.1 \pm 13.9$ | $100.4 \pm 51.6$ |
| RTT | CBDV 2mg/Kg | $173.8 \pm 63.4$ | $101.996 \pm 8.3$ | $95.8 \pm 26.6$ |
| RTT | CBDV 20mg/Kg | $109.1 \pm 36.3$ | $82.207 \pm 17.1$ | $76.6 \pm 23.3$ |
| RTT | CBDV 100mg/Kg | $89.8 \pm 24.2$ | $96.0 \pm 3.7$ | $85.8 \pm 48.2$ |

Data are mean $\pm$ SEM. Hippocampal BDNF an IGF-1 levels were calculated performing ELISA assays and were expressed respect to WT $= 100$. Western blot assay was used to quantify hippocampal levels of Ribosomal protein S6 (S6tot) and its phosphorylated form (phS6). rpS6 activity was expressed as ratio phS6/S6tot levels, respect to WT $= 100$. MeCP2-308 hemizygous male mice (RTT); wild-type littermates (WT); Cannabidivarin (CBDV).

hippocampal levels of lipid-activated G protein-coupled receptor GPR55, a recently identified cannabinoid receptor, in a RTT mouse model.

Present data provide convincing evidence that the CBDV treatment rescues a number of behavioural and phenotypic alterations

in a validated RTT mouse model. In line with previous reports (Woods et al., 2012), we found that RTT mice show abnormal sociability in the three-chamber social test. These results are consistent with the increasing literature providing evidence of a link between cannabinoids and social behaviour in humans (Wei et al., 2017) and in animal models (Kaplan et al., 2017; Kramar et al., 2017; Marco et al., 2015). In particular, the ECS is suggested to control the molecular mechanisms underpinning social anxiety (Viveros et al., 2005; Wei et al., 2017). In this line, we found that RTT mice exhibited avoidance of the social stimulus, rather than a lack of preference for the social vs the inanimate one. This abnormal behavioural profile was largely attenuated by the CBDV treatment.

Of note, a normalization of the compromised general health status in RTT mice was also observed. This effect was attributable to improvements in a number of parameters which are relevant for this disorder such as mobility, gait, kyphosis and tremors. Moreover, these beneficial effects of the CBDV treatment were accompanied by a partial restoration of motor coordination and spontaneous locomotor activity in the home cage. Increasing evidence suggests the potential therapeutic efficacy of phCBs in a number of disorders characterized by motor dysfunctions, such as Alzheimer's, Huntington's and Parkinson's disease (Dowie et al., 2009; Maroof et al., 2014; Pisani et al., 2011). Taken together, present findings suggest that CBDV may provide significant beneficial effects on RTT-related motor defects. Further studies specifically tailored to confirm this hypothesis are however needed (De Filippis et al., 2015b).

Another important finding of the present study concerns the normalization of brain atrophy in CBDV-treated RTT mice. Microcephaly is a peculiar feature of RTT and several studies have reported reduced brain weight in the mouse models (Zhou et al., 2017). It is generally acknowledged that such reduction is attributable to cell atrophy due to abnormalities in the cytoskeleton, rather than cell death (neurodegeneration is not observed in RTT mice or patients) (Guy et al., 2007). Given that the ECS is known to modulate the actin cytoskeleton (Njoo et al., 2015; Roland et al., 2014), one intriguing hypothesis concerns the possibility that the CBDV treatment may have restored the structural integrity of neurons and astrocytes or the cytoarchitecture of the cortex, which are abnormal in RTT mouse brain (Bittolo et al., 2016; Fukuda et al., 2005; Maezawa et al., 2009).

In the present study, we provide the first evidence that GPR55 levels are increased in the hippocampus of early symptomatic RTT mice. Considering previous studies linking GPR55 with social behaviour (Kaplan et al., 2017; Kramar et al., 2017), motor function (Bjursell et al., 2016) and spatial memory (Marichal-Cancino et al., 2018), it is conceivable that CBDV-mediated antagonism of GPR55 may account for the rescue of RTT-related alterations we report in the present study. Although further studies are needed to verify this possibility, our results provide a new pharmacological target for the treatment of RTT. In this line, it is worth noting that GPR55 has been suggested to be involved in the regulation of energetic metabolism (Simcocks et al., 2014). Given that mitochondrial dysfunction is emerging as crucial in the pathogenesis of RTT (De Filippis et al., 2015c; Valenti et al., 2017), we suggest that further studies aimed at verifying whether abnormal GPR55 levels may account for defective mitochondrial energy production in RTT mouse brain should be performed.

Interestingly, the CBDV treatment provided different effects in different paradigms depending on the dose used. The social defect was in fact contrasted by the low and the intermediate dose of CBDV (2 and 20 mg/kg), whereas the defective general health status and motor coordination appeared more efficaciously contrasted by the high and the intermediate dose (20 and 100 mg/kg). Present results support the intermediate dose of 20 mg/kg as the most

efficacious and highlight the need for further studies aimed at clarifying the molecular mechanisms underlying CBDV beneficial effects on RTT symptomatology. In fact, similar differential effects of low and high doses have been already reported for other molecules, including CBD, that were explained by actions on different molecular pathways (Han et al., 2014; Kaplan et al., 2017).

In the present study, using early symptomatic RTT mice we were not able to detect some behavioural and molecular alterations in veh-injected RTT mice that were previously reported in this RTT mouse model (De Filippis et al., 2012, 2014). One explanation for such discrepancies may reside in the age of the experimental animals which were younger compared to previous experiments (5 months vs at least 7 months of age) (De Filippis et al., 2014). This is the case for the cognitive abilities of RTT mice in the Y maze test as well as brain neurotrophins levels and the phosphorylation level of rpS6. Indeed, these cognitive and molecular deficits have been reported at 7−8 months of age in this RTT mouse model compared to WT controls (De Filippis et al., 2014), but they have never been assessed at 5 months of age. In fact, most of the studies carried out so far in such RTT mouse model have focussed on clearly symptomatic mice (Moretti et al., 2006; Shahbazian et al., 2002) and only one study has addressed the progression of symptoms (De Filippis et al., 2010). Present results provide new relevant information regarding the progression of RTT-related behavioural and molecular abnormalities in MeCP2-308 mice (De Filippis et al., 2010) and highlight the importance of studies aimed at testing the potential value of innovative therapeutic strategies for RTT at different stages of the disease.

Increasing evidence suggests that modulation of neurotrophins, such as BDNF and IGF1, can improve RTT symptomatology and neuropathological signs in mouse models (Castro et al., 2014) and in patients (Katz, 2014; Pini et al., 2012). Besides this, numerous findings argue for a role of ECS in modulation of brain neurotrophin levels (Keimpema et al., 2014). Based on these evidences, we aimed at evaluating the effect of CBDV on the altered levels of relevant neurotrophins in the brain of RTT mice (Katz, 2014). In contrast to previous studies on older mice, in this study we could only identify abnormalities in the hippocampus of RTT mice concerning reduced NGF levels, which were not modulated by the CBDV treatment. Furthermore, no effects of the treatment on BDNF and IGF1 levels were evidenced. Even though we cannot exclude that the CBDV treatment might impact a defective BDNF/IGF1 signalling at an advanced stage of the disease, present results suggest that the reported phenotypic improvement by CBDV treatment in RTT mice at the tested age involves different signalling pathways.

We also evaluated CBDV treatment effects on the defects in mTOR/S6 activation known to be characteristic of RTT mouse brain (De Filippis et al., 2014; Ricciardi et al., 2011). Indeed, even though no studies have so far addressed CBDV effects on mTOR activation, this signalling pathway plays a crucial role in a number of neurodevelopmental disorders (Troca-Marín et al., 2012) and is critically involved in regulation of synaptic plasticity and memory processes (Costa-Mattioli et al., 2009). Moreover, previous reports suggest that ECS modulation can impact mTOR signalling (Busquets-Garcia et al., 2013; Puighermanal et al., 2012). Based on these evidences, we reasoned that the CBDV treatment may normalize the defective activation of the mTOR pathway in RTT mouse brain. Unfortunately, at this early symptomatic stage of the disease we did not find any defect in the phosphorylation level of the rpS6, a downstream target of mTOR and S6 kinase, in the brain of MeCP2-308 mice. This is consistent with the lack of cognitive defects in 5 month-old RTT mice we report in the present study. Present results do not allow us to exclude that the CBDV treatment might impact the defective mTOR pathway at a more advanced stage of the disease in the brain of RTT mice, thus restoring cognitive deficits.

## 5. Conclusions

No cure is currently available for patients suffering from RTT, a devastating neurodevelopmental disorder with a huge burden for families. Present data provide evidence that the CBDV treatment rescues several behavioural and phenotypic defects in a mouse model of RTT, thus representing a potential therapeutic approach for this disorder. Moreover, GPR55 was herein for the first time suggested to be a potential target for the treatment of RTT. Even though further studies are needed to clarify the mechanisms of action of CBDV, present data highlight for the first time the potential therapeutic efficacy of a molecule which bears a high translational value. CBDV is in fact currently under investigation in the clinical setting and is involved in a clinical trial in children affected by Autism Spectrum Disorders.

## Founding and disclosure

## Acknowledgements

## Appendix A. Supplementary data

Supplementary data related to this article can be found at https://doi.org/10.1016/j.neuropharm.2018.07.029.

## References

Anavi-Goffer, S., Baillie, G., Irving, A.J., Gertsch, J., Greig, I.R., Pertwee, R.G., Ross, R.A., 2012. Modulation of L-alpha-lysophosphatidylinositol/GPR55 mitogen-activated protein kinase (MAPK) signaling by cannabinoids. J. Biol. Chem. 287, 91—104.

Berrendero, F., Maldonado, R., 2002. Involvement of the opioid system in the anxiolytic-like effects induced by Delta(9)-tetrahydrocannabinol. Psychopharmacology (Berl) 163, 111—117.

Bittolo, T., Raminelli, C.A., Deiana, C., Baj, G., Vaghi, V., Ferrazzo, S., Bernareggi, A., Tongiorgi, E., 2016. Pharmacological treatment with mirtazapine rescues cortical atrophy and respiratory deficits in MeCP2 null mice. Sci. Rep. 6, 19796.

Bjursell, M., Ryberg, E., Wu, T., Greasley, P.J., Bohlooly, Y.M., Hjorth, S., 2016. Deletion of Gpr55 results in subtle effects on energy metabolism, motor activity and thermal pain sensation. PLoS One 11, e0167965.

Brodie, M.J., Ben-Menachem, E., 2018. Cannabinoids for epilepsy: what do we know and where do we go? Epilepsia 59, 291—296.

Busquets-Garcia, A., Gomis-Gonzalez, M., Guegan, T., Agustin-Pavon, C., Pastor, A., Mato, S., Perez-Samartin, A., Matute, C., de la Torre, R., Dierssen, M., Maldonado, R., Ozaita, A., 2013. Targeting the endocannabinoid system in the treatment of fragile X syndrome. Nat. Med. 19, 603—607.

Castro, J., Garcia, R.I., Kwok, S., Banerjee, A., Petravicz, J., Woodson, J., Mellios, N., Tropea, D., Sur, M., 2014. Functional recovery with recombinant human IGF1 treatment in a mouse model of Rett Syndrome. Proc. Natl. Acad. Sci. U. S. A. 111, 9941—9946.

Chakrabarti, B., Persico, A., Battista, N., Maccarrone, M., 2015. Endocannabinoid signaling in autism. Neurotherapeutics 12, 837—847.

Chang, Q., Khare, G., Dani, V., Nelson, S., Jaenisch, R., 2006. The disease progression of Mecp2 mutant mice is affected by the level of BDNF expression. Neuron 49, 341—348.

Cheng, D., Low, J.K., Logge, W., Garner, B., Karl, T., 2014. Chronic cannabidiol treatment improves social and object recognition in double transgenic APPswe/PS1E9 mice. Psychopharmacology (Berl) 231, 3009—3017.

Chiu, P., Olsen, D.M., Borys, H.K., Karler, R., Turkanis, S.A., 1979. The influence of cannabidiol and delta 9-tetrahydrocannabinol on cobalt epilepsy in rats. Epilepsia 20, 365—375.

Clarke, D.J., Stuart, J., McGregor, I.S., Arnold, J.C., 2017. Endocannabinoid dysregulation in cognitive and stress-related brain regions in the Nrg1 mouse model of schizophrenia. Prog. Neuro-Psychopharmacol. Biol. Psychiatry 72, 9—15.

Costa-Mattioli, M., Sossin, W.S., Klann, E., Sonenberg, N., 2009. Translational control

of long-lasting synaptic plasticity and memory. Neuron 61, 10—26.

De Filippis, B., Fabbri, A., Simone, D., Canese, R., Ricceri, L., Malchiodi-Albedi, F., Laviola, G., Fiorentini, C., 2012. Modulation of RhoGTPases improves the behavioral phenotype and reverses astrocytic deficits in a mouse model of Rett syndrome. Neuropsychopharmacology 37, 1152—1163.

De Filippis, B., Lyon, L., Taylor, A., Lane, T., Burnet, P.W., Harrison, P.J., Bannerman, D.M., 2015a. The role of group II metabotropic glutamate receptors in cognition and anxiety: comparative studies in GRM2(-/-), GRM3(-/-) and GRM2/3(-/-) knockout mice. Neuropharmacology 89, 19—32.

De Filippis, B., Musto, M., Altabella, L., Romano, E., Canese, R., Laviola, G., 2015b. Deficient purposeful use of forepaws in female mice modelling Rett syndrome. Neural Plast. 326184, 2015.

De Filippis, B., Nativio, P., Fabbri, A., Ricceri, L., Adriani, W., Lacivita, E., Leopoldo, M., Passarelli, F., Fuso, A., Laviola, G., 2014. Pharmacological stimulation of the brain serotonin receptor 7 as a novel therapeutic approach for Rett syndrome. Neuropsychopharmacology 39, 2506—2518.

De Filippis, B., Ricceri, L., Laviola, G., 2010. Early postnatal behavioral changes in the Mecp2-308 truncation mouse model of Rett syndrome. Genes Brain Behav. 9, 213—223.

De Filippis, B., Valenti, D., Chiodi, V., Ferrante, A., de Bari, L., Fiorentini, C., Domenici, M.R., Ricceri, L., Vacca, R.A., Fabbri, A., Laviola, G., 2015c. Modulation of Rho GTPases rescues brain mitochondrial dysfunction, cognitive deficits and aberrant synaptic plasticity in female mice modeling Rett syndrome. Eur. Neuropsychopharmacol 25, 889—901.

Devinsky, O., Cross, J.H., Laux, L., Marsh, E., Miller, I., Nabbout, R., Scheffer, I.E., Thiele, E.A., Wright, S., Cannabidiol in Dravet Syndrome Study, G., 2017. Trial of cannabidiol for drug-resistant seizures in the Dravet syndrome. N. Engl. J. Med. 376, 2011—2020.

Di Marzo, V., 2011. Endocannabinoid pathways and their role in multiple sclerosis-related muscular dysfunction. Expert Rev. Neurother. 11, 9—14.

Di Marzo, V., Stella, N., Zimmer, A., 2015. Endocannabinoid signalling and the deteriorating brain. Nat. Rev. Neurosci. 16, 30—42.

Dowie, M.J., Bradshaw, H.B., Howard, M.L., Nicholson, L.F., Faull, R.L., Hannan, A.J., Glass, M., 2009. Altered CB1 receptor and endocannabinoid levels precede motor symptom onset in a transgenic mouse model of Huntington's disease. Neuroscience 163, 456—465.

El Manira, A., Kyriakatos, A., 2010. The role of endocannabinoid signaling in motor control. Physiology 25, 230—238.

Fukuda, T., Itoh, M., Ichikawa, T., Washiyama, K., Goto, Y., 2005. Delayed maturation of neuronal architecture and synaptogenesis in cerebral cortex of Mecp2-deficient mice. J. Neuropathol. Exp. Neurol. 64, 537—544.

Geffrey, A.L., Pollack, S.F., Bruno, P.L., Thiele, E.A., 2015. Drug-drug interaction between clobazam and cannabidiol in children with refractory epilepsy. Epilepsia 56, 1246—1251.

Griebel, G., Stemmelin, J., Scatton, B., 2005. Effects of the cannabinoid CB1 receptor antagonist rimonabant in models of emotional reactivity in rodents. Biol. Psychiatr. 57, 261—267.

Guy, J., Cheval, H., Selfridge, J., Bird, A., 2011. The role of MeCP2 in the brain. Annu. Rev. Cell Dev. Biol. 27, 631—652.

Guy, J., Gan, J., Selfridge, J., Cobb, S., Bird, A., 2007. Reversal of neurological defects in a mouse model of Rett syndrome. Science 315, 1143—1147.

Guy, J., Hendrich, B., Holmes, M., Martin, J.E., Bird, A., 2001. A mouse Mecp2-null mutation causes neurological symptoms that mimic Rett syndrome. Nat. Genet. 27, 322—326.

Hagberg, B., 2002. Clinical manifestations and stages of Rett syndrome. Ment. Retard. Dev. Disabil. Res. Rev. 8, 61—65.

Hagberg, B., Hanefeld, F., Percy, A., Skjeldal, O., 2002. An update on clinically applicable diagnostic criteria in Rett syndrome. Comments to Rett syndrome clinical criteria consensus panel satellite to European paediatric neurology society meeting, baden baden, Germany, 11 september 2001. Eur. J. Paediatr. Neurol. 6, 293—297.

Han, S., Tai, C., Jones, C.J., Scheuer, T., Catterall, W.A., 2014. Enhancement of inhibitory neurotransmission by GABAA receptors having alpha2,3-subunits ameliorates behavioral deficits in a mouse model of autism. Neuron 81, 1282—1289.

Hill, A.J., Mercier, M.S., Hill, T.D., Glyn, S.E., Jones, N.A., Yamasaki, Y., Futamura, T., Duncan, M., Stott, C.G., Stephens, G.J., Williams, C.M., Whalley, B.J., 2012. Cannabidivarin is anticonvulsant in mouse and rat. Br. J. Pharmacol. 167, 1629—1642.

Iannotti, F.A., Hill, C.L., Leo, A., Alhusaini, A., Soubrane, C., Mazzarella, E., Russo, E., Whalley, B.J., Di Marzo, V., Stephens, G.J., 2014. Nonpsychotropic plant cannabinoids, cannabidivarin (CBDV) and cannabidiol (CBD), activate and desensitize transient receptor potential vanilloid 1 (TRPV1) channels in vitro: potential for the treatment of neuronal hyperexcitability. ACS Chem. Neurosci. 5, 1131—1141.

Jenniches, I., Ternes, S., Albayram, O., Otte, D.M., Bach, K., Bindila, L., Michel, K., Lutz, B., Bilkei-Gorzo, A., Zimmer, A., 2016. Anxiety, stress, and fear response in mice with reduced endocannabinoid levels. Biol. Psychiatr. 79, 858—868.

Jiang, W., Zhang, Y., Xiao, L., Van Cleemput, J., Ji, S.P., Bai, G., Zhang, X., 2005. Cannabinoids promote embryonic and adult hippocampus neurogenesis and produce anxiolytic- and antidepressant-like effects. J. Clin. Invest. 115, 3104—3116.

Jung, K.M., Sepers, M., Henstridge, C.M., Lassalle, O., Neuhofer, D., Martin, H., Ginger, M., Frick, A., DiPatrizio, N.V., Mackie, K., Katona, I., Piomelli, D., Manzoni, O.J., 2012. Uncoupling of the endocannabinoid signalling complex in a mouse model of fragile X syndrome. Nat. Commun. 3, 1080.

Kano, M., Ohno-Shosaku, T., Hashimotodani, Y., Uchigashima, M., Watanabe, M., 2009. Endocannabinoid-mediated control of synaptic transmission. Physiol.

Rev. 89, 309—380.

Kaplan, J.S., Stella, N., Catterall, W.A., Westenbroek, R.E., 2017. Cannabidiol attenuates seizures and social deficits in a mouse model of Dravet syndrome. Proc. Natl. Acad. Sci. U. S. A. 114, 11229—11234.

Katz, D.M., 2014. Brain-derived neurotrophic factor and Rett syndrome. Handb. Exp. Pharmacol. 220, 481—495.

Keimpema, E., Hokfelt, T., Harkany, T., Doherty, P., 2014. The molecular interplay between endocannabinoid and neurotrophin signals in the nervous system and beyond. Eur. J. Neurosci. 39, 334—343.

Kramar, C., Loureiro, M., Renard, J., Laviolette, S.R., 2017. Palmitoylethanolamide modulates GPR55 receptor signaling in the ventral Hippocampus to regulate mesolimbic dopamine activity, social interaction, and memory processing. Cannabis Cannabinoid Res. 2, 8—20.

Linge, R., Jimenez-Sanchez, L., Campa, L., Pilar-Cuellar, F., Vidal, R., Pazos, A., Adell, A., Diaz, A., 2016. Cannabidiol induces rapid-acting antidepressant-like effects and enhances cortical 5-HT/glutamate neurotransmission: role of 5-HT1A receptors. Neuropharmacology 103, 16—26.

Lyon, L., Burnet, P.W., Kew, J.N., Corti, C., Rawlins, J.N., Lane, T., De Filippis, B., Harrison, P.J., Bannerman, D.M., 2011. Fractionation of spatial memory in GRM2/3 (mGlu2/mGlu3) double knockout mice reveals a role for group II metabotropic glutamate receptors at the interface between arousal and cognition. Neuropsychopharmacology 36, 2616—2628.

Maezawa, I., Swanberg, S., Harvey, D., LaSalle, J.M., Jin, L.W., 2009. Rett syndrome astrocytes are abnormal and spread MeCP2 deficiency through gap junctions. J. Neurosci. 29, 5051—5061.

Marco, E.M., Rapino, C., Caprioli, A., Borsini, F., Laviola, G., Maccarrone, M., 2015. Potential therapeutic value of a novel FAAH inhibitor for the treatment of anxiety. PLoS One 10, e0137034.

Marichal-Cancino, B.A., Fajardo-Valdez, A., Ruiz-Contreras, A.E., Mendez-Diaz, M., Prospero-Garcia, O., 2017. Advances in the physiology of GPR55 in the central nervous system. Curr. Neuropharmacol. 15, 771—778.

Marichal-Cancino, B.A., Fajardo-Valdez, A., Ruiz-Contreras, A.E., Mendez-Diaz, M., Prospero-Garcia, O., 2018. Possible role of hippocampal GPR55 in spatial learning and memory in rats. Acta Neurobiol. Exp. 78, 41—50.

Maroof, N., Ravipati, S., Pardon, M.C., Barrett, D.A., Kendall, D.A., 2014. Reductions in endocannabinoid levels and enhanced coupling of cannabinoid receptors in the striatum are accompanied by cognitive impairments in the AbetaPPswe/PS1DeltaE9 mouse model of Alzheimer's disease. J. Alzheimers Dis. 42, 227—245.

Micale, V., Di Marzo, V., Sulcova, A., Wotjak, C.T., Drago, F., 2013. Endocannabinoid system and mood disorders: priming a target for new therapies. Pharmacol. Ther. 138, 18—37.

Morales, P., Hurst, D.P., Reggio, P.H., 2017. Molecular targets of the phytocannabinoids: a complex picture. Prog. Chem. Org. Nat. Prod. 103, 103—131.

Morel, A., Demily, C., 2017. Social cognition in children with neurogenetic syndromes: a literature review. Arch. Pediatr. 24, 757—765.

Moretti, P., Levenson, J.M., Battaglia, F., Atkinson, R., Teague, R., Antalffy, B., Armstrong, D., Arancio, O., Sweatt, J.D., Zoghbi, H.Y., 2006. Learning and memory and synaptic plasticity are impaired in a mouse model of Rett syndrome. J. Neurosci. 26, 319.

Njoo, C., Agarwal, N., Lutz, B., Kuner, R., 2015. The cannabinoid receptor CB1 interacts with the WAVE1 complex and plays a role in actin dynamics and structural plasticity in neurons. PLoS Biol. 13, e1002286.

Patel, S., Rademacher, D.J., Hillard, C.J., 2003. Differential regulation of the endocannabinoids anandamide and 2-arachidonylglycerol within the limbic forebrain by dopamine receptor activity. J. Pharmacol. Exp. Therapeut. 306, 880—888.

Pini, G., Scusa, M.F., Congiu, L., Benincasa, A., Morescalchi, P., Bottiglioni, I., Di Marco, P., Borelli, P., Bonuccelli, U., Della-Chiesa, A., Prina-Mello, A., Tropea, D., 2012. IGF1 as a potential treatment for Rett syndrome: safety assessment in six Rett patients. Autism Res. Treat 2012, 679801.

Pisani, V., Madeo, G., Tassone, A., Sciamanna, G., Maccarrone, M., Stanzione, P., Pisani, A., 2011. Homeostatic changes of the endocannabinoid system in Parkinson's disease. Mov. Disord. 26, 216—222.

Puighermanal, E., Busquets-Garcia, A., Maldonado, R., Ozaita, A., 2012. Cellular and intracellular mechanisms involved in the cognitive impairment of cannabinoids. Philos. Trans. R. Soc. Lond. B Biol. Sci. 367, 3254—3263.

Rett, A., 1966. On a unusual brain atrophy syndrome in hyperammonemia in childhood. Wien Med. Wochenschr. 116, 723—726.

Ricceri, L., De Filippis, B., Fuso, A., Laviola, G., 2011. Cholinergic hypofunction in MeCP2-308 mice: beneficial neurobehavioural effects of neonatal choline supplementation. Behav. Brain Res. 221, 623—629.

Ricceri, L., De Filippis, B., Laviola, G., 2012. Rett syndrome treatment in mouse models: searching for effective targets and strategies. Neuropharmacology 68, 106—115.

Ricciardi, S., Boggio, E.M., Grosso, S., Lonetti, G., Forlani, G., Stefanelli, G., Calcagno, E., Morello, N., Landsberger, N., Biffo, S., Pizzorusso, T., Giustetto, M., Broccoli, V., 2011. Reduced AKT/mTOR signaling and protein synthesis dysregulation in a Rett syndrome animal model. Hum. Mol. Genet. 20, 1182—1196.

Roland, A.B., Ricobaraza, A., Carrel, D., Jordan, B.M., Rico, F., Simon, A., Humbert-Claude, M., Ferrier, J., McFadden, M.H., Scheuring, S., Lenkei, Z., 2014. Cannabinoid-induced actomyosin contractility shapes neuronal morphology and growth. Elife 3, e03159.

Sanderson, D.J., Gray, A., Simon, A., Taylor, A.M., Deacon, R.M., Seeburg, P.H., Sprengel, R., Good, M.A., Rawlins, J.N., Bannerman, D.M., 2007. Deletion of glutamate receptor-A (GluR-A) AMPA receptor subunits impairs one-trial spatial memory. Behav. Neurosci. 121, 559—569.

Shahbazian, M.D., Young, J.I., Yuva-Paylor, L.A., Spencer, C.M., Antalffy, B.A., Noebels, J.L., Armstrong, D.L., Paylor, R., Zoghbi, H.Y., 2002. Mice with truncated MeCP2 recapitulate many Rett syndrome features and display hyperacetylation of histone H3. Neuron 35, 243—254.

Simcocks, A.C., O'Keefe, L., Jenkin, K.A., Mathai, M.L., Hryciw, D.H., McAinch, A.J., 2014. A potential role for GPR55 in the regulation of energy homeostasis. Drug Discov. Today 19, 1145—1151.

Smith, S.E., Li, J., Garbett, K., Mirnics, K., Patterson, P.H., 2007. Maternal immune activation alters fetal brain development through interleukin-6. J. Neurosci. 27, 10695—10702.

Stahlhut, M., Downs, J., Leonard, H., Bisgaard, A.M., Nordmark, E., 2017. Building the repertoire of measures of walking in Rett syndrome. Disabil. Rehabil. 39, 1926—1931.

Troca-Marín, J.A., Alves-Sampaio, A., Montesinos, M.L., 2012. Deregulated mTOR-mediated translation in intellectual disability. Prog. Neurobiol. 96, 268—282.

Turner, S.E., Williams, C.M., Iversen, L., Whalley, B.J., 2017. Molecular pharmacology of phytocannabinoids. Prog. Chem. Org. Nat. Prod. 103, 61—101.

Valenti, D., de Bari, L., Vigli, D., Lacivita, E., Leopoldo, M., Laviola, G., Vacca, R.A., De Filippis, B., 2017. Stimulation of the brain serotonin receptor 7 rescues mitochondrial dysfunction in female mice from two models of Rett syndrome. Neuropharmacology 121, 79—88.

Viveros, M.P., Marco, E.M., File, S.E., 2005. Endocannabinoid system and stress and anxiety responses. Pharmacol. Biochem. Behav. 81, 331—342.

Wei, D., Allsop, S., Tye, K., Piomelli, D., 2017. Endocannabinoid signaling in the control of social behavior. Trends Neurosci. 40, 385—396.

Wilcox, R.R., 1987. New designs in analysis of variance. Annu. Rev. Psychol. 38, 29—60.

Woods, R., Vallero, R.O., Golub, M.S., Suarez, J.K., Ta, T.A., Yasui, D.H., Chi, L.H., Kostyniak, P.J., Pessah, I.N., Berman, R.F., LaSalle, J.M., 2012. Long-lived epigenetic interactions between perinatal PBDE exposure and Mecp2308 mutation. Hum. Mol. Genet. 21, 2399—2411.

Zhou, H., Wu, W., Zhang, Y., He, H., Yuan, Z., Zhu, Z., Zhao, Z., 2017. Selective preservation of cholinergic MeCP2 rescues specific Rett-syndrome-like phenotypes in MeCP2stop mice. Behav. Brain Res. 322, Part A 51—59.
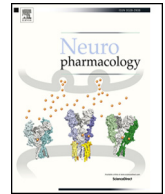
# Rescue of prepulse inhibition deficit and brain mitochondrial dysfunction by pharmacological stimulation of the central serotonin receptor 7 in a mouse model of CDKL5 Deficiency Disorder

Daniele Vigli[a], Laura Rusconi[b], Daniela Valenti[c], Paolo La Montanara[b], Livia Cosentino[a], Enza Lacivita[d], Marcello Leopoldo[d], Elena Amendola[e], Cornelius Gross[f], Nicoletta Landsberger[g], Giovanni Laviola[a], Charlotte Kilstrup-Nielsen[b], Rosa A. Vacca[c], Bianca De Filippis[a],*

[a] Center for Behavioral Sciences and Mental Health, Istituto Superiore di Sanità, 00161 Rome, Italy
[b] Department of Biotechnology and Life Sciences and Center of Neuroscience, University of Insubria, 21052 Busto Arsizio, Italy
[c] Institute of Biomembranes, Bioenergetics and Molecular Biotechnologies, National Council of Research, 70126 Bari, Italy
[d] Dept. Pharmacy, University of Bari "Aldo Moro", 70125 Bari, Italy
[e] Molecular Medicine and Medical Biotechnologies, University of Naples "Federico II", 80131 Napoli, Italy
[f] Mouse Biology Unit, European Molecular Biology Laboratory (EMBL) 00015 Monterotondo, Italy
[g] Department of Medical Biotechnology and Translational Medicine, University of Milan, 20090 Segrate, Italy

## HIGHLIGHTS

- Characterization of behavioural phenotype in fully symptomatic *Cdkl5*-null mice.
- The 5HT7R agonist LP-211 normalizes prepulse inhibition defects in *Cdkl5*-null mice.
- LP-211 treatment rescues brain mitochondrial dysfunction in *Cdkl5*-null mice.
- The abnormal phosphorylation of rpS6 in *Cdkl5*-null cortex is restored by LP-211.

## ABSTRACT

Mutations in the X-linked *cyclin-dependent kinase-like 5* (*CDKL5*) gene cause CDKL5 Deficiency Disorder (CDD), a rare neurodevelopmental syndrome characterized by severe behavioural and physiological symptoms. No cure is available for CDD. CDKL5 is a kinase that is abundantly expressed in the brain and plays a critical role in neurodevelopmental processes, such as neuronal morphogenesis and plasticity. This study provides the first characterization of the neurobehavioural phenotype of 1 year old *Cdkl5*-null mice and demonstrates that stimulation of the serotonin receptor 7 (5-HT$_7$R) with the agonist molecule LP-211 (0.25 mg/kg once/day for 7 days) partially rescues the abnormal phenotype and brain molecular alterations in *Cdkl5*-null male mice. In particular, LP-211 treatment completely normalizes the prepulse inhibition defects observed in *Cdkl5*-null mice and, at a molecular level, restores the abnormal cortical phosphorylation of rpS6, a downstream target of mTOR and S6 kinase, which plays a direct role in regulating protein synthesis. Moreover, we demonstrate for the first time that mitochondria show prominent functional abnormalities in *Cdkl5*-null mouse brains that can be restored by pharmacological stimulation of brain 5-HT$_7$R.

## 1. Introduction

CDKL5 Deficiency Disorder (CDD) (OMIM #300672) is a rare neuropathological condition that is caused by mutations in the X-linked *cyclin-dependent kinase-like 5* (*CDKL5*) gene (Kalscheuer et al., 2003). This disorder is characterized by a variety of behavioural and physiological symptoms that include the onset of seizures in the first months of life, severe global developmental delay resulting in intellectual disability (ID) and poor motor control, and the presence of peculiar hand

stereotypies (Bahi-Buisson et al., 2008; Fehr et al., 2016). No cure exists for patients affected by CDD.

*CDKL5* encodes a serine/threonine kinase expressed in various tissues, with the brain showing the highest levels of expression (Rusconi et al., 2008; Kilstrup-Nielsen et al., 2012). Available data point to a crucial role of Cdkl5 in fundamental neurodevelopmental processes such as activity-dependent regulation of neuronal morphogenesis and plasticity (Fuchs et al., 2014; Zhou et al., 2017). These processes require a fine-tune regulation of Cdkl5 localization in neurons, with the

shuttling between the cytoplasm and the nucleus being regulated by the activation of extra-synaptic NMDA receptors (Rusconi et al., 2011), and protein localization on the post-synaptic side of excitatory synapses being regulated by the association of the kinase with PSD-95 (Ricciardi et al., 2012). These neuronal alterations are accompanied by a number of behavioural deficits in mice lacking Cdkl5, including motor dysfunction, autistic-like behaviours and memory deficits (Jhang et al., 2017; Okuda et al., 2018).

The serotonin receptor 7 (5-HT$_7$R) is a G protein-coupled receptor broadly expressed in the central nervous system that is involved in a variety of neurophysiological phenomena relevant for CDD, such as sleep, cognitive processes and synaptic plasticity (Hedlund et al., 2003; Cifariello et al., 2008; Matthys et al., 2011). Pharmacological stimulation of the 5-HT$_7$R by the brain penetrant agonist LP-211 has provided promising results in preclinical studies for disorders associated with syndromic IDs, such as Fragile X syndrome and Rett syndrome (RTT) (Costa et al., 2012; De Filippis et al., 2014a, 2015b). Of note, the beneficial effects of LP-211 treatment extend beyond intellectual deficits and impact other domains, such as motor function and autistic-like behaviours in a mouse model of RTT (De Filippis et al., 2014a, 2015b), a syndrome that presents several symptoms in common with CDD (Fehr et al., 2013). Moreover, 5-HT$_7$R stimulation by LP-211 impacts a number of behavioural domains and molecular pathways that have been demonstrated to be altered in Cdkl5-null mouse brain and in induced-pluripotent stem cell (iPSCs)-derived neurons from CDKL5 patients (Ricciardi et al., 2012; Amendola et al., 2014), as it promotes a rearrangement of neuronal morphology, facilitates synaptogenesis and modulates the activation of the Akt/mTOR/S6 pathway (De Filippis et al., 2014a; Speranza et al., 2017).

Based on these pieces of evidence, in the present study we evaluated whether the stimulation of 5-HT$_7$R might represent a potential therapeutic approach for CDD. To test this hypothesis, 9–12-months old Cdkl5-null male mice and wild-type littermate controls received a repeated systemic intraperitoneal (i.p.) treatment with LP-211 (0.25 mg/kg once/day for 7 days) (De Filippis et al., 2015b). We reasoned that the translational relevance of the treatment under investigation might be increased if the relief of symptoms was demonstrated at an advanced and more severely affected stage of the disease (1-year-old mice). Male mice were used based on clinical evidences of CDD in males (Elia et al., 2008) and on the effects of mosaic CDKL5 expression due to random X-chromosome inactivation in females. To evaluate therapeutic efficacy, a battery of behavioural analyses was carried out at the end of the treatment specifically tailored to detect CDD-related behavioural alterations. Behavioural testing started at least 7 days after the end of the i.p. treatment and the brains of the experimental mice were collected two months after the last i.p. injection, based on previous data suggesting long-term effects of a seven-day-long treatment with LP-211 (De Filippis et al., 2015b).

In the brain of Cdkl5-null mice treated with either LP-211 or vehicle, Rac1 activation and mitochondrial functionality were evaluated, since recent data suggest a role for 5-HT$_7$R in the activation of brain Rho GTPases and in the regulation of the oxidative phosphorylation (OXPHOS) apparatus, the mitochondrial molecular machinery responsible for the majority of cell energy production (De Filippis et al., 2015a, 2015d; Valenti et al., 2017), central players in several pathological conditions associated with ID (De Filippis et al., 2014b; Valenti et al., 2014). We also verified whether the expression and the activation of Rho GTPase-dependent pathways are abnormal in Cdkl5-null mouse brain and LP-211 treatment effects thereon, based on previous data pointing to a pathogenic role of a disrupted interaction between Cdkl5 and the Rho GTPases Rac1 (Chen et al., 2010; Barbiero et al., 2017). In particular, we explored whether the LP-211 treatment impacts group I PAKs, the leading molecules by which Rho GTPases affect actin cytoskeleton dynamics (De Filippis et al., 2014b), and the activation of the rpS6 and its upstream regulator Akt, a pathway that is modulated by Rho GTPases and is involved in protein synthesis (Ricciardi et al., 2011;

De Filippis et al., 2014a).

## 2. Materials and methods

### 2.1. Subjects

The experimental subjects were 9–12-months old Cdkl5-null male mice and wild-type littermates (wt) backcrossed to C57BL/6N mice for at least 10 generations (Amendola et al., 2014). Experimental mice were obtained by crossing Cdkl5 heterozygous ( − / + ) female mice and wt male mice and weaned at postnatal day 25. After weaning, mice were housed according to sex in groups of two or three in polycarbonate transparent cages (33 × 13 × 14 cm) with sawdust bedding and kept on a 12-h light-dark schedule (lights off at 8:00 am). Temperature was maintained at 21 ± 1 °C and relative humidity at 60 ± 10%. Animals were provided *ad libitum* with tap water and a complete pellet diet (Altromin, 1324 - 10 mm pellets, Germany). All experimental procedures were conducted in conformity with the European Directive 2010/63/EU and the Italian legislation on animal experimentation, D.Lgs. 26/2014.

### 2.2. Genotyping

DNA has been prepared from a small tail-tip biopsy taken at weaning, as previously described (De Filippis et al., 2014a). The Cdkl5 alleles have been identified by PCR using two sets of primers (for further details see Supplementary materials). PCR products were electrophoresed through a 2% NuSieve 3:1 agarose gel (Cambrex Bio Science, Rockland, ME, USA) containing 0.1 μl/ml GelRed™ and examined under UV light.

### 2.3. Drug and treatment

LP-211 was prepared following the same synthetic procedure described in (Leopoldo et al., 2008). The compound, which has a half-life 65 min, was dissolved in a vehicle solution of 1% dimethyl sulfoxide (DMSO) in saline (0.9% NaCl). Cdkl5-null mice and wt littermate controls were randomly assigned to be daily i.p. injected (between 9.00 and 11.00 a.m.) for 7 consecutive days with either LP-211 (0.25 mg/kg) or vehicle (1% of DMSO in saline).

### 2.4. Behavioural testing

A comprehensive test battery was carried out aimed at assessing treatment effects on the behavioural domains that are compromised in CDD. The selection of the tests to be performed was based on previous literature addressing the neurobehavioural phenotype of Cdkl5-*null* mice (Amendola et al., 2014; Okuda et al., 2018) and on our lasting experience on the study of mouse models of RTT, a syndrome that has many symptoms in common with CDD (De Filippis et al., 2010, 2015c). Mice were experimentally naïve at the start of the behavioural test battery. All behavioural testing took place during the dark phase of the L/D cycle, between 9.00 a.m. and 3.00 p.m., and was carried out by experimenters blind to the mouse genotypes. A minimum of 24 h was left between tests.

#### 2.4.1. Prepulse inhibition (PPI) paradigm

Sensorimotor gating was evaluated 7 days after the last i.p. with the prepulse inhibition (PPI) paradigm (Swerdlow et al., 2001). The apparatus consisted of two Plexiglas rectangular boxes (startle cages) (9 × 7 cm), placed in sound-attenuated chambers with a red light and a fan ventilator (Med associates inc. St Albans, VT, United States of America). Background white (62 db) noise and acoustic bursts were conveyed by two separate speakers, properly spaced from the startle cage so as to produce a fine-tuned regulation of sound. Both speakers and startle cages were connected to a main PC computer, which

detected and analyzed all chamber variables by means of a specific software. Two slightly different protocols were adopted on two cohorts of mice, that differed in the range of prepulse intensities under investigation. On the first cohort of mice, prepulse intensities were as follows: 67, 70, 73 or 76 db (Macri et al., 2015). On the second cohort, 78, 82 or 84 dB pre-pulse intensities were applied (Chao et al., 2010). To evaluate sensorimotor gating capabilities in Cdkl5-*null* mice, the % PPI was calculated as follows: (100-[(mean startle amplitude for pre-pulse + pulse trials/mean startle amplitude for pulse-alone trials) x 100]) (for further details see Supplementary materials).

### 2.4.2. General health score

The general health of the experimental mice was qualitatively evaluated 1 and 28 days after the last injection, by a trained observer, blind to the genotype of the experimental mice, according to a method that has been developed to assess the health status of RTT mice (Guy et al., 2007; De Filippis et al., 2014a). Briefly, mice received a score (ranging from 0 – normal appearance-to 4- highly compromised) for each of the following parameters: gait, mobility, breathing, kyphosis, fur, hind limb clasping, tremors and general conditions. The individual scores for each category were subsequently averaged to obtain a semi-quantitative measure of the general health status.

### 2.4.3. Nest building evaluation

Nest building ability was scored 21 days from the last i.p. injection to assess purposeful and coordinated forepaw use to unravel whether *Cdkl5*-null mice display alterations and LP-211 effects thereon, as previously described (De Filippis et al., 2015a). The quality of the nests was evaluated 24 h after nest material provision (for further details see Supplementary materials).

### 2.4.4. Home cage locomotor activity

To verify whether LP-211 treatment affects the daily locomotor activity in *Cdkl5*-null mice, spontaneous locomotor activity in the home-cages was evaluated 33 days after the last i.p. injection. Levels of activity were monitored continuously by means of an automatic device using small passive infrared sensors positioned on the top of each cage (ACTIVISCOPE system, NewBehaviour Inc., Zurich, Switzerland) as previously described (De Filippis et al., 2013) (for further details see Supplementary materials). To avoid confounding effects due to cage clean procedures and/or room entrances, the analysis was performed during two 6-h intervals, during the dark and the light phase, in which animals were left undisturbed.

### 2.4.5. Open field test

Locomotor activity was assessed in the Open Field test 30 days after the last i.p injection, to complement the home-cage recording (Ricceri et al., 2011) (for further details see Supplementary materials).

### 2.4.6. Fear conditioning task

The fear conditioning task was carried out 14 days after the last i.p. injection to evaluate cognitive abilities in *Cdkl5*-null mice and LP-211 effect thereon (Wang et al., 2012). An automated system was used (UgoBasile S.R.L.), which consisted in a soundproof cubic apparatus with inside a mouse cage (21(d) x 24(w) x 30(h) cm) with electrified grid floor. The task consisted of a two-days-long protocol in which freezing frequency and duration were measured with an automatic freezing detector (UgoBasile S.R.L.). Throughout the task, mice were exposed to a white noise (WN- 60 db, 2000 Hz). On the first day (training), animals were placed in the fear conditioning apparatus for 180s (baseline, BL) and then exposed for three times to the acoustic conditioned stimulus (CS; 2000 Hz–68 db, 30s). Each CS on the first day was paired with a 0.7 mA shock released during the last 2s (unconditioned stimulus; US). A 95s inter trial interval (ITI) was used. On the second day(test), mice were placed in the same chamber and, after a 180s BL, were exposed to fifteen trials consisting in 30s of CS plus 10s of

ITI. Contextual fear memory was established by measuring the time spent in freezing behaviour during the baseline on the testing day compared to levels shown during the baseline on the training day. Freezing behaviour in response to the CSs on the test day was also evaluated. Before the starting of each session the grid floor of the apparatus was cleaned with 70% ethanol.

### 2.5. Neurobiological analyses

Two months after the last i.p. injection, the brains of the experimental mice were dissected and cortices, a behaviourally relevant brain area in which 5-HT$_7$R (Hedlund, 2009) and Cdkl5 (Wang et al., 2012) are highly expressed, were immediately frozen in dry ice for G-LISA Assay and western blot analyses (De Filippis et al., 2015b).

For mitochondrial analyses, the hemispheres from additional subjects were cryopreserved, as previously described (Valenti et al., 2017). Previous data in fact demonstrate that cryopreserved brain tissues show mitochondrial membrane potential, outer and inner membrane integrity and mitochondrial ATP production capacity comparable to mitochondria isolated from fresh brains (Valenti et al., 2014).

#### 2.5.1. RAC-1 G-LISA assay

Rac1 G-Lisa Activation Assay BiochemkitTM (Cytoskeleton, Denver, CO) (n = 4–5) was used to measure Rac1 activity in mouse cortices according to the manufacturer's recommendations.

#### 2.5.2. Western blot analysis

Cortices were homogenized in lysis buffer and centrifuged. Then the supernatant was collected and the protein content was quantified by bicinchonic acid assay. For western blotting analysis, 20 μg of total proteins were separated on a 12% SDS-PAGE and membranes incubated with the appropriate primary and secondary antibodies. Images of the membranes were acquired by a CCD camera (Syngene, G-Box Chemi XRQ) and optical densities (O.D.) of the protein signals calculated for each sample with Image J software and normalized with the corresponding housekeeping signal (Fig. 4 A, C); the O.D. ratios were then compared and expressed as the average fold increase, with 1 (wt control) as baseline (for further details see Supplementary materials).

#### 2.5.3. Mitochondrial analysis

*Measurement of mitochondrial respiratory chain complex (MRC) activities.* MRC activities were evaluated in mitochondrial membrane-enriched fractions obtained from isolated mitochondria. Measurement of MRC complex activities were performed essentially as in (Manente et al., 2013), by three assays which rely on the sequential addition of reagents to measure the activities of: i) NADH: ubiquinone oxidoreductase (complex I) followed by ATP synthase (complex V), ii) succinate: ubiquinone oxidoreductase (complex II) and iii) cytochrome c oxidase (complex IV) followed by cytochrome c oxidoreductase (complex III) (for further details see Supplementary materials).

*Measurement of mitochondrial ATP production rate.* The rate of ATP production by OXPHOS was determined in isolated mitochondria, as previously described in (Valenti et al., 2010) (for further details see Supplementary materials).

*Measurement of mouse brain ATP levels.* Half brain was weighted (approx. 20 mg) and subjected to perchloric acid extraction as described in (Khan, 2003) (for further details see Supplementary materials). The amount of tissue ATP was determined enzymatically in KOH neutralized extracts, as described in (Valenti et al., 2010).

### 2.6. Statistical analysis

Data were analyzed using the ANOVA model, including genotype and treatment as between-subjects factors, or applying repeated measures ANOVAs if there was a within-subjects factor, using Statview vers. 5.0 (Sas, Institute Inc., Cary, NC). The alpha level was set to 5%. To
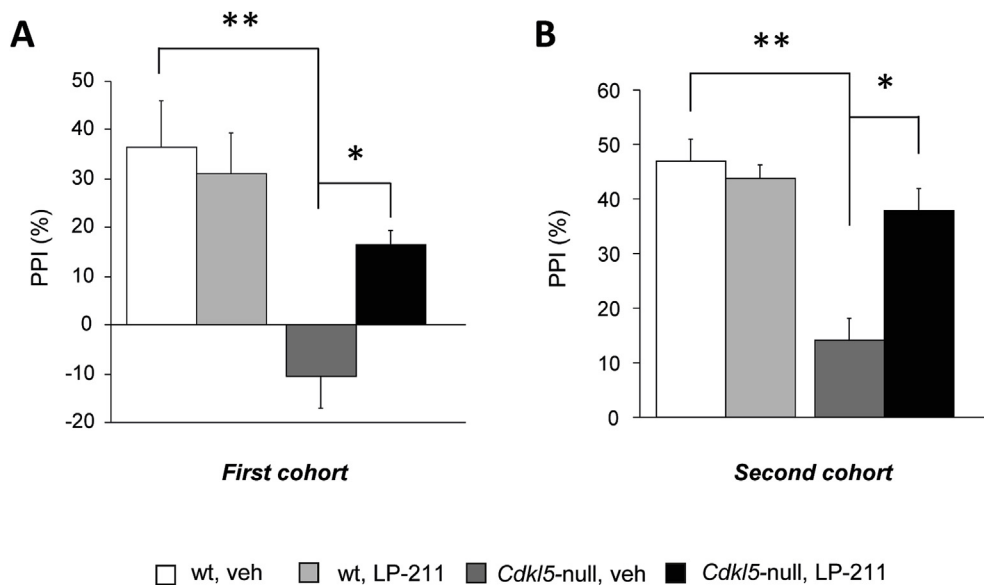
**Fig. 1. LP-211 treatment selectively rescues prepulse inhibition (PPI) deficit in *Cdkl5*-null mice at an advanced stage of the disease.** PPI evaluation was carried out on two cohorts of animals using protocols adopting different ranges of prepulse intensities; (**A-B**) *Cdkl5*-null mice show a severe impairment in PPI compared to wt mice. LP-211 treatment rescues the abnormal sensory motor gating in *Cdkl5*-null mice (cohort 1: wt, Veh = 4; wt, LP-211 = 7; *Cdkl5*-null, Veh = 8; *Cdkl5*-null, LP-211 = 9; cohort 2: wt, Veh = 11; wt, LP-211 = 12; *Cdkl5*-null, Veh = 7; *Cdkl5*-null, LP-211 = 7). The histograms show the average of all prepulse intensities. Data are mean ± SEM. Statistical significance was calculated by two-way ANOVA. **p < 0,01; *p < 0,05 after Tukey's *post-hoc* tests.

□ wt, veh   ◻ wt, LP-211   ◼ *Cdkl5*-null, veh   ■ *Cdkl5*-null, LP-211

unravel the presence of outliers, the Grubbs' test was applied. *Post-hoc* comparisons were performed using Tukey HSD (Wilcox, 1987).

## 3. Results

### 3.1. LP-211 treatment selectively rescues PPI deficit in mice lacking Cdkl5 at an advanced stage of the disease

To evaluate the efficacy of the LP-211 treatment for CDD, a broad test battery was carried out.

*Prepulse inhibition (PPI).* The evaluation of the sensorimotor gating showed significant deficits in PPI capacity in *Cdkl5*-null mice compared to wild–type (wt) controls, in the absence of changes in the acoustic startle response (see Fig. S1 A-B). This genotype effect was replicated on two cohorts of animals using protocols adopting different ranges of prepulse intensities [Fig. 1A cohort 1: Genotype*Treatment interaction: F (1,22) = 12.2, p = 0.021; *post-hoc:* p < 0.01; Fig. 1B cohort 2: Genotype*Treatment interaction: F (1,33) = 7.3, p = 0.011; *post-hoc*: p < 0.01].The LP-211 treatment significantly improved this abnormal behaviour in *Cdkl5*-null mice compared to vehicle (veh)-treated *Cdkl5*-null mice in both cohorts of animals [Fig. 1A, Genotype*Treatment; *post-hoc*: p < 0.01; Fig. 1B; Genotype*Treatment; *post-hoc:* p < 0.05]. No significant prepulses intensities*genotype*treatment interactions were found (Fig. S1 C-D).

*General health status.* We found that fully symptomatic *Cdkl5*-null mice showed worse general health conditions in comparison to wt mice [Fig. 2A; Genotype: F (1,35) = 7.8; p = 0.008]. The LP-211 treatment did not significantly improve general health status in *Cdkl5*-null mice (Fig. 2A). No differences between the first and the second evaluation (1 and 28 days from the last i.p.), and no interaction of the repeated measures with genotype and treatment were found. Fig. 2A represents the genotype*treatment interaction, in which the general health scores obtained at 1 and 28 days after the last i.p. injections were averaged.

*Nest building ability.* Nest building ability was slightly, but significantly impaired in *Cdkl5*-null mice in comparison to wt controls [Genotype: F (1,35) = 4.9; p = 0.032], thus confirming defective co-ordination of forepaws (De Filippis et al., 2015a; Fuchs et al., 2018b). The LP-211 treatment did not affect the quality of the nests built by *Cdkl5*-null mice (wt veh: 2.3 ± 1.2; *Cdkl5*-null veh: 1.8 ± 1.4; wt LP-211: 2.5 ± 1.2; *Cdkl5*-null LP-211: 1.3 ± 1.0).

*Home cage locomotor activity.* The evaluation of spontaneous home cage locomotor activity highlighted a hypoactive profile in *Cdkl5*-null mice compared to wt controls, as demonstrated by the lower number of

beam breaks they performed during the dark/active phase of the Light/ Dark cycle [Fig. 2B; Phase*Genotype*Treatment interaction: F (1,28) = 3.3; p = 0.082; *post-hoc:* p < 0.05]. The LP-211 treatment did not affect the abnormal locomotor profile shown by *Cdkl5*-null mice in the home cage.

*Open field test.* We found that *Cdkl5*-null mice show hyperactivity when exposed to a novel environment compared to wt controls, as demonstrated by the increased distance they moved in the open field [Fig. 2C; Genotype: F (1,33) = 13.6; p < 0.001] as well as the number of entrances in the central zone of the arena [Genotype: F (1,33) = 5.9, p < 0.021]. Increased locomotion was confirmed throughout the 60-min Open Field test, with no differences between the initial and the last 5-min blocks (Fig. S2). LP-211 treatment did not exert any effects on the total distance moved (Fig. 2C) as well as the number of entrances in the central zone of the arena (wt veh:191.5 ± 65.1; *Cdkl5*-null mice veh: 222.4 ± 83.9; wt LP-211: 176.6 ± 55.2; *Cdkl5*-null mice LP-211: 252.6 ± 60.7). No difference between *Cdkl5*-null mice and wt controls was found in time spent in the central/intimidating zone of the arena, an index of anxiety-like behaviours (*data not shown*).

*Fear conditioning test.* Defective contextual fear memory was found in *Cdkl5*-null mice, as demonstrated by the reduced freezing levels they displayed compared to wt controls when exposed to the context in which they received the footshock on the previous day [Fig. 2D; Day*Genotype*Treatment interaction: F (1,35) = 3.1; p = 0.086; *post-hoc:* p < 0.01]; no significant LP-211 treatment effect was highlighted on this hippocampus-dependent cognitive deficit. Reduced freezing in response to the presentation of the 15 CSs on the second day of testing compared to wt controls was also evident in *Cdkl5*-null mice [Genotype: F (1,35) = 11.6; p < 0.001]. The LP-211 treatment did not improve this abnormal freezing response shown by *Cdkl5*-null mice (wt veh:27.9 ± 10.2; *Cdkl5*-null mice veh: 16.3 ± 12.0; wt LP-211: 24.1 ± 11.8; *Cdkl5*-null mice LP-211: 16.5 ± 12.8).

### 3.2. The LP-211 treatment activates Rac1 and rescues the abnormal activation of rpS6 in the cortex of Cdkl5-null mice

Based on available data suggesting that Rac1 signaling may be defective in CDD (Chen et al., 2010), the activation of Rac1 and of the Rho GTPases downstream molecules PAKs and rpS6 was evaluated in *Cdkl5*-null mouse cortex, to verify whether they are abnormal and whether pharmacological stimulation of the 5-HT$_7$R may recover them.

*Rac1 activation.* No genotype difference was found in the activation of Rac1 in *Cdkl5*-null mouse cortex. The LP-211 treatment significantly
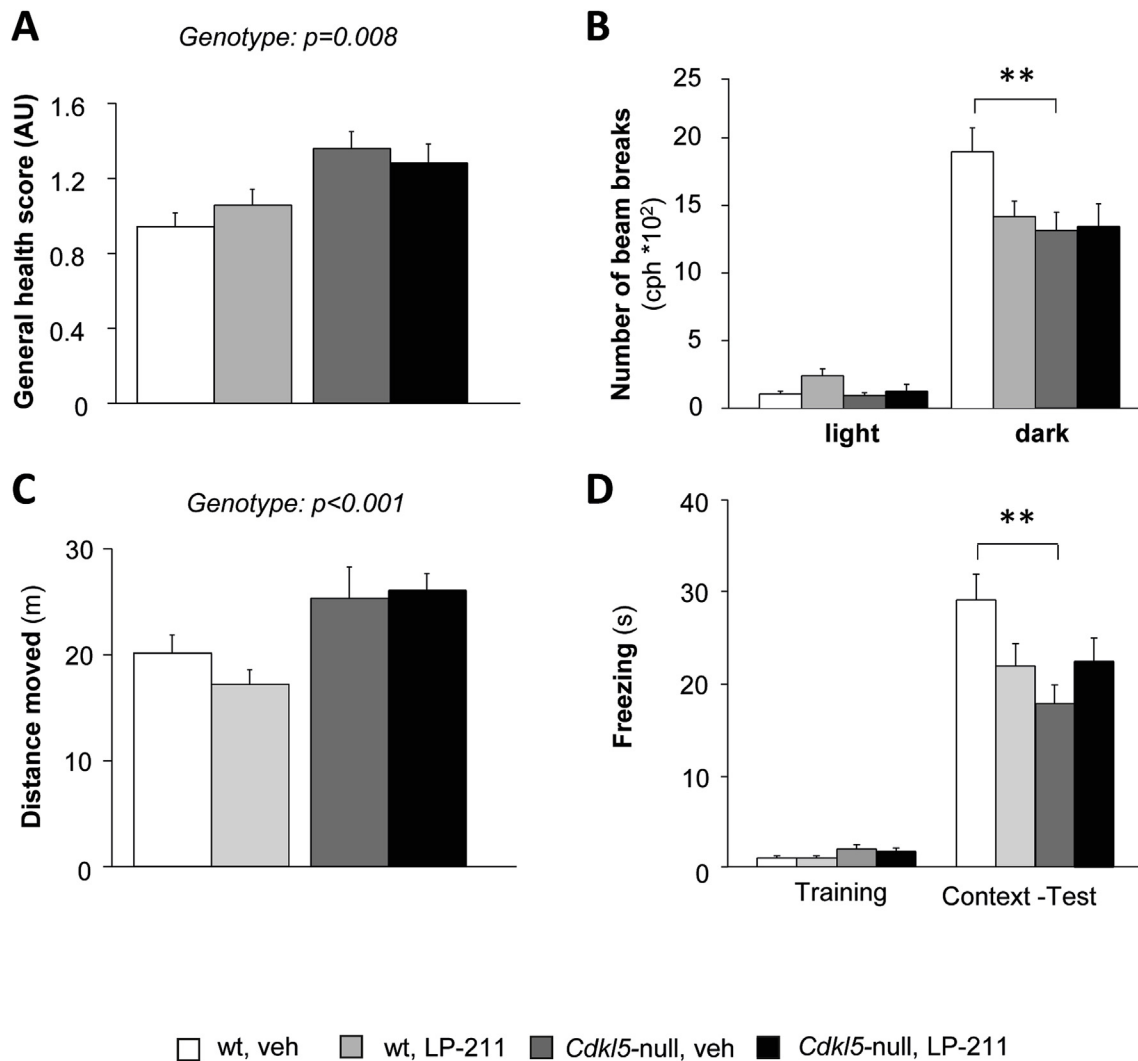
**Fig. 2. *Cdkl5*-null mice show severe behavioural alterations at an advanced stage of the disease. (A)** *Cdkl5*-null mice present a higher general health score compared to wt controls, thus confirming a worse general health status (score = 0–4). No treatment effects are found (wt, Veh = 11; wt, LP-211 = 12; *Cdkl5*-null, Veh = 8; *Cdkl5*-null, LP-211 = 8). **(B)** *Cdkl5*-null mice show hypoactivity in the home cage in comparison to wt mice during the dark/active phase of the circadian cycle. The LP-211 treatment does not affect this parameter. The infrared sensors detect any movement of mice with a frequency of 20 events per second (20 Hz). Scores are obtained as counts per hour (cph) expressed during 1-h periods, and the profile of daily activity is obtained by averaging 6-h of continuous registration per phase (Dark vs Light; 1–6pm - 2–8am) (wt, Veh = 8; wt, LP-211 = 10; *Cdkl5*-null, Veh = 7; *Cdkl5*-null, LP-211 = 7). (C) A hyperactive profile is evident in the open field task, with *Cdkl5*-null mice moving more than wt controls, that is not affected by the LP-211 treatment. (wt, Veh = 11; wt, LP-211 = 12; *Cdkl5*-null, Veh = 8; *Cdkl5*-null, LP-211 = 8). **(D)** *Cdkl5*-null mice show reduced freezing behaviour in comparison to wt mice in the fear conditioning task, suggesting defective contextual fear memory. The LP-211 treatment does not affect the performance in this cognitive test (wt, Veh = 11; wt, LP-211 = 12; *Cdkl5*-null, Veh = 8; *Cdkl5*-null, LP-211 = 8). Data are mean ± SEM. Statistical significance was calculated by two-way ANOVA. **p < 0,01; *p < 0,05 after Tukey's *post-hoc* tests.

increased Rac1 activation in both genotypes [Fig. 3, Treatment: F (1,15) = 5.8; p = 0.028].

*Expression and activation of RhoGTPase-dependent signaling pathways.* We found that phospho-PAK(p-PAK)/total PAK ratio, which provides an index of the net functionality of the kinase, was shifted toward increased activation in *Cdkl5*-null mouse cortex compared to wt controls [Fig. 4A and B; Genotype: F (1,17) = 15.7; p < 0.001]. The LP-211 treatment increased PAK activation in the cortex of both genotypes, as demonstrated by increased p-PAK/total PAK ratio [Fig. 4B, Treatment: F (1,17) = 11.7; p = 0.003].

In *Cdkl5*-null mouse cortex, we also observed increased ribosomal protein S6 (rpS6) activation (Fig. 4C representative blots), as demonstrated by increased phospho-rpS6 (240/244) (p-rpS6)/total rpS6 ratio, which was normalized by the LP-211 treatment [Fig. 4D; Genotype*-Treatment interaction: F (1,18) = 3.2, p = 0.089; *post-hoc:* p < 0.05]. No genotype or treatment effects were found on the phosphorylation levels of the rpS6 at Ser235/236 in the cortex (Fig. 4E).

*Akt activation levels.* In the cortex of *Cdkl5*-null mice, no genotype difference and no LP-211 treatment was detected for the activation of Akt quantified as the ratio phospho-Akt (p-Akt)/Akt total (Fig. S3).

*Cdkl5 levels.* Interestingly, the LP-211 treatment slightly, but significantly increased Cdkl5 protein levels in the cortex of LP-211-treated wt mice, in comparison to wt controls [Genotype*Treatment interaction: F (1,18) = 11.6, p = 0.003; *post-hoc:* p < 0.01; wt, veh: 100 ± 0.2 and wt, LP-211: 140 ± 0.2 (% relative to wt)]. As expected, Cdkl5 was not detected in the brain of mutant mice.

*5-HT$_7$R levels.* We also evaluated whether the levels of the 5-HT$_7$R differ in the brain of *Cdkl5*-null mice compared to wt controls and LP-211 effects thereon. No significant genotype or treatment effects were found in cortex (Fig. S4).
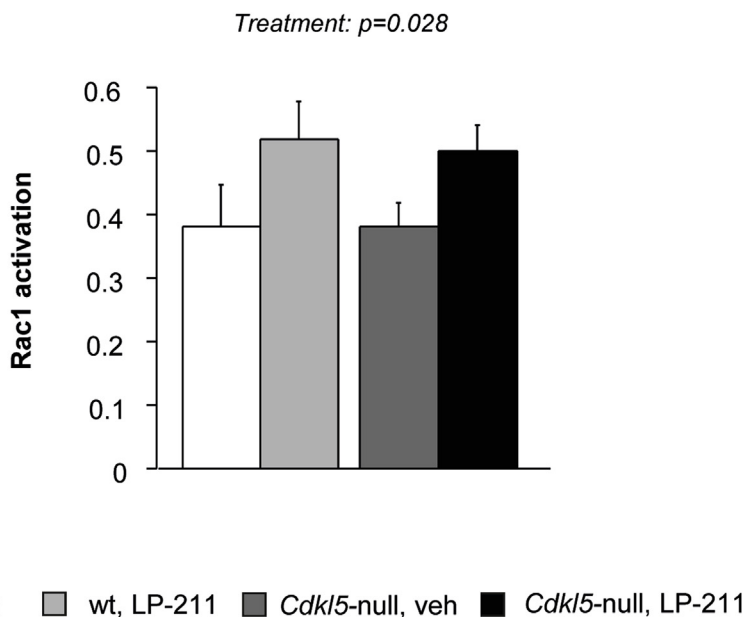
*Treatment: p=0.028*

**Fig. 3. The LP-211 treatment significantly increases Rac1 activation in both genotypes**. The activation of Rac1 protein was evaluated in mouse cortical brain areas by G-Lisa Activation Assay. No differences were found between *Cdkl5*-null mice and wt littermates. LP-211 treatment increases Rac1 activation levels in both genotypes (wt, Veh = 5; wt, LP-211 = 5; *Cdkl5*-null, Veh = 5; *Cdkl5*-null, LP-211 = 4). Data are mean ± SEM. Statistical significance was calculated by two-way ANOVA.

☐ wt, veh    ☐ wt, LP-211    ■ *Cdkl5*-null, veh    ■ *Cdkl5*-null, LP-211

### 3.3. Cdkl5-null mouse brain shows defective mitochondrial functionality that is rescued by the LP-211 treatment

Based on recent evidence suggesting a role for 5-HT$_7$R and Rho GTPases in the regulation of brain mitochondrial functionality (De Filippis et al., 2015c, 2015d; Valenti et al., 2017), we analyzed mitochondrial functionality in *Cdkl5*-null mouse brains.

*Activity of Mitochondrial Respiratory Chain (MRC) complexes.* We



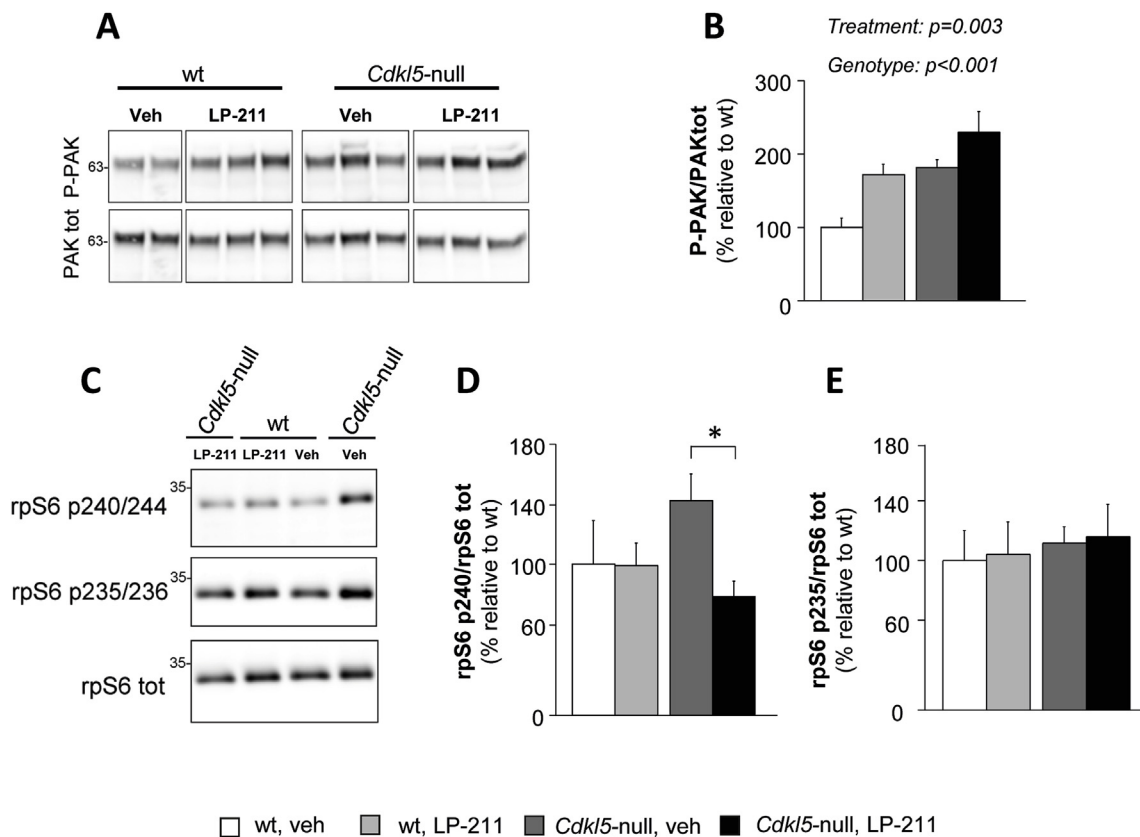☐ wt, veh    ☐ wt, LP-211    ■ *Cdkl5*-null, veh    ■ *Cdkl5*-null, LP-211

**Fig. 4. The LP-211 treatment rescues the abnormal activation of rpS6 in the cortex of *Cdkl5*-null mice.** Representative Western blot analysis (summarized view corresponding to one or three animals per group) of (**A**) phospho-PAK (p-PAK) and PAK tot, (**C**) rpS6 p240/244, rpS6 p235/236 and rpS6 tot proteins in cortical brain areas. (**B**) The LP-211 treatment increases the activation of group I PAKs, measured as p-PAK/PAK tot ratio in the cortex of *Cdkl5*-null and wt mice. This leads to an exacerbation of the overactivation of PAK in *Cdkl5*-null mouse cortex. (**D**) The LP-211 treatment normalizes the abnormal level of the p-rpS6(240/244)/rpS6tot ratio in*Cdkl5*-null mouse cortex. The LP-211 treatment does not affect cortical levels of the p-rpS6(235/236)/rpS6 tot ratio (**E**) (wt, Veh = 4; wt, LP-211 = 6; *Cdkl5*-null, Veh = 6; *Cdkl5*-null, LP-211 = 6). Data are expressed as percentage of wt veh controls (100). Data are mean ± SEM. Statistical significance was calculated by two-way ANOVA. **p < 0,01; *p < 0,05 after Tukey's *post-hoc* tests.
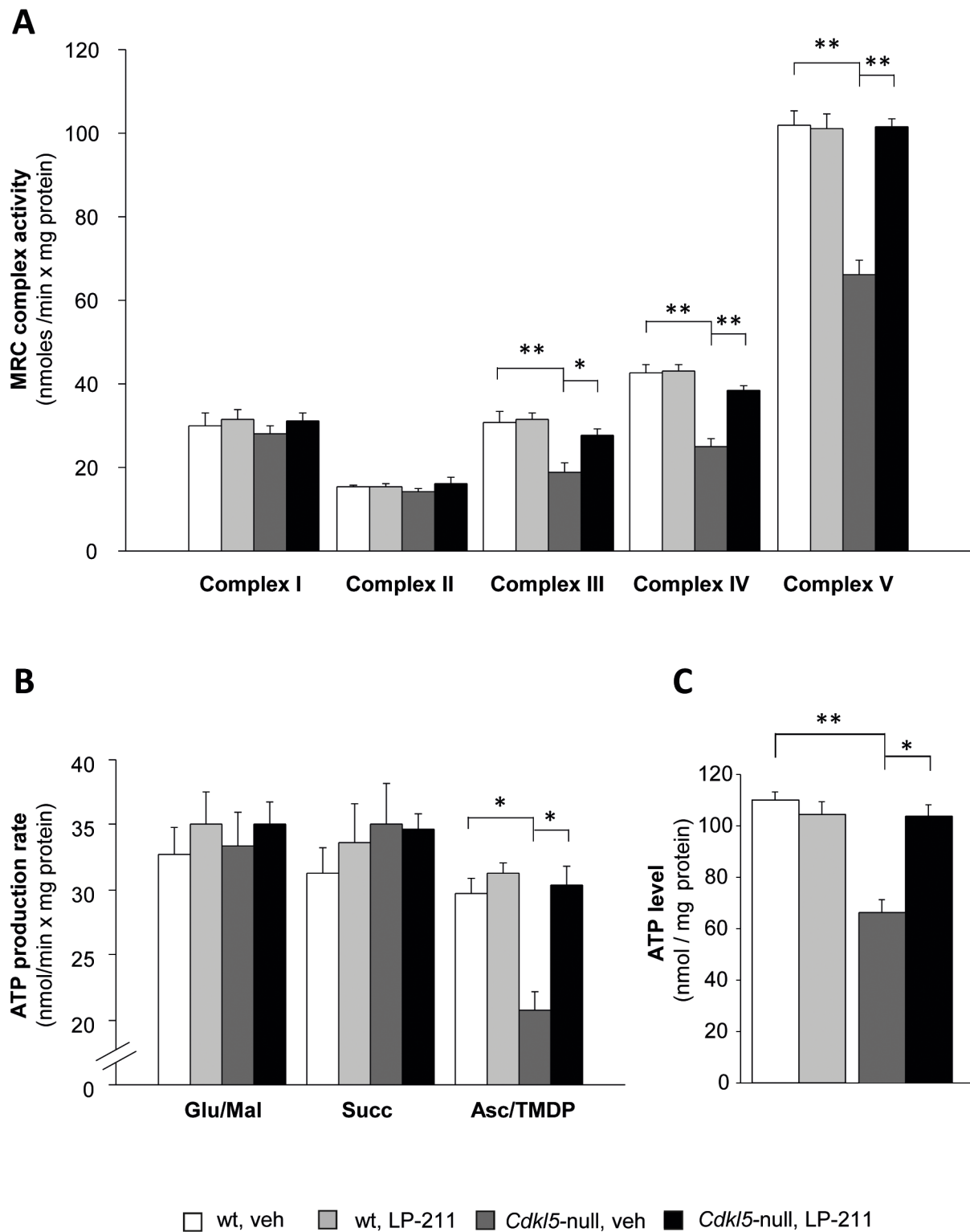
**Fig. 5.** *Cdkl5*-null mouse brain shows defective mitochondrial functionality that is rescued by the LP-211 treatment. (**A**) Reduced activity of mitochondrial respiratory chain (MRC) complexes III, IV, V is evident in *Cdkl5*-null mouse brain compared to wt controls. LP-211 treatment rescues these alterations. (**B**) Mitochondrial ATP production rate and (**C**) ATP level are lower in the brain of *Cdkl5*-null mice. The LP-211 rescues the defective energy status in the brain of *Cdkl5*-null mice (**B, C**) (wt, Veh = 3; wt, LP-211 = 3; *Cdkl5*-null, Veh = 3; *Cdkl5*-null, LP-211 = 3). Data are mean ± SEM. Statistical significance was calculated by two-way ANOVA. \*\*p < 0,01; \*p < 0,05 after Tukey's *post-hoc* test.

found reduced activity of the MRC complexes III, IV and V in *Cdkl5*-null mouse brains compared to wt controls [Fig. 5A; Repeated measure*Genotype*Treatment interaction: F (4,32) = 13.4; p < 0.001; *post-hoc*: p < 0.01]. No difference was found in the activity of complexes I and II (Fig. 5A). A complete restoration in the activity of the defective MRC complexes in LP-211-treated *Cdkl5*-null mice was found [Fig. 5A; Repeated measure*Genotype*Treatment interaction; *post-hoc*: p < 0.01 compared to vehicle-treated *Cdkl5*-null mice for complexes

IV and V and p < 0.05 compared to vehicle-treated *Cdkl5*-null mice for complex III].

*Brain energy status evaluation.* To evaluate if normalization of the activity of MRC complexes was associated with a normalization of their bioenergetic efficiency, the ATP production rate and ATP whole brain levels were measured (Fig. 5 B, C). In line with the results on complexes activity, *Cdkl5*-null mouse mitochondria showed a significant reduction in mitochondrial ATP production rate when supplied with the substrate for complex IV (ascorbate/TMDP), as energy source [Fig. 5B; Repeated measure*Genotype*Treatment interaction: F (2,16) = 3.2; p = 0.066; *post-hoc:* p < 0.05]. No changes were found when substrates for complexes I and II were used (Fig. 5B). Importantly, whole brain ATP levels were also reduced in *Cdkl5*-null mouse brain in comparison to wt controls [Fig. 5C; Genotype*Treatment interaction: F(1,12) = 20.2; p < 0.001; *post-hoc:* p < 0.01]. LP-211 treatment completely rescued the defective mitochondrial ATP production and the reduced brain ATP levels in *Cdkl5*-null mice [Fig. 5B; ATP production: Repeated measure*Genotype*Treatment interaction; *post-hoc:* p < 0.05; Fig. 5C; whole brain ATP level: Genotype*Treatment interaction; *post-hoc:* p < 0.01].

## 4. Discussion

This study provides the first characterization of the behavioural phenotype of *Cdkl5*-null mice at an advanced stage of the disease and demonstrates that 5-HT$_7$R modulation, with the 5-HT$_7$R agonist LP-211, partially rescues the abnormal neurobehavioural phenotype of fully symptomatic *Cdkl5*-null male mice. In particular, in *Cdkl5*-null mice receiving the LP-211 treatment we found a normalization of PPI deficits and a complete restoration of rpS6 activation in cortical brain areas. Moreover, we demonstrate for the first time that mitochondria, the powerhouses of the cells, show important abnormalities at the functional level in *Cdkl5*-null brain and that such functional alterations can be persistently restored by modulation of brain 5-HT$_7$R.

In spite of the progressive nature of CDD, mouse studies have been so far focused on young animals (i.e. 2–4 months of age) and no information is available on behavioural as well as brain molecular alterations in *Cdkl5*-null mice at an advanced stage of the disease. The present study provides the first comprehensive characterization of the behavioural phenotype displayed by 9–12-months old *Cdkl5*-null male mice. In particular, we found marked alterations in the general health status and in the locomotor profile, with *Cdkl5*-null mice showing an hypolocomotor profile in the home cage and hyperlocomotion in the open field, thus confirming previous data in young animals (Amendola et al., 2014; Jhang et al., 2017). An abnormal profile was also observed in the fear conditioning task, suggestive of a profound cognitive impairment in fully symptomatic *Cdkl5*-null mice. We cannot however exclude that the hyperactive profile shown by *Cdkl5*-null mice when exposed to novel contexts may account for the reduced freezing behaviour in this cognitive task (Amendola et al., 2014; Jhang et al., 2017).

Furthermore, the comprehensive battery of behavioural tests we carried out allowed us to identify the presence of severe PPI deficits in fully symptomatic *Cdkl5*-null mice, a measure of sensorimotor gating of the startle reflex (Swerdlow et al., 2001) that is known to be affected in patients with several neuropsychiatric disorders including schizophrenia (Braff et al., 2001), and in rodent models (Schwabe and Krauss, 2017). As PPI can be easily assessed in patients (Braff et al., 2001), present results provide to the clinical setting an innovative, non-invasive tool to test the efficacy of potential treatments for CDD. Further studies are however needed to uncover the developmental course of this behavioural alteration as a reduction in PPI was previously reported in two-months old *Cdkl5*-null mice, that just missed statistical significance (Okuda et al., 2018).

Of note, the LP-211 treatment rescued this behavioural alteration in *Cdkl5*-null mice. A link between PPI deficits and abnormal serotonin signaling has been clearly established, with either an increase or a decrease in serotonin signaling leading to PPI disruption (Fletcher et al.,

2001). Moreover, based on human studies demonstrating that 5-HT$_7$R mRNA is downregulated in the dorsolateral prefrontal cortex of schizophrenics (East et al., 2002), several works have addressed and demonstrated the involvement of 5-HT$_7$R in regulation of the PPI response in rodents (Pouzet et al., 2002b; Semenova et al., 2008). Our results similarly suggest that 5-HT$_7$R may be critically involved in serotonin-dependent regulation of the sensorimotor gating processing. Since we did not observe any change in the levels of the 5-HT$_7$R in *Cdkl5*-null mouse brain, our results suggest that stimulation of the 5-HT$_7$R might have indirectly rescued 5-HT$_7$R-independent defects in *Cdkl5*-null mouse brain. Indeed, several serotonin receptors have been found to be involved in the regulation of PPI (Pouzet et al., 2002a; Mitchell and Neumaier, 2008; Pogorelov et al., 2017). Moreover, other neurotransmitter systems including glutamate and dopamine play a role in regulating sensorimotor gating (reviewed in (Geyer et al., 2001)).

Another important finding of the present study concerns the demonstration that *Cdkl5*-null mouse brains display impaired mitochondrial OXPHOS and a consequent decrease in brain energy status. We found reduced activity of the complexes III, IV, V and decreased ATP production and defective whole brain energy status. How the lack of Cdkl5 produces such a mitochondrial dysfunction in mouse brain is not yet clear. Both transcriptional and post-translational mechanisms may be involved (De Filippis et al., 2015b). Of note, high levels of oxidative stress markers have been found in CDKL5 patients (Pecorelli et al., 2011), that have been proposed to be due to mitochondrial dysfunction (Pecorelli et al., 2015). We clearly demonstrate here the occurrence of multilevel dysfunctions of brain mitochondria in *Cdkl5*-null mice, thus providing support to this hypothesis.

Interestingly, reactivation of mitochondrial respiratory chain complexes in *Cdkl5*-null mouse brain by the LP-211 treatment rescued the defective brain energy status. Present results are in line with previous studies reporting the beneficial effect of the LP-211 treatment on brain mitochondrial function of two mouse models of RTT (Valenti et al., 2017). Taken together, these data strengthen the suggested link between 5-HT$_7$R and mitochondria in mouse brain and add relevant information to previous studies demonstrating a role for the serotonergic system in the regulation of mitochondria homeostasis (Chen et al., 2007; de Oliveira, 2016).

In the present study, we focused on RhoGTPases signaling, based on previous evidence suggesting that these pathways may be altered in CDD (Chen et al., 2010). Contrary to our expectation, we found normal activation levels of Rac1 in *Cdkl5*-null mouse cortex at the tested age. These results are in contrast with previous *in vitro* studies suggesting that defective Rac1 activation may play a role in CDD pathogenesis (Chen et al., 2010; Barbiero et al., 2017). Since no data on younger animals are currently available we cannot however exclude that such inconsistency may be due to the advanced age of the experimental mice. Indeed, a recent study aimed at evaluating Rac1 signaling in the brain of Fragile X mouse model has uncovered an age-dependent effect, with the observed Rac1 overactivation disappearing in older animals (Pyronneau et al., 2017).

Evidence that CDKL5 pathogenesis changes as the disease progresses is in fact provided by the increased activation of rpS6 (p 240/244) and the lack of genotype differences in Akt activation we found in *Cdkl5*-null mouse cortex at an advanced stage of the disease, which are in contrast with the previously reported reductions in younger animals (9–12 months of age vs postnatal day 27 and 60) (Amendola et al., 2014; Della Sala et al., 2016). Moreover, recent evidence demonstrated age-dependent efficacy of pharmacological treatment strategies in *Cdkl5*-null mice, with drugs exerting promising beneficial effects in two-month old *Cdkl5*-null mice losing their effectiveness at an advanced stage of the disease (Fuchs et al., 2018a). Altogether, these data highlight the need for studies aimed at evaluating the developmental progression of the disease and for innovative therapeutic strategies to be applied at an advanced stage of the disease, when previously efficacious therapies may lose their effectiveness.

We found that the LP-211 treatment normalized the unexpected overactivation of rpS6 in *Cdkl5*-null cortex, in addition to PPI deficits and mitochondrial dysfunction. Given that Rac1 and AkT activation were found to be normal and were not affected by the LP-211 treatment, present results suggest that different upstream molecules of rpS6 are altered in *Cdkl5*-null mouse brain at an advanced stage of the disease, that may account for the beneficial effects of the treatment under investigation (Bokoch, 2003; Biever et al., 2015). Indeed, the 5-HT$_7$R activation is known to stimulate several signaling cascades (Speranza et al., 2013; Guseva et al., 2014). Interestingly, among them, PKA activation has been intriguingly linked to de-phosphorylation of rpS6 at Ser240/244 (Bonito-Oliva et al., 2013) and to regulation of PPI (Kelly et al., 2007).

Besides the overactivation of rpS6, increased activation of group I PAKs was also evident in *Cdkl5*-null mouse brain, that was exacerbated by the LP-211 treatment. This family of proteins is crucially involved in several neuronal processes potentially relevant for CDD. In fact, group I PAKs play a crucial role in modulating ultrastructural neuronal morphology *in vivo* and in regulating activity-dependent actin dynamics, underlying synaptic plasticity (Hayashi-Takagi et al., 2010; De Filippis et al., 2014b; Duffney et al., 2015). Moreover, overactivation of the Rac/Pak pathway affects fear memory (Das et al., 2017), social learning (Molosh et al., 2014) and synaptic plasticity (Hayashi et al., 2004, 2007; Martinez and Tejada-Simon, 2011). Taken together, these results highlight the overactivation of Group I PAKs as a potential innovative target for the treatment of CDD at an advanced stage of the disease. Group I PAKs inhibitors are in fact increasingly recognized as promising candidates for the treatment of Fragile X and schizophrenia (Dolan et al., 2013; Hayashi-Takagi et al., 2014).

In conclusion, the present study provides the first evidence that the LP-211 treatment partially rescues the abnormal neurobehavioural phenotype of clearly symptomatic *Cdkl5*-null male mice. Abnormal PPI and reduced brain energy status due to mitochondrial dysfunction were also uncovered, for the first time, in *Cdkl5*-null mice at an advanced stage of the disease, thus providing innovative endophenotypes for CDD. Moreover, we provide here the first *in vivo* evidence that Cdkl5 in mouse cortex is involved in regulation of group I PAKs, a family of proteins that are crucially involved in several neuronal processes potentially relevant for CDD. Altogether, the present data highlight innovative endophenotypes and druggable molecular targets for this devastating disorder.

## Funding

## Disclosure/conflicts of interest

None of the authors declare financial interests or potential conflict of interests.

## Acknowledgements

## Appendix A. Supplementary data

Supplementary data to this article can be found online at https://doi.org/10.1016/j.neuropharm.2018.10.018.

## References

Amendola, E., Zhan, Y., Mattucci, C., Castroflorio, E., Calcagno, E., Fuchs, C., Lonetti, G., Silingardi, D., Vyssotski, A.L., Farley, D., Ciani, E., Pizzorusso, T., Giustetto, M., Gross, C.T., 2014. Mapping pathological phenotypes in a mouse model of CDKL5 disorder. PLoS One 9, e91613.

Bahi-Buisson, N., Nectoux, J., Rosas-Vargas, H., Milh, M., Boddaert, N., Girard, B., Cances, C., Ville, D., Afenjar, A., Rio, M., Heron, D., N'Guyen Morel, M.A., Arzimanoglou, A., Philippe, C., Jonveaux, P., Chelly, J., Bienvenu, T., 2008. Key clinical features to identify girls with CDKL5 mutations. Brain 131, 2647–2661.

Barbiero, I., Peroni, D., Tramarin, M., Chandola, C., Rusconi, L., Landsberger, N., Kilstrup-Nielsen, C., 2017. The neurosteroid pregnenolone reverts microtubule derangement induced by the loss of a functional CDKL5-IQGAP1 complex. Hum. Mol. Genet. 26, 3520–3535.

Biever, A., Valjent, E., Puighermanal, E., 2015. Ribosomal protein S6 phosphorylation in the nervous system: from regulation to function. Front. Mol. Neurosci. 8, 75.

Bokoch, G.M., 2003. Biology of the p21-activated kinases. Annu. Rev. Biochem. 72, 743–781.

Bonito-Oliva, A., Pallottino, S., Bertran-Gonzalez, J., Girault, J.A., Valjent, E., Fisone, G., 2013. Haloperidol promotes mTORC1-dependent phosphorylation of ribosomal protein S6 via dopamine- and cAMP-regulated phosphoprotein of 32 kDa and inhibition of protein phosphatase-1. Neuropharmacology 72, 197–203.

Braff, D.L., Geyer, M.A., Swerdlow, N.R., 2001. Human studies of prepulse inhibition of startle: normal subjects, patient groups, and pharmacological studies. Psychopharmacology 156, 234–258.

Chao, H.T., Chen, H., Samaco, R.C., Xue, M., Chahrour, M., Yoo, J., Neul, J.L., Gong, S., Lu, H.C., Heintz, N., Ekker, M., Rubenstein, J.L., Noebels, J.L., Rosenmund, C., Zoghbi, H.Y., 2010. Dysfunction in GABA signalling mediates autism-like stereotypies and Rett syndrome phenotypes. Nature 468, 263–269.

Chen, Q., Zhu, Y.C., Yu, J., Miao, S., Zheng, J., Xu, L., Zhou, Y., Li, D., Zhang, C., Tao, J., Xiong, Z.Q., 2010. CDKL5, a protein associated with rett syndrome, regulates neuronal morphogenesis via Rac1 signaling. J. Neurosci. 30, 12777–12786.

Chen, S., Owens, G.C., Crossin, K.L., Edelman, D.B., 2007. Serotonin stimulates mitochondrial transport in hippocampal neurons. Mol. Cell. Neurosci. 36, 472–483.

Cifariello, A., Pompili, A., Gasbarri, A., 2008. 5-HT(7) receptors in the modulation of cognitive processes. Behav. Brain Res. 195, 171–179.

Costa, L., Spatuzza, M., D'Antoni, S., Bonaccorso, C.M., Trovato, C., Musumeci, S.A., Leopoldo, M., Lacivita, E., Catania, M.V., Ciranna, L., 2012. Activation of 5-HT7 serotonin receptors reverses metabotropic glutamate receptor-mediated synaptic plasticity in wild-type and Fmr1 knockout mice, a model of Fragile X syndrome. Biol. Psychiatry 72, 924–933.

Das, A., Dines, M., Alapin, J.M., Lamprecht, R., 2017. Affecting long-term fear memory formation through optical control of Rac1 GTPase and PAK activity in lateral amygdala. Sci. Rep. 7, 13930.

De Filippis, B., Musto, M., Altabella, L., Romano, E., Canese, R., Laviola, G., 2015a. Deficient purposeful use of forepaws in female mice modelling rett syndrome. Neural Plast. 2015, 326184.

De Filippis, B., Chiodi, V., Adriani, W., Lacivita, E., Mallozzi, C., Leopoldo, M., Domenici, M.R., Fuso, A., Laviola, G., 2015b. Long-lasting beneficial effects of central serotonin receptor 7 stimulation in female mice modeling Rett syndrome. Front. Behav. Neurosci. 9, 86.

De Filippis, B., Nativio, P., Fabbri, A., Ricceri, L., Adriani, W., Lacivita, E., Leopoldo, M., Passarelli, F., Fuso, A., Laviola, G., 2014a. Pharmacological stimulation of the brain serotonin receptor 7 as a novel therapeutic approach for Rett syndrome. Neuropsychopharmacology 39, 2506–2518.

De Filippis, B., Ricceri, L., Fuso, A., Laviola, G., 2013. Neonatal exposure to low dose corticosterone persistently modulates hippocampal mineralocorticoid receptor expression and improves locomotor/exploratory behaviour in a mouse model of Rett syndrome. Neuropharmacology 68, 174–183.

De Filippis, B., Ricceri, L., Laviola, G., 2010. Early postnatal behavioral changes in the Mecp2-308 truncation mouse model of Rett syndrome. Gene Brain Behav. 9, 213–223.

De Filippis, B., Romano, E., Laviola, G., 2014b. Aberrant Rho GTPases signaling and cognitive dysfunction: in vivo evidence for a compelling molecular relationship. Neurosci. Biobehav. Rev. 46 (2), 285–301.

De Filippis, B., Valenti, D., Chiodi, V., Ferrante, A., de Bari, L., Fiorentini, C., Domenici, M.R., Ricceri, L., Vacca, R.A., Fabbri, A., Laviola, G., 2015c. Modulation of Rho GTPases rescues brain mitochondrial dysfunction, cognitive deficits and aberrant synaptic plasticity in female mice modeling Rett syndrome. Eur. Neuropsychopharmacol 25, 889–901.

De Filippis, B., Valenti, D., de Bari, L., De Rasmo, D., Musto, M., Fabbri, A., Ricceri, L., Fiorentini, C., Laviola, G., Vacca, R.A., 2015d. Mitochondrial free radical overproduction due to respiratory chain impairment in the brain of a mouse model of Rett syndrome: protective effect of CNF1. Free Radic. Biol. Med. 83, 167–177.

de Oliveira, M.R., 2016. Fluoxetine and the mitochondria: a review of the toxicological aspects. Toxicol. Lett. 258, 185–191.

Della Sala, G., Putignano, E., Chelini, G., Melani, R., Calcagno, E., Michele Ratto, G., Amendola, E., Gross, C.T., Giustetto, M., Pizzorusso, T., 2016. Dendritic spine instability in a mouse model of CDKL5 disorder is rescued by insulin-like growth factor 1. Biol. Psychiatry 80, 302–311.

Dolan, B.M., Duron, S.G., Campbell, D.A., Vollrath, B., Shankaranarayana Rao, B.S., Ko, H.Y., Lin, G.G., Govindarajan, A., Choi, S.Y., Tonegawa, S., 2013. Rescue of fragile X syndrome phenotypes in Fmr1 KO mice by the small-molecule PAK inhibitor FRAX486. Proc. Natl. Acad. Sci. U. S. A. 110, 5671–5676.

Duffney, L.J., Zhong, P., Wei, J., Matas, E., Cheng, J., Qin, L., Ma, K., Dietz, D.M.,

Kajiwara, Y., Buxbaum, J.D., Yan, Z., 2015. Autism-like deficits in shank3-deficient mice are rescued by targeting actin regulators. Cell Rep. 11, 1400–1413.

East, S.Z., Burnet, P.W., Kerwin, R.W., Harrison, P.J., 2002. An RT-PCR study of 5-HT(6) and 5-HT(7) receptor mRNAs in the hippocampal formation and prefrontal cortex in schizophrenia. Schizophr. Res. 57, 15–26.

Elia, M., Falco, M., Ferri, R., Spalletta, A., Bottitta, M., Calabrese, G., Carotenuto, M., Musumeci, S.A., Lo Giudice, M., Fichera, M., 2008. CDKL5 mutations in boys with severe encephalopathy and early-onset intractable epilepsy. Neurology 71, 997–999.

Fehr, S., Downs, J., Ho, G., de Klerk, N., Forbes, D., Christodoulou, J., Williams, S., Leonard, H., 2016. Functional abilities in children and adults with the CDKL5 disorder. Am. J. Med. Genet. 170, 2860–2869.

Fehr, S., Wilson, M., Downs, J., Williams, S., Murgia, A., Sartori, S., Vecchi, M., Ho, G., Polli, R., Psoni, S., Bao, X., de Klerk, N., Leonard, H., Christodoulou, J., 2013. The CDKL5 disorder is an independent clinical entity associated with early-onset encephalopathy. Eur. J. Hum. Genet. 21, 266–273.

Fletcher, P.J., Selhi, Z.F., Azampanah, A., Sills, T.L., 2001. Reduced brain serotonin activity disrupts prepulse inhibition of the acoustic startle reflex. Effects of 5,7-dihydroxytryptamine and p-chlorophenylalanine. Neuropsychopharmacology 24, 399–409.

Fuchs, C., Fustini, N., Trazzi, S., Gennaccaro, L., Rimondini, R., Ciani, E., 2018a. Treatment with the GSK3-beta inhibitor Tideglusib improves hippocampal development and memory performance in juvenile, but not adult, Cdkl5 knockout mice. Eur. J. Neurosci. 47, 1054–1066.

Fuchs, C., Gennaccaro, L., Trazzi, S., Bastianini, S., Bettini, S., Martire, V.L., Ren, E., Medici, G., Zoccoli, G., Rimondini, R., Ciani, E., 2018b. Heterozygous CDKL5 knockout female mice are a valuable animal model for CDKL5 disorder. Neural Plast. 2018, 9726950.

Fuchs, C., Trazzi, S., Torricella, R., Viggiano, R., De Franceschi, M., Amendola, E., Gross, C., Calza, L., Bartesaghi, R., Ciani, E., 2014. Loss of CDKL5 impairs survival and dendritic growth of newborn neurons by altering AKT/GSK-3beta signaling. Neurobiol. Dis. 70, 53–68.

Geyer, M.A., Krebs-Thomson, K., Braff, D.L., Swerdlow, N.R., 2001. Pharmacological studies of prepulse inhibition models of sensorimotor gating deficits in schizophrenia: a decade in review. Psychopharmacology 156, 117–154.

Guseva, D., Wirth, A., Ponimaskin, E., 2014. Cellular mechanisms of the 5-HT7 receptor-mediated signaling. Front. Behav. Neurosci. 8, 306.

Guy, J., Gan, J., Selfridge, J., Cobb, S., Bird, A., 2007. Reversal of neurological defects in a mouse model of Rett syndrome. Science 315, 1143–1147.

Hayashi-Takagi, A., Araki, Y., Nakamura, M., Vollrath, B., Duron, S.G., Yan, Z., Kasai, H., Huganir, R.L., Campbell, D.A., Sawa, A., 2014. PAKs inhibitors ameliorate schizophrenia-associated dendritic spine deterioration in vitro and in vivo during late adolescence. Proc. Natl. Acad. Sci. U. S. A. 111, 6461–6466.

Hayashi-Takagi, A., Takaki, M., Graziane, N., Seshadri, S., Murdoch, H., Dunlop, A.J., Makino, Y., Seshadri, A.J., Ishizuka, K., Srivastava, D.P., Xie, Z., Baraban, J.M., Houslay, M.D., Tomoda, T., Brandon, N.J., Kamiya, A., Yan, Z., Penzes, P., Sawa, A., 2010. Disrupted-in-Schizophrenia 1 (DISC1) regulates spines of the glutamate synapse via Rac1. Nat. Neurosci. 13, 327–332.

Hayashi, M.L., Choi, S.Y., Rao, B.S., Jung, H.Y., Lee, H.K., Zhang, D., Chattarji, S., Kirkwood, A., Tonegawa, S., 2004. Altered cortical synaptic morphology and impaired memory consolidation in forebrain- specific dominant-negative PAK transgenic mice. Neuron 42, 773–787.

Hayashi, M.L., Rao, B.S., Seo, J.S., Choi, H.S., Dolan, B.M., Choi, S.Y., Chattarji, S., Tonegawa, S., 2007. Inhibition of p21-activated kinase rescues symptoms of fragile X syndrome in mice. Proc. Natl. Acad. Sci. U. S. A. 104, 11489–11494.

Hedlund, P.B., 2009. The 5-HT7 receptor and disorders of the nervous system: an overview. Psychopharmacology 206, 345–354.

Hedlund, P.B., Danielson, P.E., Thomas, E.A., Slanina, K., Carson, M.J., Sutcliffe, J.G., 2003. No hypothermic response to serotonin in 5-HT7 receptor knockout mice. Proc. Natl. Acad. Sci. U. S. A. 100, 1375–1380.

Jhang, C.L., Huang, T.N., Hsueh, Y.P., Liao, W., 2017. Mice lacking cyclin-dependent kinase-like 5 manifest autistic and ADHD-like behaviors. Hum. Mol. Genet. 26, 3922–3934.

Kalscheuer, V.M., Tao, J., Donnelly, A., Hollway, G., Schwinger, E., Kubart, S., Menzel, C., Hoeltzenbein, M., Tommerup, N., Eyre, H., Harbord, M., Haan, E., Sutherland, G.R., Ropers, H.H., Gecz, J., 2003. Disruption of the serine/threonine kinase 9 gene causes severe X-linked infantile spasms and mental retardation. Am. J. Hum. Genet. 72, 1401–1411.

Kelly, M.P., Isiegas, C., Cheung, Y.F., Tokarczyk, J., Yang, X., Esposito, M.F., Rapoport, D.A., Fabian, S.A., Siegel, S.J., Wand, G., Houslay, M.D., Kanes, S.J., Abel, T., 2007. Constitutive activation of Galphas within forebrain neurons causes deficits in sensorimotor gating because of PKA-dependent decreases in cAMP. Neuropsychopharmacology 32, 577–588.

Khan, H.A., 2003. Bioluminometric assay of ATP in mouse brain: determinant factors for enhanced test sensitivity. J. Biosci. 28, 379–382.

Kilstrup-Nielsen, C., Rusconi, L., La Montanara, P., Ciceri, D., Bergo, A., Bedogni, F., Landsberger, N., 2012. What we know and would like to know about CDKL5 and its involvement in epileptic encephalopathy. Neural Plast. 2012, 728267.

Leopoldo, M., Lacivita, E., De Giorgio, P., Fracasso, C., Guzzetti, S., Caccia, S., Contino, M., Colabufo, N.A., Berardi, F., Perrone, R., 2008. Structural modifications of N-(1,2,3,4-tetrahydronaphthalen-1-yl)-4-aryl-1-piperazinehexanamides: influence on lipophilicity and 5-HT7 receptor activity. Part III. J. Med. Chem. 51, 5813–5822.

Macri, S., Ceci, C., Onori, M.P., Invernizzi, R.W., Bartolini, E., Altabella, L., Canese, R., Imperi, M., Orefici, G., Creti, R., Margarit, I., Magliozzi, R., Laviola, G., 2015. Mice repeatedly exposed to Group-A beta-Haemolytic Streptococcus show perseverative behaviors, impaired sensorimotor gating, and immune activation in rostral diencephalon. Sci. Rep. 5, 13257.

Manente, A.G., Valenti, D., Pinton, G., Jithesh, P.V., Daga, A., Rossi, L., Gray, S.G., O'Byrne, K.J., Fennell, D.A., Vacca, R.A., Nilsson, S., Mutti, L., Moro, L., 2013. Estrogen receptor beta activation impairs mitochondrial oxidative metabolism and affects malignant mesothelioma cell growth in vitro and in vivo. Oncogenesis 2, e72.

Martinez, L.A., Tejada-Simon, M.V., 2011. Pharmacological inactivation of the small GTPase Rac1 impairs long-term plasticity in the mouse hippocampus. Neuropharmacology 61, 305–312.

Matthys, A., Haegeman, G., Van Craenenbroeck, K., Vanhoenacker, P., 2011. Role of the 5-HT7 receptor in the central nervous system: from current status to future perspectives. Mol. Neurobiol. 43, 228–253.

Mitchell, E.S., Neumaier, J.F., 2008. 5-HT6 receptor antagonist reversal of emotional learning and prepulse inhibition deficits induced by apomorphine or scopolamine. Pharmacol. Biochem. Behav. 88, 291–298.

Molosh, A.I., Johnson, P.L., Spence, J.P., Arendt, D., Federici, L.M., Bernabe, C., Janasik, S.P., Segu, Z.M., Khanna, R., Goswami, C., Zhu, W., Park, S.J., Li, L., Mechref, Y.S., Clapp, D.W., Shekhar, A., 2014. Social learning and amygdala disruptions in Nf1 mice are rescued by blocking p21-activated kinase. Nat. Neurosci. 17, 1583–1590.

Okuda, K., Takao, K., Watanabe, A., Miyakawa, T., Mizuguchi, M., Tanaka, T., 2018. Comprehensive behavioral analysis of the Cdkl5 knockout mice revealed significant enhancement in anxiety- and fear-related behaviors and impairment in both acquisition and long-term retention of spatial reference memory. PloS One 13, e0196587.

Pecorelli, A., Belmonte, G., Meloni, I., Cervellati, F., Gardi, C., Sticozzi, C., De Felice, C., Signorini, C., Cortelazzo, A., Leoncini, S., Ciccoli, L., Renieri, A., Jay Forman, H., Hayek, J., Valacchi, G., 2015. Alteration of serum lipid profile, SRB1 loss, and impaired Nrf2 activation in CDKL5 disorder. Free Radic. Biol. Med. 86, 156–165.

Pecorelli, A., Ciccoli, L., Signorini, C., Leoncini, S., Giardini, A., D'Esposito, M., Filosa, S., Hayek, J., De Felice, C., Valacchi, G., 2011. Increased levels of 4HNE-protein plasma adducts in Rett syndrome. Clin. Biochem. 44, 368–371.

Pogorelov, V.M., Rodriguiz, R.M., Cheng, J., Huang, M., Schmerberg, C.M., Meltzer, H.Y., Roth, B.L., Kozikowski, A.P., Wetsel, W.C., 2017. 5-HT2C agonists modulate schizophrenia-like behaviors in mice. Neuropsychopharmacology 42, 2163–2177.

Pouzet, B., Didriksen, M., Arnt, J., 2002a. Effects of the 5-HT(6) receptor antagonist, SB-271046, in animal models for schizophrenia. Pharmacol. Biochem. Behav. 71, 635–643.

Pouzet, B., Didriksen, M., Arnt, J., 2002b. Effects of the 5-HT(7) receptor antagonist SB-258741 in animal models for schizophrenia. Pharmacol. Biochem. Behav. 71, 655–665.

Pyronneau, A., He, Q., Hwang, J.Y., Porch, M., Contractor, A., Zukin, R.S., 2017. Aberrant Rac1-cofilin signaling mediates defects in dendritic spines, synaptic function, and sensory perception in fragile X syndrome. Sci. Signal. 10.

Ricceri, L., De Filippis, B., Fuso, A., Laviola, G., 2011. Cholinergic hypofunction in MeCP2-308 mice: beneficial neurobehavioural effects of neonatal choline supplementation. Behav. Brain Res. 221, 623–629.

Ricciardi, S., Boggio, E.M., Grosso, S., Lonetti, G., Forlani, G., Stefanelli, G., Calcagno, E., Morello, N., Landsberger, N., Biffo, S., Pizzorusso, T., Giustetto, M., Broccoli, V., 2011. Reduced AKT/mTOR signaling and protein synthesis dysregulation in a Rett syndrome animal model. Hum. Mol. Genet. 20, 1182–1196.

Ricciardi, S., Ungaro, F., Hambrock, M., Rademacher, N., Stefanelli, G., Brambilla, D., Sessa, A., Magagnotti, C., Bachi, A., Giarda, E., Verpelli, C., Kilstrup-Nielsen, C., Sala, C., Kalscheuer, V., Broccoli, V., 2012. CDKL5 ensures excitatory synapse stability by reinforcing NGL-1-PSD95 interaction in the postsynaptic compartment and is impaired in patient iPSC-derived neurons. Nat. Cell Biol. 14, 911–923.

Rusconi, L., Kilstrup-Nielsen, C., Landsberger, N., 2011. Extrasynaptic N-methyl-D-aspartate (NMDA) receptor stimulation induces cytoplasmic translocation of the CDKL5 kinase and its proteasomal degradation. J. Biol. Chem. 286, 36550–36558.

Rusconi, L., Salvatoni, L., Giudici, L., Bertani, I., Kilstrup-Nielsen, C., Broccoli, V., Landsberger, N., 2008. CDKL5 expression is modulated during neuronal development and its subcellular distribution is tightly regulated by the C-terminal tail. J. Biol. Chem. 283, 30101–30111.

Schwabe, K., Krauss, J.K., 2017. What rodent models of deep brain stimulation can teach us about the neural circuit regulation of prepulse inhibition in neuropsychiatric disorders. Schizophr. Res. 198, 45–51.

Semenova, S., Geyer, M.A., Sutcliffe, J.G., Markou, A., Hedlund, P.B., 2008. Inactivation of the 5-HT(7) receptor partially blocks phencyclidine-induced disruption of prepulse inhibition. Biol. Psychiatry 63, 98–105.

Speranza, L., Chambery, A., Di Domenico, M., Crispino, M., Severino, V., Volpicelli, F., Leopoldo, M., Bellenchi, G.C., di Porzio, U., Perrone-Capano, C., 2013. The serotonin receptor 7 promotes neurite outgrowth via ERK and Cdk5 signaling pathways. Neuropharmacology 67, 155–167.

Speranza, L., Labus, J., Volpicelli, F., Guseva, D., Lacivita, E., Leopoldo, M., Bellenchi, G.C., di Porzio, U., Bijata, M., Perrone-Capano, C., Ponimaskin, E., 2017. Serotonin 5-HT7 receptor increases the density of dendritic spines and facilitates synaptogenesis in forebrain neurons. J. Neurochem. 141, 647–661.

Swerdlow, N.R., Geyer, M.A., Braff, D.L., 2001. Neural circuit regulation of prepulse inhibition of startle in the rat: current knowledge and future challenges. Psychopharmacology 156, 194–215.

Valenti, D., de Bari, L., De Filippis, B., Henrion-Caude, A., Vacca, R.A., 2014. Mitochondrial dysfunction as a central actor in intellectual disability-related diseases: an overview of Down syndrome, autism, Fragile X and Rett syndrome. Neurosci. Biobehav. Rev. 46 Pt 2, 202–217.

Valenti, D., de Bari, L., Vigli, D., Lacivita, E., Leopoldo, M., Laviola, G., Vacca, R.A., De Filippis, B., 2017. Stimulation of the brain serotonin receptor 7 rescues mitochondrial dysfunction in female mice from two models of Rett syndrome. Neuropharmacology 121, 79–88.

Valenti, D., Tullo, A., Caratozzolo, M.F., Merafina, R.S., Scartezzini, P., Marra, E., Vacca, R.A., 2010. Impairment of F1F0-ATPase, adenine nucleotide translocator and

adenylate kinase causes mitochondrial energy deficit in human skin fibroblasts with chromosome 21 trisomy. Biochem. J. 431, 299–310.

Wang, I.T., Allen, M., Goffin, D., Zhu, X., Fairless, A.H., Brodkin, E.S., Siegel, S.J., Marsh, E.D., Blendy, J.A., Zhou, Z., 2012. Loss of CDKL5 disrupts kinome profile and event-related potentials leading to autistic-like phenotypes in mice. Proc. Natl. Acad. Sci. U. S. A. 109, 21516–21521.

Wilcox, R.R., 1987. New designs in analysis of variance. Annu. Rev. Psychol. 38, 29–60.

Zhou, A., Han, S., Zhou, Z.J., 2017. Molecular and genetic insights into an infantile epileptic encephalopathy - CDKL5 disorder. Front. Biol. 12, 1–6.

## Glossary

*CDKL5 Deficiency Disorder:* CDD
*Cyclin-dependent kinase-like 5:* CDKL5
*Serotonin receptor 7:* 5-HT$_7$R
*Intellectual disability:* ID
*Rett syndrome:* RTT
*Induced-pluripotent stem cells:* iPSCs

*Ribosomal protein:* rp
*Intraperitoneal:* i.p.
*Oxidative phosphorylation:* OXPHOS
*Wild-type:* wt
*Prepulse inhibition:* PPI
*Mitochondrial Respiratory Chain:* MRC
*Dimethyl sulfoxide:* DMSO
*White noise:* WN
*BL:* baseline
*CS:* conditioned stimulus
*US:* unconditioned stimulus
*Inter trial interval:* ITI

## Nomenclature

*LP-211:* N-(4-cyanophenylmethyl)-4-(2-diphenyl)-1-piperazinehexanamide
*PubChem:* CID:25107716